Durham E-Theses

Advanced Algorithms for Automatic Wind Turbine Condition Monitoring

ZAPPALA, DONATELLA

Advanced Algorithms for Automatic Wind Turbine Condition Monitoring

by

Donatella Zappalá

A thesis submitted as part of the
degree of Doctor of Philosophy

Supervisors: Prof. Peter Tavner & Prof. Simon Hogg

School of Engineering and Computing Sciences
Durham University
United Kingdom

November 2014

Dedicated to my beloved daughter Caterina

Abstract

Reliable and efficient condition monitoring (CM) techniques play a crucial role in minimising wind turbine (WT) operations and maintenance (O&M) costs for a competitive development of wind energy, especially offshore. Although all new turbines are now fitted with some form of condition monitoring system (CMS), very few operators make use of the available monitoring information for maintenance purposes because of the volume and the complexity of the data.

This Thesis is concerned with the development of advanced automatic fault detection techniques so that high on-line diagnostic accuracy for important WT drive train mechanical and electrical CM signals is achieved.

Experimental work on small scale WT test rigs is described. Seeded fault tests were performed to investigate gear tooth damage, rotor electrical asymmetry and generator bearing failures. Test rig data were processed by using commercial WT CMSs.

Based on the experimental evidence, three algorithms were proposed to aid in the automatic damage detection and diagnosis during WT non-stationary load and speed operating conditions. Uncertainty involved in analysing CM signals with field fitted equipment was reduced, and enhanced detection sensitivity was achieved, by identifying and collating characteristic fault frequencies in CM signals which could be tracked as the WT speed varies.

The performance of the gearbox algorithm was validated against datasets of a full-size WT gearbox, that had sustained gear damage, from the National Renewable Energy Laboratory (NREL) WT Gearbox Condition Monitoring Round Robin project.

The fault detection sensitivity of the proposed algorithms was assessed and quantified leading to conclusions about their applicability to operating WTs.

Declaration

This thesis is based on the work carried out by Donatella Zappalá, under the supervision of Prof. Peter Tavner and Prof. Simon Hogg as a part of the Energy Group, School of Engineering and Computing Sciences, Durham University. No part of this thesis has been submitted elsewhere for any other degree or qualification. The content of this thesis is all my own work unless referenced to the contrary in the text.

Acknowledgements

Publications

Peer reviewed publications

Journal papers

1) **Zappalá, D.,** Tavner, P.J., Crabtree, C.J. & Sheng, S. (2014). Side-band algorithm for automatic wind turbine gearbox fault detection and diagnosis. *IET Renewable Power Generation* **8**(4): 380-389.

2) Delorm, T.M., **Zappalá, D.** and Tavner, P.J. (2012). Tidal stream device reliability comparison models. *Proceedings of the Institution of Mechanical Engineers, Part O: Journal of Risk and Reliability* **226**(1): 6-17.

Conference proceedings

1) **Zappalá, D.,** Crabtree, C.J., Vilchis-Rodriguez, D.S., Tavner, P.J., Djurović, S. & Smith, A.C. (2014). Advanced Algorithms for Automatic Wind Turbine Generator Fault Detection and Diagnosis. In *Proceedings of the Scientific Track of the European Wind Energy Association Conference*. Barcelona, Spain.

2) Crabtree, C.J., **Zappalá, D.,** Tavner, P.J. and Hogg, S.I. (2014). Electrical Fault Detection Using Mechanical Signals. In *Proceedings of the Scientific Track of the European Wind Energy Association Conference*. Barcelona, Spain.

3) **Zappalá, D.,** Tavner, P.J., Crabtree, C.J. & Sheng, S. (2013). Sideband Algorithm for Automatic Wind Turbine Gearbox Fault Detection and Diagnosis. In *Proceedings of the Scientific Track of the European Wind Energy Association Conference*. Vienna, Austria.

4) **Zappalá, D.,** Tavner, P.J. & Crabtree, C.J. (2012). Gear Fault Detection Automation Using WindCon Frequency Tracking. In *Proceedings of the Scientific Track of the European Wind Energy Association Conference*. Copenhagen, Denmark.

Technical Reports

1) Chen, B., **Zappalá, D.,** Crabtree, C.J. and Tavner, P.J. (2014). 'Survey of Commercially Available SCADA Data Analysis Tools for Wind Turbine

Health Monitoring'. Durham University School of Engineering and Computing Sciences and the SUPERGEN Wind Energy Technologies Consortium.

2) Crabtree, C.J., **Zappalá, D**. and Tavner, P.J. (2014). 'Survey of Commercially Available Condition Monitoring Systems for Wind Turbines'. Durham University School of Engineering and Computing Sciences and the SUPERGEN Wind Energy Technologies Consortium.

Table of Contents

List of Figures

List of Tables

List of Abbreviations

BMS	Blade Monitoring System
CBM	Condition Based Maintenance
CDS	Condition Diagnostics System
CM	Condition Monitoring
CMS	Condition Monitoring System
DAQ	Data Acquisition
DAS	Data Acquisition System
DECC	Department of Energy & Climate Change
DFIG	Doubly Fed Induction Generator
DFT	Discrete Fourier Transform
DSP	Digital Signal Processor
EC	European Commission
EU	European Union
EWEA	European Wind Energy Association
FFT	Fast Fourier Transform
GRC	Gearbox Reliability Collaborative
GWEC	Global Wind Energy Council
HPF	Harmonic Power Factor
HS	High-Speed
HSS	High-Speed Shaft
IG	Induction Generator
IS	Intermediate-Speed
ISS	Intermediate-Speed Shaft
LS	Low-Speed
LSS	Low-Speed Shaft
LWK	Landwirtschaftskammer Schleswig-Holstein
MCSA	Motor Current Signal Analysis
MV	Medium Voltage

NAREC	New & Renewable Energy Centre
NI	National Instruments
NREL	National Renewable Energy Laboratory
NWTC	National Wind Technology Centre
OEM	Original Equipment Manufacturer
O&M	Operations and Maintenance
PSD	Power Spectral Density
SB	Sideband
SBPF	Sideband Power Factor
SCADA	Supervision Control and Data Acquisition
SHM	Structural Health Monitoring
TCM	Turbine Condition Monitoring
TSD	Tidal Stream Device
WF	Wind Farm
WMEP	Wissenschaftlichen Mess und Evaluierungsprogramm
WRIG	Wound Rotor Induction Generator
WT	Wind Turbine
WTCMTR	Wind Turbine Condition Monitoring Test Rig

Nomenclature

A_{mn}	Amplitude of the amplitude modulation function
B_{mn}	Amplitude of the phase modulation function
$a_m(t)$	Amplitude modulation function
$b_m(t)$	Phase modulation function
CWT_{local}	Localised Continuous Wavelet Transform
D_b	Rolling-element diameter
D_c	Bearing pitch diameter
f	Frequency
f_{BPFI}	Inner raceway ball passing frequency
f_{BPFO}	Outer raceway ball passing frequency
f_{HSS}	HSS rotational frequency
f_{LSS}	LSS rotational frequency
f_{mesh}	Gear meshing frequency
$f_{mesh,HS}$	HS stage meshing frequency
$2xf_{mesh,HS}$	HS stage meshing frequency second harmonic
$f_{mesh,LS}$	LS stage meshing frequency
$2xf_{mesh,LS}$	LS stage meshing frequency second harmonic
f_{rm}	Rotor mechanical speed
f_{rot}	Shaft rotational frequency
f_s	Fundamental stator supply frequency
f_{samp}	Sampling frequency
f_{syn}	Synchronous speed
HPF	Harmonic power factor
$\%HPF$	Harmonic power factor detection sensitivity
$IDFT_{local}$	Iterative Localised Discrete Fourier Transform

j	$\sqrt{-1}$
M	Number of tooth-meshing harmonics
M'	Number of SBs around the meshing harmonics
N	Length of a discrete signal
N_b	Number of rolling elements
N_t	Number of gear teeth
$P(k)$	Power spectrum or PSD
SB_i	ith Sideband
$SBPF_{gear}$	Gear SBPF
$\%SBPF_{gear}$	Gear SBPF detection sensitivity
$SBPF_{rotor}$	Rotor SBPF
$\%SBPF_{rotor}$	Rotor SBPF detection sensitivity
s	Induction generator fractional slip
T_{samp}	Sampling period
t	Time
X	Frequency order
X_m	Amplitude of the mth meshing harmonic
$X(f)$	Fourier transform
$x(t)$	Continuous-time signal
$X[k]$	Discrete Fourier transform
$x[n]$	Discrete-time signal
W_N	Principal Nth root of unity
$(W_N)^k$	Complex roots of unity
$w[n]$	Window function
$y(t)$	Modulated vibration signal
$y'(t)$	Meshing vibration signal
α_{mn}	Phase of the amplitude modulation function

β	Contact angle
β_{mn}	Phase of the phase modulation function
ϕ_m	Phase of the mth meshing harmonic
ω	Machine rotational speed

1

Introduction

1.1. Background

The exploitation of renewable energy sources plays a key role in the strategy developed by the European Union (EU) in order to meet its environmental and energy policy goals, including its obligation to reduce greenhouse gases under the Kyoto Protocol (EC, 2002b) and the aim of securing its energy supply (EC, 2002a). The EU has committed to a legally binding target to meet 20% of its energy consumption through renewable energy by 2020. To achieve this, there is an expectation that 34% of electricity will need to be generated by renewables (EC, 2009). In its recently published communication on "a policy framework for climate and energy in the period from 2020 to 2030" the EU proposes an objective of increasing the share of renewable energy to at least 27% of the EU's energy consumption by 2030 as part of the commitment to decarbonise the economy by 80% to 95% by 2050 (EC, 2014).

Thanks to recent technological advances and commercial growth, wind energy has been the strongest growing renewable source of energy in the world over the last 30 years. Wind energy plays a central role in an increasing number of countries' immediate and longer term energy plans. At the end of 2013 the global installed wind capacity stood at 318.1 GW (Fried et al., 2014) with 117.3 GW installed in the EU: 110.7 GW onshore and 6.6 GW offshore. As shown in Figure 1.1, the annual wind power installations in the EU have increased steadily over the past 13 years from 4.4 GW in 2001 to 11.2 GW in 2013, representing an average annual growth rate of over 10%. 2013 was a record year for offshore installations, with 1,567 MW of new capacity grid connected. Offshore wind power installations represent over 14% of the annual EU wind energy market. The EU current wind power

capacity would, in a normal wind year, produce 257 TWh of electricity, enough to cover 8% of EU's gross electricity demand (Pineda et al., 2014).
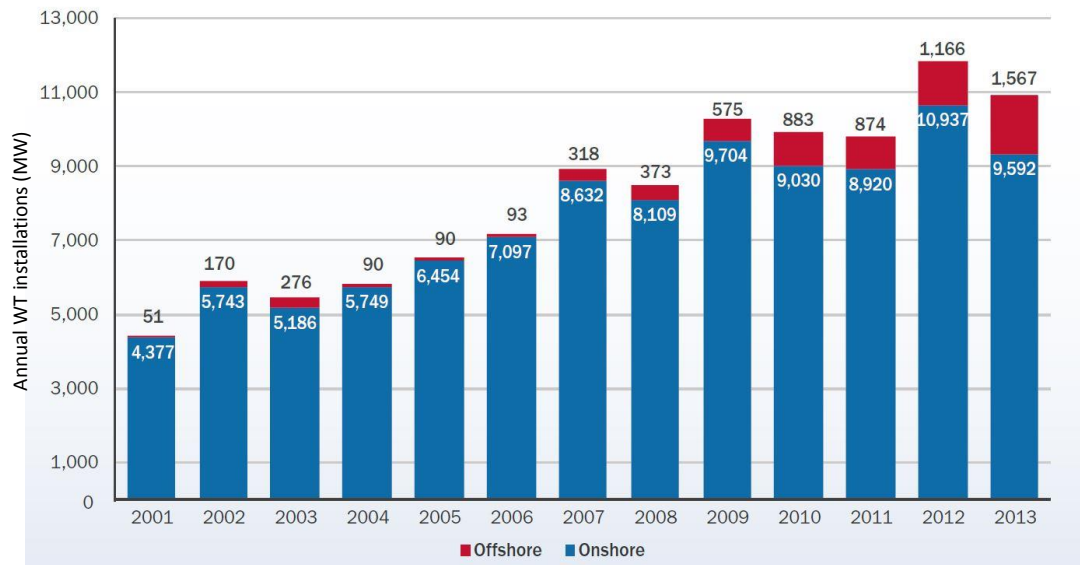
Figure 1.1: Annual onshore and offshore installations (MW) in EU (Pineda et al., 2014).

According to the European Wind Energy Association (EWEA) scenarios, 230 GW of wind capacity will be installed in Europe by 2020, 400 GW by 2030 and 735 GW by 2050 (Moccia et al., 2011). Offshore wind has significant generation potential in Europe with increasingly large-scale sites identified as suitable for offshore development and benefiting from a favourable wind resource. Offshore wind is therefore expected to play a significant role in meeting these targets. However, this poses several technical and economic challenges which need to be addressed.

1.1.1. Wind Energy: Going Offshore

Compared to onshore, offshore installations present less problematic visual intrusion, significantly higher yields due to stronger wind profiles, which generally increase with distance from shore, less turbulence and larger WT ratings. Today, more than 90% of installations are in European waters, in the

North, Baltic and Irish Seas, however, offshore development in China is starting to take off, followed by Japan, South Korea, Taiwan and the US.

Since the world's first offshore wind farm (WF) was built in shallow waters off the coast of Denmark in 1991 at Vindeby, wind technology has matured, turbine size has increased from 450 kW up to 8 MW, WF total capacity has grown significantly and projects have moved further from the coast. Figure 1.2 represents the current offshore trends in distances to shore and water depths for the on-line WFs along with the ones under construction and already consented in Europe. The bubble size represents the total WF capacity. Current commercial fixed bottom substructures are economically limited to 50 m maximum water depth, i.e. shallow to transitional depths (Kaldellis and Kapsali, 2013). To date, the majority of on-line large-scale WFs have been built 20 km or less from the shore and in up to 20 m water depth using shallow water technology, such as the monopile and gravity-based structures, although the idea of going deeper is gradually moving closer to implementation. A large amount of consented and under construction offshore WFs are already located in depths of over 40 m and up to 100 km from shore. Thanks to the deployment of deep offshore technologies, for example floating turbines, WFs could be located even further offshore into deeper (> 50 m) water in the near future (Arapogianni et al., 2013) but the capital costs will be significantly higher.

With its extensive wind resources, the UK is the world leader in offshore wind development. The seas surrounding Scotland are estimated to have a quarter of Europe's potential wind energy capacity. Both the UK and Scottish Governments are committed to increasing offshore wind deployment. The UK's planned expansion of offshore wind will enable the country to meet binding EU targets to source 15% of all energy from renewables by 2020. The installation of offshore wind in Scotland will make a significant contribution to Scotland's target to meet the equivalent of 100% of the country's electricity

demand from renewables by 2020. Currently, the total installed offshore capacity in UK is 3.7 GW. The largest WF in the world, the London Array, rated 630 MW from 175 WTs, became operational in 2013. A further 5.7 GW is either under construction or has planning approval, and a further 12.3 GW is in the planning system. Industry projections see a total of 8 GW of capacity by 2016 and around 18 GW by 2020, supplying 18-20% of national electricity demand (RenewableUK, 2014).
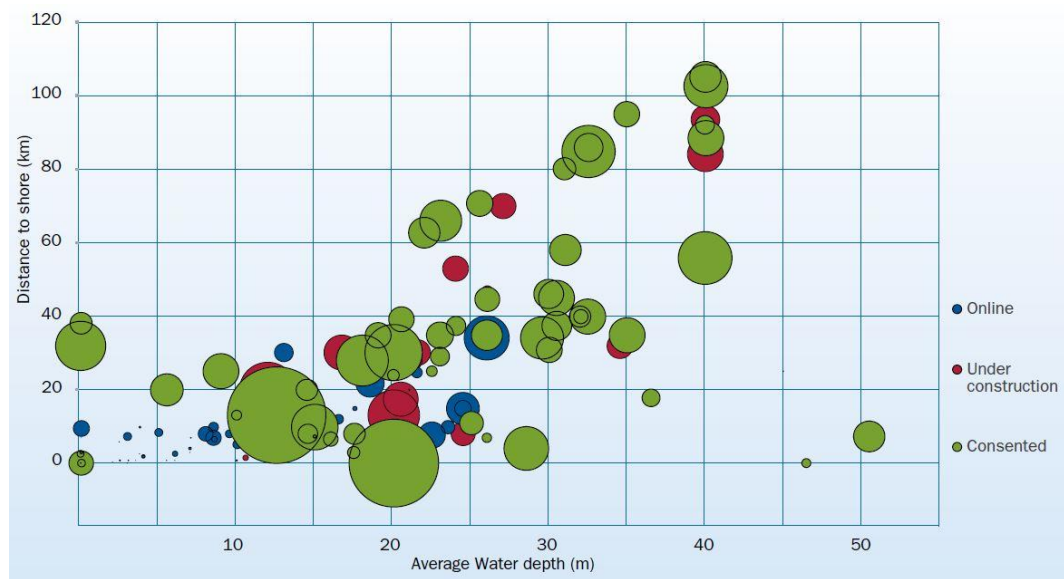
Figure 1.2: Average water depth and distance to shore for on-line, under construction and consented offshore WFs (Arapogianni et al., 2013).

1.1.2.   Cost of Energy

Despite the considerable offshore potential and the progress made so far, the offshore wind industry market is not growing as fast as expected. The primary reasons for this are that offshore generation is still more expensive than conventional generators at current fuel prices because of the high capital cost of the installation. It also imposes a higher risk of a lower return on invested capital than current onshore WFs because of uncertain installation costs and lower reliability of offshore generation. As more and more offshore assets are commissioned and the number of operational WTs

continues to grow, the technical and commercial challenges of operating offshore projects is starting to receive greater attention.

Wind energy at onshore coastal sites is already close to competitiveness compared to conventional power plants (Krohn et al., 2009). The estimated cost of offshore energy varies depending on the site and project, however offshore wind projects are still significantly more costly than onshore. Recent WF projects around the UK coast have indicated that Cost of Energy has stabilised at around £140/MWh (Arwas et al., 2012). The most critical priority for offshore wind power is to significantly lower its cost of energy in order to become competitive with conventional power generation and establish itself as an economically sustainable, stable and long-term energy source. According to the UK Renewable Energy Roadmap, the offshore cost of energy needs to reach the challenging target of £100/MWh by 2020 (DECC, 2011) in order to gain a significant market foothold and parity with other forms of generation. To achieve this goal, capital and operational expenditures must be optimized. Capital expenditure (CAPEX) for a WT is primarily the cost of the turbine itself, the supporting and electrical infrastructures. Operational expenditure (OPEX) for a WT includes the cost of running the site, planned O&M, and unplanned maintenance due to poor reliability.

1.1.3.   Operations & Maintenance

As WT designs become adapted to offshore conditions, the achievement of favourable economic solutions depends upon controlling the WF system full life-cycle cost. Based on an analysis of a representative offshore WF of 500 MW capacity, Figure 1.3 illustrates a breakdown of typical total system costs (GL Garrad Hassan, 2013).
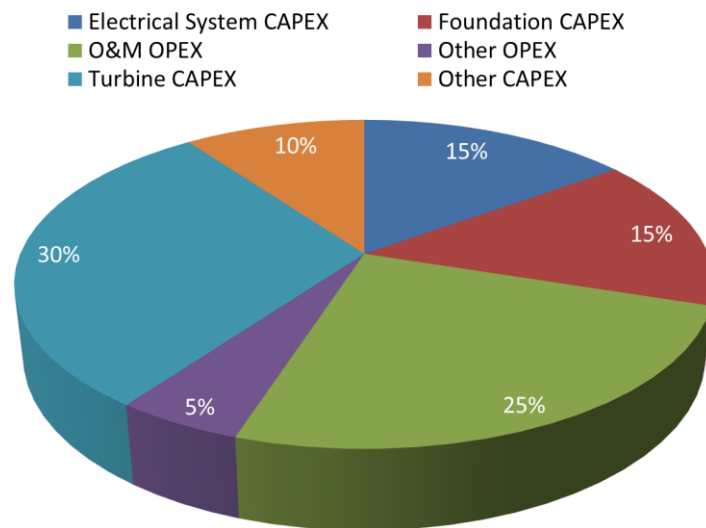
Figure 1.3: Breakdown of cost of energy for representative offshore WF, based on data from (GL Garrad Hassan, 2013).

CAPEX currently makes up around 70% of the overall cost of energy for offshore wind, as WTs are capital intensive, and the OPEX is around 30%, however, this percentage will fall as capital loans are paid off and costs of energy will fall. In the OPEX category, around 5% is accounted for by ongoing expenditures such as grid usage fees, leases, back-office support and other items. The remaining 25% is apportioned to the O&M activities, which follow commissioning to ensure the safe and economic running of the project. The objective is to make sure the project achieves the best balance between running cost and electricity output. O&M occurs throughout the life of the project, which is critical to project profitability and is nominally 20 years, although it could be extended if WTs prove reliable. To date most O&M has been contracted to the WT suppliers to run in parallel with key equipment warranties, typically for the first 5 years of offshore operation. O&M costs broadly scale with the number of turbines, as this governs the number of offshore transfers required per year and the number of parts used. Assuming WTs of 6 MW in size, a distance from O&M port of 55 km and O&M strategy of work boats with helicopter support, the total OPEX, as seen by the WF

owner, is estimated by GL Garrad Hassan as around £430,000 per turbine per year, averaged over a 20 year design life (GL Garrad Hassan, 2013).

O&M strategy is a significant factor to be considered when evaluating the economic viability of large offshore WFs. Reducing O&M costs could result in greater competitiveness of electricity generated by offshore WTs in the electricity market.

1.1.4.   Maintenance Strategies and Optimisation

Operations represent a small proportion of O&M expenditure and refer to activities contributing to the high level management of the asset such as remote monitoring, environmental monitoring, electricity sales, marketing, administration and other back office tasks. Maintenance accounts for a large portion of O&M effort, cost and risk. The purpose of maintenance is to enable desired component performance by maintaining or returning the component's ability to function correctly.

Figure 1.4 shows common maintenance strategies employed, which can be divided into corrective and preventive maintenance. The primary difference between these two strategies is that a problem in the system must exist before corrective maintenance actions are taken, whilst preventive tasks are intended to prevent occurrence of a problem in the first place.

Corrective maintenance is undertaken after a breakdown or when obvious failure has been located. For failures on critical functions, it has to be performed immediately and unscheduled downtime will result. However, for failures that have no or little consequence on the comprehensive system function, the maintenance can be deferred in time to a better suited occasion.

Preventive maintenance is performed to avoid failure and can be further subdivided into calendar based and condition based maintenance.

- Calendar based maintenance is performed on scheduled times and is independent on the machinery operating status between maintenance visits. It is suitable for failures that are age-related and for which the probability distribution of failure can be established. Scheduled maintenance activities in wind power takes generally 2-3 days per WT and include, among the others, lubrication oil and oil filter changes, check of generator brushes and slip-rings, inspection with respect to leakage, test of safety systems and brake pad, strength testing and retightening bolts, oil sampling and analysis for the gearbox and visual inspection of the blades. This maintenance is based on manufacturer recommendations. Onshore, it is generally performed every three months during the first year of the WT, and later on every six months or year depending on the type of service maintenance tasks and WT model. However, due to higher transportation costs and production losses, WTs located offshore are routinely serviced only once a year during spring or summer (Besnard, 2009). Reducing failures in this way comes at the cost of completing maintenance tasks more frequently than absolutely necessary and not exhausting the full life of the various components already in service.

- Condition based maintenance (CBM) is performed on the basis of the actual health of the component, and thus it requires reliable monitoring systems, with on line monitoring and/or inspections and alarm limits that can be programmed or specified to alert attention if the condition exceeds specified accepted levels. In-depth analysis of the monitored data provides a diagnosis and prognosis of an incipient fault and gives input to decide maintenance actions on a dynamic preventive schedule (Bengtsson, 2004). This involves acquisition, processing, analysis and interpretation of data and selection of optimal maintenance actions and is achieved using CMS. CBM has been shown to minimise the costs of maintenance, improve operational safety, and

reduce the quantity and severity of in-service system failures (Byon and Ding, 2010; McMillan and Ault, 2008).

Unscheduled maintenance work is likely to result in WT downtime and loss of production. In contrast, planned maintenance activity is not critical to production and can be carried out when winds are light and access is easier, or during periods of low demand for electricity.
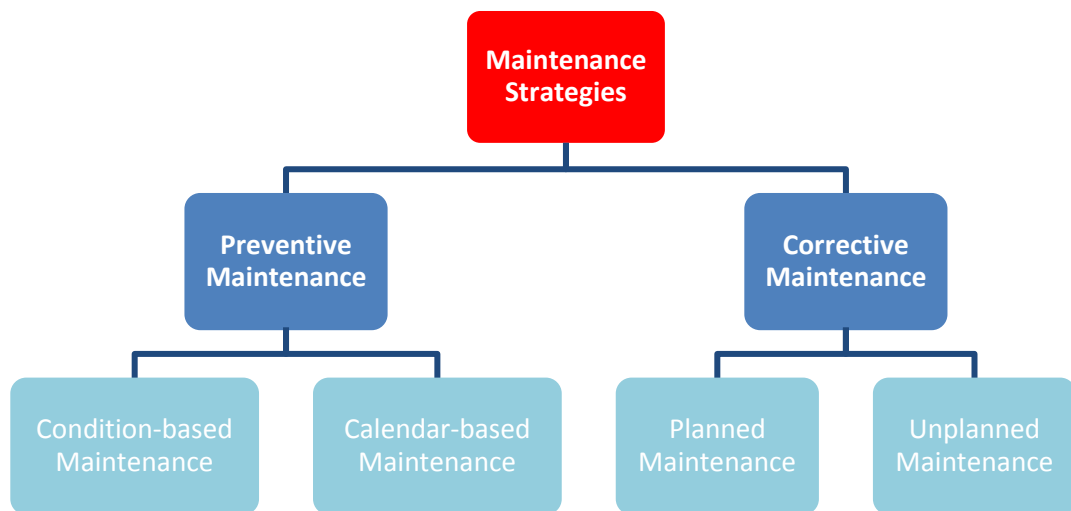
Figure 1.4: Types of maintenance strategies (Wiggelinkhuizen et al., 2008).

The current O&M practice adopted for existing onshore and offshore WFs is corrective maintenance. Essentially, when an item fails and the WT becomes non-operational a maintenance expedition is launched at the first opportunity to carry out the repair, this being an additional visit to the WT over any planned routine preventive calendar-based maintenance visit (Karyotakis, 2011). Failed items are generally repaired in situ or by exchange so the corrective maintenance strategy ensures the WT is returned to full operational state as quickly as practically possible.

Offshore O&M tasks are influenced by distance to shore, weather and sea conditions, site exposure, WF size, WT reliability and maintenance strategy and transportation means. WF accessibility for maintenance can be

restricted by harsh sea, wind or visibility conditions for many days, or even weeks, at a time, especially during winter. In addition, offshore conditions require special costly equipment, such as supply vessels, barges or helicopters, to move, change-out or install major subassemblies. Such equipment is in high demand in the offshore industry and may not be available at short notice or can be locally sourced. High average offshore wind speed poses a triple challenge to O&M activity:

- Increasing the likelihood of faults occurring, due to the rigorous operating conditions;

- Making access more challenging and reducing the opportunities for the turbines to be repaired and returned to full operation; and

- Increasing the cost of failure, as turbines generate most power during windy conditions the foregone revenue of lost energy production is highest during high wind speeds.

Owing to the reduced site accessibility and the high cost of specialist personnel and equipment involved, offshore O&M costs can be quantified as three to five times higher than those on land (McMillan and Ault, 2007; Musial and Ram, 2010). A considerable part of these costs, typically up to 70%, is associated with unscheduled maintenance which results in unexpected WT downtime, reduced availability and lost revenue (Tavner et al., 2008b; Van Bussel and Schöntag, 1997; Walford, 2006). Moreover, man-day costs can amount up to €1000 for offshore unscheduled maintenance (Nilsson and Bertling, 2007). O&M costs could potentially increase even more when considering next WF development further offshore in higher average wind speeds and more challenging sea-states. These high figures emphasise the need for optimising the O&M strategy for offshore WFs to reduce the turbine downtime and improve the availability (Sheng and Veers, 2011). Achieving high WT availability is paramount to providing affordable and cost-effective wind energy. In this context, high operational reliability and adequate maintenance capability are two interrelated and critical issues for

safeguarding the long-term operation of an offshore WF, in both technical and economic terms.

Corrective maintenance strategies, successfully employed onshore with minimal interference from environmental conditions, are largely impractical offshore because of difficulties in accessing WFs in harsher environmental conditions and in transporting maintenance teams and spares (Andrawus et al., 2007; Musial et al., 2006). O&M work at sea is significantly more challenging, time consuming and costly. For unmanned offshore WFs optimisation of maintenance strategies is required to minimise the maintenance costs in order to achieve competitive prices for the produced electricity (Sørensen, 2009). The adoption of a CBM strategy can contribute significantly to minimising the offshore O&M costs by lowering the number of inspection visits and corrective maintenance actions (Garcia Marquez et al., 2012). This maintenance approach involves the repair or replacement of parts based on their actual condition and the individual operating history of the particular machine, rather than on a schedule based on the predicted operating conditions of the average machine (Hyers et al., 2006). Advanced techniques are needed to plan CBM using data from the Supervisory Control Data Acquisition (SCADA) and CMSs fitted to the WTs.

1.2. Research Motivation and Aims

WTs have exceptionally good monitoring cover because of their unmanned remote robotics operation (Tavner, 2012). All new WTs are now fitted with some form of CMS by either the manufacturer or user. However, these systems usually collect large, complex, unmanageable volumes of data, still requiring a large degree of expert manual analysis. Owing to the amount and complexity of the data, very few operators are currently making use of the monitoring information for maintenance purposes. To use CM information successfully for optimising the O&M strategies, systems that can

automatically analyse and interpret the large volumes of CM data are required.

Current efforts in the wind CM industry are aimed at automating the data interpretation and improving the accuracy and the reliability of the diagnostic decisions, especially in the light of impending large-scale, offshore WF generation. The development of reliable and cost-effective CM techniques, with automatic damage detection and diagnosis of the WT components, plays a pivotal role in establishing technically and economically viable CBM strategies, particularly for unattended WTs located in remote and difficult-to-access locations. Autonomous on-line CM systems allow the early warning of mechanical and electrical defects to prevent major component failures (Hameed et al., 2009). Faults can be detected while the defective component is still operational and thus necessary repair actions can be planned in time to minimise WT downtime, improve reliability, maximise availability and improve profitability.

This work attempts to target this research area by experimentally defining three algorithms that could be easily incorporated into current CMSs for automatic gearbox and generator fault detection and diagnosis. The main aim of this research is to devise automatic techniques to improve CM reliability using field-fitted equipment. The implementation of these algorithms could reduce WF operators' workload, dramatically cutting down the quantity of the information handled and the complexity of carrying out manual data analysis, and provide improved detection for timely decision-making.

1.3.   SUPERGEN Wind Energy Technologies Consortium

This research has been funded by a UK EPSRC doctoral training award as part of the Phase 2 of the SUPERGEN Wind Energy Technologies programme, EP/H018662/1 (SUPERGEN Wind, 2014).

The SUPERGEN Wind Energy Technologies Consortium is a UK wind energy research consortium which was originally established by the EPSRC on 23rd March 2006 as part of its Sustainable Power Generation and Supply (SUPERGEN) programme. The project successfully renewed for another four years, starting from 23rd March 2010. Phase 2 has run under the Energy Programme of Research Councils UK, led by EPSRC.

The SUPERGEN Wind Consortium was led by Strathclyde and Durham Universities and consisted of 7 research partners with expertise in WT technology, aerodynamics, hydrodynamics, materials, electrical machinery, control, reliability and CM. The Consortium had the active support of 18 industrial partners including WF operators, manufacturers and consultants. The Consortium's principal objective for Phase 2 was: "*To undertake research to achieve an integrated, cost-effective, reliable & available offshore wind power station*".

The project had three parallel initiating themes during the first two years:
- Theme 1: The Farm, dealing with research into the physics and engineering of the offshore WF ;
- Theme 2: The Turbine, looking more specifically at improving the reliability and performance of individual WTs, building on the work in SUPERGEN Wind Phase 1;
- Theme 3: The Connection, addressing the technical barriers to the WF connection and associated grid capacity issues.

In the third and fourth years of the project, the results of these three themes have been fed into a fourth gathering theme, Theme 4: The Wind Farm, which considered the WF as a power station looking at how the power station should be designed, operated and maintained for optimum reliability and what the overall economics should be.

This research was carried out as part of:

- The sub theme 2.4, Fault Detection, of Theme 2, whose objective, was to develop turbine monitoring targeted at improving the reliability and availability of offshore WFs.
- The sub theme 4.3, Asset management, of Theme 4, whose objective was to develop a single CM and fault identification strategy for the electrical and mechanical drivetrain systems, appropriate for large offshore WT designs.

Throughout this research, the Author had the opportunity to attend several training seminars, including academic and industrial presentations, which broadened the Author's knowledge on different aspects of WT technology, WF development and economics. The Author had also the chance to present her research results during the yearly SUPERGEN Wind Phase 2 general assemblies which have always stimulated fruitful discussions with other researchers and industrial partners and have been a source of inspiration for further research.

During the preparation of this Thesis, there was a large amount of collaborative work and discussion with a number of academic and industrial partners involved in Theme 2-2.4 and Theme 4-4.3. In particular, this Thesis presents the results of the collaborative work with the University of Manchester on the investigation of generator faults.

1.4. Thesis Structure

This Thesis is organised into a number of chapters to reflect the direction, progress and results of research since October 2010.

This introduction, Chapter 1, places the research in a wider context by briefly introducing wind energy development and the research background.

The challenges to WT O&M are discussed and the aims of the research are introduced.

Chapter 2 is a comprehensive review which summarises the current knowledge in the field of WT CM. This chapter introduces and discusses the published WT reliability studies and seeks to explain why research effort should be expended upon improving reliability of WT gearbox and generator, subassemblies that are of most concern for O&M. The current state of the art of commercial available WT CMSs, their commercial benefits, their current challenges and limitations are then summarised.

The focus in this research is presented in Chapter 3 together with the theoretical basis of signal processing and fault detection analytical techniques relevant to this work. Some of the most significant principles of the theory of faults in WT gearbox and generator are then discussed. The fundamental electrical and mechanical fault equations used in this Thesis are derived.

Chapter 4 describes the methodological approach of this research. Firstly, the Durham Wind Turbine Condition Monitoring Test Rig (WTCMTR) is introduced. Secondly, the faults investigated, the rig data acquisition system and the methodology applied for data analysis and processing are described. The collaborative research with the University of Manchester, within the SUPERGEN Wind Phase 2 Consortium, on rotor electrical asymmetry and generator bearing faults is then introduced and described. Finally, a fault detection sensitivity function, which allows the comparison of the results obtained for the different faults and the relative monitoring signals investigated, is defined.

The next two chapters present the majority of the original research. In these chapters experimental results from small-scale WT test rigs and a full-scale WT gearbox, are presented and discussed.

Chapter 5 contains the results of test rig experimentation. Results from gearbox high-speed pinion tooth damage, generator rotor electrical asymmetry and generator bearing fault during non-stationary load and speed operating conditions are presented. Based on the experimental evidence, three algorithms for automatic fault detection and diagnosis are introduced, mathematically defined and applied to analyse the experimental results. Finally, this chapter presents and compares the fault detection sensitivities of the proposed algorithms for the different faults investigated.

Chapter 6 shows the successful validation of the experimentally defined algorithm for automatic gear tooth fault detection and diagnosis against signals from a full-size WT gearbox that had sustained gear damage, and had been studied in a National Renewable Energy Laboratory's (NREL) programme.

Chapter 7 draws conclusions from this research and discusses the main implications of the Thesis. The chapter concludes with a discussion of further work based on experiences from this project, including improvements that could be made to the test rig and some potential new areas for investigation.

1.5. Original Contribution

Due to the highly stochastic nature of the wind, the loading on the WT drive train components is highly variable and the analysis of CM signals is not simple. Despite recent advances, one of the main limitations of most current CMS systems is the time-consuming and costly manual handling of large amounts of complex monitoring data which requires specialist knowledge. This can result in monitoring information being neglected and costly corrective maintenance strategies adopted.

Having in mind the crucial role of reliable and effective CM methods in minimising O&M costs for a competitive development of offshore wind

energy, this Thesis aims at developing potential techniques that can be applied remotely and automatically to important WT drive train electrical and vibration CM signals. The proposed techniques are also able to indicate the severity of the fault so that a judgement can be made as to when maintenance should take place. Previous WT CM work identified signals and methods for WT fault detection. This work reduces the uncertainty involved in analysing CM signals when using field fitted equipment by concentrating on raising fault detection sensitivity so that high reliability is achieved. Enhanced detection sensitivity is obtained by identifying and collating characteristic fault frequencies in CM signals which could be tracked as the WT speed varies. This is accomplished by experimental work on small scale test rigs and technique validation by using real WT datasets. Test rig data were processed by using a commercial WT CMS, further demonstrating the practicability of what was being proposed. The analysis methods used are more advanced than those used in previous works, so it is possible to place more confidence in the results obtained.

In summary, the Author contends that the work has made a significant contribution to the economic applicability of wind turbine condition monitoring engineering.

2

Wind Turbine Monitoring

2.1. Introduction

Chapter 1 has highlighted the current need for WT O&M cost reduction through the adoption of reliable and cost effective CM techniques that allow early detection of any degeneration in system components, facilitating a proper asset management decision, improving availability, minimizing downtime and maximizing productivity. As offshore WTs operate in remote locations and harsh environments, the need for high reliability and low O&M costs is higher than for on-shore applications. For these reasons the development of reliable CMSs for WTs is essential to avoid catastrophic failures and to minimize costly corrective maintenance.

This chapter outlines the current knowledge in the field of WT CM. Firstly, recent published WT reliability studies are summarised and the subassemblies that are of most concern for O&M are identified. This is followed by a description of the state of the art in CM of WTs, looking at both new emerging techniques currently being researched and industry developed tools, with a particular focus on the economic benefits of CMSs. Conclusions are drawn about current systems challenges and limitations.

2.2. Wind Turbine Reliability

WT reliability is a critical factor in the economic success of a wind energy project. Poor reliability directly affects the project's revenue stream through both increased O&M costs and reduced availability to generate power due to turbine downtime.

The principal objective of reliability analysis is to gain feedback for improving design by identifying weaknesses in parts and subassemblies. Reliability studies play also a key role in optimising WT maintenance strategy. The main factor for optimal preventive maintenance, both from technical and economical point of view, is the time period selection for inspection. Optimum time period selection could not be achieved without a comprehensive reliability and availability analysis resulting in a ranking of critical subassemblies. In this way, WT reliability data can be used to benchmark WT performance for organising and planning future O&M, particularly offshore.

Although modern WTs currently have a shorter design life compared to traditional steam and gas turbine generator systems, i.e. 20 years and 40 years respectively, their failure rates have been estimated about three times those of conventional generation technologies (Spinato et al., 2009). Failure rates of 1-3 failure(s)/turbine/year for stoppages ≥24 hours are common onshore (Tavner et al., 2007). Despite substantial improvements in recent years, the current reliability of onshore WTs is still inadequate for the harsher offshore environment (Wilkinson et al., 2006) where maintenance attendance times are to be reduced and availability raised. For onshore WTs, high failures rates can be managed by a maintenance regime that provides regular visits. This will be costly or impossible to sustain in remote offshore WF sites. Failure rates of 0.5 failure(s)/turbine/year would be desirable offshore, where planned maintenance visits need to be kept at or below 1 per year, but are nowhere near this level yet (Spinato et al., 2009).

Detailed measurements of failure rates from offshore WTs have not yet been accumulated in statistically significant numbers in the public domain, therefore the available literature on WT reliability focused essentially on publicly available onshore data. WTs constitute a highly specialized technology and because of the commercial relevance of their failure data, due

to the important capital investment, and therefore risk, of their installation, operators and manufacturers are reluctant to disclose data about reliability or failure patterns. As a result the sources of information are restricted to a few publicly available databases, although there is a strong argument for WT operators to end this restrictive practice in aid of improving economic performance.

Whereas the standardisation of data collection practices is well established in the oil and gas industry (ISO 14224:2006), the wind industry has not yet standardised its methods for reliability data collection. However, an early wind industry reliability study, Wissenschaftlichen Mess und Evaluierungsprogramm database (WMEP) in Germany, developed a prototype data collection system described in (Faulstich et al., 2008). Based on WMEP and other work, the EU FP7 ReliaWind Consortium (Wilkinson, 2011) further developed a standard approach to WT taxonomy and data collection, catering specifically for larger WFs and making use of both automatic but filtered SCADA data and maintainers' logs. Understanding the WT failure rates and downtimes is difficult not only because of the considerable range of designs and sizes that are now in service worldwide but also since studies are conducted independently under various operating conditions in different countries (Pinar Pérez et al., 2013). It should be noted that the standardisation of WT taxonomy and data collection is of paramount importance to facilitate the exchange of information between parties and to ensure that data can be compared in a useful engineering and management way.

Figure 2.1 summarises the analysis of reliability data from three large surveys of European onshore WTs over 13 years. Failure and downtime data have been categorised by WT subassembly. The WMEP (Hahn et al., 2007), the Landwirtschaftskammer (LWK) (Eggersglüß, 1995-2004) and the Swedish (Ribrant and Bertling, 2007) surveys provide large datasets of

failure rate and downtime data which are remarkably similar and give valuable insights into the reliability of the various WT drive train subassemblies.
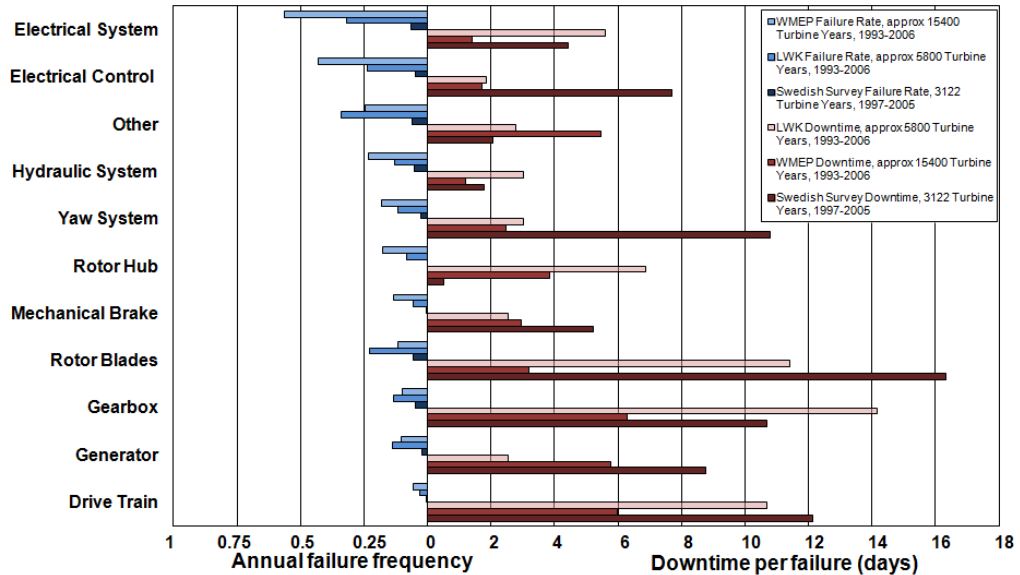
Figure 2.1: Failure rate and downtime results for onshore WTs from three large public domain reliability surveys (Ribrant and Bertling, 2007; Tavner et al., 2010).

This data highlights that the highest failure rate subassemblies onshore do not necessarily cause the most downtime. Whilst electrical subassemblies appear to have higher failure rates and shorter downtimes, mechanical subassemblies, including blades, gearbox and generator components, tend to have relatively low failure rates but the longest downtimes. Similar results have been obtained by Pinar Pérez et al. (2013) who brought together and compared data from a selection of major reliability studies in the literature. From the failure rates the long downtime of the mechanical subassemblies is clearly not due to their intrinsic design weakness but rather the complex logistical and technical repair procedures in the field. It may result from the acquisition time for the spare part, i.e. supply chain, and for the required maintenance equipment. This will be aggravated particularly offshore where special lifting equipment and vessels are required and weather conditions

have to be considered. Particularly, the gearbox exhibits one of the highest amounts of downtime per failure among all the onshore WT subassemblies and it is the most critical for WT availability. Also, the replacement of WT major components, such as the gearbox, is responsible for 80% of the cost of corrective maintenance (Besnard, 2013). This suggests that drive train sub-assemblies such as the generator and gearbox warrant the most attention.

These datasets have some important limitations. Data are taken from mixed and changing WT populations. Many of the turbines are old and some of them may be in the wear out phase of the bath tub curve, meaning that they start to deteriorate to such a degree that they have reached the end of their useful life. This phase is characterized by a rapidly increasing failure rate with time. Also, the majority of turbines are much lower power than modern turbines and use dated technologies. The more recent ReliaWind study (Wilkinson et al., 2010) attempted to address these limitations by considering only turbines that met the following requirements: rating greater than or equal to 850 kW, variable speed, pitch regulated and operating for a minimum of two years; WF with at least 15 turbines. Figure 2.2 and Figure 2.3 show the results of the ReliaWind study, which broke the turbine into a detailed taxonomy of subsystems and subassemblies to identify critical areas of interest from >4000 onshore WTyears. It should be noted that, unlike the previous data shown in Figure 2.1, for reasons of confidentiality the published ReliaWind results do not show the actual failure rate and downtime, only the percentage distribution. In spite of the diverse technologies and power ratings, the ReliaWind findings are broadly comparable with the WMEP, LWK and the Swedish surveys and the same failure rate trend emerges. However, the downtime trend shows much greater emphasis on the rotor and power modules because it is believed these newer variable speed WTs have not yet experienced major gearbox, generator or blade failures to date in service (Tavner, 2012).
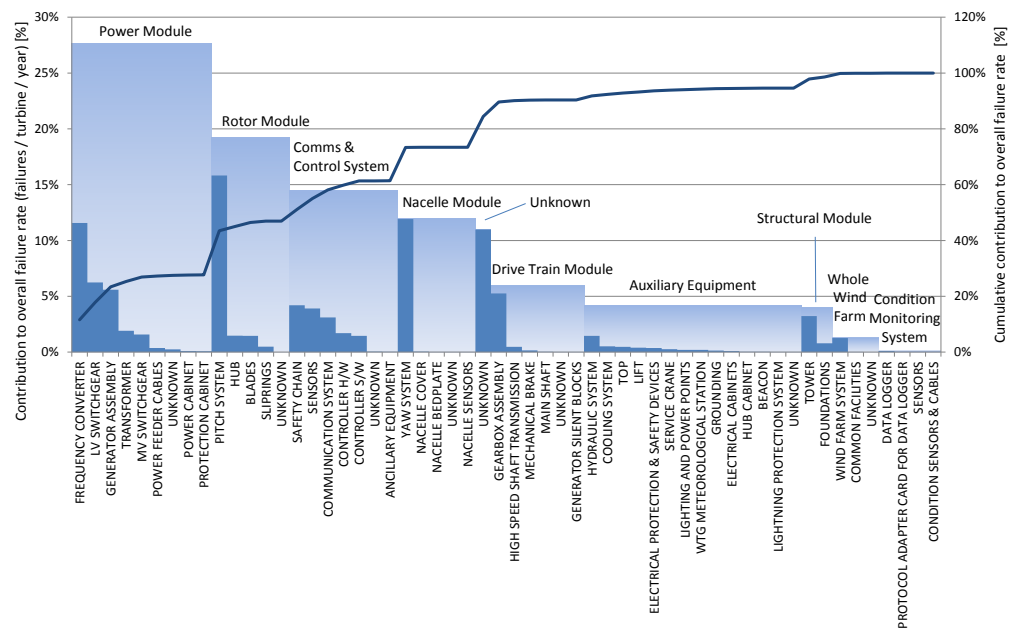
Figure 2.2: Distribution of normalised failure rate by sub-system and subassembly for WTs of multiple manufacturers from the ReliaWind survey (Wilkinson et al., 2010).
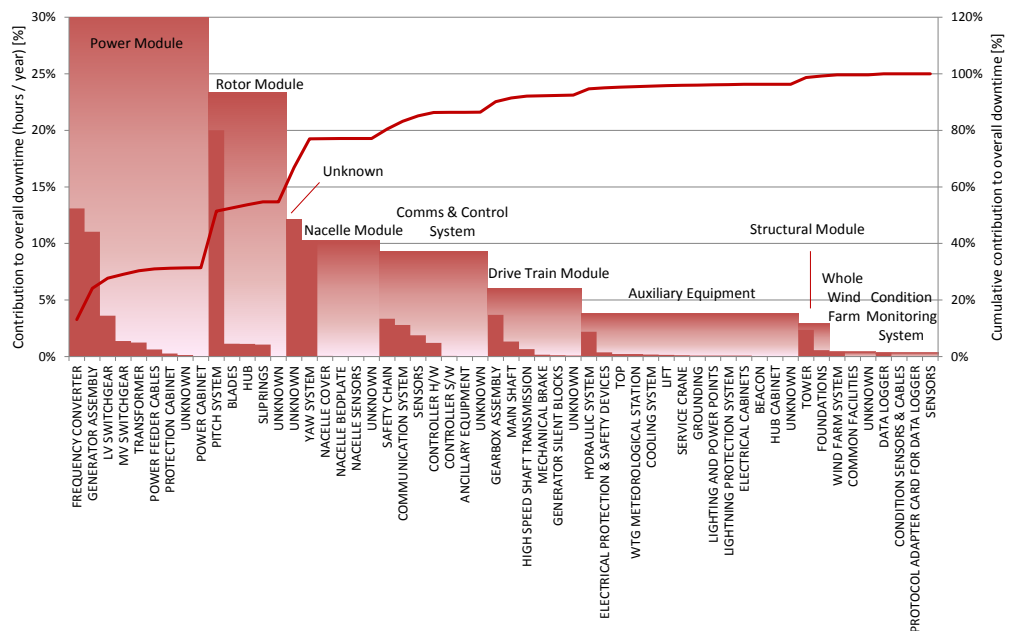
Figure 2.3: Distribution of normalised downtime by sub-system and subassembly for WTs of multiple manufacturers from the ReliaWind survey (Wilkinson et al., 2010).

23

A recent study (Faulstich et al., 2011) has shown that onshore 75% of WT failures are responsible for only 5% of the downtime, whereas only 25% of failures cause 95% of downtime. Downtime onshore is dominated by a few large faults, many associated with gearboxes, generators and blades, requiring complex and costly repair procedures. The 75% of faults causing 5% of the downtime are mostly associated with electrical faults, often caused by the system tripping, which, in the majority of cases in the onshore environment, are relatively easy to fix via remote or local resets. However, as WTs go offshore limited accessibility, longer waiting, travel and work times will amplify the influence of the 75% short duration failures on offshore WT availability. Local resets will carry high costs and difficult access conditions that are likely to significantly increase the downtime contribution of these subassemblies (Tavner et al., 2010).

As mentioned, very little field data is still publicly available for offshore WFs, although there are a number of reports published from early publicly funded projects in Europe (Feng et al., 2010). Crabtree (2012) carried out a reliability analysis of 3 years of available data from Egmond aan Zee offshore WF in the Netherlands (NoordzeeWind, 2007-2009). The WF consists of 36 Vestas V90-3MW WTs situated 10-18 km offshore and in 17-23 m water depth in the North Sea. Operational reports, available for 2007 to 2009, gave the number of stops resulting from 13 subassemblies or tasks, representing 108 WTyears of data. The results are shown in Figure 2.4 in the same format as Figure 2.1. It should be noted that, in this case, stop and not failure frequency was recorded. Direct comparison cannot be made between the onshore and offshore data sets, Figure 2.1 and Figure 2.4 respectively, as stops and failures are different concepts. However, the overall distribution is largely similar with subassemblies with high stop and failure rates not always being the worst causes of downtime. The control system dominates the number of stops, 36%, but caused only 9.5% of the total downtime. Conversely, the gearbox and generator respectively contributed only 6.7%

and 2.8% of total stops but 55% and 15% respectively of the downtime. The average energy lost per turbine per year demonstrates similar trends to the downtime (Crabtree, 2012).
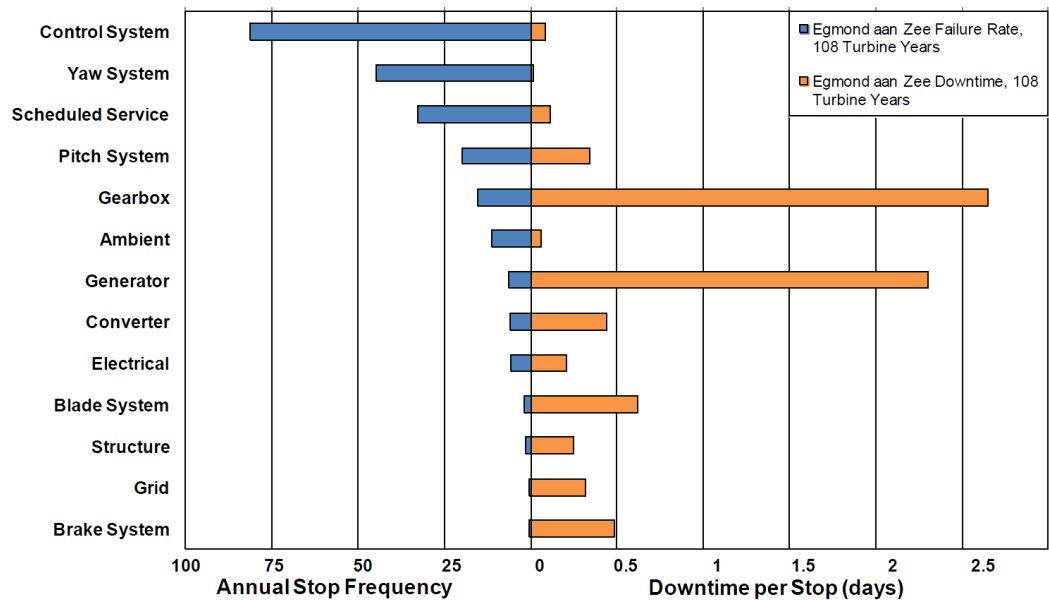
Figure 2.4: Stop rate and downtime data from Egmond aan Zee WF over 3 years (Crabtree, 2012).

For large, remote WFs to become cost effective improving WT availability is essential and requires the adoption of a number of design and operational measures, for example the choice of the most effective turbine architecture, the installation of effective CM and the application of appropriate O&M programs. Emphasis should be placed on avoiding large maintenance events that require deploying expensive and specialized equipment. However, the most important measure will be to improve the intrinsic reliability of the turbines used, achievable only through close collaboration between manufacturers, operators and research institutes, and the development of a standardised methodology for reliability data collection and analysis (Feng et al., 2010).

2.2.1. Wind versus Tidal Stream Turbine Reliability

The focus of this Thesis is WT reliability, however the Author also had the chance previously to analyse tidal stream device (TSD) reliability (Zappalá, 2010). Considering the strong architectural and technical similarities between the power generation equipment of wind and tidal turbines, an interesting comparison of their reliability has been proposed. This section is based on a publication in the Proceedings of the Institution of Mechanical Engineers, Part O: Journal of Risk and Reliability (Delorm et al., 2012), in which the Author has been involved.

A wide range of TSDs are currently in development, several of them are still at the stage of prototype or part-scale model deployment. Since extraction of tidal stream energy is a new technology, the proposed different concepts of energy converting devices present a significant uncertainty associated with the prediction of their performance. Permanently installed at selected tidal sites, TSDs may endure extreme climatic, current, and wave load conditions, and their mechanical and electrical control systems are complex. Therefore their reliability and survivability will be an engineering challenge. Due to the level of maturity of this emerging technology, there are almost no data to estimate average failures rate of the tidal turbine components. Data on failure rates is either not available due to sparse field experience or is kept confidential by the industry to secure competitive advantages.

The prediction of the prospective reliability of TSDs is a key challenge in order to develop technically and economically viable energy devices. A framework for the assessment of the reliability and the availability of competing TSDs, which could represent a valuable tool in the definition of the most suitable architecture for future full scale profitable installation, has been proposed, further details are available in Delorm et al. (2012). Historical reliability data from similarly rated WTs and other relevant marine

databases were used to populate the devised reliability models. Four horizontal-axis devices, shown in Figure 2.5, all rated 1-2 MW, with taxonomies similar to WTs, have been analysed and compared:

- TSD1: floating tethered, semi-submerged deep-water application, single-axis turbine, fixed pitch blades, induction generator, rated power 1.2 MW;

- TSD2: sea-bed pile-mounted, shallow-water application, twin-axis turbines, variable pitch blades, induction generators, rated power 2 x 0.6MW = 1.2MW;

- TSD3: sea-bed bottom-mounted, gravity base, shallow or deep water application, single-axis ducted turbine, fixed pitch blades, permanent magnet generator, rated power 1.0MW;

- TSD4: floating tethered, deep-water application, twin-axis turbines, fixed pitch blades, permanent magnet generators, rated power 2 x 0.6MW = 1.2MW.
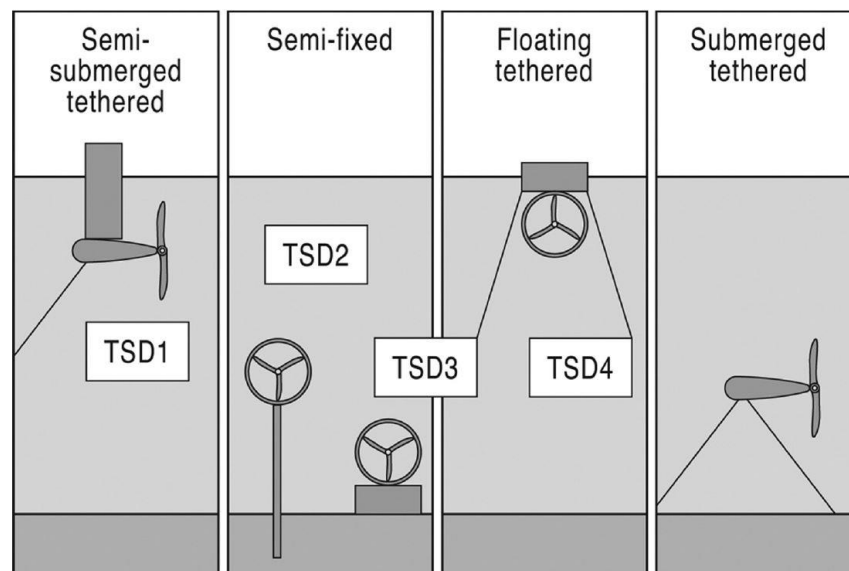
Figure 2.5: Horizontal-axis TSDs chosen for reliability comparison (Delorm et al., 2012).

The predicted reliability values obtained for the four devices have been interestingly compared with measured reliabilities of onshore WTs of similar

size (Spinato et al., 2009), as shown in Figure 2.6. The similarities of a large number of subassemblies used in the power trains of these two technologies allow this comparison to be made when the turbines operate at similar power (Val, 2009).
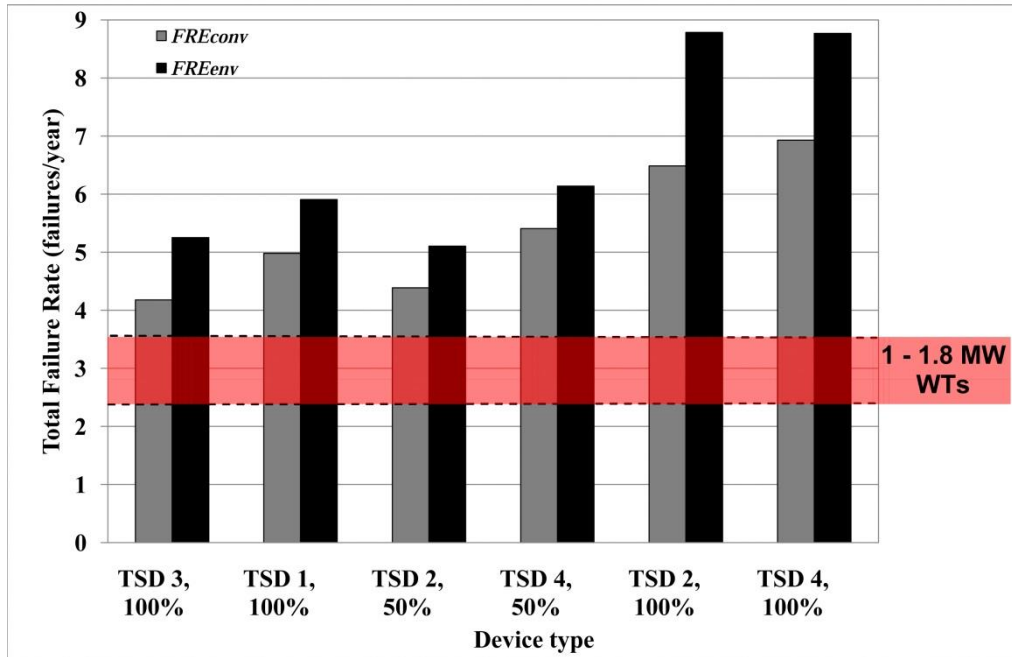
Figure 2.6: Comparison of predicted TSD & WT failure rates. FRE_{con} represents the TSD conservative failure rate estimate without adjustment of the surrogate data and FRE_{env} represents the TSD failure rate estimate with the surrogate data adjusted for the tidal environmental conditions (Delorm et al., 2012).

The horizontal band in Figure 2.6 represents the range of measured failure rates of onshore WTs of rating similar to the TSDs investigated according to (Spinato et al., 2009). The predicted failure rates for the four devices show that they are less reliable than onshore WTs of similar power output: ranging from 150% to 200% of WT failure rates. Moreover, the failure rates increase with TSD complexity. With these predictions, few devices can expect to survive more than a year in the water. The extremely high values of the predicted failure rates for the four devices would be unacceptable for a commercial device. This is to be expected, bearing in mind that the TSD

technology is in its infancy and operating in a harsher environment, but suggests that these predicted TSD failure rates are representative and that the industry either needs to reduce them in some radical way or provide more accessible methods of repair.

It should also be noted that, similarly to offshore WTs, tidal turbines work under very different environmental and operational conditions to onshore WTs. This partially controls the lower failure rates of WTs, shown in Figure 2.6, which can be attended for maintenance at any time as they are onshore, compared to tidal devices for which the shortest practical maintenance interval is likely to be one year, due to the offshore subsea location (Wolfram, 2006). This suggests that for TSDs the concept of annual maintenance is simply untenable without improvement of the device failure rate and also emphasises the need in tidal devices for effective CMS once failure rates have been improved.

2.3. Wind Turbine Monitoring Systems

The need for successfully detecting incipient faults before they develop into serious failures, to increase availability and lower cost of energy, has led to the development of a large number of WT monitoring systems. As the wind industry develops these monitoring systems are slowly being integrated together.

As described in Tavner (2012), modern WTs are equipped with monitoring systems which allow the active remote control of their functions. The WT monitoring may include a variety of systems as follows:

1. *Supervisory Control & Data Acquisition (SCADA) system*, to provide low resolution monitoring to supervise the WT operation and provide a channel for data and alarms from the WT. The status of the WT and its subassemblies is assessed using sensors

fitted to the WT which measure meteorological and turbine operating information at a low sample rate, usually at 10 minutes interval in the WT controller. SCADA is a valuable low-cost monitoring system, integrating cheap, high-volume measurement, information and communication technology. Data is used to control the WT and transmitted to a central database for large WT original equipment manufacturers (OEM), however WF operators rarely use SCADA to monitor WT & WF performance. A recent trend in wind project management is to tie the SCADA data into centralized monitoring centres, operated by either the turbine manufacturer or a service provider. This arrangement can provide 24/7 coverage for multiple projects distributed over several time zones. The volume of data from many installations in varied conditions provides better visibility of recurrent problem causes and a synergistic sharing of information. A survey of the SCADA systems available to the wind industry is given in Chen et al. (2014), in which the Author has been involved. A great benefit of SCADA is that it gives an overview of the whole WT by providing comprehensive signal information, historical alarms and detailed fault logs, as well as environmental and operational conditions. The main weaknesses of SCADA are that the large volume of data generated requires considerable analysis for on-line interpretation and that the low data rate does not allow the depth of analysis usually associated with accurate diagnosis. Potentially SCADA alarms can help a turbine operator to understand the WT and key components status, but in a large WF, these alarms are currently too frequent for rational analysis. Their added values could be explored in more detail. Recent researches (Chen et al., 2013; Gray and Watson, 2010; Zaher et al., 2009) have shown how rigorous analysis of the information

collected by SCADA systems can provide long-term fault detection, diagnosis and prognosis for the main WT subassemblies, such as the gearbox, the converter and the pitch system. Simple signal algorithms to prevent false alarms have been developed (Feng et al., 2013; Qiu et al., 2012), although the techniques need further verification. The implementation of the proposed techniques in the field would give the operators sufficient time to make more informed decisions regarding the maintenance of their machines.

2. *Structural Health Monitoring (SHM)*, to provide low-resolution signals for the monitoring of key items of the WT structure, tower and foundations. These are particularly important offshore where the structures are subjected to strong effects from the sea, wind and seabed. Structural faults are slow to develop and do not need continuous monitoring. SHM systems are frequently installed below the nacelle on large WTs, i.e. >2 MW. Low frequency sampling signals, below 5 Hz, are recorded from accelerometers or similar low frequency transducers to determine the structural integrity of the WT tower and foundation for faults driven by blade-passing frequencies, wind gusts and wave slam. A detailed review of new emerging techniques currently being researched in the SHM field is provided in (Ciang et al., 2008).

3. *Condition Monitoring System (CMS)*, to provide high-resolution monitoring of WT high-risk subassemblies for the diagnosis and prognosis of faults. Included in this area are Blade Monitoring Systems (BMS), aimed at the early detection of blade defects. In this Thesis, the attention will be focused on the investigation of novel techniques for WT CMSs. For this reason, the next section gives a detailed review of the state of the art of CMSs in wind machines.

2.4. CMS State of Art

Condition monitoring focuses on remotely measuring critical indicators of WT component health and performance, with the objective of identifying incipient failures before catastrophic damage occurs. Failures of the major components of the WT drive train are expensive due to the high costs for the spare parts, the logistic and maintenance equipment, and energy production losses. A comprehensive on-line monitoring program provides diagnostic information on the health of the turbine subsystems and alerts the maintenance staff to trends that may be developing into failures or critical malfunctions. This information can be used to schedule maintenance tasks or repairs before the problem escalates and results in a major failure or consequential damage with resultant downtime and lost revenue. Thus necessary actions can be planned in time and need not be taken immediately; this factor is of special importance for offshore plants where bad weather conditions can prevent any repair actions for several weeks. Many faults can be detected while the defective component is still operational. In some cases, remedial action can be planned to mitigate the problem. In other cases, measures can be implemented to track the problem's progression. In the worst case of an impending major failure, CM can assist maintenance staff in logistics planning to optimize manpower and equipment usage and to minimize the cost of a repair or replacement. In this condition, both the cost of the maintenance activity itself and the costs for production losses may be reduced.

CM has become increasingly important in larger turbines owing to the greater cost of the components and greater concern about their reliability. Furthermore, it represents an essential technology for offshore turbines, owing to their projected size, limited accessibility and consequent need for greater reliability. The main advantages and benefits arising from applying CM are summarised in Table 2.1 (Hameed et al., 2009).

The processes necessary for a successful CM process are:

- Detection: the essential knowledge that a fault condition exists in a machinery component and ideally its location. Without this, no preventive action can be taken to avoid possible system failure.
- Diagnosis: the determination of the nature of the fault, including its more precise location. This knowledge can be used to decide the severity of the fault and what preventive or remedial action needs to be taken (if any) ;
- Prognosis: the forecast or prediction of the remaining life or time before failure. Based on this, the most efficient and effective action to remove the fault can be planned. Prognosis has the largest potential payoff of all CM technologies, especially for offshore turbines.
- Maintenance action: repairs or replacements action to remove the cause of the fault.

Table 2.1: Characteristics of CMSs, adapted from (Hameed et al., 2009).

Characteristics	Advantages	Benefits
Early warning	Avoid breakdowns	Avoid repair costs
	Better planning of maintenance	Minimise downtime
Identification of problem	Right service at the right time	Prolonged lifetime
	Minimizing unnecessary replacements	Lowered maintenance costs
	Problems resolved before the time of guarantee expires	Quality-controlled operations during time of guarantee
Continuous monitoring	Constant information that the wind power system is working	Security. Less stress

The level of detail required for failure prevention depends very much on the type of component, its perceived value and the consequences of failure. For the main and most expensive WT subassemblies, such as the gearbox, the generator and the blades, simple fault detection is not sufficient, as their cost is usual too high to justify total replacement, and some form of diagnosis is required. Diagnosis also allows scope for prognosis: either to predict the possibility of progression from a non-critical fault to a critical fault, indicating the need to closely monitor the fault progression, or to predict the time to failure, allowing scheduling of repairs.

2.4.1. Review of CMS Techniques

The on-line monitoring and fault detection are relatively new concepts in the wind industry and are flourishing on a rapid scale. Today it is state of the art for modern onshore and offshore WTs to be equipped with some form of CMS. Measurements are recorded from sensors and different methodologies and algorithms have been developed to analyse the data with the aim of monitoring the WT performance and identifying characteristic fault indicators.

The poor early reliabilities for gearbox and drive train components have led to an emphasis in WT CM on drive train components. CM is believed to have entered the WT market about twenty years ago as a result of a series of catastrophic gearbox failures in onshore turbines, which led to insurers demanding that WT manufacturers take remedial action by utilising CM technology, already applied to other rotating machinery. However, the more recent information on WT reliability and downtime, shown in Figure 2.2 and Figure 2.3, suggests that the target for CM should be widened from the drive train towards WT electrical and control systems and blades.

In recent years, efforts have been made to develop efficient and cost-effective CM techniques and signal processing methods for WTs. There have

been several reviews on WT CM in literature, including (Amirat et al., 2007; Garcia Marquez et al., 2012; Hameed et al., 2009; Hyers et al., 2006; Lu et al., 2009; Wiggelinkhuizen et al., 2008; Wilkinson et al., 2007; Yang et al., 2014), discussing the main CM techniques, the signal processing methods proposed for fault detection and diagnosis and their applications to wind power.

For advanced CM techniques, signal processing techniques are used to extract features of interest. The selection of appropriate signal processing and data analysis techniques is crucial to WT CM success. If the fault related characteristics can be correctly extracted using these techniques, fault growth can be assessed by observing characteristic variations, and these characteristics are also important clues for fault diagnosis.

The most recent reviews by Yang et al. (2014) and Garcia Marquez et al. (2012) provide a particularly insightful and detailed summary of the state of the art in WT CMSs while also providing a comprehensive explanation of the new emerging techniques currently being researched.

The following monitoring techniques, available from different applications, which are possibly applicable for WTs, have been identified:

1. Vibration analysis
2. Oil analysis
3. Strain measurements
4. Thermography
5. Acoustic emissions
6. Electrical signals

Among these different techniques, vibration analysis and oil monitoring are the most predominantly used for WT applications due to their established successes in other industries.

Vibration analysis is a low-cost and a well-proven monitoring technology typically used to monitor the condition of WT rotating components, i.e. the drive train. Vibration techniques were the first to be used in WT CMS. The principle is based on two basic facts (Randall, 2011):

1. Each component of the drive train has a natural vibration frequency and its amplitude will remain constant under normal conditions, although varying with drive train speed.
2. The vibration signature will change if a component is deteriorating and the changes will depend on the failure mode.

The type of sensors used essentially depends on the frequency range of interest and the signal level involved. A variety of techniques have been used including low-frequency accelerometers for the main bearings and higher-frequency accelerometers for the gearbox and generator bearings and in some cases proximeters. By far the most common transducer in use today is the piezoelectric accelerometer, which is applicable to a broad range of frequencies, is inexpensive, robust, and available in a wide range of sizes and configurations.

Principles for vibration analysis are presented in detail in McGowin et al. (2006). Signal analysis usually requires specialized knowledge. Almost all of the commonly used algorithms can be classified into two categories: time and frequency domains. Time domain analysis focuses principally on statistical characteristics of vibration signal such as peak level, standard deviation, skewness, kurtosis, and crest factor. Frequency domain analysis uses Fourier methods, usually in the form of a fast Fourier transform (FFT) algorithm, to transform the time domain signal to the frequency domain. This is the most popular processing technique for vibration analysis and it is discussed in more detail in the next chapter. Further analysis is usually carried out conventionally using vibration amplitude and power spectra. The

advantage of frequency domain analysis over time domain analysis is its ability to easily identify and isolate certain frequency component of interest.

Applying vibration based CM to WTs presents a few unique challenges. WTs are variable load and speed systems operating under highly dynamic conditions, usually remote from technical support. This results in CM signals that are dependent not only on component integrity but also on the operating conditions. One limitation of the conventional fast FFT analysis is its inability to handle non-stationary waveform signals that may not yield accurate and clear component features. To overcome the problems of the conventional FFT-based techniques and find improved solutions for WT CM, a number of advanced signal processing methods, including wavelet transforms, that enable to detect defects whose vibration signature is not cyclic, time–frequency analysis, bi- or tri-spectrum and artificial intelligence techniques have been researched recently (Amirat et al., 2009; Garcia Marquez et al., 2012; Hameed et al., 2009; Yang et al., 2014; Yang et al., 2010; Yang et al., 2009b; Zaher et al., 2009). However, the interpretation of the results is more complicated for direct analysis than FFT techniques. Moreover, most new techniques are unsuitable for an on-line CM use because they are computationally intensive and have not been demonstrated yet in operating WTs.

Oil analysis is used to determine the chemical properties and content of oil coolant or lubricant with two purposes: safeguarding the oil quality and safeguarding the components involved. Although still expensive, on-line debris detection in lubricant oil is one of the most promising techniques for use in WT CM. Oil analysis focuses on one of the most critical WT components, the gearbox. Gear wheels and bearings deterioration depends mainly on the lubricant quality, i.e. particle contamination and properties of the oil and additives used to improve the performance of the oil. Oil monitoring can help detect lubricant, gear and bearing failures and is an

important factor in achieving maximum service life for WT gearboxes. Oil analysis is discussed in detail in McGowin et al. (2006). On-line oil analysis is gradually becoming more important with several on-going pilot projects.

Crucial to the value of oil debris detection is the length of the warning that it can give of impending failure, giving time to arrange for inspection and maintenance (Tavner, 2012). Little or no vibration may be evident while faults are developing, but analysis of the oil can provide early warnings. However, oil debris detection cannot locate a fault, except by distinguishing between the types of debris produced. The combined use of vibration and oil analysis, to cover a broader range of potential failures and to increase the credibility of the CM results, could be a key to WT drive train monitoring.

Strain measurements by fibre-optic sensors are proving a valuable technique for measuring blade-root bending moments as an input to advanced pitch controllers and can be used to monitor WT blades. They have been demonstrated in operation, however they are still too expensive and improvements in costs and reliability are expected. The use of mechanical strain gauges can be very useful for lifetime forecasting and protecting against high stress levels, especially in the blades. However, mechanical strain gauges are not robust on a long term, as they are prone to failure under impact and fatigue load. Developments are still necessary for the improvement of instrumentation and sensors robustness as well as for reliable fault detection algorithms.

Thermography is often used for monitoring electronic and electric components and identifying failure. Infrared thermography is a technique used to capture thermal images of components. Every object emits infrared radiation according to its temperature and its emissivity. The radiation is captured by a thermographic camera. The technique can be applied to equipment from time to time but should be done when the equipment is fully loaded, and often involves visual interpretation of hot spots that arise due to

bad contact or a system fault. At present the technique is not particularly well-established for on-line CM, but cameras and diagnostic software that are suitable for on-line process monitoring are starting to become available.

Acoustic emissions could be helpful for detecting drive train, blade or tower defects. Rapid release of strain energy takes place and elastic waves are generated when the structure of a metal is altered, and this can be analysed by acoustic emissions. Acoustic monitoring has some similarities with vibration monitoring but also a principal difference. Whereas vibration sensors are mounted on the component involved, so as to detect movement, the acoustic sensors are attached to the component by flexible glue with low attenuation. For vibration analysis the frequencies related to the rotational speeds of the components are of interest. For acoustic emission a wider bandwidth of higher frequencies is considered which can give an indication of starting defects. These sensors have lately gained much more attention in order to detect early faults and are successfully applied for monitoring bearing and gearboxes. Acoustic emission is considered more robust for low-speed operation of WT compared to the classic vibration based methods. However, this technique is still too expensive due to the data acquisition costs.

Electrical signals have been widely used for CM of rotating electric machines and their coupled drive trains (Tavner et al., 2008a) but have not been used in WTs because of lack of industry experience. Voltage, current and power measurements, used to control the generator speed and excitation, represent the newest potential source of CM information for WTs. The difficulty with these electrical signals is that they are very rich in harmonic electrical information, which must be accurately understood if diagnosis is to be performed with confidence (Yang et al., 2009b). These techniques are at the moment confined to research related activities but there is significant potential for applying them successfully in the field (Djurović et al., 2012a).

Work by Watson et al. (2010) showed the potentiality of the wavelet transform in detecting WT mechanical and electrical faults by electrical power analysis but this technique still has strong practical limitations because of its intensive calculation and consequent inefficiency in dealing with lengthy WT signals.

Some of the more recent emerging CM techniques described in the research literature (Garcia Marquez et al., 2012; Yang et al., 2014) include ultrasonic testing, potentially effective for detecting early WT blade or tower defects, shaft torque and torsional vibration measurements, for main shaft and gearbox monitoring, and shock pulse method, an on-line approach to detecting WT bearing faults.

To date, little work has been done in the area of prognosis models. Much of the research in this area is generic and being conducted by the aerospace community for civil and military aviation. Some specific research will be required to apply the principles of prognosis to the wind power industry (Hyers et al., 2006). A model for estimating the residual lifetime of generator bearings based on CMS data has been recently proposed in Fischer (2012).

2.4.2. Commercially Available CMSs

WT CMS application was requested by insurance companies in Europe, such as Germanischer Lloyd (2007), in the late 1990s following a large number of claims triggered by catastrophic gearbox failures (Tavner, 2012). As the drive train is not only one of the most valuable WT subsystems but also one of the most trouble prone, German insurers introduced this clause as a cost deterrent to encourage an improvement in its operating life.

A typical CMS should feature:

- Physical Measurement: sensors measure the machine signals, analogue or pulse signals from sensors are then filtered and converted to digital information;

- Data Acquisition System (DAS): data is transmitted from sensors to processing unit;

- Feature Extraction: characteristic information is extracted from raw sensor data;

- Pattern Classification: defect type and severity level are diagnosed;

- Life Prediction: remaining service life of the monitored component is prognosticated.

Today, a number of commercial certified WT CMSs are available to the wind industry and they are largely based upon the successful experience of monitoring conventional rotating machines which is beginning to adapt to the WT environment. A survey of the commercially available WT CMSs, conducted by the UK SUPERGEN Wind Energy Technologies Consortium, is given in Crabtree et al. (2014), to which the Author has contributed. This survey provides an up to date insight, at the time of writing, into the current state of the art of CM and shows the range of systems currently available to WT manufacturers and operators. The document contains information gathered over several years through interaction with monitoring system and turbine manufacturers and includes information obtained from various product brochures, technical documents and personal interaction with sales and technical personnel at the European Wind Energy Association Conferences from 2008 to 2014. The detailed table from the SUPERGEN Wind survey, listing the up to date commercially available CMSs for WTs, from which this summary is derived, is provided in the Appendix. The systems are grouped by monitoring technology and then alphabetically by product name.

The survey shows that the large majority of CMSs currently in use on operational WTs are based on vibration monitoring of the drive train, at a typical sampling rate up to 20 kHz, with special focus on main bearing, gear teeth and bearings. Figure 2.7 provides an example setup for a vibration-based WT CMS (Doner, 2009).
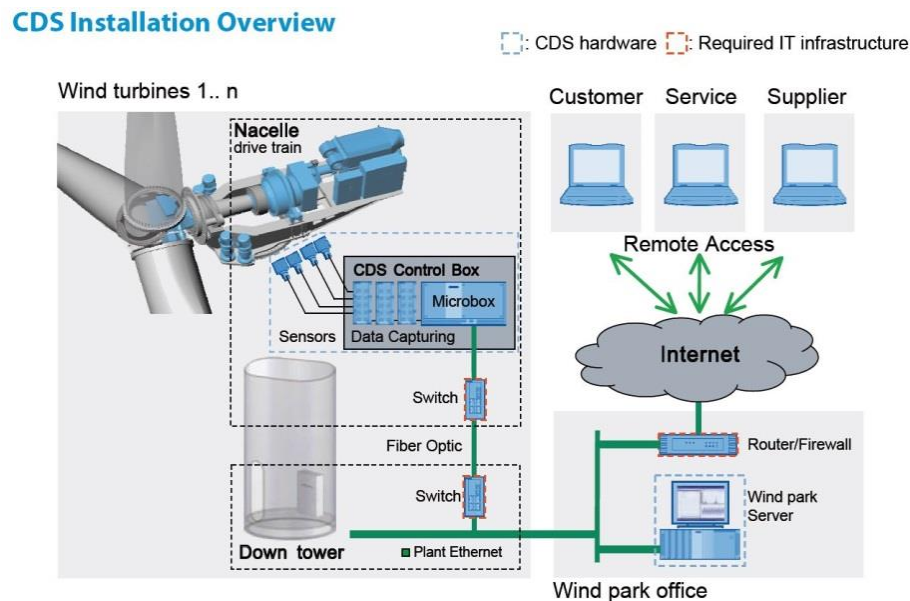
Figure 2.7: Example setup of a WT CMS, from the Winergy CDS (Doner, 2009).

The system consists of several sensors and a DAS, referred to as the condition diagnostics system (CDS) enclosure, which are located in the turbine nacelle, and a data server, CDS server, located at the wind park or a remote monitoring centre. Typically, the DAS has a channel for the shaft rotational speed signal, which is either measured by a tachometer dedicated to the CM system or supplied by the turbine controller. The communication between the DAS and the data server located at the wind park can be through Ethernet or fibre optic cables. If no data server is set up at the local wind park, the DAS normally can be configured to wirelessly transmit the test data to a server located in the remote monitoring centre, which could be anywhere around the globe. The data server normally hosts the CM software

package, which is a platform for reviewing and analysing the data, presenting the CM results, and streamlining both raw and processed data into a CM database. One wind park, typically consisting of hundreds of turbines, can be monitored by one CM software package.

Among vibration-based CM systems, the main differences are the number of sensors, measurement locations, and analysis algorithms, since almost all systems use standard accelerometers as the main physical measurement device. The typical configuration of the sensors along the WT drive train is shown in Figure 2.8, which refers to the Gram & Juhl TCM (Turbine Condition Monitoring) system architecture (Gram & Juhl A/S, 2010). Sensors are mounted on the bearing housing or gear case to detect characteristic vibration signatures for each component. The signature for each gear mesh or bearing is unique and depends on the geometry, load, and speed of the components.
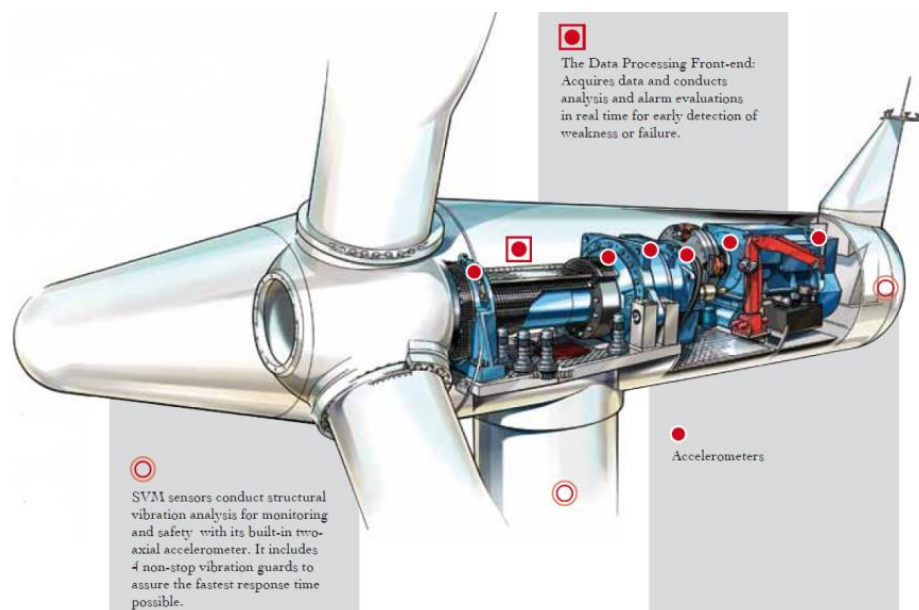
Figure 2.8: Typical sensor positions (Gram & Juhl A/S, 2010).

According to the survey, the most popular signal processing technique for the vibration monitoring of the WT drive train is the traditional FFT

analysis of the high frequency data to detect the fault-specific frequencies. Frequently, time domain parameters are used to monitor the trend of overall vibration level over time. To minimize data transmission, CMSs analyse data and transmit trends to the system microprocessor continuously, whereas spectral analysis occurs only when settings detect an unusual condition. One triggering mechanism, such as time interval-based or vibration level-based, can be set up in the time domain parameter overall trending process. Whenever it triggers, a discrete frequency analysis snapshot can be taken. Based on these snapshots, detailed examinations on the component health can be conducted. The amplitude of characteristic frequencies for gears, e.g., meshing frequency, and bearings, e.g., ball passing frequency, can also be trended over time for detecting potential failures. Such a strategy mitigates the burden of data transmission from the WT; however, it increases the risks of losing raw historic data because of limited CMS memory size.

In order to acquire data that is directly comparable between each point and, importantly, to allow spectra to be recorded in apparently stationary conditions, a number of commercial CMSs, such as the SKF WindCon 3.0, can be configured to collect the vibration spectra within limited, pre-defined speed and power ranges. This is an important point to note when using traditional signal processing methods such as the FFT which require stationary signals within the analysis time window in order to obtain a clear result.

All the vibration-based CMSs surveyed have the capability to carry out some form of automatic diagnostic procedure. The majority of them are capable of producing alarms based either on the magnitude of spectral peaks, overall vibration levels or, in some cases, rates of oil debris particle generation. However, results of automatic diagnosis must often be confirmed by vibration experts and component inspection. The level of confidence in these alarms is currently low but increases as monitoring engineers become

more familiar with systems and turbines and as analysis techniques develop. Automatic diagnosis and prognosis are recent technologies which still require further investigation.

Only 6 out of the 27 vibration-based CMSs surveyed state that they are also able to monitor the level of debris particles in the gearbox coolant and lubrication oil system to enhance their CM capabilities. Modern oil debris counters take a proportion of the lubrication oil stream and detect and count both ferrous and non-ferrous particles of varying sizes. The counts can be fed as on-line data to the CMS. However, it should be noted that increasing measurement detail increases the cost of the on-line instrument.

Some recent commercially available CMSs are beginning to adapt to the WT environment and to be fully integrated into existing SCADA systems using standard protocols, examples are the GE Energy ADAPT.wind, the Romax Technology InSight Intelligent Diagnostic System and the Gram & Juhl TCM. Thanks to this integration, the analysis of the systems installed on the wind energy plant can also directly consider any other signals or variables of the entire controller network, as for example current performance and operating condition, without requiring a doubling of the sensor system. The database, integrated into a single unified plant operations' view, allows a trend analysis of the condition of the machine. Recently patented condition-based turbine health monitoring systems, as the Brüel&Kjaer VibroSuite, the Romax Technology InSight Intelligent Diagnostic System and the Gram & Juhl TCM, claim to feature diagnostic and prognostic software unifying fleet wide CMS and SCADA, enabling the identification of both source and cause of the fault and the application of prognostics to establish the remaining operational life of the component.

Only three on-line blade CMSs based on strain measurement using fibre optic transducers have been surveyed. These systems may be fitted to WT retrospectively. Compared to vibration monitoring techniques, these systems

can be operated at low sampling rates as they are looking to observe changes in time domain. They are usually integrated in the WT control system but there are also some cases of integration, as an external input, into commercial available conventional vibration-based CMSs. As the blades continue to increase in cost and mass with the introduction of ever larger wind machines, there is a great deal of concern about their reliability. It is believed that the development of reliable and effective blade monitoring systems will be a key enabler for future megawatt-scale turbines.

No commercial CMS is offered for electronics beyond oversight by the SCADA system. However, the reliability of both power electronics and electronic controls is of significant concern, especially for offshore installations where deterioration may be accelerated in the harsh environment by corrosion and erosion.

2.4.3. Cost Justification

A CMS based on vibration analysis, such as the SKF WindCon 3.0, is in the range of €15,000 to €20,000 per WT for software, transducers, cabling and installation (Nilsson and Bertling, 2007), more expensive than SCADA and with less coverage. The robustness with respect to failure detection/forecasting is not yet completely demonstrated and there has been considerable debate in the industry about the true value of CMS (Tavner, 2012). The cost justification of CMS for wind power has not been as clear as for traditional fossil-fired or nuclear power plants. To date, there have been few cost evidence publications to support the claims of the CMS industry. This is no doubt the result of data confidentiality within the industry.

A cost-benefit analysis (Walford, 2006) shows that the lifetime savings derived from an early warning and the avoidance of the impending failures of the critical WT components would more than offset the lifetime cost of a CM system. Work by Besnard et al. (2010) shows results from Life-Cycle-Cost

model evaluated with probabilistic methods and sensitivity analysis to identify the economic benefit of using CMS in WTs. The results highlight that there is a high economic benefit of using CMS. The benefit is highly influenced by the reliability of the gearbox. Although the economics of deploying CM for a wind park is case dependent, some studies have shown the estimated return on assumed cost being better than 10:1 onshore, with total return on investment achieved in less than three years. These benefits will be even more dramatic if turbines are installed offshore where accessibility is a huge challenge (Sheng and Veers, 2011).

Yang et al. (2014) discuss gearbox failure costs and the cost advantages deriving from avoiding complete failure through successful WT CM for onshore and offshore individual 3 MW turbines and for an offshore WF, Scroby Sands (UK) comprising 30, 2 MW WTs. The work shows that, according to published failure rates, there is clearly a benefit in using WT CMS to eliminate gearbox failures. The figures for Scroby Sands offshore WF are particularly favourable and suggest that offshore WT CMS is essential for the avoidance of serious downtime and wasted offshore attendance. In addition, the Authors notice that the inclusion of other major subassemblies, such as generator, blades and converter, would make a significant contribution to the WT CMS financial case, as would an extension of WF working life but all depends upon the reliability of the WT CMS and the ability of the operator to make use of its indications.

The investment in CM equipment for traditional power generation plants is normally covered by savings of costs from reduced unplanned production losses. For onshore WTs unplanned production losses are relatively low. Although for offshore WTs unplanned production losses are higher, the investment costs should for an important part be paid back by reduction of maintenance cost and reduced costs of increased damage (Hameed et al., 2009). According to Tavner (2012) WT CMS can only be

justified if the system is capable of detecting a fault giving early enough warning to avoid full subassembly replacement, which is the most costly aspect of failure, and if that CMS detection and warning can be acted upon by operators and WT OEMs to allow scheduling for repairs.

A practical example of CMS cost justification is given in Giordano and Stein (2011) which describes the real-life experience of an onshore 25 turbine WF operator using the 01dB-Metravib OneProd Wind CMS to successfully detect a broken tooth on the sun gear of the planetary stage of the gearbox, a generator bearing inner ring defect and a main bearing outer ring defect. This work demonstrated how the CMS investment cost was less than 1% of the price of a current WT and the benefits coming from 17% failure detection were sufficient to payback it.

2.5. Current Limitations and Challenges of WT CMSs

Experience with CMSs in WFs to date is limited and shows that it is problematic to achieve reliable and cost-effective applications. The application of CM techniques has for decades been an integral part of asset management in other industries, and the technology has in recent years increasingly been adopted by the wind power industry. The general capabilities of the CM technology are therefore well known, but the adaptation to the wind industry has proven challenging for successful and reliable diagnostics and prognostics as they are unmanned and remote power plants. There is still insufficient knowledge among WT maintenance staff of the potential of CMSs and inadequate experience of their application to common WT faults. The main differences which characterize WT operation compared to other industries are variable speed operation and the stochastic characteristics of aerodynamic load. This makes it difficult to use traditional frequency domain signal processing techniques, such as FFT, and to develop effective algorithms for early fault detection and diagnosis, due to the non-

stationary signals involved. The majority of commercially available WT CMSs usually require experienced CM engineers able to successfully detect faults by comparing spectra at specific speeds and loads. Fault detection and diagnosis still require specialized knowledge of signal interpretation to investigate individual turbine behaviour, determine what analyses to perform and interpret the results with increased confidence. The lack of an ideal technique to analyse monitoring signals leads to frequent false alarms, which not only devaluate the WT CMS, but are also dangerous once a real fault occurs (Yang et al., 2009a).

One major limitation of the current commercially available CMSs is that very few operators make use of the alarm and the monitoring information available to manage their maintenance because of the volume and the complexity of the data. In particular, the frequent false alarms and costly specialist knowledge required for a manual interpretation of the complex vibration data, have discouraged WT operators from making a wider use of CMSs. This happens despite the fact that these systems are fitted to the majority of the large WTs (>1.5 MW) in Europe (Yang et al., 2014). Moreover, with the growth of the WT population, especially offshore, a manual examination and comparison of the CM data will be impractical unless a simplified monitoring process is introduced. The man-power costs of daily data analysis on an increasingly large WT population will be inappropriate to justify WT CM.

Most of the WT fault detection algorithms developed so far (Crabtree, 2011; Hameed et al., 2009; Hyers et al., 2006; Wiggelinkhuizen et al., 2008) requires time consuming post-processing of monitored signals, which slows down the fault detection and diagnostic process, and still a certain degree of interpretation of the results. These algorithms are generally based on single signal analysis. Diagnosis can be difficult on the basis of a single signal alone while a multi-parameter approach, based on comparison of independent

signals and able to recognise symptoms from different approaches, has shown an increased confidence in the practical applicability of these algorithms, potentially reducing the risk of false alarms (Feng et al., 2013).

Aspects of monitoring that particularly concern operators are the improvement of accuracy and reliability of diagnostic decisions, including level of severity evaluation, and the development of reliable and accurate prognostic techniques. It appears evident that cost effective and reliable CMSs would necessarily imply an increasing degree of data automation to deliver actionable recommendations in order to work effectively in the challenging offshore environment. The challenge is to achieve detection, diagnosis and prognosis as automatically as possible to reduce manpower and access costs. Current efforts in the wind CM industry are aimed at automating the data interpretation and improving the accuracy and the reliability of the diagnostic decisions, especially in the light of impending large-scale, offshore WF generation.

The incorporation of refined efficient monitoring algorithms and techniques into existing CMSs could represent a way to increase their automation, enhance their capabilities, simplify and improve the accuracy and user confidence in alarm signals. In particular, automatic processing is required to separate multiple vibration components. These algorithms could reduce the quantity of information that the WT operators must handle, providing improved detection and timely decision-making capabilities. Before being reported to the operators and asset managers, the raw data from remote CM stations would be processed and filtered by an on-line automatic acquisition system able to:

- detect incipient faults;
- diagnose their exact nature and give their location;
- ideally, provide a preliminary malfunction prognosis, through disciplined data management, sophisticated stochastic modelling and

computational intelligence, in order to schedule a repair/replacement of the component before failure.

The operator could then choose to examine a particular WT in more detail, if required, so that the costly mobilisation of diagnosis specialists could be minimised only to serious, repairable WT faults. This tool will then allow for a simpler and faster analysis of the different signals transferred by the CMS since the expert will just receive information relevant to the signals showing defects.

In summary, main advantages of automatic on-line CMSs with integrated fault detection algorithms are:

- appropriate management of WF data with a reduction of human workload, without losing accuracy in the phenomenon examination, and costs when handling high rate monitoring information flow from disparate remote locations;
- the elimination of data post-processing;
- the application of a multi-parameter approach, able to compare at the same time independent monitoring signals, such as vibration signature, oil debris content and electric signature, providing reliable and timely automatic warnings/alarms of the incipient fault;
- the improvement of accuracy and reliability of the diagnostic decisions;
- the improvement of O&M strategy management according to the automatic prioritisation of fault severity set by reliable alarms.

Finally, as shown in the SUPERGEN Wind survey (Crabtree et al., 2014), the majority of CMSs currently operate independently from the SCADA systems, therefore they do not use a lot of valuable information as operational parameters. It is then expected that the ultimate integration of autonomous CM and SCADA systems in the turbine controller will not only save costs but will also lead to more effective monitoring (Tavner, 2012).

3

Theoretical Background

3.1. Focus in this Research

In the previous chapter two main issues concerning WT CM have been raised:

1. The WT inherent physical conditions, such as rapidly varying speed and load conditions, make the CM signal analysis a complex and costly task.
2. It would be beneficial, from the perspective of WF operators, if the WT monitoring data could be analysed and interpreted automatically to support the operators identifying WT faults.

The objective of the research described in this Thesis is to address these key aspects by developing advanced automatic fault detection algorithms so that high on-line diagnostic accuracy and reliability for WT mechanical and electrical signals is achieved.

This research focuses on analysing faults on gearbox and generator which, as seen in previous Section 2.2, are among the most critical components for modern variable speed WT reliability and availability. According to Hyers et al. (2006), together they comprise both the most costly and the least reliable WT components. They have been chosen because of their significance either in downtime duration or failure rate and also because the developed algorithms could be easily adapted and implemented into existing CMSs avoiding costly extra transducers and data processing.

Direct drive WTs, with no gearbox but a specialised low-speed synchronous generator, turning at the same rotational speed as the blades, and fully rated converter, are, in recent years, showing increased market share. The major motivation for this is that by eliminating the costly and

trouble-prone gearbox, the system should prove to be more reliable. However, it has been shown that direct drive WTs do not necessarily have better reliability than geared drive turbines. The price paid by direct drive WTs for the reduction of failure rate by the elimination of the gearbox is a substantial increase in failure rate of electrical-related subassemblies (Tavner et al., 2008b; Tavner et al., 2006).

In this chapter, for each of the two WT subassemblies considered in this work, a short description of the technology is initially given followed by a discussion of the main issues concerning their failure. The theoretical basis of signal processing techniques underlying this Thesis is then introduced together with a brief review of previous WT gearbox and generator CM work from which this research originates.

3.2. WT Gearbox

The function of the WT gearbox is to convert the slow speed, high torque rotation of the rotor into the high-speed, low torque rotation of the generator, suitable for generating electricity. For machines rated between 300 kW and 5 MW, with rotor nominal speed in the range of 48 to 12 rpm, overall gear ratios of between about 1:31 and 1:125 are therefore demanded of the gearbox. Normally these large step-ups are achieved by three separate stages, the first of which is always planetary in order to achieve a sufficiently high ratio and share the high torque load across multiple contacts (Burton et al., 2011). Planetary gears are successful in WT applications, because they yield a high torque density in comparison with parallel stages. This means that they transfer more torque for the same amount of material required in the design. A corresponding weight reduction is desirable in WTs. Furthermore, the bearing loads are reduced and planetary gears are more compact. For large gear-driven WTs, most manufacturers use a three-stage design with a complex configuration as shown in the expanded view in Figure 3.1 (Sheng

and Veers, 2011). The low-speed shaft (LSS) planetary gear stage comprises three planet gears in a planet carrier coaxial with a sun gear and a ring gear. The planet gears rotate at the constant centres of the planet carrier. The low-speed input is from planet carrier driving motion via the planet gears to the sun gear. The intermediate-speed shaft (ISS) stage uses parallel helical gears as does the high-speed shaft (HSS), which is then coupled to generator drive end.
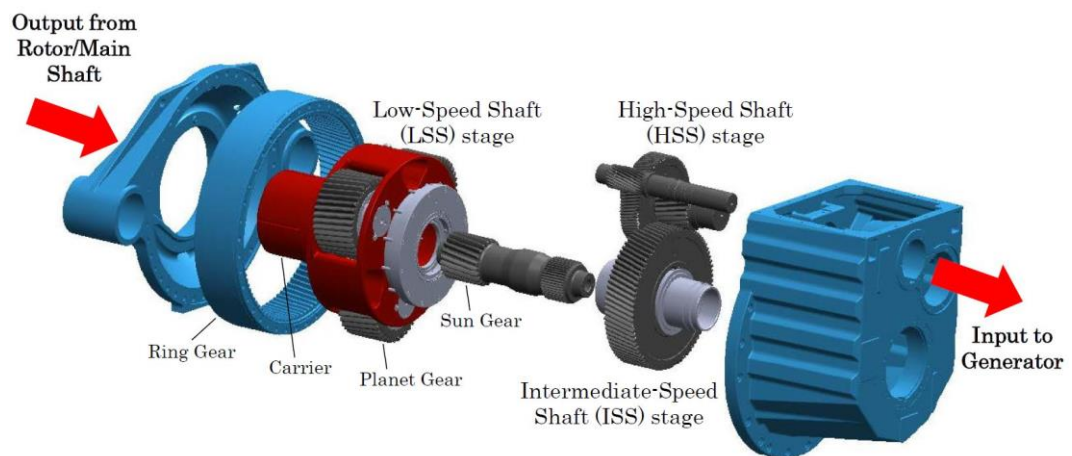
Figure 3.1: A typical WT gearbox internal components view, adapted from (Sheng and Veers, 2011).

The modern wind industry has experienced high gearbox failure rates compared to other WT subassemblies for a variety of reasons including underestimation of true operating loads during design, unexpected overloads due to unusual operating conditions, such as emergency stops, defective gearbox component design and poor maintenance. Over the last 2 decades, many lessons have been learnt by the industry to improve the reliability of gearboxes, one of the most expensive WT subassemblies. Despite reasonable adherence to internationally recognized design standards (IEC 61400-4, 2012), WT gearboxes have yet to achieve their design life goals of 20-years-plus, with most systems requiring significant repair or overhaul well before the intended life is reached. The future uncertainty of gearbox life expectancy is contributing to WT price escalation. Turbine manufacturers may add

contingencies to the sales price to cover warranty risk due to the possibility of premature gearbox failures. In addition, owners and operators request extended warranties and build contingency funds into the project financing and income expectations for problems that may show up during the warranty period. In response to gearbox reliability concerns, collaborations have been established between WT, gearbox and bearing OEMs, consultants and lubrication engineers to improve gearbox load prediction, design, manufacture and operation, for example, the gearbox reliability collaborative in the US (Musial et al., 2007).

Among the various WT components, the gearbox causes the longest downtime, as noted in previous Section 2.2, and is the most costly to maintain throughout a turbine's design life (Sheng, 2011). In a recent study, Gray and Watson (2010) showed that the gearbox alone could be responsible for up to one-third of all lost onshore WT availability. This problem is exacerbated offshore where the harsh weather and sea conditions could prevent maintenance or component replacement for long periods of time.

From a WT maintenance viewpoint, the main operators' concerns about gearbox reliability, particularly offshore, are (Feng et al., 2013)

- high replacement costs following a failure: the gearbox is about 13% of overall WT cost;
- complex repair procedures that incur high logistics costs and require favourable weather conditions;
- high revenue losses caused by a long downtime between the failures and repair completion.

Consequently, gearbox faults are widely considered a leading issue for the current commercial WT drive train CMSs, with vibration monitoring being the most popular approach despite technical challenges (Crabtree et al.,

2014; Hameed et al., 2009; Hyers et al., 2006; Wilkinson et al., 2007; Yang et al., 2014), as discussed earlier in Section 2.5.

General reliability principles for a three-stage gearbox were given by (Smolders et al., 2010) as follows:

- the high-speed parallel stage is found to be the least reliable gearbox module;
- a parallel intermediate-speed stage is more reliable than the planetary intermediate-speed stage;
- a planetary intermediate-speed stage appears less reliable than a planetary low-speed stage;
- the lubrication system has an important effect on reliability.

Failures in gearboxes are largely caused by the arduous loading regime they experience due to wind fluctuations, the consequences of which are transient off-axis loads, as well as extreme ambient conditions, which may include large temperature variation and ingress of dust, water or snow depending on location. The gear design codes used in the wind industry assume that the contact patch of the gear teeth is centred in the contacting teeth, i.e. that edge effects can be neglected (IEC 61400-4, 2012). If, however, there are significant off-axis loads caused by variable loads and transient events, such as gusts, grid faults or emergency shutdown, then there may be misalignment between the gear teeth, and the contact patch may move away from the centre resulting in higher than expected edge stresses. Gearboxes that are designed and built to specification are failing in service long before the calculated design life because the load data to which they are designed do not accurately reflect the loading they experience in service (Whittle, 2013).

Field observations have shown that common WT gearbox failure modes are bearing failures and gear tooth damage. The stochastically varying torque on the gearbox is considered to be a major root cause for bearing and gear

wear, driving gearbox failure modes and affecting gearbox life. Even the smallest gust of wind will create an uneven loading on the rotor blades, which will generate a torque on the rotor shaft that will unevenly load the bearings and misalign the gear teeth. This misalignment of the gears results in uneven teeth wear, which in turn facilitates further misalignment. Other possible causes of gear teeth and bearing failures are particulates in the oil owing to contamination during assembly, corrosion and wear; variations in rotor speed which may cause the gear teeth to chatter, causing fretting and generating particles; mechanical interference or other manufacturing problems such as heat treatments or surface finish out of specification; loss of oil or oil circulation (Hyers et al., 2006).

Gears are inherently subject to dynamic contact forces with high amplitudes. Most gear failures are initiated as localised point defects in the tooth meshing zone, where the material stress is locally very high. The defect then progresses with time due to the repeated cyclical loading during machine operation. When the gear has been in use for a while the contact forces begins to wear the teeth contact surfaces. Typical gear failure modes include pitting, scuffing, spalling, chipping and more seriously, cracks (Walford and Roberts, 2006). Missing material, due to spalling in the contact surface, implies an increased surface roughness and, without adequate lubrication oil filtration, leads to progressive damage to all other metal-to-metal surfaces in the gearbox, both gears and bearings. Tooth cracking is the end result of gear tooth deterioration. Its existence in a gearbox indicates a situation already beyond the ability of maintenance to prevent a failure and the replacement of the component is the only possibility left to retain the function of the gearbox (Mobley et al., 2008). A broken tooth on a gear generates a hit or impact, with irregular behaviour of the contact each time the defective tooth comes into meshing.

Timely and reliable detection and diagnosis of the developing gear defects within a gearbox is an essential part of minimising unplanned WT downtime.

3.3. WT Generator

A large proportion of current WTs employ high-speed induction generators (IG) for energy conversion. For commercial reasons it is common to use a voltage of only 690 V even for large generators and the generated electricity is then stepped up to the distribution level, >3.3 kV, by a transformer which is usually located in the nacelle, but may also be located at the base of the tower.

To achieve variable speed operation and, hence, enabling active power output control and performance optimisation while reducing mechanical loading, it is now common to utilise power electronic converters to decouple the turbine generator from the grid frequency. The decoupling of the electrical and rotor frequency absorbs wind speed fluctuations, allowing the rotor to act as a flywheel, and thus smoothing out spikes in power, voltage and torque. The dominant market concept for high power ($\geq$ 1.5 MW) variable speed, variable-pitch WTs typically employs a doubly fed induction generator (DFIG) so that a partially rated converter may be used. This configuration features a geared drive low voltage, 4 or 6-pole wound rotor induction generator (WRIG) with its stator connected to the medium voltage (MV) grid through a transformer and its rotor, with insulated windings, connected to the grid through slip-rings, brush-gears and a partially rated power electronic converter. The WT DFIG configuration and a cutaway view of a wound rotor induction machine are shown in Figure 3.2 and Figure 3.3, respectively.

The power converter controls the rotor frequency and thus the rotor speed to allow operation above and below the synchronous speed of the stator

field, which is determined by the network frequency and number of poles of the stator windings, e.g. 1500 rpm for a four-pole winding on a 50 Hz system. The DFIG concept supports a wide speed range operation, depending on the size of the frequency converter, which needs only to be rated to handle a fraction of the total power. The larger this fraction, the larger the achievable speed range will be (Burton et al., 2011). Typically, up to approximately 30% of the power output goes through the converter to the grid, the other part goes directly to the grid, and the window of speed variations is approximately ±30% around the synchronous speed (Li and Chen, 2008).
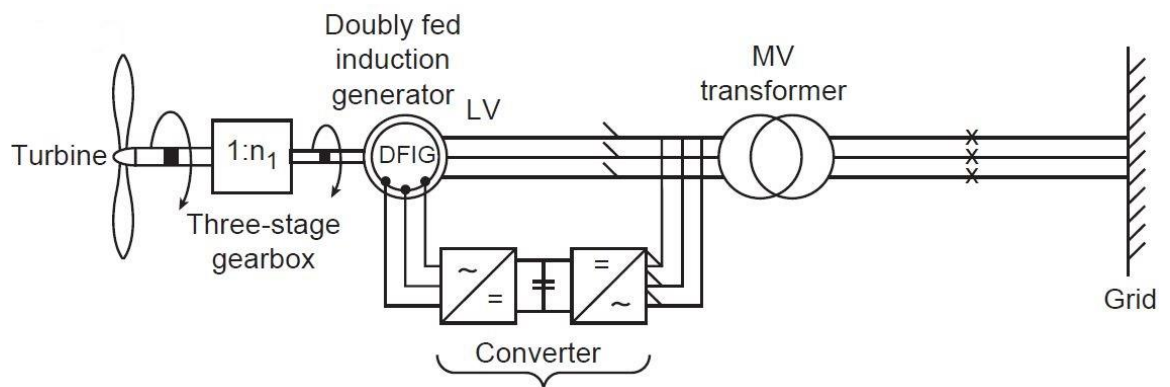
Figure 3.2: WT DFIG electrical configuration, adapted from Tavner (2012).
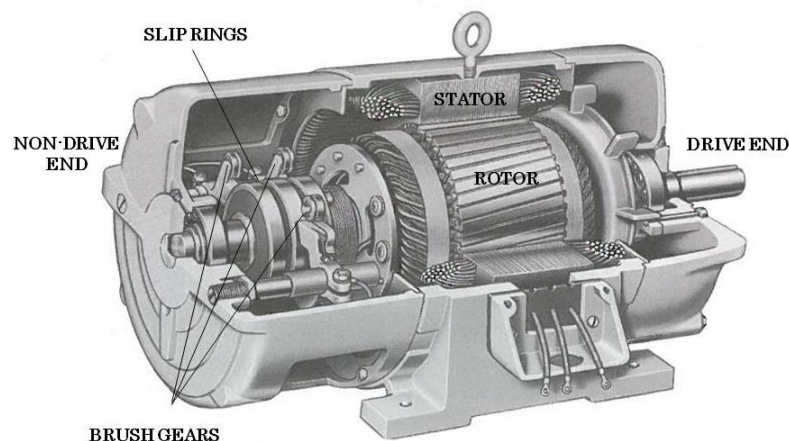
Figure 3.3: Cutaway of a wound rotor induction machine showing salient features, adapted from Chapman (1999).

DFIG generators are common in large WTs where the benefits of limited variable-speed operation are required (Van Hulle and Fichaux, 2010). The use of partially rated power electronics gives only limited speed control, but the cost paid in terms of lower efficiency is small. Whereas the cost of electrical machines is a function of torque, for power electronics it is principally a function of power. Multi-MW power electronic converters are costly, typically more than 5% of the WT total cost, and the use of a partially rated converter results in considerable savings, at the cost of increased complexity of the generator and a reduced variable speed range.

Electrical machines are usually reliable compared to other drivetrain components such as gearboxes. However, it has been found that generator failure rates in the wind energy industry compare unfavourably with other industries. Outside of the wind energy industry, a failure rate of 0.0315 to 0.0707 failures per generator per year is typical (Tavner et al., 2008a). However, in the WT industry generator failure rates of 0.1 failures per generator per year or greater are typical (Spinato et al., 2009; Tavner et al., 2006; Tavner et al., 2007). WT generator failure rates are unacceptably high, as it is has been noted in previous Section 2.2. Undetected generator faults may have a catastrophic effect on the turbine drive train resulting in costly and lengthy repairs. Attention at the incipient fault stage is required to avoid fault escalation leading to breakdown. Generator CM is significant as generator defects have been shown to make a significant contribution to WT downtime (Ribrant and Bertling, 2007; Tavner et al., 2010; Wilkinson et al., 2010). With reduced accessibility offshore, any downtime is significantly extended.

The ReliaWind study results, presented in Figure 2.3, show that 30% of annual downtime was due to converter power module failures, 30% of which resulted directly from generator failures (Wilkinson et al., 2010). WT generators are prone to electromechanical faults, mainly concentrated in the

stator, rotor and machine bearings (Zaggout et al., 2014). A recent survey of field data of over 800 failed commercial WT generators, from the US wind industry (Alewine and Chen, 2010), showed that, although bearing faults dominate total generator failures, rotor faults are significant for all WT generator sizes including the largest (>2 MW). Rotor failures accounted for 12% of the total 2MW range generator failures and exceeded 50% in smaller scale machines (Alewine and Chen, 2010). WT IG rotor electrical asymmetry represents a significant indicator of WT generator faults caused by rotor winding, brush-gear or slip-ring defects. For example, increasing resistance or open-circuit of one or more of the rotor windings or brush-gear circuits can result in rotor electrical asymmetry. Such faults are caused by a combination of magnetic, thermal and mechanical stresses acting on the rotor, varying dynamically with loading and environmental conditions (Zaggout et al., 2014). Although rotor asymmetries do not initially cause a machine to fail, they can have serious secondary effects, such as increasing losses, reducing efficiency and lowering generator and turbine reliability. The most serious consequence of these faults may be the high costs needed to repair the rotor. This could be avoided if the machines were supervised by an appropriate CMS, which should ideally employ non-invasive monitoring methods. However, monitoring of electrical faults in generators has not yet become standard practice in the wind industry. In the majority of modern WTs rotor current signals are only monitored for control purposes and, although they contain valuable information, operators often have difficulty in obtaining permission to use these signals for CM purposes. The potential advantage of using electrical signal analysis stems from the fact that these are readily available within the WT control system and, therefore require no additional sensors and infrastructure for monitoring.

The dominant source of failures in multi-MW WT generators is represented by the bearings. According to Alewine and Chen (2010), for WTs above 2 MW 58% of total generator failures originate from bearing faults.

Generator shaft bearing fault is one of the most significant in WT drive train. The most common bearing type is rolling-element. This is a class of bearing in which the main load is transferred through elements in rolling contact. The purpose is to allow constrained relative motion between loaded surfaces. Bearings are, therefore, inherently vulnerable to fatigue and wear mechanisms. Premature bearing failures can be caused by a large number of factors, the most common of which are fatigue, wear, plastic deformation, corrosion, poor lubrication, faulty installation and incorrect design (Howard, 1994). Typical WT bearing failure modes include ring or roller cracking, wear, spalling and brinelling (McGowin et al., 2006). There is an undesirable positive feedback effect with bearing deterioration in rotating electrical machines. The deterioration of bearing contact surfaces leads to increased bearing vibration and higher temperature, both of which accelerate the rate of deterioration. These phenomena are usually used for bearing CM (Howard, 1994; Tavner et al., 2008a). In addition, bearing deterioration can lead to rotor eccentricity, which places more load on the bearings, thereby aggravating the problem.

Although the cost associated with an individual bearing or gear fault is small relative to the parent component, the overall effect and cost of a component failure can be many times the part cost. Wear debris generated by spalling can initiate damage in other parts of the bearing. Misalignment due to a worn or loose bearing can overstress gear teeth and initiate surface failure or cracks. Badly damaged bearings can cause the outer race to spin in the housing, destroying the bearing seat, or create thrust loads that cause the gear case to crack. Worn generator bearings can cause rotor whirl that eventually leads to rotor bar contact with the stator or excessive stress on the end-turns of wound-rotor generator coils. Premature gear and bearing failures will quickly lead to machine malfunction, even catastrophic failure. As a result, it is essential for an advanced CMS to be capable to detect initial

faults as early as possible and to allow for remedial measures before consequential damage occurs (McGowin et al., 2006).

3.4.   Signal Processing Techniques

As introduced in Section 2.4.1, many signal processing techniques have been developed for CM of WTs in recent years. These techniques mainly depend on the types of data and components studied. The increasing capability of digital integrated circuits means that a wide range of complex operations can now be applied to real-time signals or applied to stored data. Programming environments such as MATLAB, with specialised toolboxes, allow the fast prototyping and development of digital signal processing techniques, which can later be transferred to hardware. Digital signal processors (DSPs) are specialised, dedicated programmable microprocessors with instruction sets optimised for real-time manipulation of sampled signals. Once an algorithm has been developed in software, it can often be adapted and implemented in a DSP.

For vibration and electrical signals, it is often desirable to determine their spectral content in the frequency domain to reveal information not apparent by viewing them in the time domain. Spectral analysis is the most commonly used technique for CM in geared transmission systems and electrical machines and has proved a valuable tool for fault detection and basic diagnosis (Randall, 2011; Tavner et al., 2008a). The fundamental process common to all spectral analysis techniques is the conversion of a time domain representation of the signals into a frequency domain representation. The spectral representation of a time signal is therefore a collection of components in the frequency domain, each with a specific frequency, amplitude and phase angle. A plot of the magnitude versus frequency is called the amplitude spectrum of the signal. A plot of the phase angle versus frequency is called the phase spectrum. The frequency domain methods

identify the major frequency components in the signal amplitude spectrum and then use these components and their amplitudes for trending and comparison.

Most rotating machine failures result at or near a frequency component associated with the running speed. Therefore, the ability to display and analyse the monitored signals in terms of their frequency components is extremely important. Spectral analysis compacts the data significantly, at the cost of computational time, and allows trends of change to be more easily recognised.

The spectral representation of a signal is usually achieved by using the Fast Fourier Transform (FFT) algorithm to perform a Discrete Fourier Transform (DFT) of digitised sampled data. The FFT analysis is the most popular signal processing technique used by current commercially available WT CMSs.

This section introduces and discusses the principles of the Fourier transform, its development into the DFT, for discrete signal sequence analysis, and then the FFT algorithm. The concepts of power spectrum and order analysis, which represent the basis for the signal processing developments undertaken in this Thesis and presented in Chapter 5, are then introduced. Comprehensive developments of the theory and full mathematical derivations can be found in (Bracewell, 1978; Kay, 1988; Oppenheim et al., 1999; Randall, 1987). This section cannot and does not intend to cover the area in full. Its goal is to introduce the basic terminology and the main concepts of spectral analysis, providing the equations relevant to the work presented in this Thesis.

3.4.1.   The Fourier Transform

The mathematical basis of frequency analysis is the Fourier transform. Fourier analysis is named after Jean Baptiste Joseph Fourier (1768-1830), a

French mathematician and physicist. Fourier worked on heat propagation and in his 1807 essay, *Theory of the Propagation of Heat in Solid Bodies*, showed that any continuous periodic waveform can be described or generated as the sum of an infinite series of sinusoidal components whose frequencies are integer multiples of a fundamental frequency (Smith, 1989). The originality of the paper and the surprising nature of its mathematical revelations caused great controversy and it was denied publication both in 1807 and in later years. Fourier had the support, among the examiners, of Laplace and Monge, but Lagrange was adamantly in opposition, so that Fourier's work did not appear in print until 1822, reworked into book form.

Figure 3.4 illustrates a simplified relationship between the time-domain and frequency-domain representations of a generic waveform. In this case, the complex waveform, shown over one period, is decomposed into four simple sine waves. As more terms are added the superposition of sine waves better matches the original time waveform.
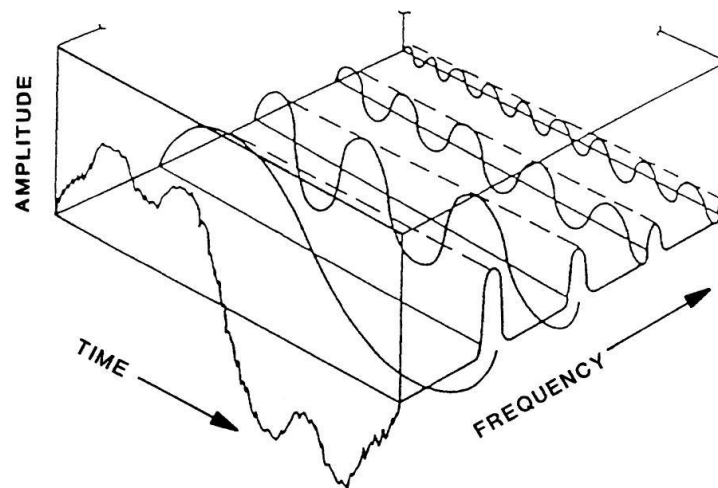
Figure 3.4: Relationship between time domain and frequency domain (Mobley, 1999).

It was later shown that any function could be expressed as an integral of sines and cosines over all frequencies from 0 to infinity, a relation called the

Fourier transform. The Fourier transform has widespread applications in engineering, science and mathematics (Bracewell, 1978).

The frequency domain representation of a continuous-time signal $x(t)$ can be described by the continuous Fourier transform, $X(f)$, which extracts its component X at the frequency f, defined as (Randall, 1987)

$$X(f) = \int_{-\infty}^{\infty} x(t)e^{-j2\pi ft}dt \tag{3.1}$$

where $j = \sqrt{-1}$ is the complex unit and, according to Euler's theorem,

$$e^{-j2\pi ft} = \cos(2\pi ft) - j\sin(2\pi ft) \tag{3.2}$$

Conversion from the frequency to the time domain can be obtained by means of the Inverse Fourier transform, defined as (Randall, 1987)

$$x(t) = \int_{-\infty}^{\infty} X(f)e^{j2\pi ft}df \tag{3.3}$$

3.4.2. The Discrete Fourier Transform

In CM a signal is a measurement of a physical quantity that conveys information about the behaviour of the system. As it is usually necessary to digitise the transducer signals for onward transmission to the processing unit in a monitoring system, data acquired with the DAQ card is usually sampled in time at a certain sampling frequency and is therefore not strictly continuous in time. In this case, the discrete Fourier transform (DFT) must be used.

Discrete sequences most commonly occur as a representation of continuous signals. They are obtained through periodic sampling of the signal. Suppose that a continuous-time signal $x(t)$ is sampled with period T_{samp} or sampling frequency

$$f_{samp} = \frac{1}{T_{samp}} \tag{3.4}$$

to obtain the discrete-time signal

$$x[n] = x(nT_{samp}) \qquad\qquad -\infty < n < +\infty \tag{3.5}$$

For the sampled discrete-time signal $x[n]$ of finite length N the DFT is defined as (Oppenheim et al., 1999)

$$X[k] = \sum_{n=0}^{N-1} x[n]\, e^{-j\frac{2\pi}{N}nk} \qquad\qquad 0 \leq k \leq N-1 \tag{3.6}$$

where the normalised discrete frequency, k/N, is related to the sampling frequency, f_{samp}, and the physical frequency, f, through the relation

$$\frac{k}{N} = \frac{f}{f_{samp}} \tag{3.7}$$

The original N-point data sequence can be determined from its complex spectrum by using the Inverse Discrete Fourier transform formula (Oppenheim et al., 1999)

$$x[n] = \frac{1}{N} \sum_{k=0}^{N-1} X[k]\, e^{j\frac{2\pi}{N}nk} \qquad\qquad 0 \leq n \leq N-1 \tag{3.8}$$

For a signal sampled with the sampling rate f_{samp}, due to the limitation imposed by the Nyquist-Shannon's sampling theorem (Oppenheim et al., 1999), components of the spectrum can only be extracted for frequencies between

$$-\frac{f_{samp}}{2} \leq f \leq \frac{f_{samp}}{2} \tag{3.9}$$

in order to obtain a faithful reconstruction of the signal from its samples, where the limiting cut-off frequency $f_{samp}/2$ is called the Nyquist frequency.

This represents the highest frequency for which the Fourier transform information would be valid. High-frequency spectrum beyond Nyquist frequency folds onto the useful spectrum, thereby causing aliasing, i.e. higher frequencies represented as lower ones, and distorting it.

3.4.3. The Fast Fourier Transform Algorithm

Direct computation of all N DFT points using equation (3.6) requires $N(N-1)$ complex additions and N^2 complex multiplications, resulting in excessive amount of computation time, particularly when a high number of samples is required. The DFT computational complexity can be reduced by the use of the very efficient Fast Fourier Transform (FFT) algorithm that computes the DFT indirectly. The FFT, first published in 1965 by J.W.Cooley and J.W.Tuckey (Cooley and Tukey, 1965), has revolutionised many fields, such as modern experimental mechanics, signal and system analysis, acoustics, where onerous computation was an impediment to progress. The FFT is a fast DFT calculation technique which is optimised with respect to computing time and memory consumption.

The algorithm is based on the fundamental principle of decomposing the computation of DFT of a sequence of length N into two DFTs of length $N/2$. It takes advantage of symmetry properties of the N distinct complex roots of unity

$$(W_N)^k = e^{j\frac{2\pi}{N}k} \qquad\qquad 0 \leq k \leq N-1 \qquad\qquad (3.10)$$

and then uses repeated clever portioning of the input sequence into two equally long sub-sequences, each of which can be separately and quickly processed, until DFTs of single points are left. In order to take full advantage of the repetitive portioning into equal two parts, the original sequence needs to be of length or periodicity, N, which is a power of 2. This allows certain symmetries to occur reducing the number of calculations, especially

multiplications, which have to be done. If the length of data set is not a power of 2, it must be padded with zeros up to the next power of 2.

As the FFT algorithm eliminates most of the repeated complex products in the DFT its execution time is much shorter. Specifically, the FFT significantly reduces the computation time by a factor of the order of $N/log_2 N$. This means that, for the typical case where $N = 2^{10} = 1024$, the FFT is about 100 times faster than the direct calculation based on the definition of the DFT. The improvement increases with N. The full details of the FFT algorithm are beyond the scope of this Thesis. An exhaustive coverage of it, including its full mathematical derivation, can be found in Oppenheim et al. (1999).

Signal transformations between time and frequency domain are feasible in near real-time using the FFT algorithm in high-performance DSPs. Implementations of the FFT algorithm as subroutines are commonly available in different programming environments, such as Mathworks' numerical computing environment MATLAB.

As discussed in previous Section 2.4.2, the majority of commercially available WT CMSs incorporate traditional FFT analysis of the high frequency data to detect fault-specific frequencies. FFT analysers provide a suitable tool for spectrum interpretation. They provide constant bandwidth on a linear frequency scale, and, by means of zoom or extended lines of resolution, they also provide very high resolution in any frequency range of interest. This permits early recognition and separation of harmonic patterns or sideband patterns and separation of closely spaced individual components.

However, the FFT traditional spectral estimation technique is only suitable for the analysis of stationary or weakly stationary signals while many of the signals encountered in a variable speed WT vary rapidly over the period of measurement. In order to acquire directly comparable data and to

allow spectra to be recorded in apparently stationary conditions in most available WT CMSs, using the traditional FFT analysis, the limits for operating conditions under which measurements are recorded can be set. This aims to produce stationary, directly comparable FFT results to increase the accuracy and reliability of the processed signals.

To overcome the conventional fast FFT analysis inability to handle non-stationary waveform signals, different time-frequency signal processing techniques appropriate for the analysis of WT non-stationary signals, such as the Short-Time Fourier transform, the Wigner Ville transform and the Wavelet transform have been proposed (Wilkinson, 2008). However they are unsuitable for practical implementation in current on-line CMSs, as they are computationally intensive, usually provide low resolution and the interpretation of the results is more complicated for direct analysis compared to FFT techniques.

3.4.4. Windowing

The FFT computation assumes that the signal is periodic in each data block, that is, it repeats over and over again and it is identical every time. When the FFT of a non-periodic signal is computed then the resulting frequency spectrum suffers from leakage. Leakage is the result of the FFT algorithm trying to handle discontinuities in the sample. The FFT sees the discontinuities as a modulating frequency. This produces spectral components where none truly exist. Leakage results in the signal energy smearing out over a wide frequency range in the FFT when it should be in a narrow frequency range. Since most signals are not periodic in the predefined data block time periods, a window must be applied to correct for leakage. However, in selecting a window it should be considered that data windowing reduces the magnitude of the spectrum at frequencies not near the signal frequency at the expense of increasing the bandwidth of the main lobe.

Different windows introduce different trade-offs between the side-lobe level and the main-lobe width expansion (Harris, 1978).

A typical window is shaped so that it smoothly attenuates the beginning and end of the data block and it has some special shape in between. This function is then multiplied with the time data block forcing the signal to be periodic. By smoothing the ends of the wave to zero, there is no discontinuity around the ends. In applying a window to the data, energy is lost. A special weighting factor must be applied so that the correct unbiased FFT signal amplitude level is recovered after the windowing. Detailed presentations of the window functions can be found in (Harris, 1978; Oppenheim et al., 1999). Their implementations are commonly available in different programming environments, such as MATLAB.

The most commonly used windows are the Hamming window

$$w[n] = 0.54 - 0.46 \cos\left(2\pi\frac{n}{N}\right) \qquad 0 \leq n \leq N \qquad (3.11)$$

and the Hann, or Hanning, window

$$w[n] = 0.5\left[1 - \cos\left(2\pi\frac{n}{N}\right)\right] \qquad 0 \leq n \leq N \qquad (3.12)$$

shown in Figure 3.5 and Figure 3.6, respectively. The window length is

$$L = N + 1 \qquad (3.13)$$
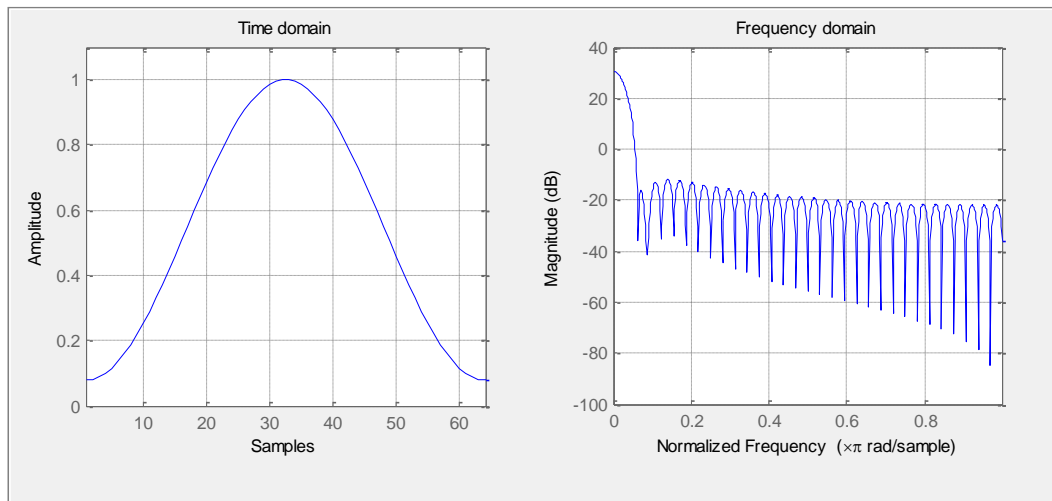
Figure 3.5: 64-point Hamming window.
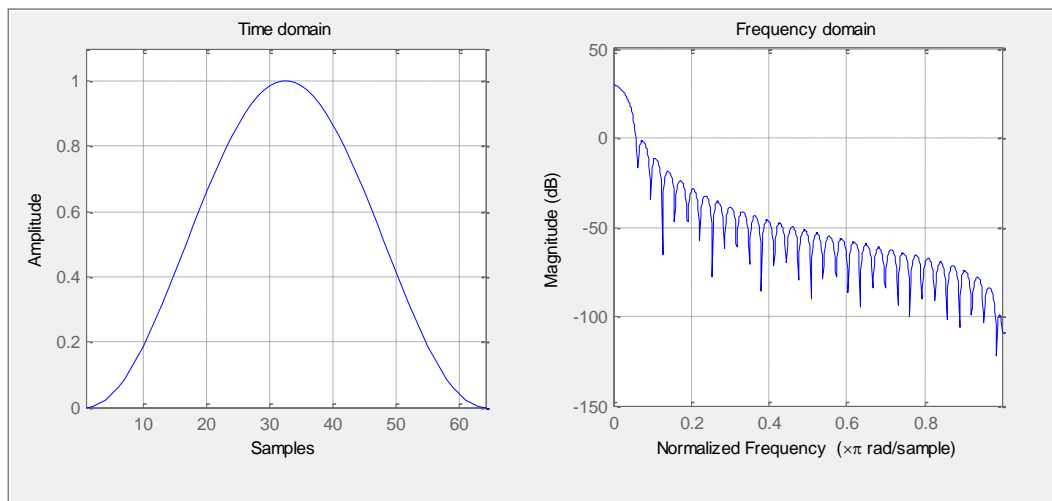
Figure 3.6: 64-point Hann, or Hanning, window.

The characteristics of the signal that is being analysed and also the nature of the system that generates the signal should be considered in choosing an appropriate truncation window. In particular, the Hanning window is recommended for signals generated by heavily damped systems and the Hamming window is recommended for use with lightly damped systems (de Silva, 1999).

72

3.4.5.   The Power Spectrum

The spectral representation of a discrete-time signal through DFT is a collection of components in the frequency domain, each with a specific frequency, amplitude and phase angle. The DFT of a real signal is then a complex quantity, having a real and an imaginary part. Both amplitude and phase information allow reconstructing entirely the original signal. The power spectrum, or power spectral density (PSD), is a scalar quantity which describes how the power of a signal is distributed among its frequency components. The power spectrum is a real valued, non-negative and, for real signals, an even function of frequency. However, phase information is lost. A plot of the power spectrum represents a useful tool to compare two signals.

One method for estimating PSD is based on using a function called the periodogram (Oppenheim et al., 1999). The power spectrum of an N-point data sequence $x[n]$ is defined as

$$P(k) = \frac{1}{N}|X[k]|^2 \qquad\qquad 0 \le k \le N-1 \qquad\qquad (3.14)$$

where $|X[k]|^2$ is the square of the magnitude of the DFT of the signal, defined in equation (3.6). The PSD can be shown to be identical to the Fourier transform of the autocorrelation function of a signal (Kay, 1988).

PSD is efficiently computable via the FFT. The power spectrum calculates the harmonic power in discrete-time, real-valued sequences. Window amplitude correction is usually used to get un-biased final spectrum reading at specific frequency.

The total power in a specific band of frequencies can be calculated by summation over the frequency band. In particular, the average power of the discrete-time signal $x[n]$ may be regarded as the sum of power associated with its individual frequency components defined in (3.14) (Shin and Hammond, 2008).

It is important to note that the power in the spectrum does not necessarily refer to the physical power. Rather, by analogy to applying a voltage across a 1 Ω resistance, the power has units of the time-domain signal squared (Wilkinson, 2008).

Extensive and complete coverage of the power spectral density and its estimation techniques can be found in (Kay, 1988; Oppenheim et al., 1999).

3.4.6.   Order Analysis

A particular issue for WT CM signal spectral analysis is that periods and amplitudes change with time, as a consequence of the continuously and rapidly changing drive train torque, and care is essential during the analysis.

Most machine components give rise to specific signals that characterize them and allow them to be separated from others, as well as distinguishing faulty from healthy condition. The distinguishing features may be because of different repetition frequencies, for example a gear meshing frequency, which characterizes a particular pair of gears, and different sideband (SB) spacing which characterizes the modulating effects of the two meshing gears on their common mesh frequency, which are discussed in detail in Section 3.5. The characteristic gear and bearing frequencies are directly proportional to the associated shaft rotational frequency. The proportionality constant depends on the element design parameters, such as the number of rolling elements or gear teeth.

Vibration signals are rich in harmonic information, which must be accurately understood if diagnosis is to be performed with confidence. Since the shaft rotational frequency normally varies significantly during the data acquisition, vibration signals are characterized by a frequency variation of their spectral components. In analysing rotating machine vibrations it is often desired to have a frequency x-axis based on harmonics of shaft speed (de Silva, 1999). In this case, rotating machinery diagnostic analysers must

have the ability to measure shaft speed from either a single or multi-pulse per revolution tachometer. The tachometer input measures the machine speed concurrently with the normal acquisition of measurement signals.

When the vibration frequency is considered with respect to the rotational speed of the machine it is expressed in a dimensionless ratio called order (X). The general relationship between the frequency order X, the machine rotational speed, ω, in rev/min, and the frequency, f, in Hz, is

$$f = X \frac{\omega}{60}$$

(3.15)

Spectra where the frequency axis is normalised with shaft rotation frequency are denoted normalised order spectra.

Spectral order is introduced as a non-dimensional frequency parameter and it remains constant with shaft speed. This enables to easily identify relative overtone amplitudes of the rotational speed as the rotation speed develops. In an ordinary spectrum the peaks will shift in frequency in correspondence to the change in shaft speed. In contrast, in normalised order spectra, the vibration signature peak positions are speed-invariant. This invariance property simplifies spectra interpretation. If the frequency axis is normalised to the shaft rotation frequency any cyclic event synchronised with the shaft rotation will produce a spectral component at a fixed position even under the variable speed conditions. With order analysis, it is possible to identify and isolate vibration patterns to analyse the performance and health of each machine component individually. The use of the order analysis is extremely important in the fault diagnosis. The main advantage of this approach is that it is easier to focus on a specific cyclic mechanism.

3.5. Gearbox Condition Monitoring

In a rotating machine, the moving parts impart vibratory forces into the structure and these forces occur at specific frequencies determined by the dynamics of the moving element. These vibrations can be detected by using non-intrusive transducers to measure vibration signals at the machine casing. Each specific machine element produces its own characteristic fairly stable vibration pattern, known as vibration signature, when it is in normal operation. This signature provides a basis for later comparison in order to locate those frequencies in which significant increases in vibration level have occurred (Davies, 1998).

Almost all failure modes in the rotating elements in geared transmission systems will cause some change in the vibration signature, and many will produce material debris and/or increased friction causing a change in surface temperature. Vibration monitoring techniques use the modified vibration signature to detect, localise, diagnose, and possibly prognosticate, the defective element so that relevant maintenance can be planned. However, it should be noted that, as the gearbox vibration amplitude varies with the mean load, for CM purposes vibration measurements should only be compared under the same load conditions.

On-line continuous vibration analysis can provide a wealth of information about the mechanical health of WT gears. Timely and reliable gear tooth defect detection and diagnosis is an important capability of any WT CMS and it is a fundamental input to advanced diagnostic techniques for a mature preventive maintenance strategy.

Historically gear defects within a WT gearbox have been difficult to diagnose at an early enough stage for defect maintenance to be scheduled in advance. The process in which the gear teeth on the input shaft roll and slide on the output shaft gear teeth is called gear meshing. Most WT gearboxes

have several speed increasing stages which each produce a different characteristic gear meshing frequency. The gearboxes also transfer a very large torque from the main rotor to the generator through these gear meshes resulting in relatively high energy gear mesh frequencies when compared to the energy level of signals produced by a small gear defect. Because of the overpowering gear mesh frequencies, gear defect signatures can often be obscured in the overall vibration signal and be difficult to diagnose. Most modern techniques for gear diagnostics are based on the analysis of vibration signals picked up from several accelerometer sensors mounted in strategic locations on the WT gearbox. As the vibration signatures for machinery faults tend to be small relative to other vibration signatures, techniques to improve the signal to noise are needed to remove frequencies associated with nominal components, while preserving the fault signatures. The common target is to detect the presence and the type of fault at an early stage of development and to monitor its evolution, in order to estimate the machine's residual life and choose an adequate plan of maintenance.

In Section 5.4, this Thesis presents a novel algorithm, the Gear Sideband Power Factor ($SBPF_{gear}$), specifically developed to aid in the detection of WT gear tooth damage in non-stationary vibration monitoring signals. $SBPF_{gear}$ is a gear condition indicator generated from fault patterns produced in vibration signatures when damaged components interact with their environment (Zappalá et al., 2014b). It auto-detects and distinguishes gear defect signatures within an overall vibration signal by extrapolating only one relevant parameter from each spectrum, significantly simplifying the complex and time consuming manual analysis. $SBPF_{gear}$ also indicates the fault severity and provides an early detection and diagnosis warning of developing gear damage.

The focus of this section is to give the preliminary basis on the theory and application of gear defect detection using machine casing vibration underlying the $SBPF_{gear}$ development.

3.5.1. Gear Characteristics

In a geared transmission system, the main vibration source is the meshing action of the gears. All non-defective gears have their own characteristic vibration signatures determined by their design parameters and their conditions. The characteristic features of gear vibrations are due to the cyclically varying gear meshing forces. These meshing forces generate vibrations that are transmitted to the gearbox casing where they can be measured.

The geometry of the gear profile has a crucial effect on the vibration behaviour. The gear meshing frequency is the rate at which gear teeth engage together in the pitch point and is defined as the product of the number of teeth on the gear and its turning speed. In the case of a parallel helical stage, a gear with N_t teeth on a shaft rotating with a frequency f_{rot} generates the fundamental meshing frequency, f_{mesh}, defined as

$$f_{mesh} = N_t f_{rot}$$
(3.16)

Any two meshing gears must have the same gear mesh frequency. A perfectly sinusoidal meshing force would imply a perfect single tone vibration spectrum. In real gears, the surfaces are not ideally smooth and the tooth shape is not ideal, hence, the vibration spectrum will always contain harmonics of the fundamental meshing frequency

$$nf_{mesh} = nN_t f_{rot} \qquad n = 2,3,\dots\dots$$
(3.17)

A gear with teeth perfectly uniform, or identical, in profile and pitch generates a line spectrum described by equations (3.16) and (3.17). The amplitude of each line depends on the actual shape of the meshing force.

In practice, as the teeth deform under load, a meshing error is introduced even when the tooth profiles are perfect. In addition, because of the gear manufacturing errors there are geometric deviations from the ideal profiles (Mark et al., 2010; Randall, 2011). All gears are manufactured with finite tolerances, the profile and pitch always vary slightly from tooth to tooth and tooth surfaces have roughness. These mechanisms cause amplitude and phase modulations of the meshing forces resulting in small amplitude SBs, that always occur in pairs around the tooth meshing frequency and its harmonics and that are periodic with the rotation frequency of the gear (Fan and Zuo, 2006; Wieringa et al., 1986). The SBs are frequency components equally spaced around a centre frequency, called carrier frequency.

The most important components in gear vibration spectra are the tooth meshing frequencies and their harmonics, together with the modulation SBs caused by mean geometric errors on the tooth profiles, machining errors and wear, as shown in Figure 3.7.

As faults develop, amplitude changes in the gear mesh frequency and its harmonics compared to the base line vibration measurements are not always detectable. That is, the mesh frequency itself can be largely unaffected by the development of a fault. Prior attempts to monitor gears for ongoing deterioration have involved, for example, extracting and trending mesh frequency and harmonic amplitudes. It has been found that this method does not work well as it has relatively low sensitivity to developing faults.
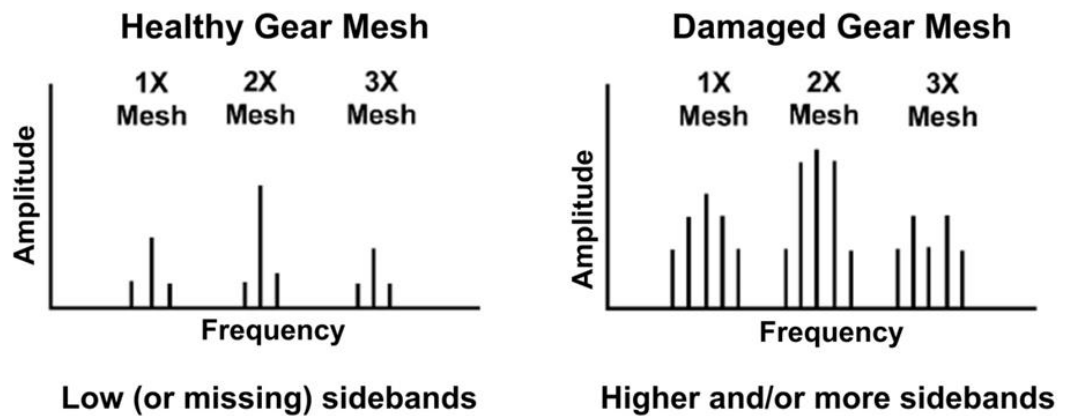
Figure 3.7: Graphical representation of typical vibration spectra for a healthy (left) and a damaged (right) gear mesh system (Hatch et al., 2012).

However, there is a phenomenon that occurs as faults develop in a gear mesh. The vibration becomes modulated by the defect. The fault engages in the gear mesh and modulates the amplitude and phase of the gear mesh frequency. This results in characteristic amplitude increases in the modulation SBs in the frequency domain. For gearboxes in good condition, the SB level generally remains constant with time. Therefore an increment in the number and the amplitude of such SBs may indicate a fault condition (Dalpiaz et al., 2000).

If a specific tooth is worn, cracked or a part of a tooth is missing, then once during each revolution of the faulted gear a shock will occur between the gears. A single damaged tooth on a pinion or gear directly coupled to a shaft generates a hit or impact, with irregular behaviour of the contact each time the defective tooth comes into meshing. The short-duration impacts produced by the local tooth damage add amplitude and phase modulation effects to the meshing vibration, and in turn generate a higher level of SBs around the mesh harmonics. Moreover, the spacing of the SBs is related to their source and thus contains important diagnostic information (Randall, 1982). The SB spacing is equal to the modulation frequency, which in turn, is equal to the rotating speed of the shaft on which the fault occurs. In particular, the

localised modulation effect takes place only during the engagement of the faulted teeth, but is repeated once in each revolution of the gear. As a consequence, the spectrum presents a large number of SBs of the tooth meshing frequency and its harmonics spaced by the faulted gear rotational frequency. For example, if a gear pinion develops a broken tooth, then the spectrum will show the mesh frequency with SBs spaced at the pinion shaft speed. The SBs will have multiple harmonics as well, both above and below the centre frequency.

Typically, the more damage that occurs, the more energy there is in the SBs (Goldman, 1999). In particular, previous literature on the vibration analysis has shown that monitoring the second harmonic of the gear mesh and its SBs allows early detection of gear wear (Mobley, 1999).

3.5.2.   Basic Analysis of Gear Vibration Signals

This section presents the derivation of the basic SB components which appear evident about the gear meshing frequency and its harmonics when the meshing vibration becomes modulated due to local tooth defects. Only the case of a gear pair with teeth perfectly uniform in profile and pitch is presented here in the interests of clarity and conciseness.

For a pair of gears, which mesh under constant load and speed, assuming that all teeth are identical and equally spaced, the meshing vibration signal, $y'(t)$, of one of the gears is represented by (McFadden, 1986)

$$y'(t) = \sum_{m=0}^{M} X_m \cos(2\pi m N_t f_{rot} t + \phi_m) \tag{3.18}$$

where M is the number of tooth-meshing harmonics, X_m and ϕ_m are the amplitude and phase of the mth meshing harmonic and $N_t f_{rot}$ is the meshing frequency defined in equation (3.16). Equation (3.18) indicates that, for healthy gears with ideal profiles, the corresponding vibration signal exhibits

predominant frequency components at the fundamental and several harmonics of the meshing frequency.

A gear tooth local defect, such as a fatigue crack, produces changes in the vibration as the affected tooth meshes with the other gear teeth. These changes can be represented by the amplitude and phase modulation functions, $a_m(t)$ and $b_m(t)$, respectively. As the modulation is periodic with the gear shaft rotation frequency, f_{rot}, these functions may be represented by the following discrete Fourier series

$$a_m(t) = \sum_{n=0}^{M'} A_{mn} \cos(2\pi n f_{rot} t + \alpha_{mn}) \tag{3.19}$$

$$b_m(t) = \sum_{n=0}^{M'} B_{mn} \cos(2\pi n f_{rot} t + \beta_{mn}) \tag{3.20}$$

where M' is the number of SBs around the meshing harmonics, A_{mn} and B_{mn} are amplitudes of the amplitude and phase modulation signals, respectively, at the nth SBs around the mth meshing harmonic, and α_{mn} and β_{mn} are phases of the amplitude and phase modulation signals, respectively, at the nth SBs around the mth meshing harmonic. Note that the modulation functions may differ with m.

The modulated vibration signal, $y(t)$, produced by a pair of meshing gears with a tooth fault is therefore given by

$$y(t) = \sum_{m=0}^{M} X_m \left(1 + a_m(t)\right)\cos\left(2\pi m N_t f_{rot} t + \phi_m + b_m(t)\right) \tag{3.21}$$

substitution of equations (3.19) and (3.20) into equation (3.21) leads to

$$y(t) = \sum_{m=0}^{M} X_m \left(1 + \sum_{n=0}^{M'} A_{mn} \cos(2\pi n f_{rot} t + \alpha_{mn}) \right) \cos \left(2\pi m N_t f_{rot} t \right.$$
$$\left. + \phi_m + \sum_{n=0}^{M'} B_{mn} \cos(2\pi n f_{rot} t + \beta_{mn}) \right) \qquad (3.22)$$

In the frequency domain, the Fourier transform of the foregoing function will comprise the fundamental and harmonics of the meshing frequency surrounded by modulation SBs (McFadden, 1986). According to equation (3.22), additional frequency components, such as $(m N_t f_{rot} \pm n f_{rot})$, will appear in the faulty gear set frequency spectrum due to modulation phenomena.

Vibration-based CM is one of the most effective techniques to detect WT gearbox failure especially in the high-speed side rather than low-speed side. This is attributed to the inherent sensitivity of the accelerometers to high frequency vibration.

In gear analysis, the presence of sidebands and their amplitudes can prove to be very valuable when diagnosing gear defects. However, for the analysis of suspected gear problems, a high resolution spectrum analyser is required to enable a high frequency range spectrum to be taken without loss of sideband data. Sidebands are very important in gear fault detection as they also enable the analyst to determine which of the two meshing gears is faulty but they are normally only detectable with very narrowband analysis.

Due to variable unsteady shaft/gear rotating speed and load, the vibration signal collected from a WT gearbox is usually non-stationary and SB distance may vary with time. For WTs, the load can vary over a very wide range in less than a minute. As a result, the spectral composition of the collected vibration signal often changes with time and conventional Fourier analysis might be unable to reveal such characteristics. To overcome this

problem, the majority of current CMS used by the wind industry collects the signals within limited, pre-defined speed and power range. The use of signal sections selected for a particular load range allows spectra to be recorded in apparently stationary conditions.

3.6. Generator Condition Monitoring

3.6.1. Rotor Electrical Asymmetry

Established induction machine monitoring techniques, including Motor Current Signal Analysis (MCSA), typically use non-invasive, spectral-based machine terminal quantity analysis. Previous work (Tavner, 2008; Thomson and Fenger, 2001) showed that induction motor cage faults can be detected by either current or power analysis.

Steady-state winding fault detection in WRIGs based on analysis of readily available current or power signals has been widely researched (Crabtree et al., 2010a; Crabtree et al., 2010b; Djurović et al., 2009; Gritli et al., 2009; Shah et al., 2009; Stefani et al., 2008; Williamson and Djurović, 2009; Yazidi et al., 2010). The reported literature range from analysis of experimental data only, investigation based on both simulation and experimental data (Gritli et al., 2009; Shah et al., 2009; Stefani et al., 2008) or analytic explanations of the origins of fault frequencies (Gritli et al., 2009; Shah et al., 2009; Williamson and Djurović, 2009; Yazidi et al., 2010). Fault modelling was based on connecting either resistive or inductive elements to machine windings (Crabtree et al., 2010a; Crabtree et al., 2010b; Gritli et al., 2009; Stefani et al., 2008) or actual short and open circuit fault simulation (Shah et al., 2009; Williamson and Djurović, 2009; Yazidi et al., 2010). Changes in the WRIG stator and rotor current spectral content, originating from winding faults, were reported in (Crabtree et al., 2010a; Crabtree et al., 2010b; Djurović et al., 2009; Gritli et al., 2009; Stefani et al., 2008; Williamson and Djurović, 2009; Yazidi et al., 2010). Theoretical and

analytical explanations of fault frequencies and their generation were attempted in (Gritli et al., 2009; Williamson and Djurović, 2009; Yazidi et al., 2010). The analyses in (Djurović et al., 2009; Gritli et al., 2009; Stefani et al., 2008; Williamson and Djurović, 2009; Yazidi et al., 2010) focused on steady-state stator and rotor current signals to identify winding fault spectral indicators.

As part of this research, a valuable collaborative relationship has been forged within the SUPERGEN Wind Energy Technologies Consortium with the University of Manchester.

The University of Manchester has developed a time-stepped model of the machine including its construction, air gap field and harmonic conductor distributions, described in detail in (Djurović and Williamson, 2008; Djurović et al., 2009; Williamson and Djurović, 2009). The model incorporates a set of analytical expressions (Williamson and Djurović, 2009) which represent all frequencies in the current and power spectra of both wound rotor and doubly-fed induction machines. These expressions not only take into account basic fault frequencies present in the machine but also those that are dependent on air-gap field space harmonics from the machine layout and supply time harmonics in the stator current.

Based on this previous work, Djurović et al. (2012a) have investigated the influence of rotor electrical asymmetry on the stator line current and total instantaneous power spectra of WT-WRIGs and DFIGs. The research has been verified using experimental data measured on both Durham and Manchester test rigs, from 4-pole 30kW wound rotor induction machines, and numerical predictions obtained from the time-stepped DFIG electromagnetic model (Djurović et al., 2009). The Manchester rig operates as either a DFIG or WRIG at user-defined fixed speeds. The Durham rig features a WRIG with variable resistance in the rotor circuits, driven at either constant speed or with non-stationary, variable speed conditions. Both machines operated

synchronised with the grid with star connected rotor and stator windings. A steady-state study of current and power spectra for healthy and faulty conditions was initially performed to identify fault-specific signal changes and consistent slip-dependent fault-indicators on both test rigs. To enable real-time fault frequency tracking and give a clear indication of rotor electrical asymmetry in induction machines, a set of concise analytic expressions, describing fault frequency variation with operating speed, were then defined and validated by measurement. Simulation and experimental results confirmed that a convenient analysis and interpretation of identified fault frequencies in stator line current and power spectra lead to an effective rotor electrical fault detection and diagnostic procedure.

In particular, the work by Djurović et al. (2012a) has shown that rotor unbalance induces a change of considerable magnitude in a number of frequencies in the current and power spectra. These are $2sf_s$ sidebands on dominant spectral components, where f_s is the fundamental stator supply frequency and s is the induction generator fractional slip defined as

$$s = \frac{f_{syn} - f_{rm}}{f_{syn}} \tag{3.23}$$

where f_{syn} is the synchronous speed and f_{rm} is the actual mechanical speed of the rotor. These sidebands have been shown to be most pronounced at the fundamental and third harmonic of the supply frequency, in the case of stator line current spectra, and at the second harmonic of the supply frequency for total power spectra (Crabtree, 2011).

The identified fault-specific components are also present in healthy machine current and power spectrum, but with significantly lower magnitudes. During healthy machine operation these can originate from any pre-existing rotor excitation unbalance or inherent manufacturing imperfections (Djurović et al., 2009; Williamson and Djurović, 2009).

86

However, real current and power spectra can be complex, noisy and difficult to interpret. The frequency ranges have to be kept wide to ensure all relevant harmonics and sidebands are visible, resulting in unwieldy, difficult to interpret spectra which require individual impractical manual examination to observe a trend over time.

This Thesis builds on the research in Djurović et al. (2012a) to present a novel fault indicator, the Rotor Sideband Power Factor ($SBPF_{rotor}$), specifically developed to aid in the automatic detection of WRIG rotor asymmetry when analysing the non-stationary signals produced by modern WT variable speed operation. $SBPF_{rotor}$ reduces each FFT spectrum to only one parameter for each data acquisition and avoids time consuming manual spectra comparison (Zappalá et al., 2014a). This novel diagnostic method, discussed in detail in Section 5.4, is based on the frequency analysis of the stator terminal electrical current spectra presented by (Djurović et al., 2012a) and it has been shown to be a suitable tool for automatic diagnosis of WRIG rotor electrical asymmetry which could be easily embedded in current commercial WT CMSs.

Vibration and torque signal analysis for electrical fault detection has received significantly less attention in literature compared to the analysis of electrical signals. This is due to claimed lower sensitivity, but it was shown to be feasible for open-circuit faults in stator phase windings, as described in Djurović et al. (2012b) and Vilchis-Rodriguez et al. (2013a). Based on the principle illustrated in Djurović et al. (2012b) it follows that rotor electrical unbalances manifest themselves as electromagnetic torque oscillations as they pass through the stator magnetic field that can induce mechanical vibration at the same frequencies in the machine frame. Given the close relationship between torque and power the frequencies that appear in the torque spectrum, as consequence of rotor electrical asymmetry, should also be present in the power signal. Therefore, the frequencies resulting from the

rotor unbalance can be present in both the stator total power signal, as referred to in Djurović et al. (2012a), and the generator vibration signal (Djurović et al., 2012b). As the torque pulsations are transmitted as vibration to the machine frame, they could consequently be used to assist the conventional CMSs based on vibration analysis in achieving electrical fault detection and diagnosis. Building on these observations the Author has investigated the experimental analysis of generator vibration signature for rotor electrical unbalance detection and the possible development of automatic fault detection algorithms (Zappalá et al., 2014a). The details of this analysis are given in Chapter 5.

3.6.2.   Generator Bearing Faults

As part of the collaborative work with the University of Manchester, the Author has also developed a high sensitivity algorithm, the Harmonic Power Factor (*HPF*), for automatic generator bearing fault detection by using conventional FFT analysis of vibration data. The aim of the *HPF* algorithm is to automatically analyse and interpret the large volumes of bearing vibration spectra usually produced by a CMS in a WF, significantly reducing the large degree of manual analysis currently required. In this work, discussed in detail in Section 5.5., tests have been performed on the Manchester test rig and the Author has led the data analysis (Zappalá et al., 2014a).

In this section a brief summary of the bearing characteristic defects frequencies relevant for the analysis of the vibration data in this Thesis and underlying the development of the *HPF* algorithm is given.

The most popular type of bearing is rolling-element bearings. A bearing generally consists of four parts: an inner raceway, an outer raceway, a set of rolling elements (balls or rollers) and a cage. The rolling elements are used to maintain the motion between the fixed supporting structure (i.e. housing) and the rotating shaft. The geometry of rolling-element bearing is shown in

Figure 3.8 where D_c is the bearing pitch diameter, D_b is the rolling-element diameter and β is the contact angle. The contact angle β is defined as the angle between the line joining the points of contact of the roller and the raceways in the radial plane, along which the load is transmitted from one raceway to another, and a line perpendicular to the bearing axis.
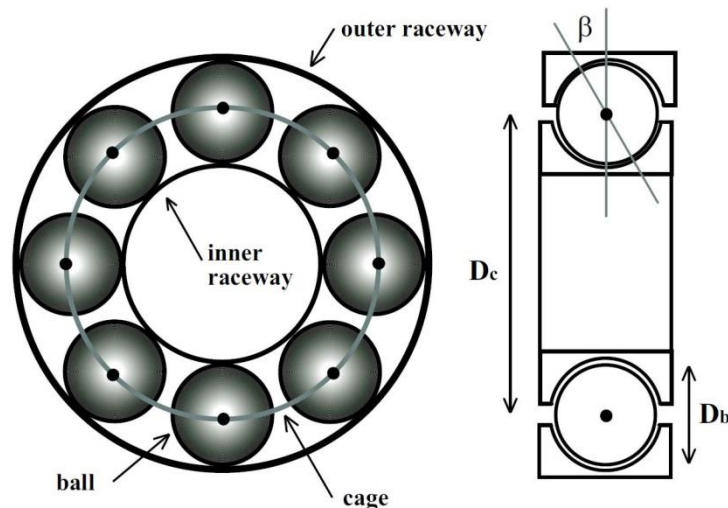
Figure 3.8: Geometry of a rolling-element bearing (Blödt et al., 2008).

The mechanical nature of a bearing fault is such that it results in vibration of the machine frame at predictable frequencies related to the machine's bearing geometry, rotational speed and fault location (Blödt et al., 2008). Consequently vibration analysis is the method conventionally used for bearing fault detection in current WT CMSs.

With each type of single-point bearing fault, a characteristic defect frequency can be associated. This frequency is equivalent to the periodicity by which an anomaly appears due to the existence of the fault. For example, in case the outer raceway is flawed, as the rolling elements move over the defect, a high-level short duration impulse is produced which causes the bearing to vibrate at a given frequency which is the rate at which the elements roll over the flaw.

Depending on the number of bearing rolling elements, the geometric relationship between its parts and their shaft rotational speed, f_{rot}, a set of defect characteristic rotational frequencies can be defined for the different bearing components. The inner and outer raceway ball passing frequencies for a rolling bearing, f_{BPFI} and f_{BPFO} respectively, are given by (Randall, 2011)

$$f_{BPFI} = f_{rot} \frac{N_b}{2} \left(1 + \frac{D_b}{D_c} \cos \beta \right) \tag{3.24}$$

$$f_{BPFO} = f_{rot} \frac{N_b}{2} \left(1 - \frac{D_b}{D_c} \cos \beta \right) \tag{3.25}$$

where N_b is the number of rolling elements. Depending if a bearing fault is located on the inner or outer raceway, vibration will be produced at one of the characteristic ball passing frequencies given by equations (3.24) and (3.25). These frequencies find their main application in CM, where the synchronous impulsive excitation caused by faults may be detected to give early warning of the onset of bearing failure.

Full mathematical derivations of the bearing component characteristic defect frequencies can be found in (Howard, 1994), however only equations (3.24) and (3.25) are relevant to the work presented in Section 5.5 of this Thesis.

3.7. Summary

The focus of this research is condition monitoring of WT gearboxes and generators, which, according to the WT reliability analysis presented in previous Chapter 2, are the drive train sub-assemblies that warrant the most attention. This chapter gave a short description of the WT gearbox and generator technology followed by a discussion of the main issues concerning their failure. Field observations have shown that one of the most common WT gearbox failure modes is gear tooth damage and that, although bearing faults

dominate total generator failures, rotor electrical asymmetry faults are significant for all WT generator sizes including the largest ones.

For vibration and electrical signals, it is often desirable to determine their spectral content in the frequency domain to reveal information not apparent by viewing them in the time domain. Spectral analysis is the most commonly used technique for CM in geared transmission systems and electrical machines, and has proved a valuable tool for fault detection and basic diagnosis.

The principles of the Fourier transform and the theoretical basis of signal processing and fault detection analytical techniques undertaken in this Thesis, and presented and discussed in detail next in Chapter 5, including the concepts of power spectrum and order analysis, were also introduced in this chapter.

Finally, a review of previous CM work on WT gearbox and generator fault detection from which this research originates was presented. Some of the most significant principles of the theory of faults in WT gearbox and generator were discussed. The main vibration source in geared transmission system and a basic analysis of modulated gear vibration signals were described together with the principles of spectrum analysis of electrical and vibration signals in case of generator rotor electrical asymmetry and bearing faults. The fundamental electrical and mechanical fault equations used in this Thesis were then derived.

4

Methodological Approach

4.1. Introduction

Chapter 2 has shown that reliable and cost-effective CM techniques, with automatic damage detection and diagnosis of the WT components, are critical for the successful, reliable exploitation of offshore wind power.

CM research in the field is often a difficult task. One of the difficulties in gaining practical industry experience of CM on real WTs is the lack of collaboration needed from WT operators and manufacturers due to data confidentiality, particularly when faults are present (Yang et al., 2010). Moreover, in the event that an operator allows access to WT CMS data for research purposes, the researcher must wait for a fault condition, but has no control over the nature and the severity of the fault, nor when it will occur.

The work presented in this Thesis is based on experimental research on small scale test rigs aimed at the investigation of CM signals and the development of convenient signal processing algorithms for automatic fault detection and diagnosis. Subsequent verification has depended on the availability from operators and OEMs of data from full-size, operational WTs or their components. Test rig results were obtained by the Author from the Durham Wind Turbine Condition Monitoring Test Rig (WTCMTR) to investigate gear tooth damage and rotor electrical asymmetry. Further experimental data, relative to generator bearing faults, have been provided to the Author for analysis and processing from the University of Manchester as part of a collaborative work within the SUPERGEN Wind Phase 2 Consortium.

The Durham and Manchester rigs were designed to act as a model for a WT drive train with the purpose of producing signals comparable to those encountered on an operational WT. The Durham rig features a WRIG driven at either constant speed or at non-stationary, variable speed conditions to reflect the stochastic effects of wind torque driving. The Manchester rig operates as either a DFIG or WRIG at user-defined fixed speeds. Seeded-fault conditions can be induced or removed from the test rig drive trains as required enabling several electrical and mechanical faults to be implemented repeatedly on demand and under controlled driving conditions. This allows to increase confidence when applying the developed algorithms to field data from operational WTs and to reduce uncertainty and risk in applying CM techniques automatically in the field.

A test rig in the laboratory environment presents a number of advantages over full-scale WT field tests. It provides a more accessible, reliable, controllable and economical test facility with the benefit of allowing additional instrumentation without the need for site access. This is particularly true for operational offshore WTs, where the collection of reliable data can be difficult.

In this chapter the methodological approach undertaken in this research is presented. The chapter begins by describing the Durham WTCMTR and the faults investigated in this Thesis. A summary of the experimental work carried out on the Durham WTCMTR is given. The rig was equipped with a commercial WT CMS, used for analysis purposes in this work, and this is described in detail. The collaborative experimental work undertaken at the University of Manchester is then presented. Finally, the methodology applied for data analysis and processing, leading to the development of automatic fault detection algorithms, is introduced together with the definition of an algorithm fault detection sensitivity function for the comparison of the results obtained under different fault conditions.

4.2. Durham Wind Turbine Condition Monitoring Test Rig

The Durham CM test rig was built in 2003 using funding from the New & Renewable Energy Centre (NAREC) in Blyth, now part of the Offshore Renewable Energy Catapult, and has been developed over several years.

The initial test rig configuration and its instrumentation is due to the postgraduate research of Michael Wilkinson who, assessed different measurement and signal processing techniques using both a 10 kW permanent magnet generator and a 30 kW induction machine (Wilkinson, 2008).

Significant improvements were made by Christopher Crabtree, as part of his postgraduate research, who refined the instrumentation, the signal conditioning and the control systems and reconfigured the test rig to be more robust but adaptable. A detailed description of the test rig and its instrumentation, including also its full specification, can be found in (Crabtree, 2011).

The rig, configured as a variable speed WT-driven WRIG, features a 54 kW DC motor driving a 4-pole, 30 kW WRIG through a two-stage gearbox with the gear ratio of 1:5. A schematic diagram of the rig is shown in Figure 4.1 and two photographs are shown in Figure 4.2. The DC machine simulates the WT rotor input. Its speed is controlled through a Eurotherm 590+ variable speed DC drive, either manually or remotely using a National Instruments (NI) LabVIEW control environment, allowing the test rig to be driven under either constant or variable, transient conditions. The test rig generator is a wound rotor singly fed induction machine, which can be synchronised with the grid through a contactor circuit. In this configuration, while the DC drive is controlled with a speed feedback loop using a DC tachometer, there is no control on the generator-side which is open loop. The

rig is equipped with an SKF WindCon 3.0 unit, a commercial CMS currently used on full-size operational WTs.

Recently, during his postgraduate research, Mahmoud Zaggout has further developed the test rig closing the generator control loop with a Voltage Source Converter, allowing the rig to operate as a fully variable speed WT-driven DFIG (Zaggout, 2013).

Currently, the test rig is configured to run as a variable speed WT-driven WRIG or DFIG depending on the user.
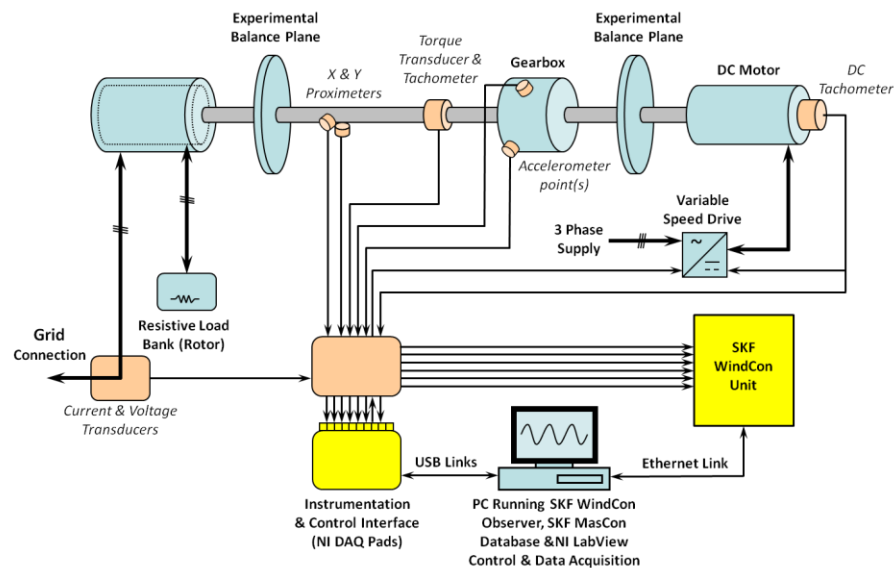
Figure 4.1: Schematic diagram of the Durham WTCMTR equipped with the gearbox (Crabtree, 2011).
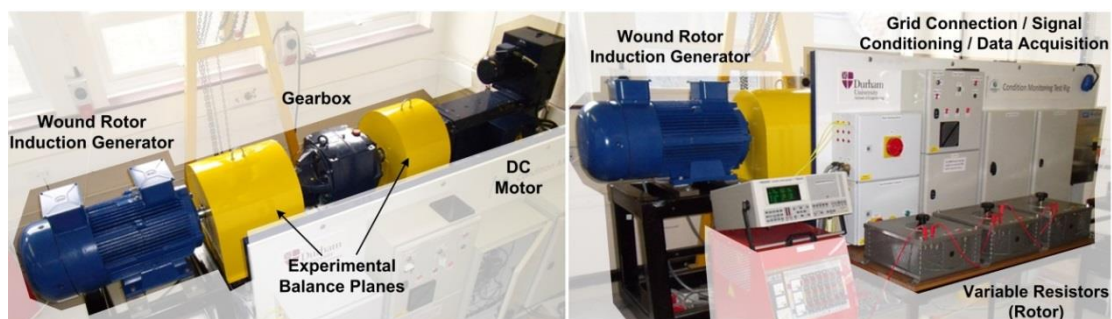
Figure 4.2: Durham WTCMTR equipped with the gearbox: main components, instrumentation and control systems (Crabtree, 2011).

This Thesis is based on experimental research conducted on the WTCMTR configured as a variable speed WT-driven WRIG. The WTCMTR configuration equipped with the gearbox, shown in Figure 4.1 and Figure 4.2, was used to acquire data for this project with the aim of investigating gear tooth damage. Another set of experiments were performed using this same configuration but with the gearbox removed with the aim of investigating rotor electrical asymmetry, this allowed the generator to carry a higher applied load. A schematic diagram of the rig without gearbox is shown in Figure 4.3 and two photographs are shown in Figure 4.4.
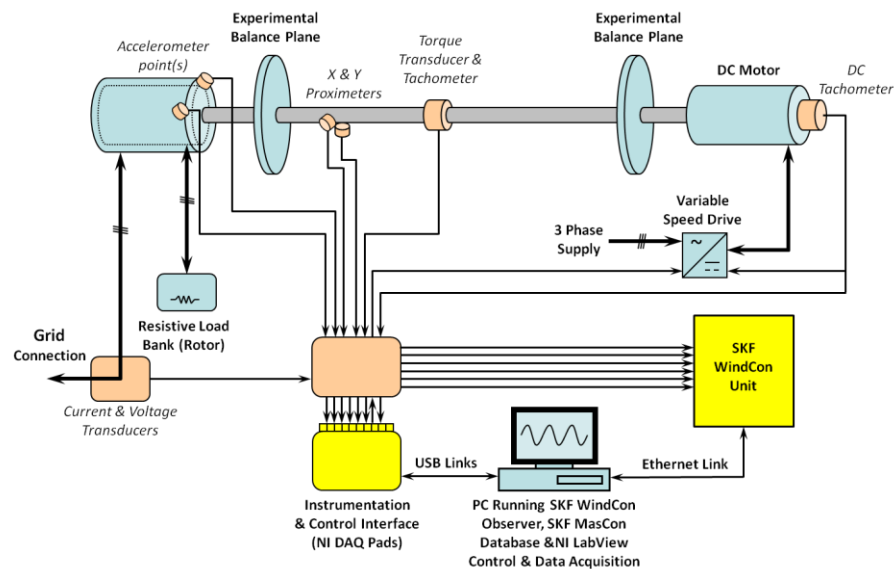
Figure 4.3: Schematic diagram of the Durham WTCMTR without gearbox.

Figure 4.4: Durham WTCMTR without gearbox: main components, instrumentation and control systems.

The WTCMTR and its evolution to the current configuration over the last 10 years has been described very thoroughly in (Crabtree, 2011; Wilkinson, 2008; Zaggout, 2013). This chapter gives only a detailed description of the main test rig mechanical and electrical components and its instrumentation relevant to the experimental work presented in this Thesis.

4.2.1.   Gearbox

The WTCMTR gearbox is a two-stage helical gears parallel shaft unit manufactured by a Brook Hansen Transmissions, with the catalogue number of SFN64E. The nomenclature for the gearbox internal elements and the gear teeth number are described in the schematic in Figure 4.5 and listed in Table 4.1.

The gearbox was configured such that the LSS was at the DC motor end. This reflects the arrangement of a geared WT, where the blades are on the high torque, LSS and the generator is on the lower torque, higher speed shaft.
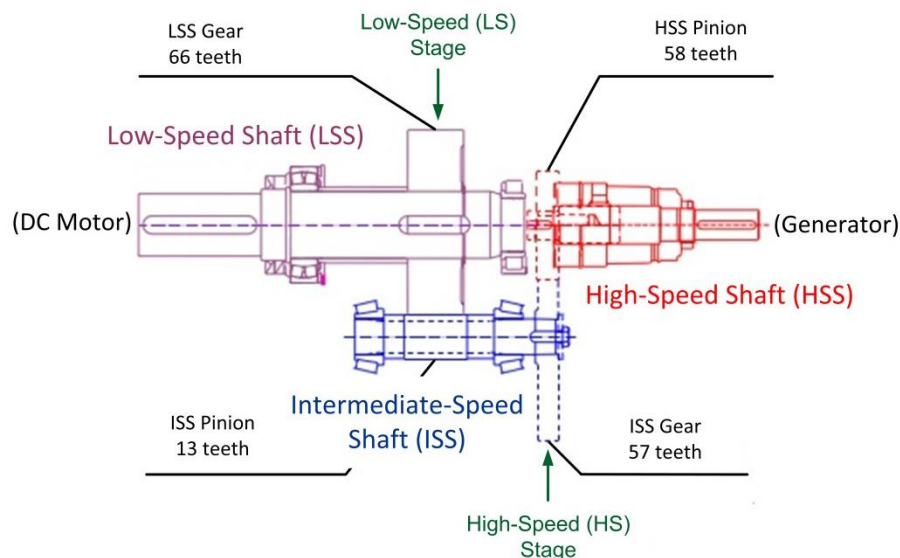
Figure 4.5: Schematic diagram of the Durham WTCMTR gearbox transmission stages (not in scale), adapted from (Hsu, 2008).

Table 4.1: Durham WTCMTR gearbox nomenclature and teeth number.

Gear Element	Location	Number of Teeth	Mate Teeth	Ratio
LSS Gear	LS Parallel Stage	66	13	–
ISS Pinion	LS Parallel Stage	13	66	–
				5.077
ISS Gear	HS Parallel Stage	57	58	–
HSS Pinion	HS Parallel Stage	58	57	–
				0.983
Overall ratio				4.9894

The gearbox first low-speed (LS) stage with 66/13 teeth and the second high-speed (HS) stage with 57/58 teeth provide an overall gear ratio of 1:4.9894 between input and output shafts, referred to as 1:5 for simplicity.

Since this is a two-stage transmission system, there are two machine speed dependant gear meshing frequencies, which, based on the information in Figure 4.5 and Table 4.1, can be calculated using equation (3.16):

1. the LS stage meshing frequency, $f_{mesh,LS}$, corresponding to the LSS Gear and the ISS Pinion mesh, given by

$$f_{mesh,LS} = 66 f_{LSS} = \frac{13}{57}(58 f_{HSS}) \qquad (4.1)$$

2. the HS stage meshing frequency, $f_{mesh,HS}$, corresponding to the ISS Gear and the HSS Pinion mesh, given by

$$f_{mesh,HS} = 58 f_{HSS} = \frac{66}{13}(57 f_{LSS}) \qquad (4.2)$$

where f_{LSS} and f_{HSS} are the LSS and HSS rotational frequencies, respectively.

4.2.2. Induction Generator

The WTCMTR generator is a 3-phase, 4-pole WRIG rated at 30 kW, manufactured by Marelli Motori, with the catalogue number of E4F 225 M4 B3. The power output from the generator stator is directly fed into the three-phase mains.

As seen in Section 3.3, modern WT generators are typically WRIGs configured as DFIGs. However, the control of such a machine is complex and in the test rig application presented in this Thesis it has been simplified to facilitate the CM research. The slip-ring rotor allows the electrical characteristics of the rotor to be influenced from the outside. By changing the electric resistance in the rotor circuit, greater slip can be attained and with it a degree of speed compliance for direct coupling to the fixed-frequency grid. A generator speed increase can be achieved by adding resistance into the rotor circuit using external controlled resistors (Hau, 2006).

The rig WRIG was operated with the rotor circuit coupled via slip-rings to an adjustable three-phase resistance load bank, shown in Figure 4.2 and Figure 4.4, rather than as a fully controlled DFIG (Crabtree, 2011). Connection of external controlled resistors to the rotor circuit allowed variation of the generator torque-speed characteristics.

Figure 4.6 shows the torque-speed characteristics for the two WTCMTR configurations considered in this Thesis, i.e. equipped with or without the gearbox, for different values of rotor resistance with the corresponding generator electrical power limits. Data were collected using a power analyser connected on the stator output and a Magtrol 3410 Torque Display to give the generator shaft speed and torque, with the generator being driven up to the limit of the driving DC machine armature current of 131 Amps. The rig generator rotor itself has a resistance of 0.032 Ω per phase (including winding

and brush-gear resistances) and, as a result, the possible slip speed variation is very small, given the limitations of the driving motor.
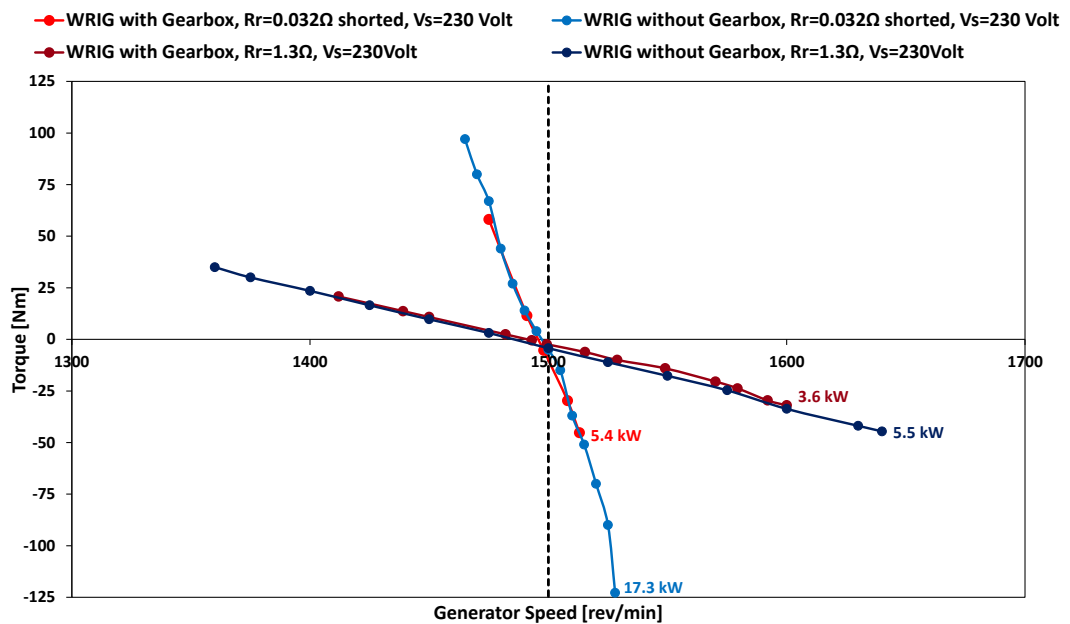
Figure 4.6: Test Rig Generator torque-speed characteristics showing electrical power limits.

In this research, in order to simulate the speed variation representative of real WT wind conditions and test the necessary signal processing techniques, the balanced 3-phase rotor resistances of the generator were increased by the adjustable external resistors connected into the rotor circuit via the machine slip-rings. Balanced rotor phase resistances of 1.3 Ω allowed a super-synchronous generator speed variation of around 100 rev/min, from 1500 to 1600 rev/min, which will be acceptable for experimental CM research purposes.

It should be emphasised that with the generator driven through a gearbox the DC motor delivered torque at a lower speed and the armature current limit was reached at lower generator torque. With the generator driven without a gearbox higher generator speed, torque and power range were achieved.

4.2.3. Instrumentation and Data Acquisition

This section gives a brief overview of the WTCMTR instrumentation, described in detail by Crabtree (2011), which was suitable for use in this research. In particular, the focus is on the transducers used to investigate the gearbox and generator fault conditions in this work and the test rig data acquisition environments.

The test rig is instrumented with a wide range of transducers:

- A Magtrol TMB 313/431 torque transducer, positioned on the high-speed shaft, with a rated torque of 500 Nm and sensitivity of 10^{-2} V/Nm. The transducer is capable of outputting 60 pulses per revolution and it is then also used as shaft pulse tachometer. A frequency to voltage converter was implemented giving linear operation over the required speed range. Additionally, a frequency divider circuit was included to ensure the speed pulse signal was within range for the SKF WindCon digital input (Crabtree, 2011).

- A DC motor tachometer supplied by Eurotherm Drives, fitted to the DC machine no-load side end-plate, to give the LSS speed reading and to provide speed feedback to the Eurotherm drive. The DC tachometer signal is primary for reference rather than analysis. It contained low frequency commutator noise which was removed by using a 20 Hz low pass filter (Crabtree, 2011).

- Two Brüel&Kjaer 4513-002 Deltatron accelerometers. These are piezoelectric Shear accelerometers with integral electronics, a sensitivity of 500 mV/g, a frequency range of 1 to 10 kHz and 10 g peak dynamic measuring range. They can be placed at various points on either the gearbox or generator. These transducers do not require any additional signal conditioning apart from their standard charge amplifiers.

- Transducer boards installed to measure the three phase generator stator terminal voltages and currents. The transducers produce a voltage proportional to the corresponding measured value. The bandwidth of these transducer boards is DC-100 kHz.

- Two Kaman KD2300-4S1 proximeters located at 90° to each other on the HSS at the generator end measuring the vertical and horizontal shaft displacement. The transducer bandwidth is 0 to 50 kHz. These eddy current sensors do not require additional signal conditioning other than their standard charge amplifiers.

In order to minimize experimental noise from the laboratory environment and improve the safety for the operator, all instrumentation was isolated from mains voltage electrical signals and power supplies within lockable steel cabinets.

The rig is equipped with two independent Data Acquisition Systems (DASs).

1. Signals from transducers positioned along the drive train are transmitted to two NI 6015 data acquisition (DAQ) pads which are in turn connected, via shielded USB connection, to the NI LabVIEW environment which also operates as control environment of the rig, as described in detail next in Section 4.2.4. The DAQs perform A/D conversion of signals from sensors and D/A conversion of signals from the computer. The DAQ pads are configured to record 15 data channels, with a sampling frequency of 5 kHz. The data recorded are: timestamp, DC motor speed and armature current, HSS speed and torque, three stator phase voltage waveforms, three stator line current waveforms, vertical and horizontal shaft proximeter signals and two accelerometer signals. The phase stator terminal voltages and currents are combined in LabVIEW to give the generator electrical power using the two-wattmeter method.

2. Signals from the transducers are also recorded and processed by an SKF WindCon 3.0 unit, a commercial CMS used in WT industry, which has been used for analysis purposes throughout this work. The test rig was implemented with the WindCon CMS for comparison with industrial data and results. Its main features are described in detail next in Section 4.5.

4.2.4. Control and Driving Conditions

The test rig is controlled from the NI LabVIEW environment, developed by Crabtree (2011). The LabVIEW environment allows the operator to run the machine up to its synchronous speed before waiting for confirmation of grid connection and running up to the test starting speed.

The driving speed is read from a spreadsheet containing a time and speed vector defined by the operator. The LabVIEW control environment then transmits a control signal, proportional to speed demand, to the Eurotherm variable speed drive in real time.

The WTCMTR can be operated either at constant or variable speed depending on the operator's requirements.

Variable speed machine testing is performed by using the driving data derived from a WT model. This model, developed by the University of Strathclyde, as part of the SUPERGEN Wind Energy Technologies Consortium, incorporates the properties of natural wind and the mechanical behaviour of a 2 MW variable speed WT operating under closed-loop conditions. A variety of wind speeds and turbulence intensities, defined as the measure of the overall level of turbulence (Burton et al., 2011), were applied to the model. The driving conditions were then scaled to the test rig based on the generator speed data from the model (Crabtree, 2011).

As discussed earlier in Section 3.3, typically in a variable speed WT 4-pole DFIG the window of speed variations is approximately ±30% around the synchronous speed. WTs usually operate under generator speed control, below rated wind speed, and under blade pitch control above rated wind speed. In the case of the experimental research presented in this Thesis, the WTCMTR has been configured as a variable speed WT-driven WRIG operating entirely in super-synchronous mode, above 1500 rev/min. However, the use of the 2 MW variable speed WT driving model has allowed the simulation of the different dynamic speed behaviours that a full-size WT 4-pole DFIG exhibits both below and above rated wind speed.

Scaled generator variable speed signals used for testing in this research, shown in Figure 4.7, are

1. 7.5 m/s mean, 6% turbulence intensity, representative of a low mean wind speed with low turbulence, with the WT operating at or below rated wind speed under generator speed control;

2. 15 m/s mean, 20% turbulence intensity, representative of a high mean wind speed with high turbulence, with the WT operating above rated wind speed under blade pitch control.
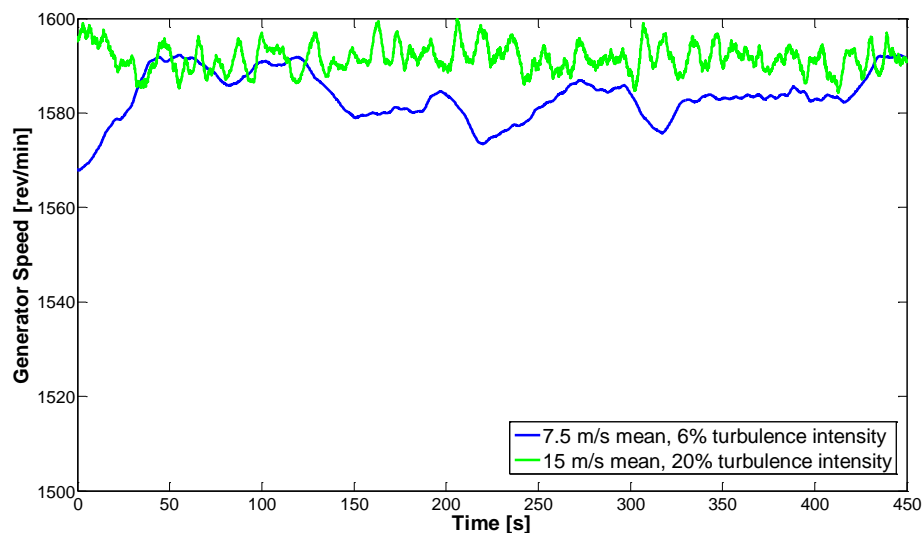
Figure 4.7: WTCMTR generator variable speed test conditions.

4.2.5. Previous Fault Detection Algorithm Work

The WTCMTR has been used successfully to investigate various electrical and mechanical drive train faults over the last few years.

Wilkinson (2008) applied various mechanical and electrical fault-like perturbations to the test rig operated with two different generators: a 10 kW permanent magnet generator, to represent a direct-drive WT, and a 30 kW induction machine, operated as a WRIG, to represent a geared-drive WT. The aim of that research was to investigate different measurement and signal processing techniques and their fault detectability.

Two frequency tracking algorithms for the analysis of discretely sampled CM signals have been developed and proved successful on data from the Durham test rig configured as a variable speed WT-driven WRIG:

- the adaptive Localised Continuous Wavelet Transform algorithm, CWT_{local}, initially proposed by Yang et al. (2010) and then further developed by Crabtree (2011);
- the Iterative Localised Discrete Fourier Transform algorithm, $IDFT_{local}$, developed by Crabtree (2011).

The fundamental idea of these algorithms was to reduce the computing demand for standard signal processing by tracking only the speed-dependant fault-related frequencies of interest in non-stationary monitoring signals, rather than analysing wide frequency bandwidth signals.

The CWT_{local} and the $IDFT_{local}$ algorithms were used to post-process the electrical and mechanical data recorded from the LabVIEW data acquisition system under three fault-like conditions:

- WRIG rotor electrical asymmetry;
- High-speed gear tooth damage and ultimate failure;
- High-speed shaft mass unbalance.

105

The comparison between the two algorithms in terms of clarity of result and computational intensity showed that, although the CWT_{local} produced a slightly improved result for gear tooth fault detection, given the impulsive nature of the response in vibration signals, the processing time required was significant and considered to be impractical for continuous application on large WT populations. The $IDFT_{local}$ algorithm produced results of better quality for rotor electrical asymmetry and high-speed mass unbalance with reduced computing time. However, the main $IDFT_{local}$ limitations were the requirement for off-line analysis to achieve implementation, the inability to discriminate fault severity, particularly in the case of gear tooth failure, and the relatively low detection sensitivity of its results.

This Thesis builds on the previous research done on the Durham WTCMTR, configured as a variable speed WT-driven WRIG, to develop advanced high sensitivity algorithms specifically designed to aid in the automatic on-line detection of mechanical and electrical faults when using field fitted commercial WT CMSs. Test rig data are analysed and processed by using a commercial WT CMS, further demonstrating the practicability of what is being proposed.

4.3. Faults Investigated

In this research seeded-fault testing was performed on the Durham WTCMTR to investigate mechanical and electrical conditions.

Two classes of faults were applied to the test rig:

- High-speed pinion tooth damage, representing the effect of a mechanical fault in the WT gearbox;
- Generator rotor electrical asymmetry, representing the effect of a winding fault, brush imbalance or air gap eccentricity in the WT generator.

106

A further class of faults will be considered on a test rig at Manchester:

- Rotor bearing damage in the WT generator.

4.3.1.   High-Speed Pinion Tooth Damage

As discussed earlier in Section 3.2, timely and reliable detection and diagnosis of the developing gear defects within a gearbox is an essential part of minimising an unplanned WT downtime. In order to develop algorithms suitable for on-line WT gearbox CM, experimental research was conducted in the controlled laboratory environment.

Thanks to the WTCMTR gearbox construction, its HSS pinion and the output shaft can be removed as one assembly without the need to remove the complete gearbox from the test rig, as shown in Figure 4.8. This allowed the easy investigation of high-speed pinion tooth damage through seeded-fault testing, as shown in Figure 4.8(d), such faults being introduced by manual filing based upon photographs from actual damage to WT gearbox gear teeth. A replica gear manufactured externally was used to exactly replace the original Hansen pinion.

Experiments were conducted to investigate the progression of a tooth defect on the gearbox HSS pinion, which was introduced into the WTCMTR at constant or variable generator load and constant or variable speed. The behaviour of a healthy pinion and of four faults of increasing severity were investigated by introducing progressive damage to the leading contact edge of one tooth of the gearbox HSS pinion.
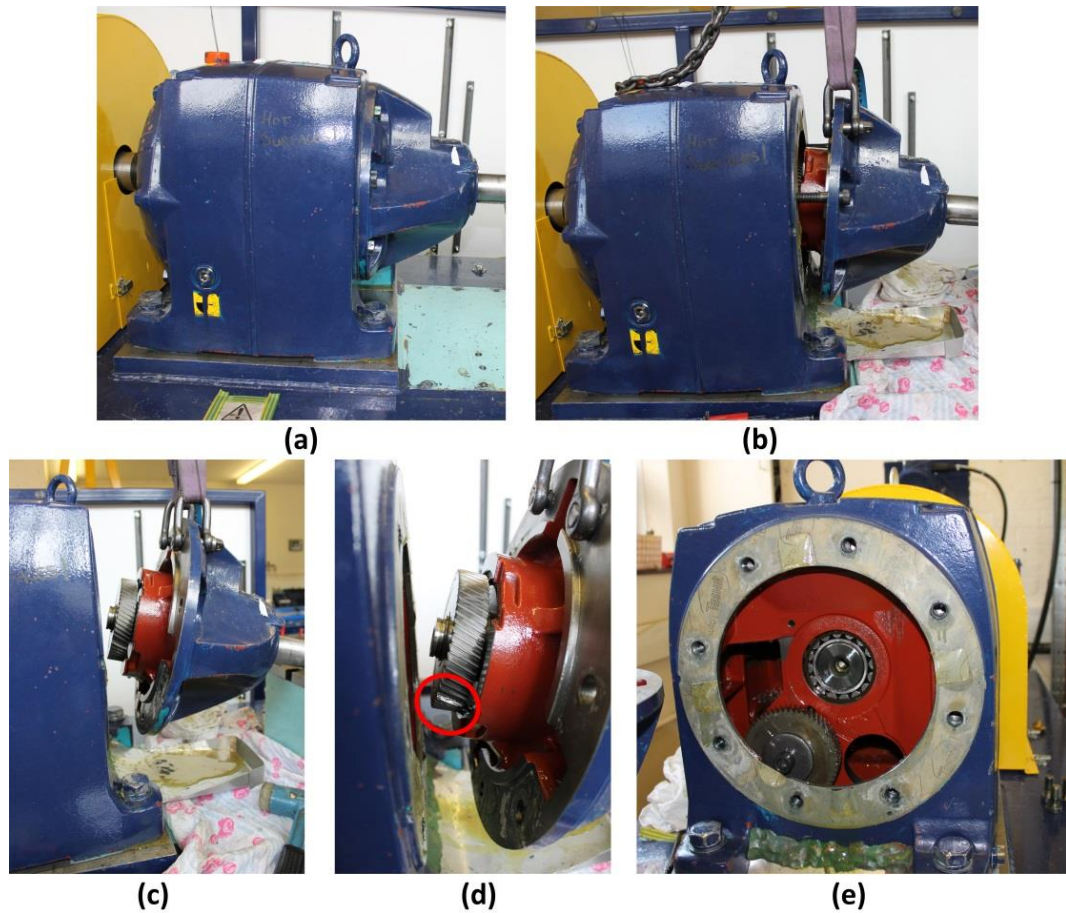
Figure 4.8: (a) WTCMTR gearbox; (b) and (c) High-speed shaft and pinion assembly; (d) Detail of applied seeded-fault used for testing; (e) Gearbox internal construction.

The gearbox high-speed assembly was removed between each test and the next fault ground by hand to give four faults of increasing severity, with a geometry based upon observed damage of full-size WT gearboxes. The fault was progressively moved across the tooth face until the entire tooth was removed except for a small amount of the root, based upon practical knowledge of the progression of gear teeth faults. Figure 4.9(a) shows the healthy pinion, Figure 4.9(b)–(d) show the early stages of tooth wear, while Figure 4.9(e) depicts the entire tooth missing.
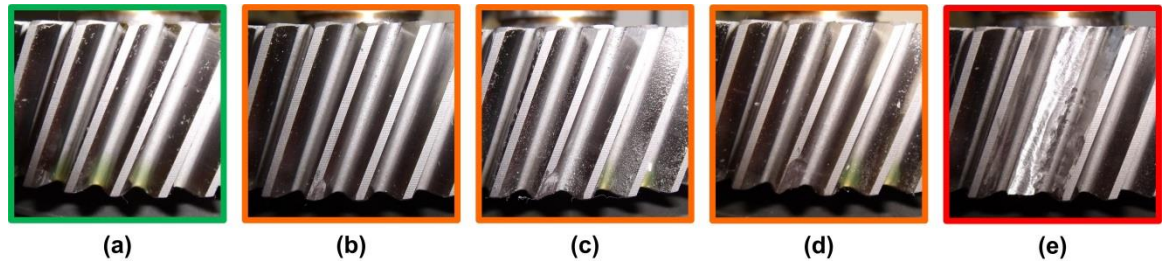
Figure 4.9: HSS pinion conditions investigated during the seeded-fault tests: (a) healthy; early stage of tooth wear: (b) 3 mm x 2 mm chip; (c) 5 mm x 5 mm chip; (d) 7 mm x 5 mm chip; (e) missing tooth.

4.3.2. Rotor Electrical Asymmetry

Different fault conditions including rotor winding, brush-gear or slip-ring defects in a WRIG typically result in uneven rotor current distributions, causing rotor electrical asymmetry (Djurović et al., 2012a). As discussed earlier in Section 3.3, according to Alewine and Chen (2010), rotor faults are significant for all WT generator sizes, second only to bearing faults in medium scale WTs (1-2 MW).

In this research, in order to develop algorithms suitable for on-line WT generator CM, experimental research was conducted in the controlled laboratory environment to investigate rotor resistive unbalance. Experiments were performed using the WTCMTR configuration with the gearbox removed shown schematically in Figure 4.3. Rotor electrical asymmetry was simulated on the test rig WRIG by using a load bank externally connected to the rotor circuit via the machine slip-rings to vary the resistance into one rotor phase winding circuit. An experimental resistive load bank, shown in Figure 4.4, has been designed and installed on the test rig under the direction of the Author. The load bank allows an increase of the rotor balanced phase resistances, for a wider generator speed variation, and small asymmetry to be introduced into one phase of the rotor circuit in a more controllable fashion compared to the fully variable 0-4 Ω resistors used in the original test rig configuration, shown in Figure 4.2.

The details of the generator rotor circuit taking into account the external resistive load bank are shown in Figure 4.10.
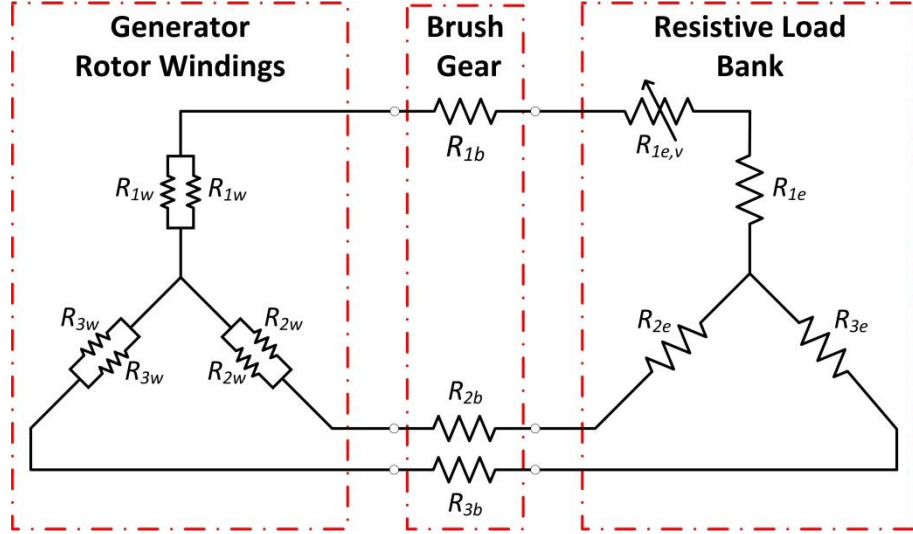
Figure 4.10: WRIG rotor circuit diagram.

From Figure 4.10, the balanced rotor phase resistances, R_{1h}, R_{2h} and R_{3h}, are given, respectively, by

$$R_{1h} = \frac{R_{1w}}{2} + R_{1b} + R_{1e} \tag{4.3}$$

$$R_{2h} = \frac{R_{2w}}{2} + R_{2b} + R_{2e} \tag{4.4}$$

$$R_{3h} = \frac{R_{3w}}{2} + R_{3b} + R_{3e} \tag{4.5}$$

where, R_{1w}, R_{2w} and R_{3w} are the three rotor winding phase resistances, R_{1b}, R_{2b} and R_{3b} are the three rotor brush-gear phase resistances and R_{1e}, R_{2e} and R_{3e} are the three external resistances.

The phases are balanced, giving

$$R_{1h} = R_{2h} = R_{3h} = 1.4\Omega \tag{4.6}$$

The rotor resistance per phase when balanced is 1.4 Ω here, slightly higher in magnitude than that previously used for the investigation of gearbox fault and set through the original test rig external fully variable resistors, i.e. 1.3 Ω.

The resistive load bank allows fault levels to be implemented on the test rig by adding a variable external resistance, $R_{1e,v}$, to phase 1 of the three-phase rotor circuit. The faulted phase 1 resistance, R_{1f}, is given by

$$R_{1f} = \frac{R_{1w}}{2} + R_{1b} + R_{1e} + R_{1e,v} \tag{4.7}$$

Since the rotor circuit is star connected, the absolute rotor electrical asymmetry, δR, can be described by

$$\delta R = \left| R_{1f} e^{i\theta_1} + R_{2h} e^{i\theta_2} + R_{3h} e^{i\theta_3} \right| \tag{4.8}$$

where $i = \sqrt{-1}$, $\theta_1 = 0$, $\theta_2 = \frac{2\pi}{3}$ and $\theta_3 = \frac{4\pi}{3}$.

The rotor electrical asymmetry, ΔR, can be expressed as a percentage of the balanced phase resistance by

$$\Delta R(\%) = \frac{\delta R}{R_{1h}} \times 100 = \frac{\delta R}{R_{2h}} \times 100 = \frac{\delta R}{R_{3h}} \times 100 \tag{4.9}$$

In this work, for experimental purposes, two fault levels were implemented on the test rig by successively adding two additional external resistances of 0.3 Ω and 0.6 Ω, respectively, to phase 1 of the rotor circuit through the external load bank. According to equation (4.9), these gave 21% and 43% rotor electrical asymmetry, respectively.

The asymmetry levels investigated in this research compare favourably to levels used in previous rotor electrical unbalance or brush-gear damage work such as Djurović et al. (2012a), Gritli et al. (2009) and Stefani et al. (2008).

4.4. Summary of experiments

For each fault investigated, the test rig was operated such that tests were carried out for each healthy or faulted condition for each driving condition. In particular, the DC motor was driven at constant and wind-like variable speed conditions, at low wind speed, low turbulence and high wind speed, high turbulence, Figure 4.7, to cover the super-synchronous generator speed range allowed by the external variable resistors connected to the rotor circuit.

The experimental work performed on the Durham WTCMTR during the research described in this Thesis is summarised in Table 4.2. For each seeded-fault investigated, the WTCMTR configuration used for testing, the fault levels investigated, the test conditions and the corresponding CM signal analysed are defined.

Table 4.2: Summary of the experimental work performed on the Durham WTCMTR.

Seeded-fault	WTCMTR configuration	Fault Level	Generator Speed	Test Duration	Balanced Rotor Phase Resistances	Generator Max Power Output	CM signal
HSS Pinion Tooth Damage	WRIG driven through the gearbox (Figure 4.1)	Healthy 3x2 mm Chip 5x5 mm Chip 7x5 mm Chip Missing Tooth	Constant, ranging between 1500-1600 rpm with a 5 rpm step Variable, 7.5 m/s, 6% turb. 15 m/s, 20% turb.	300 s 450 s	1.3 Ω	3.6 kW	Vibration from a single axis, vertically mounted accelerometer on the gearbox high-speed end
Rotor Electrical Asymmetry	WRIG driven without gearbox (Figure 4.3)	Balanced Rotor 21% Asymmetry 43% Asymmetry	Constant, ranging between 1500-1600 rpm with a 10 rpm step Variable, 7.5 m/s, 6% turb. 15 m/s, 20% turb.	300 s 450 s	1.4 Ω	3.4 kW	Stator line current Vibration from two accelerometers on the generator load side end-plate

4.5.   Data acquisition: SKF WindCon System

In this research, signals from the transducers were recorded and processed by using an SKF WindCon 3.0 unit, a commercial CMS producing FFT spectra, as currently used on the full-size operational WTs. This was done to demonstrate that the research proposals in this Thesis could be implemented on a practicable, industrial CMS.

Figure 4.11 shows the operational structure of the SKF WindCon system installed on the test rig. MasCon 16W is the WindCon hardware and has 16 analogue and 2 digital inputs. Each channel is equal to a sensor input. In its current configuration there are 6 active analogue channels enabled in MasCon configured to record: the vertical and horizontal shaft proximeter signals, the 2 accelerometer signals (named Accelerometer 1 and Accelerometer 2, respectively), HSS torque and one phase stator line current.
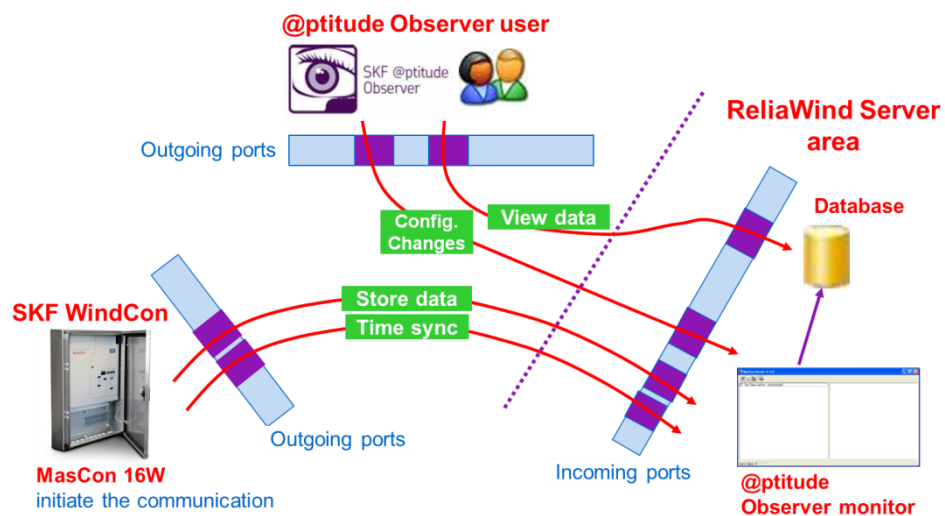
Figure 4.11: Architecture of the SKF WindCon system installed on the WTCMTR.

For operation and analysis purposes the system requires that a pulsed speed signal be applied to one of the digital inputs as a reference signal for other measurements and as a trigger for Fourier transform analysis, as all

frequency analysis and diagnosis is reliant on the machine operating condition. For the test rig this requirement is met by the shaft tachometer signal, set as a digital channel, named Generator Speed, with 60 pulses per revolution.

The configuration of the MasCon unit can be done remotely via the WindCon software, SKF @ptitude Observer, which has been installed by the Author to replace the old SKF ProCon version. This software is also used for data management and analysis. Data are stored on a recently built dedicated server, called ReliaWind, accessible, via @ptitude Observer, across the Durham University School of Engineering and Computing Science network. @ptitude Observer Monitor is the server software which works as the connector between MasCon system, database, and @ptitude Observer users. This software performs the communication and database storage allowing the use of @ptitude Observer as an on-line system.

Different types of measurement points are available and can be performed in the channels of the WindCon MasCon 16W unit. Several measurement points can be attached to one channel. They are classified into two main categories, details of which are available in (SKF Reliability Systems, 2010):

- Spectra and time waveform based measurement points, which include Vibration, Envelope, Harmonic, Process FFT;
- Trend based measurement points, which include Process, Speed, Running hours, Counts, Counts rate, Derived point.

For the purpose of this research, according to the sensors currently connected to the test rig, 7 measurement points have been set and are listed in Table 4.3.

Main feature of the vibration points in WindCon is the possibility to set the spectral analysis, which is carried out using FFT and so requires

stationary input signals. In order to analyse CM data of variable speed and load WTs, for each point the spectral analysis can be configured according to an active range, which sets the limits for operating conditions under which spectra are sampled. In particular, the measurement point active range is set in terms of speed, load and the allowable change in these during the measurement period. In this way quasi-stationary signals can be processed avoiding issues associated with variable speed and load conditions and increasing the confidence in the resultant spectra which are directly comparable by the operator. During the test rig operation, time series data have been configured to be recorded at 0.08 minute intervals, while spectra from the vibration signals at 1 minute intervals, when the speed is within the active range set in the spectral analysis settings.

Table 4.3: Test rig WindCon system measurement point configuration.

Measurement Point Name	Point Type	MasCon Channel
HSS Speed	Speed	Generator Speed (digital)
HSS Torque	Process	HSS Torque
Accel1	Vibration	Accelerometer 1
Accel2	Vibration	Accelerometer 2
Line Current	Vibration	Line Current
VertProx	Vibration	Vertical Proximeter
HorizProx	Vibration	Horizontal Proximeter

The Observer software features a powerful diagnostic tool, the *machine parts*, which allows the creation of a mechanical model of the machine, where the features of its main components can be specified, as, for example, the gear type and tooth number. The software also features a large bearing database which stores geometrical data from approximately 20,000 different bearings

from several different manufacturers. This allows detailed specifications to be attached to each individual bearing. The WTCMTR mechanical model is shown in Figure 4.12.
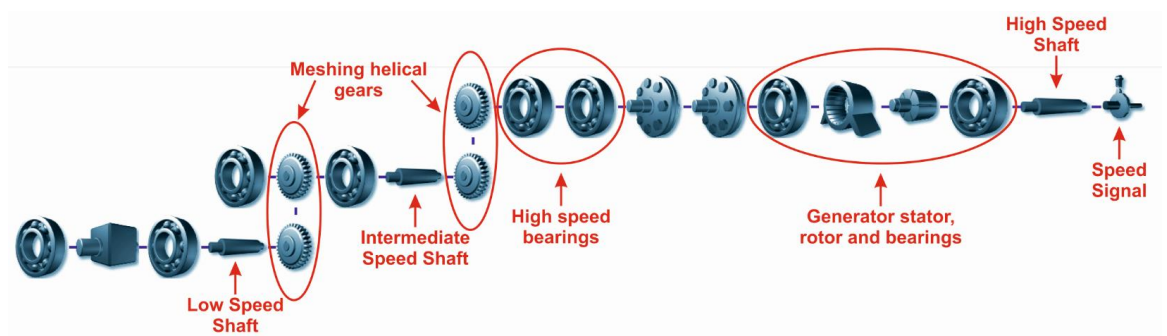
Figure 4.12: SKF Observer machine parts of the Durham WTCMTR, equipped with the gearbox, including main component of interest.

The machine parts mechanical data provides a tool aiding the user to automatically calculate the characteristic frequency signature of each component at any rotational speed. For a given FFT spectrum, the component-specific, speed dependent characteristic fault frequencies can be easily identified by selecting them from a menu of all possible components in the machine diagram and displayed as vertical bars. The cursor function enables user to select peaks, harmonics and sidebands in the spectrum to aid FFT interpretation and to increase the diagnostic capability of frequency analysis. A harmonic cursor is a set of markers indicating all members of a specific harmonic family with a very fine resolution. A sideband cursor similarly depicts a family of sidebands with a given spacing around a specified central carrier frequency (Randall, 2011). The software built-in diagnostic system also provides the user with the probability that a selected unidentified frequency in a spectrum, including harmonics, belongs to a specific machine part. This allows the identification of the part of the machine which causes a high peak at a specific frequency.

As a result, the software user, however inexperienced, has a much improved ability to understand vibration spectra from the complex drive train

and to find out which machine component is generating a certain anomaly in the frequency spectra. However, accurate fault detection and diagnosis still require time-consuming and costly manual analysis for spectra comparison as specialised knowledge is required for signal interpretation.

For each measurement point, individual automatic or adaptive warning and alarm settings can be configured in Observer. The level for the active alarms can be set by the user or automatically calculated by the system after a minimum specific number of historical values have been stored in the database. The alarms can be used to give an overall picture of the machine health, but do not necessarily indicate the exact location of a fault, due to their general nature. In order to speed up the diagnostic process, alarms can be set based on the fault frequencies for different components within the drive train. However, recent work about the use of WindCon on operational onshore WTs in the field (Crabtree, 2011) has shown that, given the WT noisy variable speed and load environment, alarms could not be relied upon with any great confidence and, albeit following an alarm signal, faults always required manual investigation in order to gain confidence in the result.

The current status of the machine can be visualised through the *process overview* graphic interface, configured to display the rig measurement point alarm status. For operational onshore and offshore WTs, once reliable and effective alarms are set, the process overview represents an easy to use and understandable tool for control rooms and operators.

The software also features the machine *diagnosis* tool, including ready-made formulas which link together frequencies and harmonics with the correct machine part and correct cause of error. Sophisticated built-in diagnosis rules, derived from SKF's understanding and experience of rotating machine diagnostics, can be applied using defect frequencies of the whole machine, with individual alarm level for each overall or enveloped vibration measurement point and for each type of fault. Customized diagnosis rules can

also be created by the software user. In the diagnosis display, all the different diagnoses attached to a measurement point and calculated using the spectrum data stored in the database, are trended and are related to the alarm level set by the user. This allows displaying and following the progression of machine faults more simply than the alternative of manually inspecting each spectrum.

The aim of this research is to investigate and expand the potentiality of current commercial WT CMSs, such as the SKF WindCon system, by experimentally developing fault detection algorithms, with instruction sets optimised for real-time manipulation of sampled signals, which could be implemented into their software diagnosis tool. This will contribute to automate the fault detection and diagnosis process for the main WT components, improving the confidence in the alarms produced by the system and reducing uncertainty and risk in applying CM techniques directly to field data from operational WTs.

4.6. Collaborative Work with the University of Manchester

As part of this research, a valuable collaborative relationship has been forged within the SUPERGEN Wind Phase 2 Consortium with the University of Manchester.

In the case of rotor electrical asymmetry investigation, the experimental research conducted by the Author on the Durham WTCMTR has been supported by numerical predictions provided from the time-stepping electromagnetic model developed by the University of Manchester (Djurović et al., 2012a; Djurović and Williamson, 2008; Djurović et al., 2009; Williamson and Djurović, 2009), as described in detail next in Section 5.3.2.

The University of Manchester has also experimentally investigated generator bearing faults (Vilchis-Rodriguez et al., 2013b) and the collected vibration data have been provided to the Author for further analysis and processing. The Manchester test rig features a 30kW, 4-pole, WRIG of identical construction to that on the Durham test rig except the generator has been rewound to allow greater access to winding connections on both the rotor and stator side. The Manchester test rig has the ability to be run as a DFIG or as a WRIG, as for the Durham test rig, however although it is not configured for variable speed, transient driving. The Manchester rig is described in detail and compared with Durham WTCMTR in (Djurović et al., 2012a).

Experimental work on generator drive-end side bearing faults was performed on the Manchester test rig WRIG, with short circuited rotor windings, driven at constant speed by the DC motor. The generator drive-end side bearing, shown in Figure 4.13, is an SKF 6313 roller bearing with 8 rolling elements.
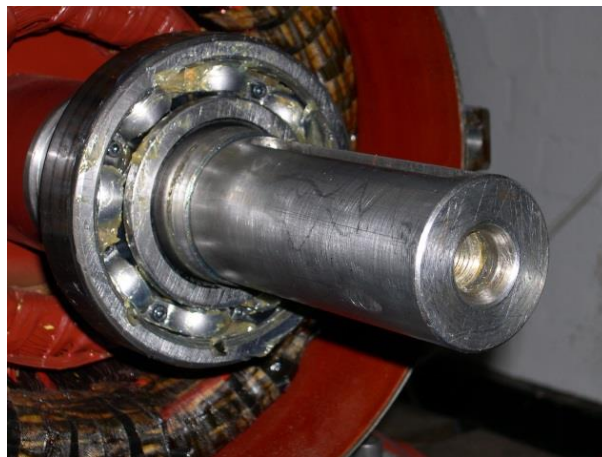
Figure 4.13: Generator drive-end side SKF 6313 bearing, photograph courtesy of the University of Manchester.

According to the bearing geometry and to equations (3.24) and (3.25), the inner and outer raceway ball passing frequencies, f_{BPFI} and f_{BPFO} respectively, are given by (Vilchis-Rodriguez et al., 2013b)

$$f_{BPFI} = 4.93 f_{rot} \qquad (4.10)$$

$$f_{BPFO} = 3.07 f_{rot} \qquad (4.11)$$

where f_{rot} is the shaft rotational speed.

Bearing faults were experimentally simulated on the Manchester test rig by drilling a hole in the middle of the bearing outer race perpendicular to the race surface on the generator drive-end side bearing. To simulate different levels of fault severity the diameter of the hole was varied from 3 to 12 mm in steps of 3 mm and 6 mm, respectively, as illustrated in Figure 4.14.
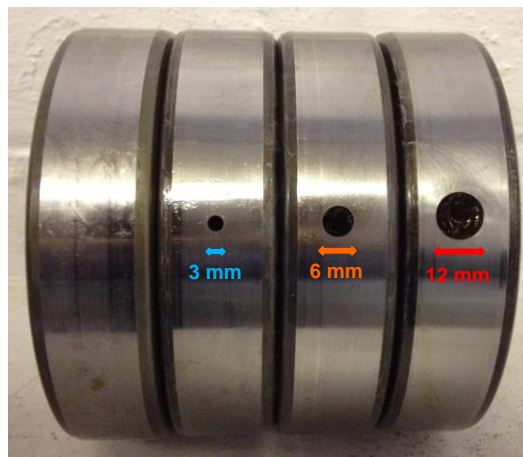
Figure 4.14: Bearing faults investigated during the tests, photograph courtesy of the University of Manchester.

For each considered hole dimension the faulted bearing was used to perform seeded-fault experiments and record the frame vibration signal. A Brüel&Kjaer Pulse system was used to record the vibration signals from two accelerometers fitted to the generator load side end-plate vertically and horizontally, respectively.

4.7. Data Analysis and Processing

In this research, the methodological approach shown schematically in Figure 4.15 has been adopted to analyse and process the experimental data, from both the Durham WTCMTR and the Manchester test rig, in order to develop automatic fault detection algorithms.

The research process consisted of 7 steps, which are briefly described as follows and presented in detail next in Chapter 5:

- **Data Collection:** Raw sensor signals from transducers positioned along the drive train have been collected during healthy and seeded-fault testing under the controlled test rig conditions.
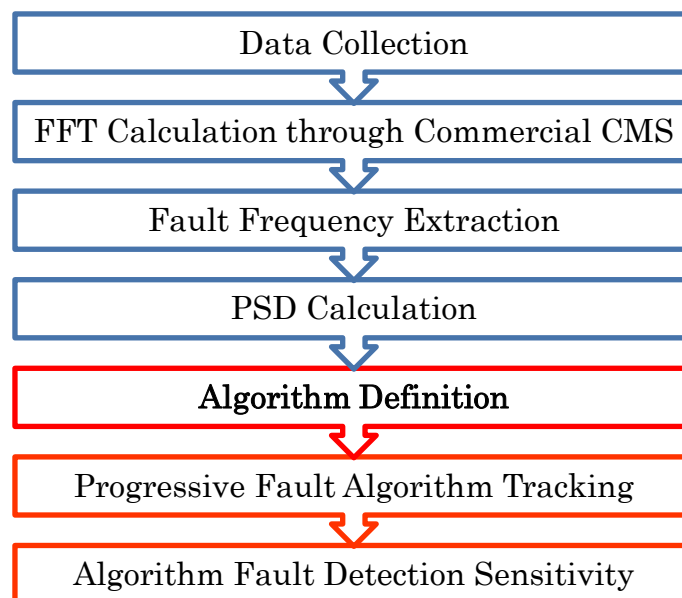
Figure 4.15: Schematic of the methodological approach.

- **FFT Calculation through Commercial CMS:** FFT spectra have been obtained by on-line processing of the transducer data using a commercial WT CMS, i.e. SKF WindCon system for the Durham WTCMTR and Brüel&Kjaer Pulse system for the Manchester test rig, respectively.

122

- **Fault Frequency Extraction:** The FFT spectra produced were compared under similar machine operating conditions in order to identify and extract the characteristic fault frequencies, introduced throughout Chapter 3, from the machine signature for further research investigation.

- **PSD Calculation:** The PSD of the extracted fault frequencies has been calculated as described in Section 3.4.5.

- **Algorithm Definition:** For each fault investigated, to enable the detection of changes in the frequency spectra, a fault detection algorithm has been defined as the total power associated with the observed characteristic fault frequencies in the CM signal. The specific definition of each algorithm depends on the nature of the fault and of the signal under investigation. In the following chapter these algorithms will be developed for each particular test rig signal. In order to automatically extract the value of the proposed algorithms from the FFT spectra provided by the CMS for each data acquisition, dedicated codes were developed and built in the MATLAB environment by the Author.

- **Progressive Fault Algorithm Tracking:** For each fault investigated, the defined algorithm has been used to track the progressive component fault introduced into the test rig, at constant and variable speed and generator load, in the case of the Durham WTCMTR, and at steady-state operating speeds for the Manchester test rig.

- **Algorithm Fault Detection Sensitivity:** Finally, a fault detection sensitivity function has been defined and used to assess the performance of the proposed algorithms and to allow direct comparison between results. As presented and discussed in detail next in Chapter 5, for each case investigated and each test condition, the algorithm detection sensitivity to the fault has been calculated as the percentage

change of the algorithm value between the faulty and healthy conditions.

4.8. Summary

This chapter describes the methodological approach adopted in this Thesis.

The Durham WTCMTR and its main mechanical and electrical components have been installed in 2003 and since then the rig has been used by various researchers to investigate CM techniques. An experimental resistive load bank has been designed and manufactured to perform generator rotor seeded-fault testing in a controllable fashion, making the original rig instrumentation suitable for use in this research.

Table 4.2 summarises the experimental work undertaken on the Durham WTCMTR under both steady-state and transient, variable speed driving conditions. In this research, two seeded-fault conditions have been investigated: high-speed pinion tooth damage and rotor electrical asymmetry. Signals from the transducers were recorded and processed by using an SKF WindCon CMS.

A summary of the collaborative work with the University of Manchester has been also described. During this collaboration, model simulations of generator rotor electrical asymmetry and tests on generator bearing faults were carried out at the University of Manchester and the Author has led the data analysis.

Finally, Figure 4.15 introduces the methodological approach adopted to process the experimental results from the Durham WTCMTR and the Manchester test rig, which leads to the development of automatic fault detection algorithms and represents the most original research contribution of the Author. Data analysis and processing procedures are presented and discussed in detail next in Chapter 5.

5

Experimental Results

5.1. Introduction

Chapter 4 has presented the methodological approach adopted in this Thesis. A number of seeded-fault conditions were investigated to demonstrate the detection of faults with different characteristics and in different signals. For the Durham WTCMTR, two classes of seeded-fault tests were performed:

- Gearbox high-speed pinion tooth damage;
- Generator rotor electrical asymmetry.

In addition, data from tests on generator rotor electrical asymmetry and generator bearing faults, carried out at the University of Manchester, were available to the Author for analysis.

In this chapter the experimental results from the two small-scale WT test rigs are presented and discussed. For each seeded-fault applied, experiments were conducted to investigate their detectability. Data have been collected from a number of runs of the test rigs, of up to 450 seconds duration, under both healthy and faulty conditions, and then data has been analysed retrospectively. The data analysis and processing procedure has been introduced in Section 4.7 and is presented in detail in this chapter. The rationale behind the adopted approach is that, in each case, damaged components produce specific fault patterns in the machine signature, as described in detail in Chapter 3. Characteristic fault frequencies have been extracted from these signatures and used to reflect the health of the component. Appropriate algorithms for automatic fault detection and diagnosis have been defined by collating the identified characteristic fault frequencies in the CM signals which could then be tracked as the WT speed

varies. In particular, three novel algorithms are defined and presented in this Thesis:

- the Gear Sideband Power Factor algorithm, $SBPF_{gear}$, specifically developed to aid in the detection of WT gear tooth damage;
- the Rotor Sideband Power Factor algorithm, $SBPF_{rotor}$, specifically developed to aid in the detection of WRIG rotor asymmetry;
- the Harmonic Power Factor algorithm, HPF, specifically developed to aid in the detection of generator bearing faults.

The main aim of these algorithms is to automatically analyse and interpret the large volumes of CM data usually produced by a CMS in a WF, significantly reducing the large degree of manual analysis currently required.

The use of characteristic fault frequencies extracted from the generator vibration signature as an indicator of rotor electrical asymmetry is also examined and discussed.

Finally, this chapter presents and discusses the fault detection sensitivities of the proposed algorithms for the different fault investigated.

The HS pinion tooth damage findings, along with those in Chapter 6, were presented at the Scientific Track of the European Wind Energy Association (EWEA) conference in Copenhagen, Denmark in 2012 (Zappalá et al., 2012) and in Vienna, Austria in 2013 (Zappalá et al., 2013), followed by a publication in the IET Renewable Power Generation journal (Zappalá et al., 2014b).

The rotor electrical asymmetry and generator bearing fault findings were presented at the Scientific Track of the EWEA conference in Barcelona, Spain in 2014 (Zappalá et al., 2014a).

5.2. Gearbox High-Speed Pinion Tooth Damage

5.2.1. Test Conditions

As introduced earlier in Section 4.3.1, seeded-fault testing was performed to investigate HSS pinion tooth damage introduced into the Durham WTCMTR. The vibration signature of a healthy pinion and of four faults of increasing severity were examined by introducing progressive damage to the leading contact edge of one tooth of the gearbox HSS pinion, as shown in Figure 4.9. Such faults have been introduced by manual filing based upon photographs from actual damage to WT gearbox gear teeth.

The external variable resistors connected to the rotor circuit shown in Figure 4.2 were used to increase the balanced rotor phase resistances up to 1.3 Ω and allow a super-synchronous generator speed variation of around 100 rev/min, from 1500 to 1600 rev/min, with a corresponding maximum power output of 3.6 kW, as shown in Figure 4.6. Firstly, tests were performed at steady-state, constant speed conditions to extract features indicative of the developing fault from the gearbox vibration signature and to design the detection algorithm by adding their PSD together. Secondly, in order to validate the developed algorithm, the DC motor was driven at both constant and wind-like variable speed conditions to cover the allowed speed range. Each constant speed test was run for up to 300 seconds while each variable speed test was run for up to 450 seconds, allowing a sufficient data acquisition and processing time for the WindCon unit. A summary of the HSS pinion seeded-fault experiments performed during this research is given in Table 4.3.

During the gearbox seeded-fault testing, vibration data was collected by a single axis accelerometer vertically mounted on the gearbox HS end, at a position radial to the shaft, as shown in Figure 5.1. The transducer was mounted as close as possible to the gearbox HSS pinion to get the best quality

signal. The accelerometer data was recorded and processed by the SKF WindCon system assuming a fixed sampling frequency and producing FFT spectra with an overall frequency range of 5 kHz in the 1500–1600 rev/min HSS active range. The HSS speed allowable change within the defined active range was set at 5 rev/min, in order to define the limits for the operating conditions under which spectra were sampled and to process quasi-stationary signals. The accelerometer measurement point in WindCon has been configured to provide vibration spectra which refer to a measurement time window of 1.28 seconds. The Hanning window has been applied to the vibration signals. The produced spectra have 6400 resolution lines for a 5 kHz bandwidth with a resulting frequency resolution of 0.78125 Hz/line.

Figure 5.1: Photograph of the WTCMTR gearbox showing the location of the accelerometer on the HS end gear case.

WindCon's built-in diagnostic tools were used to assist with the analysis of the spectra by tracking the machine component-specific, speed-dependent fault frequencies, their harmonics and SBs. The spectra were analysed and compared offline using the cursors produced by the Observer machine diagram to pick out and identify frequencies, and their harmonics, within the spectra and relate them to the components which generated them.

5.2.2. Vibration Signature Analysis

In the work presented in this Thesis, normalised order spectra (X), introduced earlier in Section 3.4.6, were used to facilitate the comparison of the FFT spectra and to identify the effect of the faulty tooth on the 30 kW gearbox vibration signature. A local gear defect, such as a cracked tooth, generates a disturbance in each revolution. Basically, a spectral order is introduced as a non-dimensional frequency parameter. If the frequency axis is normalised to the shaft rotation frequency any cyclic event synchronised with the shaft rotation will produce a spectral component at a fixed position even under the variable speed conditions. The advantage of this approach is that it is easier to focus on a specific cyclic mechanism.

During the tests performed on the Durham WTCMTR the HSS speed signal was recorded simultaneously with the vibration data by the WindCon software. WindCon's frequency unit has a built-in tool allowing the operator to switch easily and automatically between Hz or order frequency units. This is done by dividing the FFT frequency in Hz by the HSS rotational speed, f_{HSS}, at which the spectrum is collected. The WTCMTR gearbox characteristic vibration frequencies (4.1) and (4.2) have then been normalised by f_{HSS} and expressed in order (X) as follows

$$f_{mesh,LS} = 13.23\ X \tag{5.1}$$

$$f_{mesh,HS} = 58\ X \tag{5.2}$$

The FFT spectra produced were compared under similar machine operating conditions. To simplify the result presentation and interpretation, all signal spectra produced by Observer were extracted and re-plotted in MATLAB. Figure 5.2 shows an example of measured HSS order vibration spectra comparison between the healthy, early stages of tooth wear (i.e. 7 mm x 5 mm chip) and the missing tooth conditions at a typical operating speed of 1560 rev/min and 51% of the maximum generator output.

129
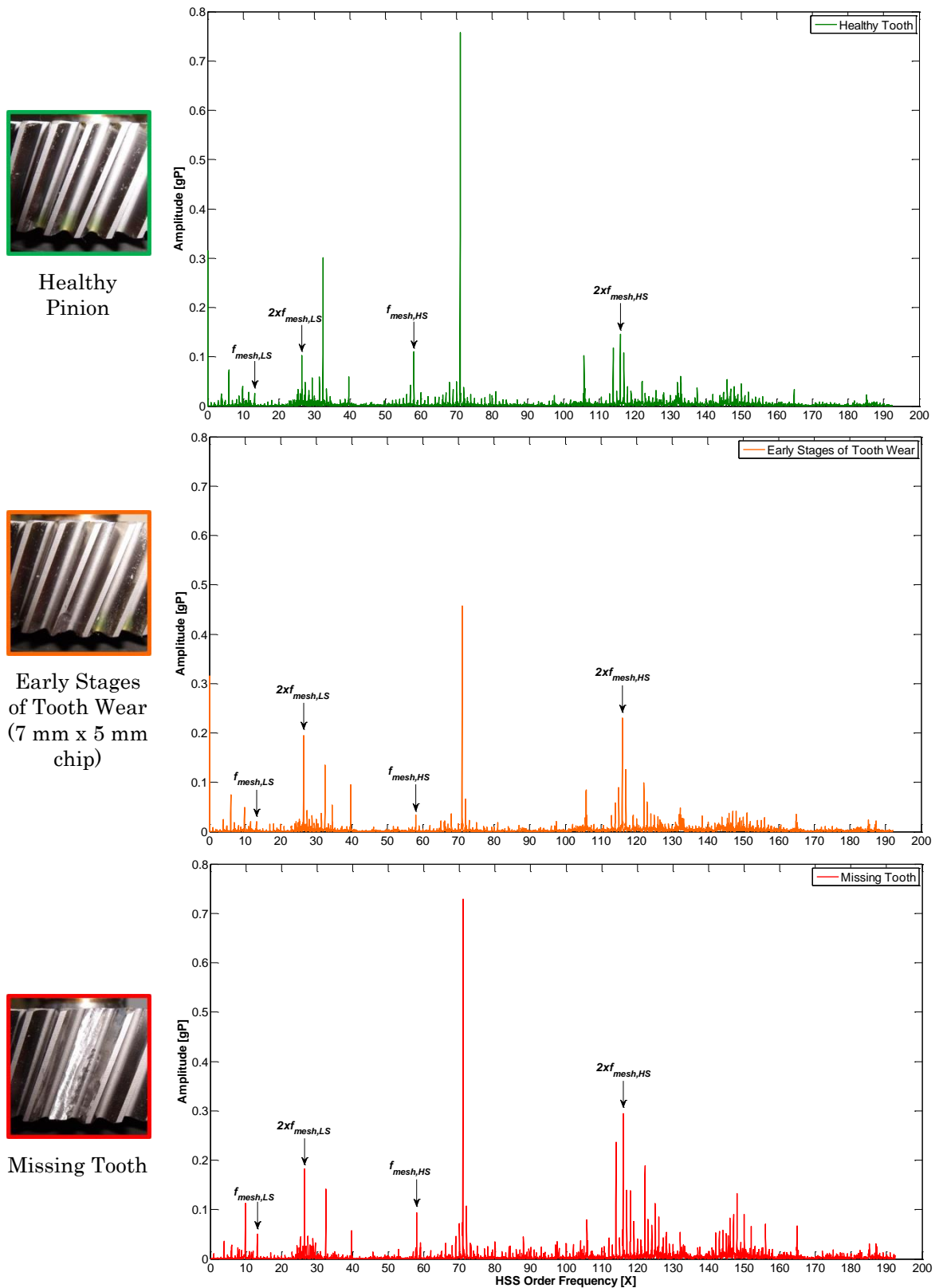
Figure 5.2: WTCMTR gearbox FFT vibration order spectra during the seeded-fault tests at 1560 rev/min and 51% of the maximum generator output.

Results obtained from the other investigated speeds are very similar to those shown in Figure 5.2 and, for conciseness, they are not presented here.

Each plot depicts the normalised LS and HS stage gearbox meshing frequencies, defined by equations (5.1) and (5.2), respectively, and their second harmonics, $2xf_{mesh,LS}$ and $2xf_{mesh,HS}$ respectively, given by

$$2xf_{mesh,LS} = 26.46\,X \qquad\qquad (5.3)$$

$$2xf_{mesh,HS} = 116\,X \qquad\qquad (5.4)$$

The spectra show an increase in the harmonic content of the signal as a result of abnormal gear set behaviour due to the progressive damage introduced to the gearbox HSS pinion. The spectra associated with the damaged pinions present richer frequency contents and relatively higher amplitude than that from the healthy pinion. The three spectra show also high-amplitude frequency content at around $71\,X$. This frequency is not a multiple of any meshing frequency. The comparison with similar spectra at different speeds allowed identifying this content as a rotating-related frequency associated with the effects of the test rig loaded conditions. However, as its amplitude does not vary substantially when passing from healthy to faulty conditions it does not represent a significant frequency to track in order to detect the gearbox failure. The HS stage meshing frequency second harmonic, $2xf_{mesh,HS}$, and its SBs are dominant in the early stages of tooth wear and missing tooth spectra.

The zoom-in view of the measured HSS order vibration spectra around the $2xf_{mesh,HS}$ second harmonic, Figure 5.3, shows that the presence of an HSS pinion faulty tooth results in clear and prominent f_{HSS} SB components of the $2xf_{mesh,HS}$ harmonic. Low-amplitude SBs are also visible in the healthy spectrum. As discussed earlier in Section 3.5.1, these SBs originate from inherent manufacturing imperfections in the existing gearbox producing slight gear tooth profile and pitch variations. However, when the gearbox

131

operates with the damaged tooth, the presence of the faulty pinion can be clearly seen in the $2xf_{mesh,HS}$ harmonic which is heavily modulated by the HSS speed, f_{HSS}, given by

$$f_{HSS} = 1\,X \tag{5.5}$$
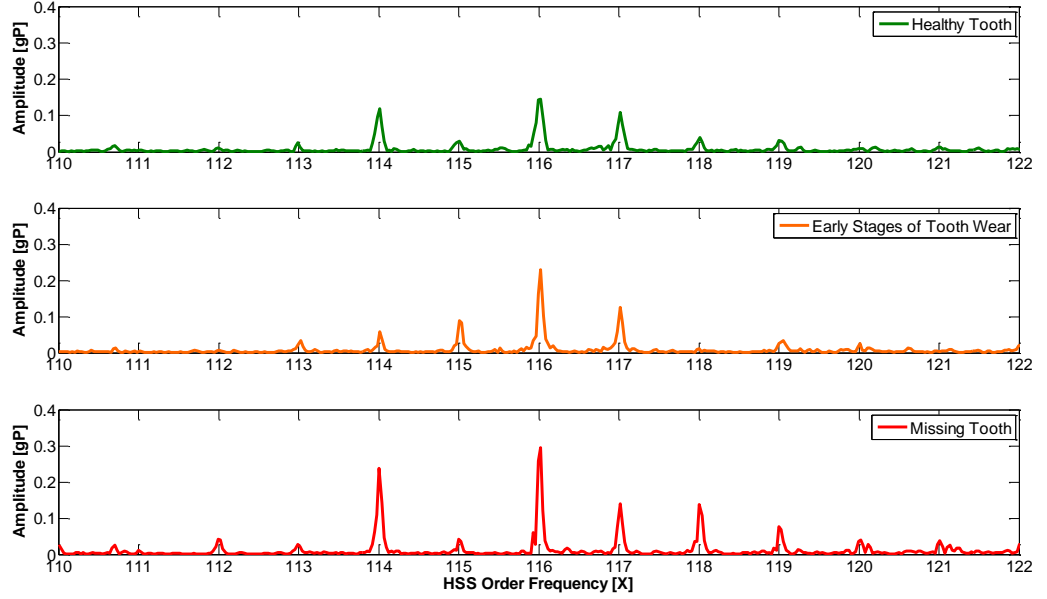
Figure 5.3: WTCMTR vibration spectra in the $[110 - 122]\,X$ HSS order frequency bandwidth during the seeded-fault tests at 1560 rev/min.

Overall, it is clear that the energy contained in the SB spikes from the faulty gearboxes is much higher than that from the healthy gearbox. The severity level of the tooth damage affects the SB amplitudes. Such a pattern is a strong indicator of abnormal behaviour of the HS gear stage.

For the early wear stage and the missing tooth spectra, ten stronger SBs of the $2xf_{mesh,HS}$ harmonic, SB_i, calculated as

$$SB_i = \left(2xf_{mesh,HS} \pm i\right) X \tag{5.6}$$

where $i = 1, 2, 3, 4, 5$, are clearly visible in the spectra in Figure 5.3. The increase in the SB amplitude content can be explained as the result of the

impact produced by the faulted HSS pinion every revolution, as discussed earlier in Section 3.5.1. This is validated by observing that the frequency of the amplitude modulation is the same as the HSS speed where the defected pinion is located. Furthermore, the gear mesh centre harmonic, surrounded by the SBs, denotes which gear mesh the damaged gear is passing through. These two pieces of information indicate that the damaged component is part of the HS stage gear mesh and is mounted on the HSS shaft.

5.3. Generator Rotor Electrical Asymmetry

5.3.1. Test Conditions

As introduced earlier in Section 4.3.2, experimental research was conducted to investigate generator rotor electrical asymmetry. Experiments were performed using the WTCMTR configuration with the gearbox removed shown schematically in Figure 4.3. The experimental resistive load bank shown in Figure 4.4 was used to increase the balanced rotor phase resistances up to 1.4 Ω to allow for a wide generator speed variation as would be found in a variable slip WRIG. Tests have been performed within the allowed 1500-1600 rev/min super-synchronous generator speed range with a corresponding maximum power output of 3.4 kW, as shown in the WTCMTR generator torque-speed characteristic in Figure 5.4. The load bank has also allowed rotor electrical asymmetry to be introduced into one phase of the rotor circuit for fault testing.

For experimental purposes, in order to represent the development of rotor electrical faults on a DFIG, such as brush-gear or slip-ring wear, two seeded-fault levels were implemented on the test rig by successively adding two additional external resistances of 0.3 Ω and 0.6 Ω, respectively, to phase 1 of the rotor circuit through the external load bank. The corresponding level of rotor electrical asymmetry, given as a percentage of the rotor balanced phase resistance, was, according to equation (4.9), 21% and 43%, respectively.

These values compare very favourably with other studies such as (Djurović et al., 2012a; Gritli et al., 2009; Stefani et al., 2008).
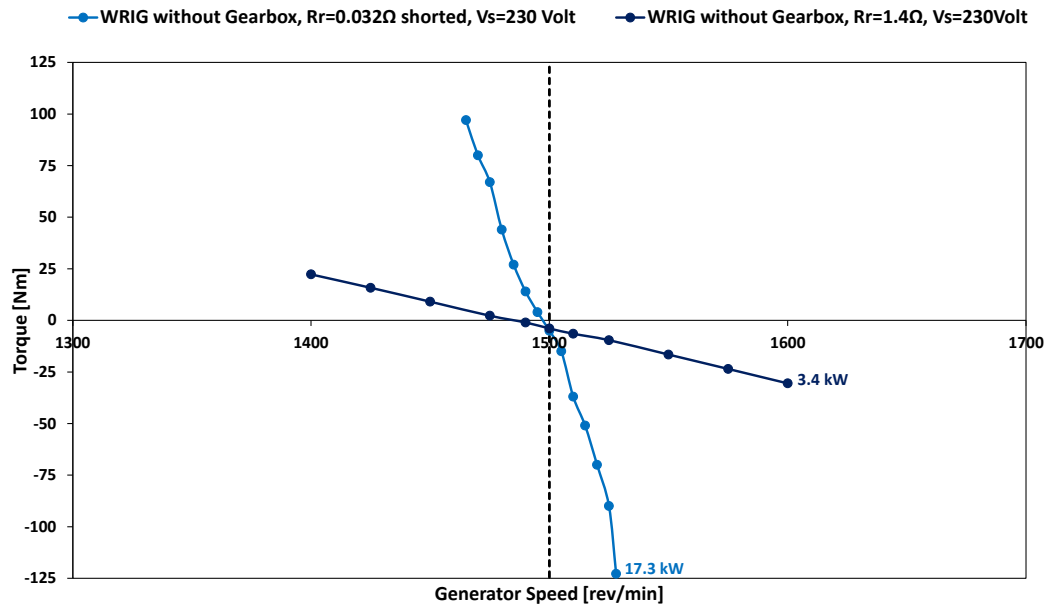
Figure 5.4: Generator torque-speed characteristics for the WTCMTR equipped without the gearbox showing electrical power limits.

Similar to the HSS pinion fault investigation, tests were performed first at steady-state, constant speed conditions to extract features indicative of the developing fault and to design the detection algorithm by adding their PSD together. Secondly, in order to validate the developed algorithm, the DC motor was driven at both constant and wind-like variable speed conditions to cover the allowed speed range. As in the previous case, in each constant speed test the rig was driven for 300 seconds while in each variable speed test it was driven for 450 seconds, allowing a sufficient data acquisition and processing time for the WindCon unit. A summary of the generator rotor electrical asymmetry experiments performed during this research is given in Table 4.3.

During the seeded-fault testing, the phase 1 stator line current signal was collected and processed by the SKF WindCon system assuming a fixed

sampling frequency and producing FFT spectra with an overall frequency range of 500 Hz in the 1500–1600 rev/min HSS active range. The HSS speed allowable change within the defined active range was set at 5 rev/min, in order to define the limits for the operating conditions under which spectra were sampled and to process quasi-stationary signals. Only one line current signal is presented and analysed here, as is usually the case for MCSA (Crabtree, 2011). The stator line current measurement point in WindCon has been configured to provide FFT spectra which refer to a measurement time window of 12.8 seconds. The Hanning window has been applied to the line current signals. The produced spectra have 6400 resolution lines for a 500 Hz bandwidth with a resulting frequency resolution of 0.078125 Hz/line.

The potential of using fault specific frequencies identified in the generator vibration signature as fault indicators of rotor electrical asymmetry was investigated on the Durham WTCMTR test rig. Data was recorded from two Brüel&Kjaer DT4394 accelerometers fitted to the generator load side end-plate. The accelerometers were installed in two planes, vertically and horizontally at positions radial to the shaft, as shown in Figure 5.5(a), with the aim of providing a comparison between fault effects in different positions on the stator frame. The accelerometer output signals were recorded for a series of experiments, of up to 300 seconds duration, at steady-state operating speeds of 1530, 1560 and 1590 rev/min for balanced rotor, 21% and 43% rotor electrical asymmetry conditions. A Brüel&Kjaer Pulse vibration analysis platform (Brüel&Kjaer, 2013) was used to record and condition the vibration signal from the accelerometers. The vibration signal FFT analysis was performed using the Pulse platform proprietary routine at 6400 line resolution for the investigated 0-1 kHz bandwidth with a resulting frequency resolution of 0.15625 Hz/line. The vibration FFT spectra refer to a measurement time window of 6.4 seconds. The results of this investigation are presented in Section 5.3.3.

As part of still ongoing collaborative research with the University of Manchester, within the SUPERGEN Wind Phase 2 Consortium, the potential of using fault specific frequencies identified in the generator vibration signature as fault indicators of rotor electrical asymmetry was also investigated on the Manchester test rig under the same steady state speed conditions. Similar to the Durham WTCMTR test settings, two Brüel&Kjaer DT4394 accelerometers were fitted vertically and horizontally to the generator load side end-plate, as shown in Figure 5.5(b), and the Brüel&Kjaer Pulse vibration analysis platform was used to collect the data.
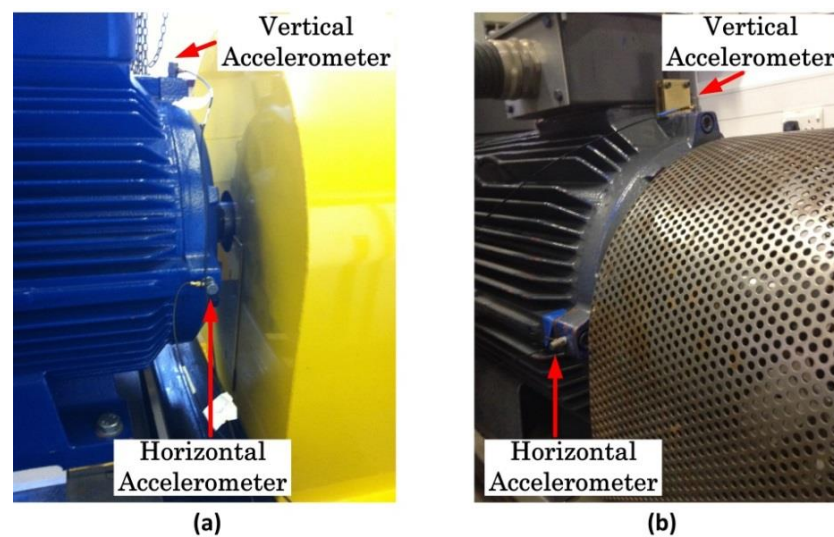
Figure 5.5: Location of the two accelerometers on generator load side end-plate: (a) WTCMTR WRIG; (b) Manchester test rig, photograph courtesy of the University of Manchester.

5.3.2.   Electrical Signature Analysis

The FFT spectra produced by Observer were compared under similar machine operating conditions. However, it should be emphasised that, unlike the HSS pinion fault investigation, in this case the analysis and comparison of the spectra was done without the aid of WindCon as it does not feature any built-in diagnostic tool for the machine electrical parts to assist with the easy tracking of the electrical machine component-specific fault frequencies. To

simplify the result presentation and interpretation, all signal spectra produced by Observer were extracted and re-plotted in MATLAB.

Figure 5.6 shows an example of measured stator line current FFT spectra comparison between the balanced rotor, 21% and 43% rotor asymmetry conditions at a typical operating speed of 1590 rev/min and 85% of the maximum generator output. Results obtained from the other investigated speeds are very similar and comparable to those presented in Figure 5.6 and, for conciseness, they are not presented here.

The full [0-500] Hz spectra are dominated by the high amplitude of the supply frequency, f_s, however when considering their zoom-in view in the [0-200] Hz frequency bandwidth a clear indication of fault signature is provided by the $|2s|f_s$ upper SBs of the supply frequency first and third harmonics, $|1-2s|f_s$ and $|3-2s|f_s$, respectively. As the fault is introduced and its severity increased changes in the amplitude of these SBs are clearly visible. The magnitude of these SBs is significantly affected by the severity level of the electrical asymmetry introduced into the generator rotor.

The $|1-2s|f_s$ amplitude shows a marked increase when the rotor 21% electrical asymmetry is introduced. A similar behaviour is shown for the 43% asymmetry condition.

A change is also apparent in the $|3-2s|f_s$ component despite its lower magnitude. The result from the $|3-2s|f_s$ component may be a useful rotor fault indicator. In Figure 5.6 it can be seen that its amplitude is negligible for balanced rotor conditions and it only becomes clearly evident when the 21% fault level is introduced.

The presence of the two fault-related slip-dependent frequencies, $|1-2s|f_s$ and $|3-2s|f_s$, in the line current experimental spectra confirms and strengthens the previous findings by (Djurović et al., 2012a).
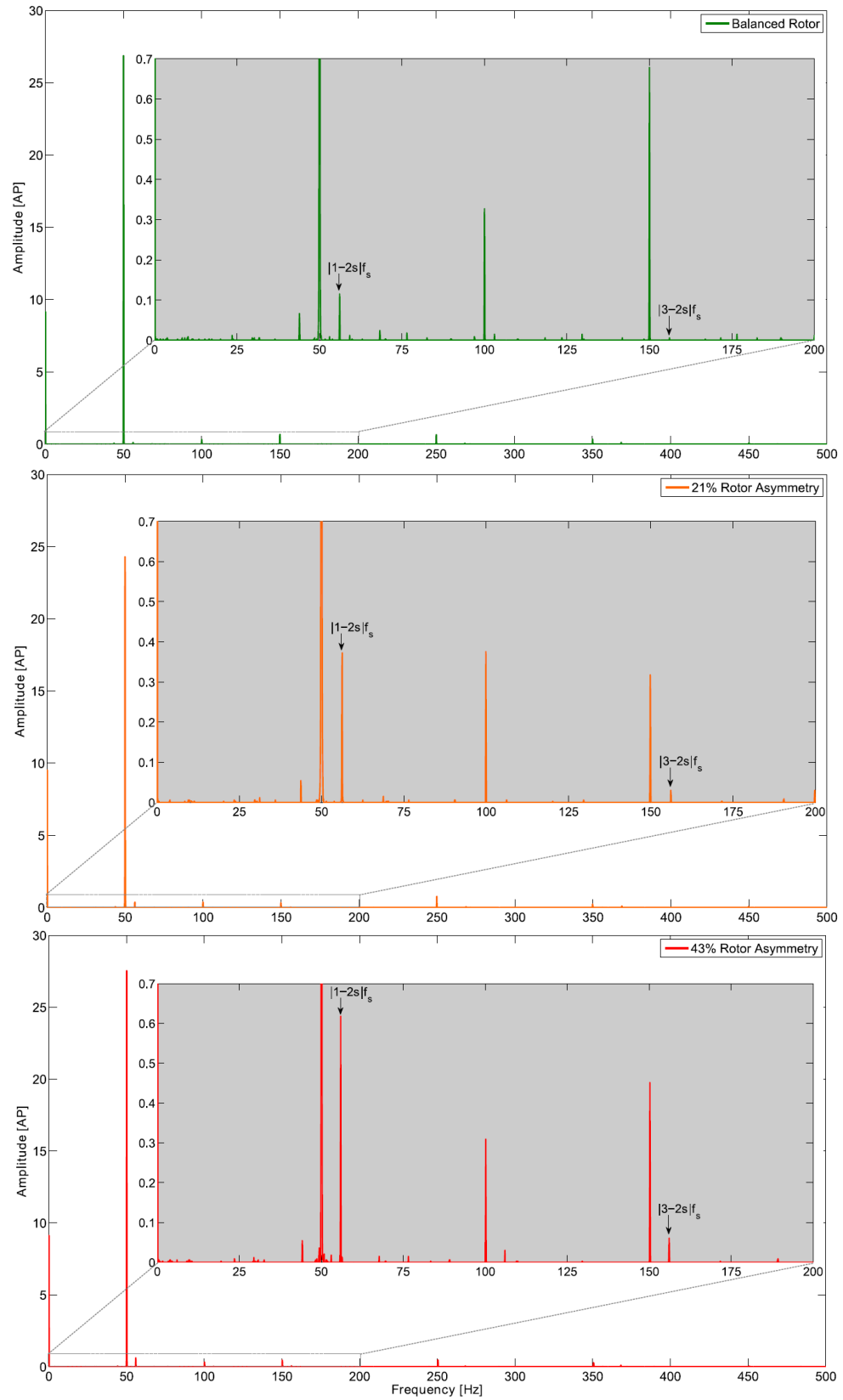
Figure 5.6: WTCMTR stator line current spectra at 1590 rev/min.

As part of the collaborative research within the SUPERGEN Wind Phase 2 Consortium, the experimental investigation of rotor electrical asymmetry through MCSA has been supported by numerical predictions provided from the time-stepping electromagnetic model developed by the University of Manchester. A model study was undertaken by Dr Damian Vilchis-Rodriguez to explore the spectral content of the line current signal for the laboratory WRIG under balanced and unbalanced rotor operating conditions. The WRIG model used in this investigation is based on the principles of generalised harmonic analysis and is presented in (Djurović et al., 2009). The model accounts for harmonic air-gap field effects when evaluating machine parameters and is convenient for frequency domain analysis of machine quantities, as demonstrated in (Djurović et al., 2012a; Djurović et al., 2009; Williamson and Djurović, 2009) and discussed earlier in Section 3.6.1. The simulations also assumed a stator/grid excitation unbalance representative of that found in the laboratory grid supply, as is generally the case for on-line operating ac machinery.

Normalised line stator current frequency spectra predicted by the Manchester model simulations for balanced rotor and 21% rotor asymmetry conditions at the super-synchronous operating speeds of 1530 rev/min, 1560 rev/min and 1590 rev/min are shown in Figure 5.7. The current amplitude values have been divided by the fundamental frequency magnitude, so that the fundamental frequency is normalised to one and the magnitude of the other components are referred to the fundamental.

The steady-state results from the Manchester generator current simulations are found to be very consistent with those from the Durham experimental tests. They clearly show that the SBs around the first and third harmonics of the supply frequency are related to the rotor electrical asymmetry, thus confirming the validity of the experimental approach.
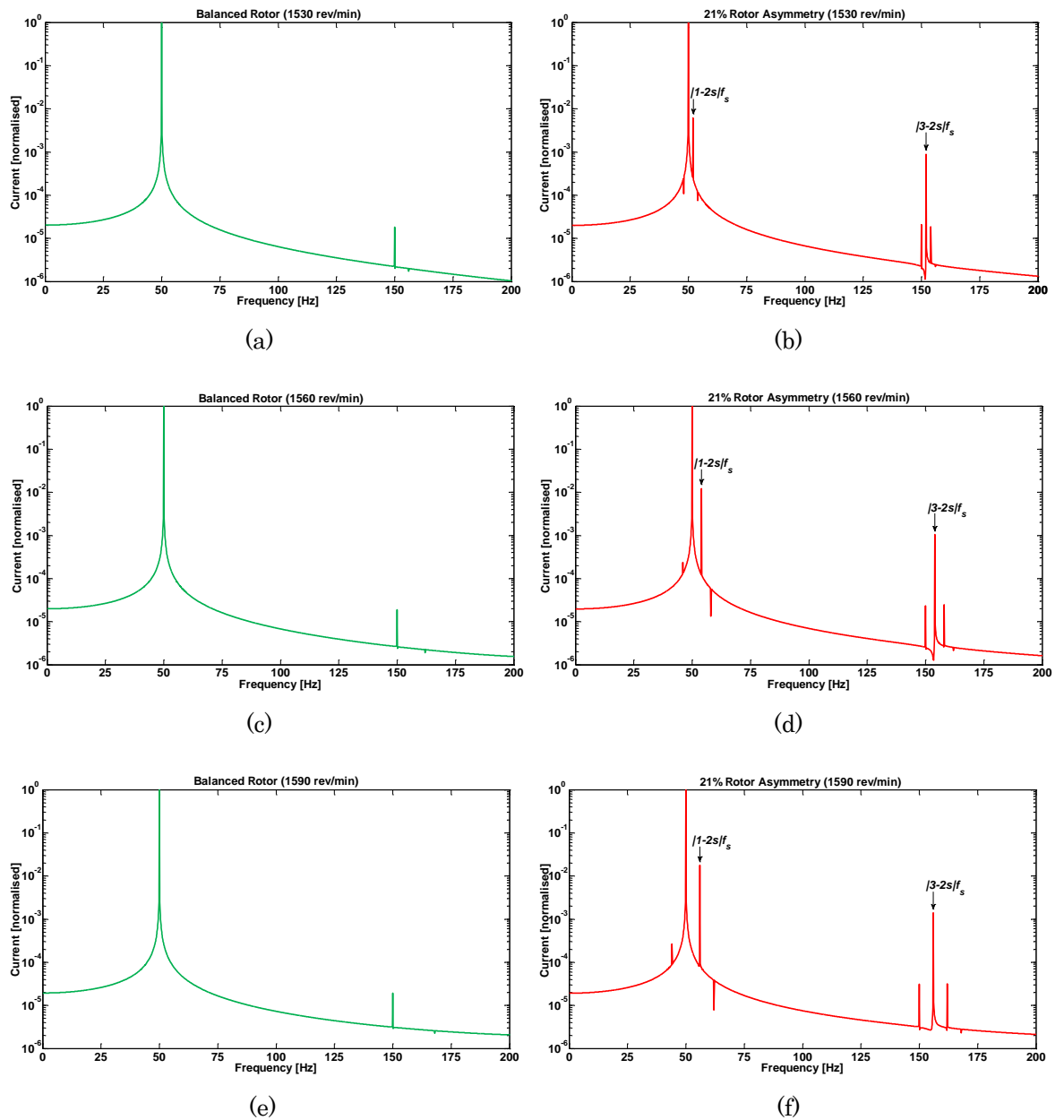
Figure 5.7: Line current spectra from Manchester simulations for balanced and 21% rotor asymmetry conditions at: (a) and (b) 1530 rev/min; (c) and (d) 1560 rev/min; (e) and (f) 1590 rev/min.

The SB on the third harmonic is only present when the supply third order time harmonic exists in conjunction with the rotor electrical fault. In the simulation results the $|3 - 2s|f_s$ amplitude is larger than that of the supply frequency third harmonic because non-linear phenomena, such as saturation and hysteresis, and slotting effects, such as permeance harmonics,

that may contribute to the harmonic component magnitude, are not considered in the model. Furthermore, no noise is considered in the simulations giving a very high signal to noise ratio even for very small frequencies. This results in the presence of the second harmonic of the $|3 - 2s|f_s$ component in the faulty spectra as shown in Figure 5.7(b), Figure 5.7(d) and Figure 5.7(f).

The simulation results confirm that the $|1 - 2s|f_s$ and $|3 - 2s|f_s$ slip-dependant frequencies are useful rotor electrical asymmetry detection indicators under practical WT operating conditions when supply unbalance is unavoidable.

5.3.3.   Vibration Signature Analysis

As discussed in previous Section 3.6.1, based on principles presented in (Djurović et al., 2012b), rotor electrical asymmetry results in electromagnetic torque pulsations at predictable frequencies that will also be manifested mechanically on the machine frame as vibration. Given the close relationship between torque and power the frequencies that appear in the torque spectrum, as consequence of rotor electrical asymmetry, should also be present in the power signal. Therefore, the frequencies resulting from the rotor asymmetry will be present in both the stator total power signal, as referred to in (Djurović et al., 2012a), and the generator vibration signal. The same characteristics in line current, shown in Figure 5.6 and Figure 5.7, are then expected in the vibration signals, but down-shifted by the fundamental frequency close to DC.

Based on this observation, simulations have been run by Dr Damian Vilchis-Rodriguez to explore the total power spectral content under balanced rotor and 21% rotor electrical asymmetry conditions. An example of the estimated total power spectra is given in Figure 5.8 for the super-synchronous operating speed of 1590 rev/min. As expected, the calculated

141

faulty power spectrum indicates that rotor electrical asymmetry induces a change of considerable magnitude in the $|2s|f_s$ upper SBs of the fundamental harmonic at zero Hz, $|2s|f_s$, and of the second harmonic of the supply frequency, $|2 - 2s|f_s$. Results obtained from the other investigated speeds are very similar and comparable to those presented in Figure 5.8 and, for conciseness, they are not presented here.
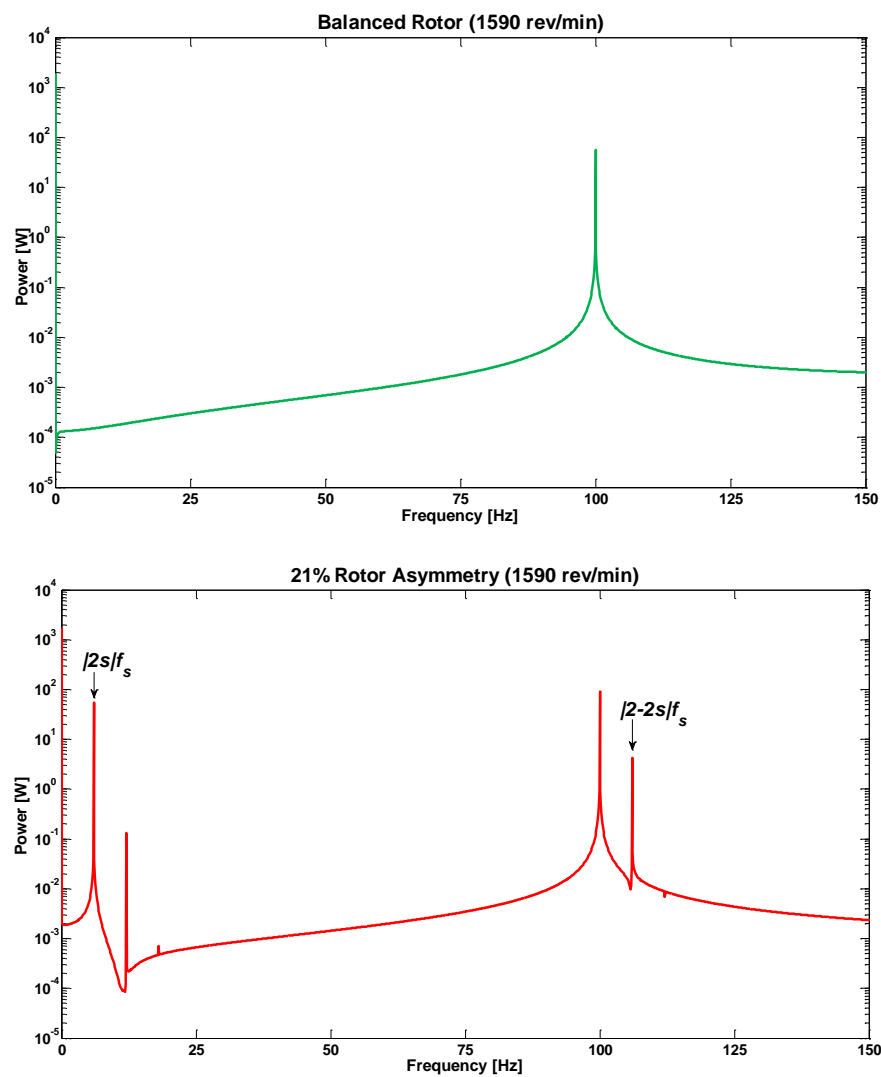
Figure 5.8: Total power spectra from Manchester simulations for balanced and 21% rotor asymmetry conditions at 1590 rev/min.

In the case of the experimental investigation on the Durham WTCMTR, tests were performed for balanced rotor, 21% and 43% rotor electrical

asymmetry conditions under steady-state operating speed conditions. The analysis of the measured vibration spectra obtained from the two accelerometers fitted to the generator load side end-plate did not show any significant change in the amplitude of the $|2s|f_s$ upper SB around zero when rotor electrical asymmetry was introduced for all the three steady-state machine operation speeds tested. This component yielded no change as a result of either the level of asymmetry tested or the variation in the overall signal. However, as shown in Figure 5.9, relevant changes in the amplitude of the $|2s|f_s$ upper SB of the supply frequency second harmonic, $|2 - 2s|f_s$, were instead clearly visible in the spectra measured from both accelerometers when introducing the two rotor asymmetry levels. The results show a marked increase in the magnitude of the fault frequency component for the most severe asymmetry case.

As part of still ongoing collaborative research with the University of Manchester, within the SUPERGEN Wind Phase 2 Consortium, at the time of writing, preliminary seeded-fault tests were performed on the Manchester test rig for balanced rotor, 500% and 1000% rotor electrical asymmetry conditions under the same steady-state conditions investigated in the Durham test rig. However, preliminary results obtained so far are unclear and equivocal, showing not significant effect of rotor asymmetry on the machine vibration spectra obtained from the two accelerometers. This is thought to be the result of the very large rotor asymmetries applied to the Manchester generator rotor, i.e. 500% and 1000%, respectively, compared to those investigated on the Durham WTCMTR, i.e. 21% and 43%, respectively. Further investigation, implying a new set of tests on both rigs under similar rotor asymmetry conditions and a study of the effect of rotor resistance and machine configuration on the generator vibration signature, will be performed as part of the ongoing collaborative relationship with the University of Manchester.
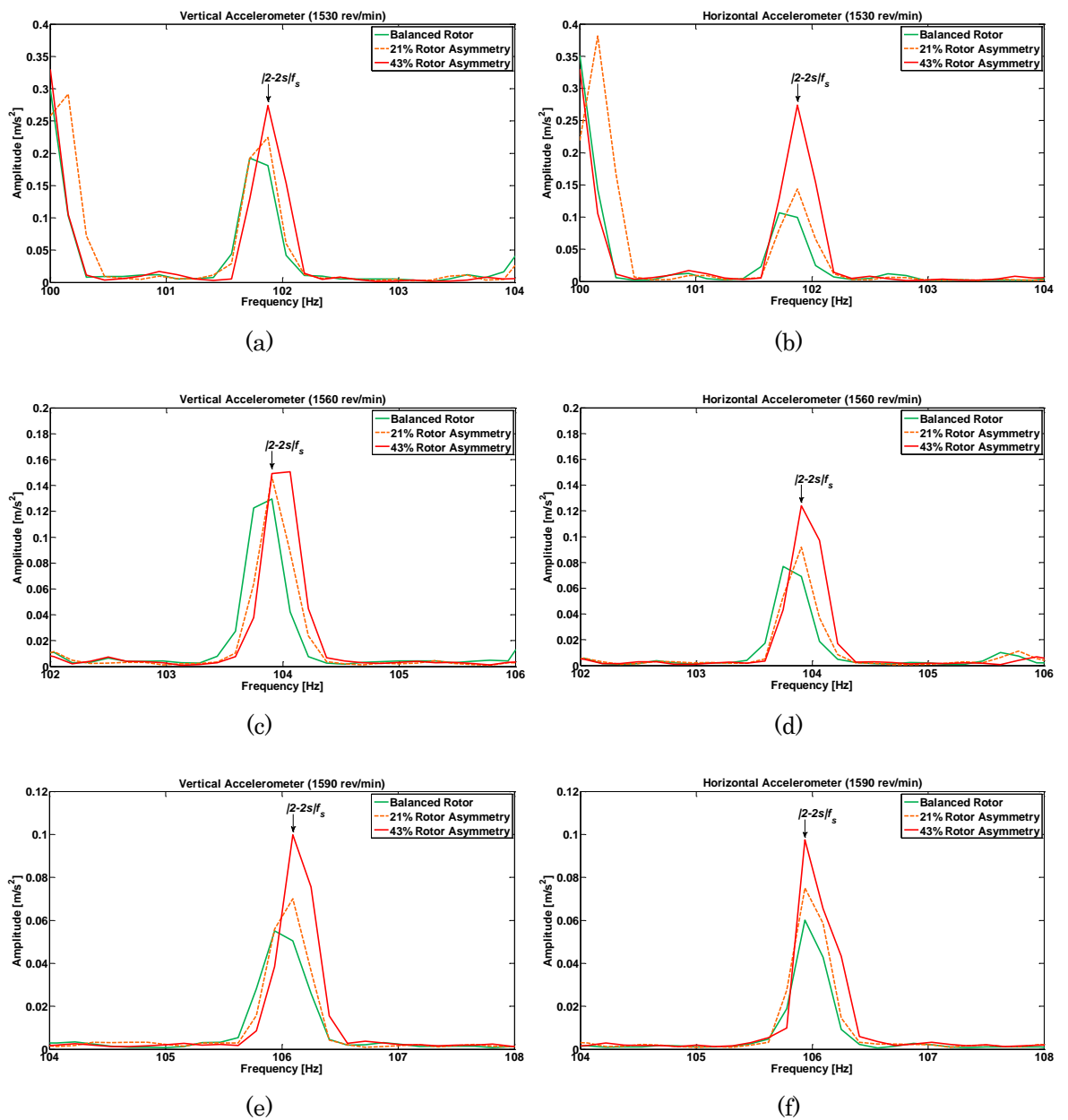
Figure 5.9: Durham vertical and horizontal accelerometer vibration spectra around the $|2 - 2s|f_s$ SB for balanced rotor, 21% and 43% rotor asymmetry conditions at: (a) and (b) 1530 rev/min; (c) and (d) 1560rev/min; (e) and (f) 1590 rev/min.

5.4. Sideband Power Factor (SBPF) Algorithms

The HS pinion tooth damage and rotor electrical asymmetry seeded-fault tests conducted on the Durham WTCMTR have shown that the presence of characteristic fault frequencies and their amplitudes could be valuable for detecting and diagnosing WT gearbox and generator faults, respectively. As described in previous Sections 5.2.2 and 5.3.2, faults manifest themselves as changes in the magnitude of defined spectral components, which are modulation SBs of characteristic frequencies of the gearbox vibration and generator stator line current signatures, respectively. Therefore, faults could be detected by examining these component magnitudes over time, taking into account of the variable operating conditions. However, even with the aid of a WT CMS built-in diagnostic system, the manual analysis of the spectra, needed to compare the changes in the SB amplitudes for different conditions, requires significant time-consuming work load because of the great number of frequency bands to be monitored. CMSs produce large amounts of data that often require the user to have some degree of expertise in order to extrapolate useful information and distinguish a normal operating condition from a potential failure mode. Moreover, the small amplitudes of the characteristic fault frequencies in the spectrum often make it difficult to correctly judge the health condition of a machine, in particular when the fault-related features are wholly or partially hidden by significant background noise. WT CM results are also usually coupled with load variations, which further increase the difficulty of obtaining reliable fault information. Once monitoring is carried out on large WT populations, the amount of manual analysis increases dramatically and would be impractical for operators or maintainers unless the process is simplified further. Therefore single component health indicators, which can be trended under the variable WT speed and load conditions, are needed.

This calls for intelligent monitoring strategies that are able to detect the faulty signal in an automatic way. The challenge is to develop gearbox and generator CM indicators that can provide early evidence of impending problems. The suggestion is to track the overall power of the spectra associated with the characteristic SBs identified in the gearbox vibration and in the generator current spectra, respectively.

Based on the experimental evidence, for each fault investigated on the Durham WTCMTR, a fault detection algorithm has been defined. The proposed algorithms track the overall power of the fault-frequency signal by collating the identified SBs in the vibration and line current spectra, respectively, in order to enhance the fault sensitivity detection.

The algorithm process can be summarised as:

- Extract the FFT spectrum from the CMS for analysis;
- Extract the HSS speed and the machine load associated with the FFT;
- Calculate the corresponding speed-dependant SB frequencies of interest;
- Extract the faulty SBs and their amplitude from the dataset;
- Calculate the corresponding PSD using the periodogram method described in Section 3.4.5;
- Calculate the algorithm value by summing the PSD of the faulty SBs;
- Repeat the process with the next unanalysed FFT provided by the CMS.

The specific definition of each algorithm depends on the nature of the fault and of the signal under investigation as described in the following sections. The proposed algorithms facilitate the monitoring analysis, reducing each FFT spectrum to only one parameter for each data acquisition and avoiding a time-consuming manual spectra comparison. In order to automatically extract and trend the value of the algorithms from each FFT

spectrum provided by the CMS, dedicated codes were developed and built in the MATLAB environment by the Author.

5.4.1.   Gearbox High-Speed Pinion Tooth Damage

Based on the experimental results from the Durham WTCMTR, presented in Section 5.2.2, monitoring the HS stage meshing frequency second harmonic, $2xf_{mesh,HS}$, narrowband window including its 10 neighbouring SBs spaced at the HSS rotational speed, f_{HSS}, has been assumed as the most reliable and consistent indicator of HSS pinion fault. The SB spacing is equal to the modulation frequency, which in turn, is equal to the rotating speed of the shaft on which the fault occurs, giving crucial diagnostic information.

A gearbox condition indicator, the Gear SB Power Factor algorithm, $SBPF_{gear}$, has been proposed to evaluate the gear damage during the WT non-stationary load and speed operating conditions. It evaluates the gear health conditions by using the characteristic amplitude increase in the modulation SBs of the HS stage meshing frequency second harmonic in presence of a fault. The $SBPF_{gear}$ sums the power spectrum amplitudes of the HS stage meshing frequency second harmonic and its first 5 SB peaks on each side. It is calculated by using

$$SBPF_{gear} = PSD\left(2xf_{mesh,HS}\right) + \sum_{i=-5}^{+5} PSD(SB_i) \qquad (5.7)$$

where $PSD\left(2xf_{mesh,HS}\right)$ and $PSD(SB_i)$, with $i = \pm1, \pm2, \pm3, \pm4, \pm5$, are the power spectrum amplitudes of the $2xf_{mesh,HS}$ harmonic and of its first 5 SBs spaced at the HSS rotational speed, respectively, as shown in Figure 5.10.
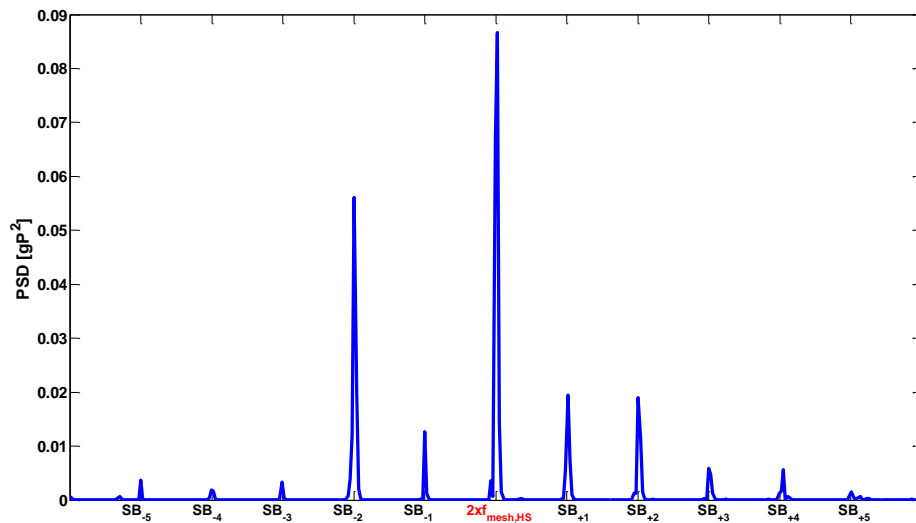
Figure 5.10: Typical FFT power spectrum around the $2xf_{mesh,HS}$ harmonic in the case of a faulty HSS pinion.

In order to test both the sensitivity and robustness of the $SBPF_{gear}$ algorithm, HSS pinion seeded-fault experiments were performed on the Durham WTCMTR over a wide range of speeds and loads. The influence of the fault severity and the variable load operating conditions on the $SBPF_{gear}$ values has been investigated by performing both constant and wind-like variable speed tests on the WTCMTR at a load of up to 3.6 kW. The resulting $SBPF_{gear}$ values are shown in Figure 5.11 against the load, expressed as a percentage of the maximum generator output in this condition, for the HSS pinion healthy conditions, for the early stages of tooth wearing and for a missing tooth. No frequency averaging, consisting of averaging together a given number of FFT spectra, has been performed on the data obtained by the WindCon software before the extraction of the $SBPF_{gear}$ values.

The experimental results show that the $SBPF_{gear}$ magnitude is proportional to the magnitude of the gear fault and power levels. The former is because as damage develops on a gear tooth passing through the gear mesh, the SBs increase in amplitude, resulting in the larger $SBPF_{gear}$ values. For each seeded-fault condition, the trend of the obtained $SBPF_{gear}$ values can

be fitted by exponential curves, relating vibration spectra power increase with machine load. In the full range of the load investigated, the $SBPF_{gear}$ values for the missing tooth case are higher than both the healthy and the early tooth wear cases, indicating clear fault detection. The proposed algorithm works successfully even at the early stages of the tooth failure, showing a higher effectiveness at the percentage loads above 20%.
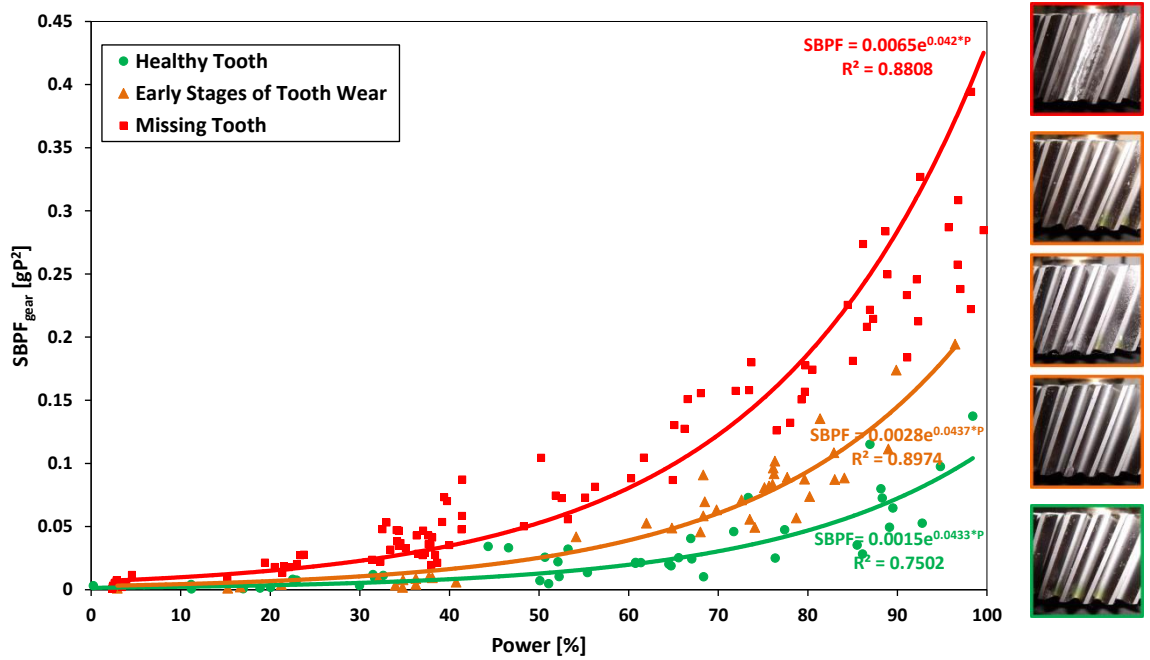
Figure 5.11: Influence of the HSS pinion fault severity and the variable load operating conditions on the $SBPF_{gear}$ values during the seeded-fault tests.

5.4.2.   Generator Rotor Electrical Asymmetry

Based on the generator current simulations, provided by the University of Manchester, experimentally validated using the Durham WTCMTR, presented in previous Section 5.3.2, monitoring the $|2s|f_s$ upper SBs of the first and third harmonics of the supply frequency, $|1-2s|f_s$ and $|3-2s|f_s$ respectively, has been considered as the most reliable and consistent indicator of rotor electrical asymmetry.

A generator fault indicator, the Rotor Sideband Power Factor algorithm, $SBPF_{rotor}$, has been proposed to evaluate rotor asymmetry during the WT non-stationary load and speed operating conditions. $SBPF_{rotor}$ monitors the rotor health conditions by using the observed characteristic amplitude increase in the modulation SBs which have been shown to be pronounced in the stator line current spectra in presence of a fault. Similarly to the previously defined $SBPF_{gear}$, $SBPF_{rotor}$ sums the power spectrum amplitudes of the $|2s|f_s$ upper SBs of the supply frequency first and third harmonics, $PSD(|1-2s|f_s)$ and $PSD(|3-2s|f_s)$, respectively, and it is given by

$$SBPF_{rotor} = PSD(|1-2s|f_s) + PSD(|3-2s|f_s) \qquad (5.8)$$

In order to test both the sensitivity and robustness of the $SBPF_{rotor}$ algorithm generator rotor seeded-fault tests were performed on the Durham WTCMTR over a wide range of speeds and loads. The influence of the fault severity and the variable load operating conditions on the $SBPF_{rotor}$ values has been investigated by performing both constant and wind-like variable speed tests on the WTCMTR at a load of up to 3.4 kW. Figure 5.12 shows the $SBPF_{rotor}$ values against the load, expressed as a percentage of the maximum generator output, for balanced rotor, 21% and 43% rotor asymmetry levels. No frequency averaging has been performed on the data before the extraction of the $SBPF_{rotor}$ values.

The experimental results show that the $SBPF_{rotor}$ magnitude is proportional to the magnitude of the rotor fault and power level. For a balanced rotor the $SBPF_{rotor}$ magnitude does not vary significantly with the load. For the faulty conditions the trend of the obtained $SBPF_{rotor}$ values can be fitted by an exponential curve. The results demonstrate effective operation of the $SBPF_{rotor}$ as an indicator of rotor fault for the full range of the investigated load levels. The algorithm is seen to enable clear fault detection, for both early and advanced stages of rotor fault.
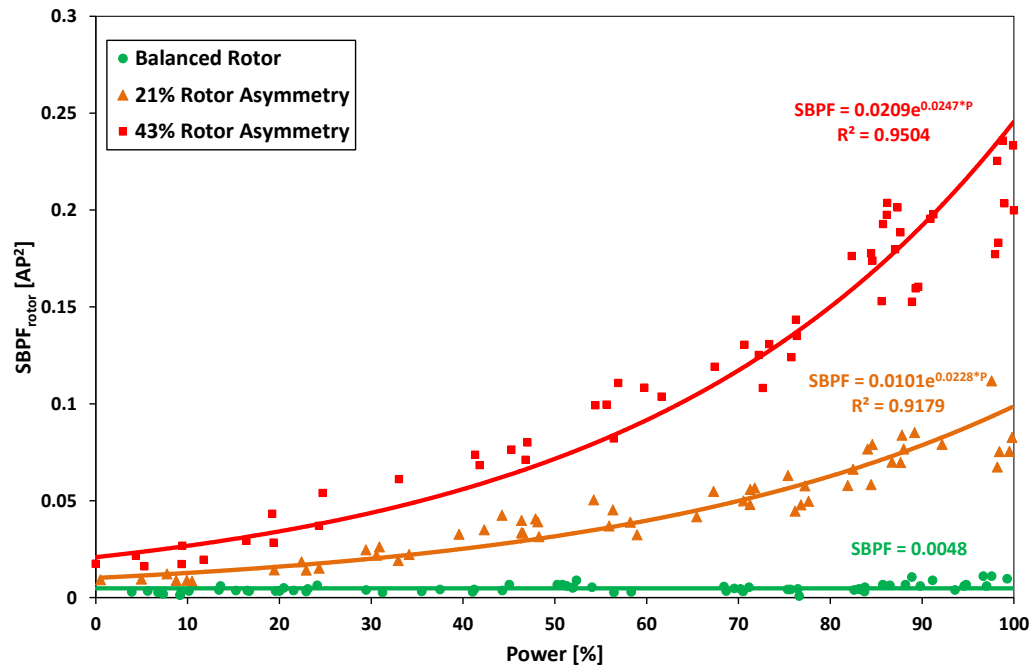
Figure 5.12: Influence of the rotor fault severity and the variable load operating conditions on the $SBPF_{rotor}$ values during the seeded-fault tests.

5.5. Collaborative work on Generator Bearing Monitoring

5.5.1. Test Conditions

Based on the collaborative research described earlier in Section 4.6, seeded-fault testing was performed to investigate generator drive-end side bearing faults introduced into the Manchester test rig. Bearing faults were introduced by drilling a hole in the middle of the outer race perpendicular to the race surface. Different levels of fault severity have been simulated as shown in Figure 4.14. For each seeded-fault test, the generator frame vibration signal was recorded by using two Brüel&Kjaer DT4394 accelerometers fitted to the generator load side end-plate and mounted

vertically and horizontally, respectively, at positions radial to the shaft, as shown in Figure 5.5(b).

The accelerometer output signals were recorded for a series of seeded-fault tests at steady-state operating speeds of 1530, 1560 and 1590 rev/min. A Brüel&Kjaer Pulse vibration analysis platform (Brüel&Kjaer, 2013) was used to record and condition the vibration signal from the accelerometers. The vibration signal FFT analysis was performed using the Pulse platform proprietary routine at 6400 line resolution for the investigated 0-1 kHz bandwidth with a resulting frequency resolution of 0.15625 Hz/line. The vibration FFT spectra refer to a measurement time window of 6.4 seconds.

5.5.2. Vibration Signature Analysis

As the investigated seeded-faults are located on the bearing outer race, the fault frequency of interest in the generator vibration signature is the outer raceway ball passing frequency, f_{BPFO}, given by equation (4.11). Repetitive impacts are generated by the rolling elements passing on the flaw of the defective outer race, causing the bearing to vibrate at the f_{BPFO} and its harmonics. As discussed in Section 3.6.2, this component is directly proportional to the shaft rotational frequency mated with the bearing, with the proportionality constant depending on the element design parameters. For this reason, normalised order spectra (X), were used to facilitate the comparison of the FFT spectra and to identify the effect of the faulty bearing on the vibration signature. The outer raceway ball passing frequency has then been normalised by its shaft rotational speed, f_{rot}, and expressed in order (X) as follows

$$f_{BPFO} = 3.07\,X \qquad\qquad (5.9)$$

The FFT spectra produced were compared under similar machine operating conditions. To simplify the result presentation and interpretation,

all signal spectra produced by the Brüel&Kjaer Pulse system were extracted and re-plotted in MATLAB.

Figure 5.13 and Figure 5.14 show an example of order vibration spectra comparison between the healthy bearing and the three different fault severities investigated during the tests, i.e. 3 mm hole, 6 mm hole and 12 mm hole, measured by the vertical and the horizontal accelerometers, respectively, at the super-synchronous operating speed of 1560 rev/min. Results obtained from the two accelerometers at the other two investigated steady-state speeds are very similar and comparable to those presented in Figure 5.13 and Figure 5.14 and, for conciseness, they are not presented here.

The spectra show an increase in the harmonic content of the vibration signal as a result the progressive damage introduced to the generator bearing. Bearing fault frequencies are evident in the measured vibration spectra, producing noticeable increments in the amplitude of the first five outer race bearing fault frequency harmonics, $i \times f_{BPFO}$, with $i = 1,2,3,4,5$, with respect to healthy machine operation.

The severity level of the bearing damage affects the harmonic amplitudes. It is clear that the overall energy contained in the f_{BPFO} harmonics in the case of faulty bearings is much higher than that from the healthy machine, progressively increasing as the fault becomes more severe.
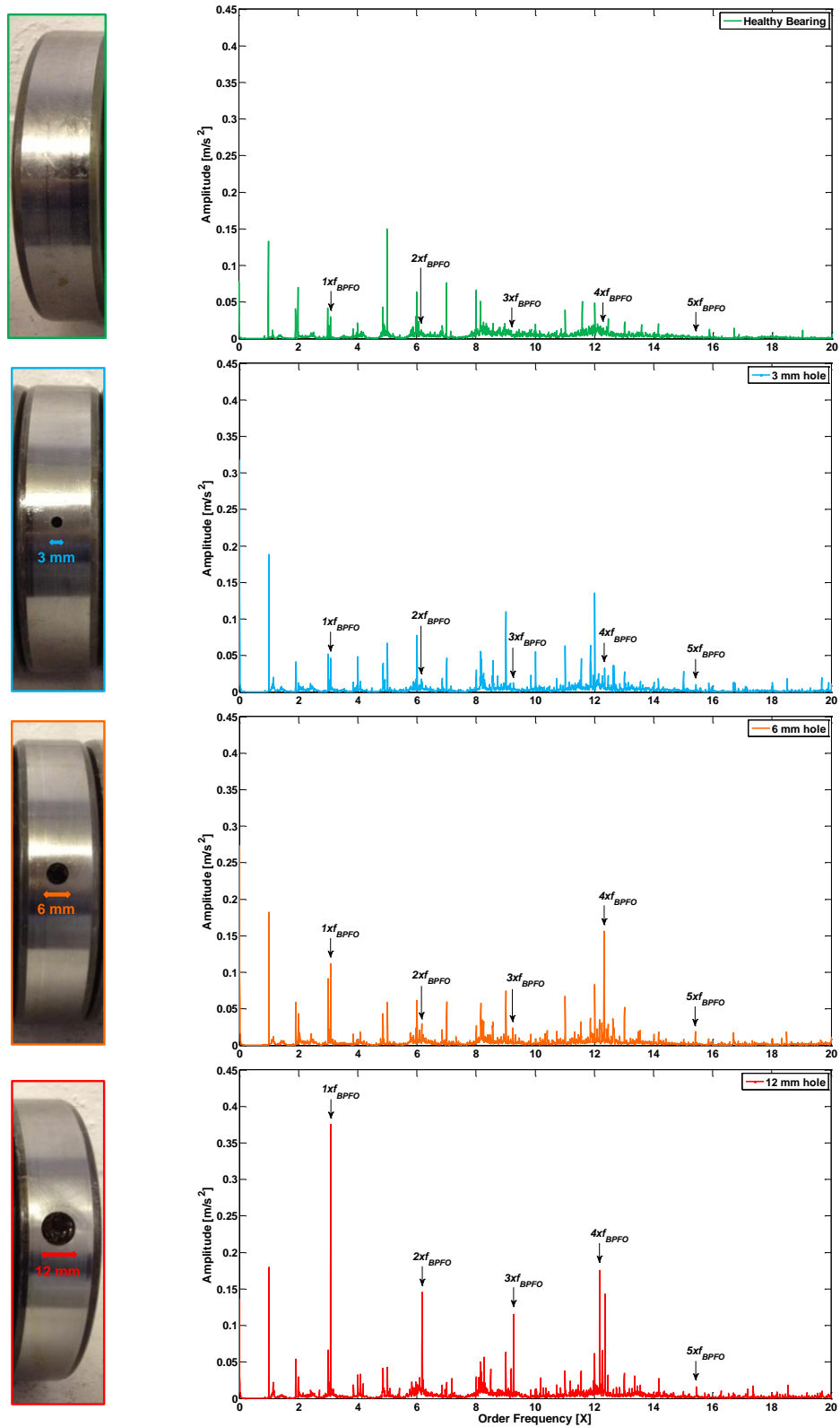
Figure 5.13: Vertical accelerometer vibration order spectra from the Manchester test rig bearing seeded-fault tests at 1560 rev/min.

154
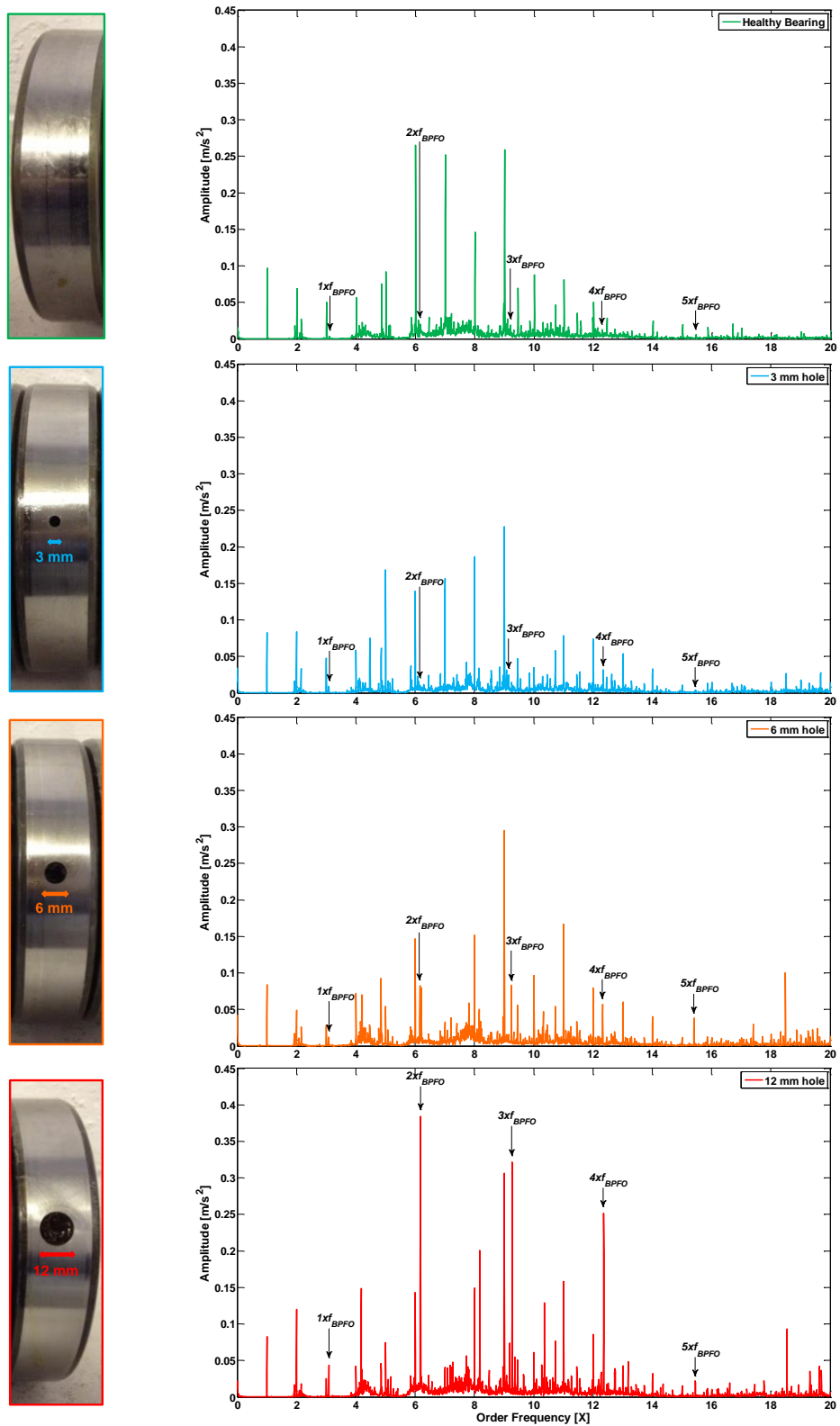
Figure 5.14: Horizontal accelerometer vibration order spectra from the Manchester test rig bearing seeded-fault tests at 1560 rev/min.

5.6. Harmonic Power Factor (*HPF*) Algorithm

The analysis of measured vibration signals has shown that at different generator speeds, generator localised outer race bearing faults result in clear amplitude increases of the first five outer race bearing fault frequency harmonics. Such pattern is a strong indicator of abnormal bearing behaviour and it has been assumed as the most reliable and consistent indicator of fault.

Based on the experimental evidence, a generator bearing outer race fault indicator, the Harmonic Power Factor algorithm, *HPF*, has been proposed in order to reduce each spectrum to only one parameter for each data acquisition and avoid time-consuming manual spectra comparison. Adopting the same approach used to define the *SBPF* algorithms presented in previous Section 5.4, the *HPF* sums the power spectrum amplitudes of the first five outer race bearing fault frequency harmonics, $PSD(i \times f_{BPFO})$, and it is given by

$$HPF = \sum_{i=1}^{5} PSD(i \times f_{BPFO}) \qquad (5.10)$$

In order to automatically extract and trend the value of the *HPF* algorithm from each FFT spectrum provided by the Brüel&Kjaer CMS, a dedicated code was developed and built in the MATLAB environment by the Author.

The sensitivity and robustness of the *HPF* algorithm have been tested by estimating its values at the different steady-state operating speeds investigated during the seeded-fault tests. Figure 5.15 and Figure 5.16 show the influence of the bearing fault severity and the investigated operating speeds on the *HPF* values for the data collected by the vertical and the horizontal accelerometers, respectively.
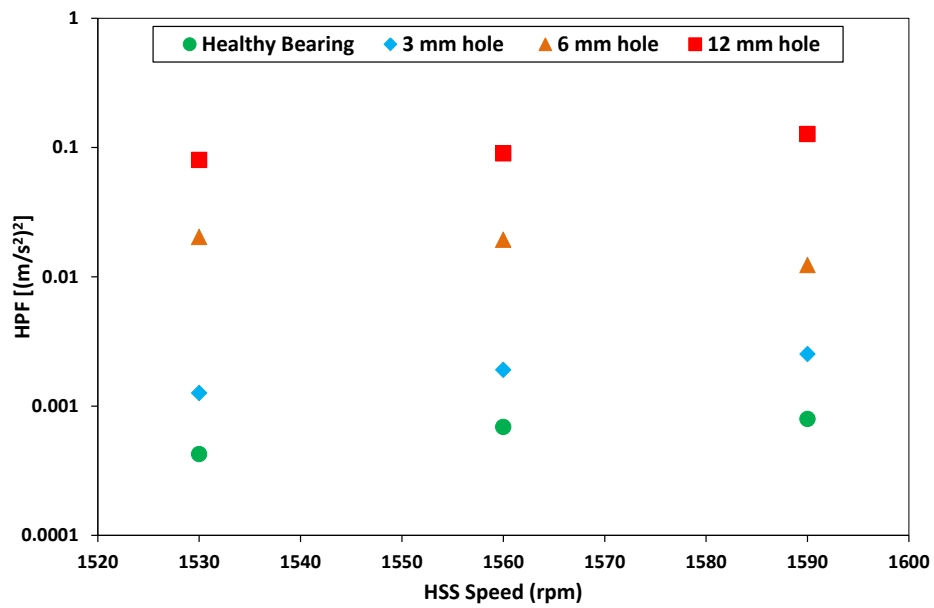
Figure 5.15: Influence of the bearing fault severity and the speed operating conditions on the *HPF* values for the vertical accelerometer dataset.
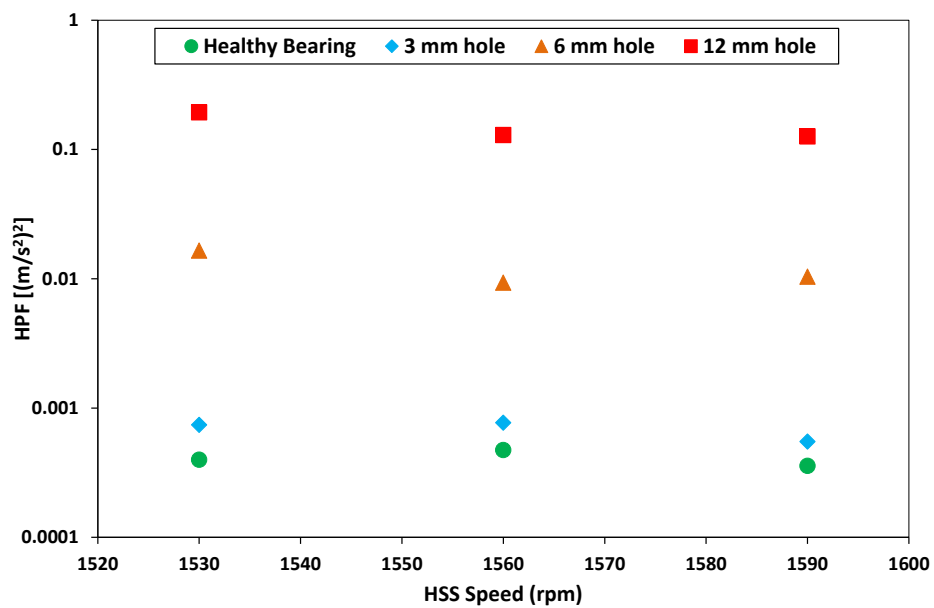
Figure 5.16: Influence of the bearing fault severity and the speed operating conditions on the *HPF* values for the horizontal accelerometer dataset.

It is clear from Figure 5.15 and Figure 5.16 that the *HPF* values derived from the measured generator frame vibration could be a reliable indicator of outer race bearing faults. The results show that the *HPF* magnitude increases

157

proportionally with the bearing fault level for both datasets, demonstrating its suitability as fault severity trend indicator. For the investigated operating conditions the proposed algorithm works successfully, achieving clear fault detection from early to more severe levels of bearing fault. The *HPF* algorithm could then be used as a suitable method to enhance the detection of bearing faults by using conventional FFT analysis and avoiding the use of more sophisticated and computing intensive post-processing techniques. In the case of the vertical accelerometer dataset, shown in Figure 5.15, for each fault severity the *HPF* values slightly increase with the HSS speed, but for the 6 mm hole at 1590 rpm speed where the value decreases. In the case of the horizontal accelerometer dataset, shown in Figure 5.16, for each fault severity the data are scattered and do not show a clear dependence of the *HPF* values on the HSS speed. Further investigation to test the *HPF* performance at the WT variable speed and load operating conditions should be the subject of further work.

5.7. Fault Detection Sensitivity

To assess the robustness and the fault signature resolution of the proposed algorithms a fault detection sensitivity function has been defined and monitored. Given that any individual monitoring signal has a different magnitude response to a particular fault level, a sensitivity function has been defined to consistently compare the results under similar operating conditions. For each proposed algorithm and each test operating conditions investigated, the algorithm detection sensitivity to the fault has been defined as its percentage change between the faulty and healthy conditions. This section presents the algorithm sensitivity calculation applied to the experimental results for each signal and each fault level investigated.

5.7.1. Gear Sideband Power Factor (*SBPF$_{gear}$*) Algorithm

Based on the experimental results from the Durham WTCMTR presented in Section 5.4.1, the $SBPF_{gear}$ detection sensitivity to HSS pinion fault, $\%SBPF_{gear}$, has been calculated as

$$\%SBPF_{gear} = \frac{\left(SBPF_{gear}\right)_f - \left(SBPF_{gear}\right)_h}{\left(SBPF_{gear}\right)_h} \times 100 \qquad (5.11)$$

where $\left(SBPF_{gear}\right)_h$ and $\left(SBPF_{gear}\right)_f$ are the healthy and faulty $SBPF_{gear}$ values, respectively, under similar operating conditions. The results are shown in Figure 5.17.
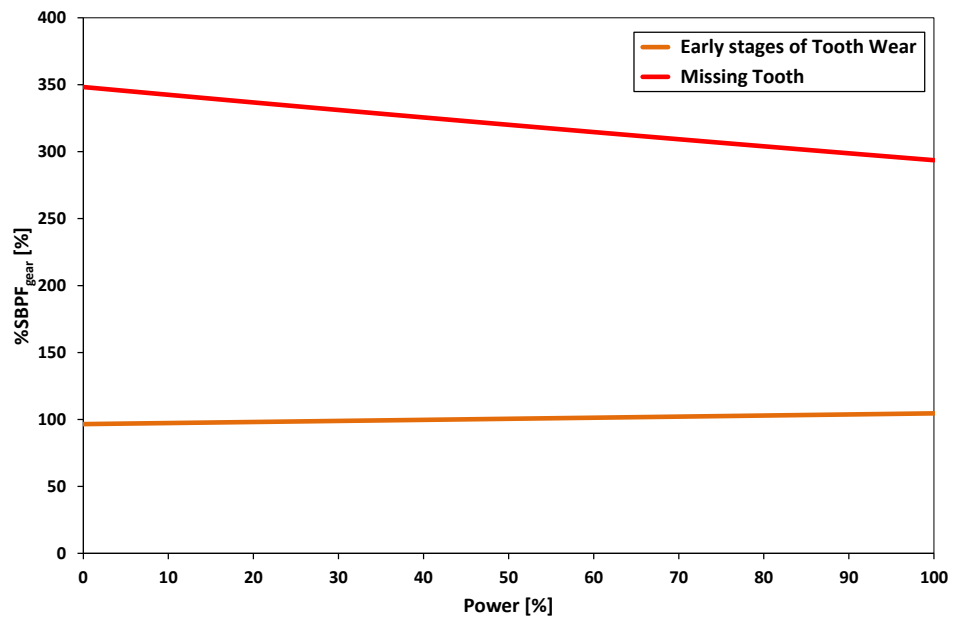
Figure 5.17: $SBPF_{gear}$ detection sensitivity to early stages of tooth wear and to tooth missing for the experimentally investigated WTCMTR power loads.

In the full range of loads investigated, the sensitivity analysis shows that the $SBPF_{gear}$ technique proves successful in the detection of both the early and the final stages of the gear tooth damage, with average detection sensitivities of 100% and 320%, respectively. The missing tooth fault is marginally easier to discriminate at lower powers, while the minor faults are

slightly easier to discriminate at higher powers. The influence of the fault severity on the $SBPF_{gear}$ detection sensitivity values is evident; the more damaged the pinion the easier it is to discriminate the fault.

5.7.2. Rotor Sideband Power Factor ($SBPF_{rotor}$) Algorithm

Similarly to the previous case, based on the Durham WTCMTR experimental results shown in Section 5.4.2, the $SBPF_{rotor}$ detection sensitivity to generator rotor electrical asymmetry, $\%SBPF_{rotor}$, has been calculated as

$$\%SBPF_{rotor} = \frac{(SBPF_{rotor})_f - (SBPF_{rotor})_h}{(SBPF_{rotor})_h} \times 100 \tag{5.12}$$

where $(SBPF_{rotor})_h$ and $(SBPF_{rotor})_f$ are the healthy and faulty $SBPF_{rotor}$ values, respectively, under similar operating conditions. The results are shown in Figure 5.18.
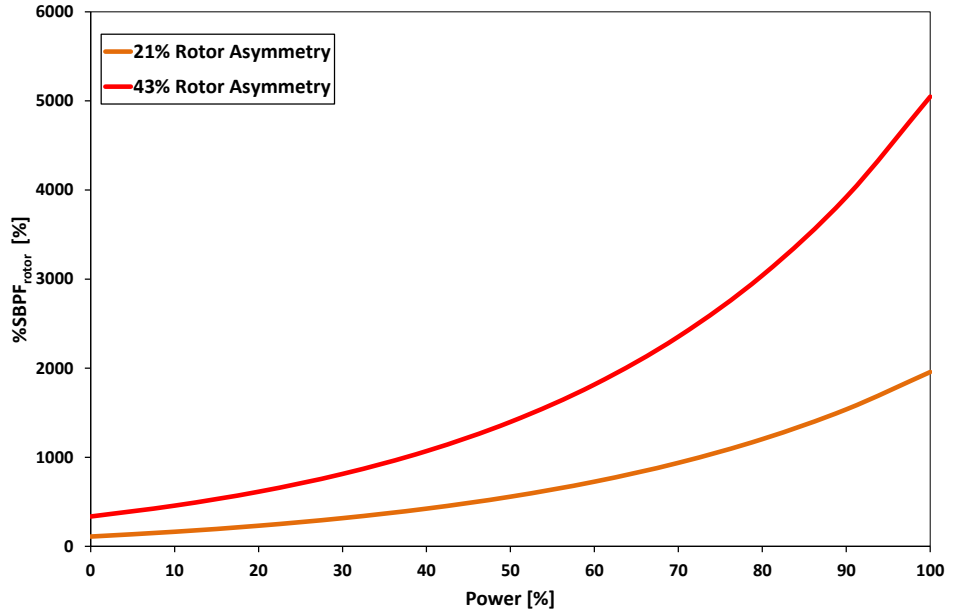
Figure 5.18: $SBPF_{rotor}$ detection sensitivity to 21% and 43% rotor asymmetry conditions for the experimentally investigated WTCMTR power loads.

As for balanced rotor the $SBPF_{rotor}$ magnitude does not vary significantly with the load, Figure 5.12, $\%SBPF_{rotor}$ varies almost

exponentially with the load for both rotor asymmetry seeded-fault datasets. The sensitivity analysis shows that $SBPF_{rotor}$ proves successful in the detection of both low and high stages of rotor fault level, with average detection sensitivities of 743% and 1897%, respectively. Under similar load conditions, the sensitivity function increases with the fault severity showing the $SBPF_{rotor}$ ability to clear discriminate the fault levels and to provide an early fault detection.

5.7.3. Harmonic Power Factor (*HPF*) Algorithm

Based on the experimental results from the Manchester test rig presented in Section 5.6, the *HPF* detection sensitivity to generator bearing outer race fault, %*HPF*, has been calculated as

$$\%HPF = \frac{HPF_f - HPF_h}{HPF_h} \times 100 \qquad (5.13)$$

where HPF_h and HPF_f are the healthy and faulty *HPF* values, respectively, under similar steady-state operating speeds conditions. Table 5.1 and Table 5.2 summarise the %*HPF* values for the generator bearing fault conditions investigated in this research and for the data collected by the vertical and the horizontal accelerometers, respectively. As expected, the average *HPF* detection sensitivity, %*HPF*, increases with the fault level. The vertical accelerometer data provides higher detection sensitivity than the horizontal accelerometer for the lowest bearing fault severity investigated, i.e. 3 mm hole. Comparable %*HPF* magnitudes are obtained for the intermediate fault condition from both accelerometers, while the horizontal accelerometer data exhibits the highest %*HPF* magnitude for the last stage of bearing fault investigated. In both cases, the results show the *HPF* algorithm ability to clearly discriminate the fault severity regardless of the generator speed.

Table 5.1: Generator drive-end side bearing damage average *HPF* detection

sensitivity for the vertical accelerometer dataset.

Generator Speed (rev/min)	Bearing Fault Severity		
	3 mm hole	6 mm hole	12 mm hole
1530	197%	4675%	18735%
1560	177%	2708%	12953%
1590	217%	1448%	15855%
Average %*HPF*	197%	2944%	15848%

Table 5.2: Generator drive-end side bearing damage average *HPF* detection sensitivity for the horizontal accelerometer dataset.

Generator Speed (rev/min)	Bearing Fault Severity		
	3 mm hole	6 mm hole	12 mm hole
1530	86%	4050%	48456%
1560	63%	1872%	27188%
1590	54%	2810%	35284%
Average %*HPF*	67%	2911%	36976%

The successful application of the *HPF* algorithm to vibration signals from the two independent accelerometers strengthens the confidence in its fault detection and diagnosis capability, eventually reducing false alarms.

5.8.   Summary

This chapter presents the experimental work conducted on two WT small-scale test rigs. The test rigs have been operated at constant and wind-like variable speed conditions and a number of seeded-faults have been applied and detected.

Seeded-fault tests have been performed by the Author on the Durham WTCMTR to investigate gearbox HS pinion tooth damage, through vibration signature analysis, and generator rotor electrical asymmetry, through

electrical and vibration signature analysis. Further experimental data, relative to the investigation of rotor electrical asymmetry and generator bearing faults, through vibration signature analysis, has been provided to the Author for analysis and processing from the University of Manchester.

In each case the relevant fault frequencies of interest, introduced throughout Chapter 3, have been investigated by using conventional FFT spectra provided by commercial WT CMSs. Identifiable fault frequencies have been extracted from the rig signatures and used to reflect the health of the component. Three novel algorithms have been then designed to track the observed fault component total power for automatic WT damage detection and diagnosis: the $SBPF_{gear}$, the $SBPF_{rotor}$ and the HPF algorithms. The main aim of these algorithms is to automatically analyse and interpret the large volumes of CM data usually produced by a CMS in a WF, significantly reducing the large degree of manual analysis currently required.

For gearbox HS pinion tooth damage, the proposed $SBPF_{gear}$ algorithm has proved to be a reliable gear health indicator, successfully allowing the assessment of the fault severity by tracking the progressive tooth damage introduced on the WTCMTR during variable speed and load conditions. The proposed algorithm has successfully detected both early and final stages of tooth damage, showing a higher effectiveness at the percentage loads above 20% and average detection sensitivity of 100% and 320%, respectively.

For generator rotor asymmetry detection through electrical signature analysis, the experimental results have demonstrated the benefits of tracking the $SBPF_{rotor}$ values as the speeds and loads vary. The algorithm has proved capable of enabling clear fault detection, for both early and advanced stages of rotor fault, with average detection sensitivity of 743% and 1897%, respectively. In the case of the Durham WTCMTR, the analysis of generator vibration signature was shown to enable rotor asymmetry detection via the

observed changes in magnitude of the $|2s|f_s$ upper SB of the supply frequency second harmonic.

Finally, the *HPF* algorithm has proved to be a reliable indicator of the outer race bearing faults investigated during the seeded-fault tests. The proposed algorithm worked successfully achieving clear fault detection, from early to more severe levels of bearing fault, under the steady-state conditions investigated during the tests, with large average detection sensitivities. The work presented in this Thesis clearly demonstrates the potential of developing WT real-time tracking applications based on the *HPF* algorithm.

6

SBPF$_{gear}$ Case Study: Validation against NREL 750kW Gearbox

6.1. Introduction

Based on the experimental evidence from the Durham WTCMTR, a novel fault detection algorithm, the Gear Sideband Power Factor, *SBPF$_{gear}$*, specifically developed to aid in the detection of WT gear tooth damage has been presented in Section 5.4.1. By tracking the overall power of the FFT spectra associated with the $2xf_{mesh,HS}$ SB frequency window, *SBPF$_{gear}$* proved effective in detecting the presence of the gear damage introduced into the 30 kW WTCMTR gearbox, that is, damage location, and in identifying the precise damaged gear, that is, damage diagnosis. In the healthy gear mesh, SBs had small amplitude compared with the centre mesh frequency or were missing resulting in low *SBPF$_{gear}$* values. As damage developed on the pinion tooth passing through the gear mesh, the SBs increased in amplitude, as well as in number, as did *SBPF$_{gear}$*. The proposed *SBPF$_{gear}$* method successfully allowed the assessment of the gear fault severity on the small-scale test rig by tracking the progressive tooth damage, from the early stages of development, during the variable wind-like speed and load conditions.

In this chapter, to validate the performance and the reliability of the proposed *SBPF$_{gear}$* technique on a full-size gearbox, the algorithm has been tested on data from the National Renewable Energy Laboratory's (NREL) wind turbine Gearbox Condition Monitoring Round project (Sheng, 2012). These vibration signals were collected from a real WT gearbox that had sustained gear damage during its field test.

6.2.   NREL Gearbox CM Round Robin project

In response to WT gearbox concerns and to help the wind industry improve its reliability and availability, the National Wind Technology Centre (NWTC) at the US Department of Energy's NREL started a project called the Gearbox Reliability Collaborative (GRC). The GRC engages key representatives in the WT gearbox supply chain, including turbine owners, operators, gearbox manufacturers, bearing manufacturers, lubricant companies and WT manufacturers, with the common goal of extending its lifetime. The main GRC's objective is to understand the possible causes of premature gearbox failures and make recommendations for reducing these failures. CM is one area of research conducted under the GRC.

One CM project was the NREL Wind Turbine Gearbox Condition Monitoring Round Robin study that took place in 2011. The study was based on gearbox data collected with various CM systems. The gearbox was first tested at the NWTC's 2.5 MW dynamometer testing facility, where it finished its run-in, and then it was sent to a nearby WF for field testing. The test gearbox was installed on the GRC test turbine, shown in Figure 6.1, which is a three-blade, stall-regulated upwind WT with a rated power of 750 kW and a rated wind speed of 16 m/s. The turbine generator operates at 1800 rev/min and 1200 rev/min nominal, on two different sets of windings, depending on the wind conditions. In the field, while the turbine was being tested, the gearbox experienced two oil loss events which resulted in some damage to its internal bearing and gear components. Additional field tests of this gearbox were terminated to prevent further damage. The gearbox was then removed from the field, reassembled and retested in the NREL test stand under controlled conditions before it was disassembled.
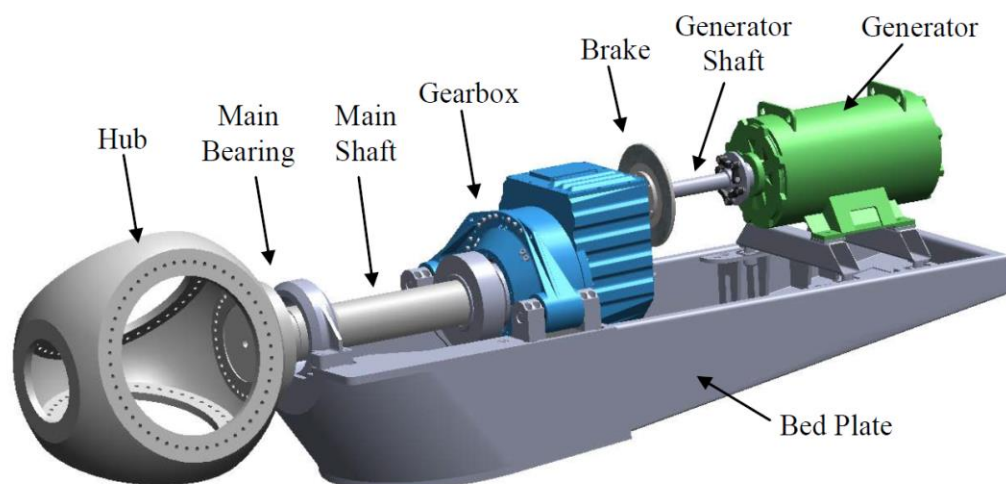
Figure 6.1: GRC test turbine (Sheng, 2012).

During the dynamometer retest, various CM data were collected, including the measurements of vibration and oil debris, along with testing condition information. This data enabled NREL to launch the Wind Turbine Gearbox Condition Monitoring Round Robin project that involved the analysis of the collected vibration data by several independent research partners and then drew conclusions from the comparison of their analysis results. The motivation was to identify some possible areas of improvement in current vibration analysis algorithms used in WT drivetrain CMSs through a blind study. The main objective of this project was use vibration data analysis support from participants to investigate different algorithms and provide guidance to the wind industry regarding best possible practices for conducting vibration-based WT CM.

NREL invited its academic and industrial partners from around the world to participate in the study. Seven university partners and nine private sector partners agreed to join this study. The vibration data collected from the gearbox, along with its configuration information, were first shared with the project partners as a blind study. Partners did not have prior knowledge of the extent or location of the actual damage within the test gearbox. They were given a time window of two months to analyse the shared vibration data

167

using any algorithm they had or could develop. After their diagnostic results were submitted to NREL, the actual damage information on the test gearbox was disclosed to them so they could further refine their results. The primary goal of the project was to verify the damage detection algorithms by comparing the damage detection results with the post-examination results. The entire project is described in the NREL report (Sheng, 2012) that contains detailed analysis algorithms and diagnostic results from eight out of the sixteen partners.

Thanks to the collaboration with Dr Shuangwen Sheng from NREL, the WT Gearbox CM Round Robin project data has been made available to the Author for validation of the $SBPF_{gear}$ algorithm performance.

6.2.1. NREL 2.5 MW Dynamometer Test Facility

The retest of the damaged gearbox was conducted in the NREL dynamometer test facility which conducts performance and reliability tests on WT drivetrain prototypes and commercial machines. A complete description of the NREL test-bed and instrumentation can be found in Musial and McNiff (2000) and NREL (2010).

A schematic diagram and a photograph of the NREL 2.5 MW dynamometer test stand with the test gearbox installed are shown in Figure 6.2 and Figure 6.3, respectively. The prime movers of the dynamometer are a 2.5 MW induction motor, a three-stage epicyclical reducer, and a variable-frequency drive, with full regeneration capacity. The rated torque provided by the dynamometer to a test article can be up to 1.4 MNm, with speeds varying from 0 rev/min to 16.7 rev/min. Non-torque loading actuators, rated up to 440 kN for radial load and 156 kN for thrust load, can also be utilized in the dynamometer to apply thrust, bending, and shear loads similar to those typically generated by a WT rotor. The complete nacelle and drivetrain was installed in the NREL dynamometer test facility and hard fixed to the floor,

without the hub, rotor, yaw bearing, or yaw drives. The actual field controller was used to provide start-up and system safety response. The gearbox was tested under simple loading conditions of fixed torque with sweeps of non-torque loading. Torque up to 75% of rated was applied.
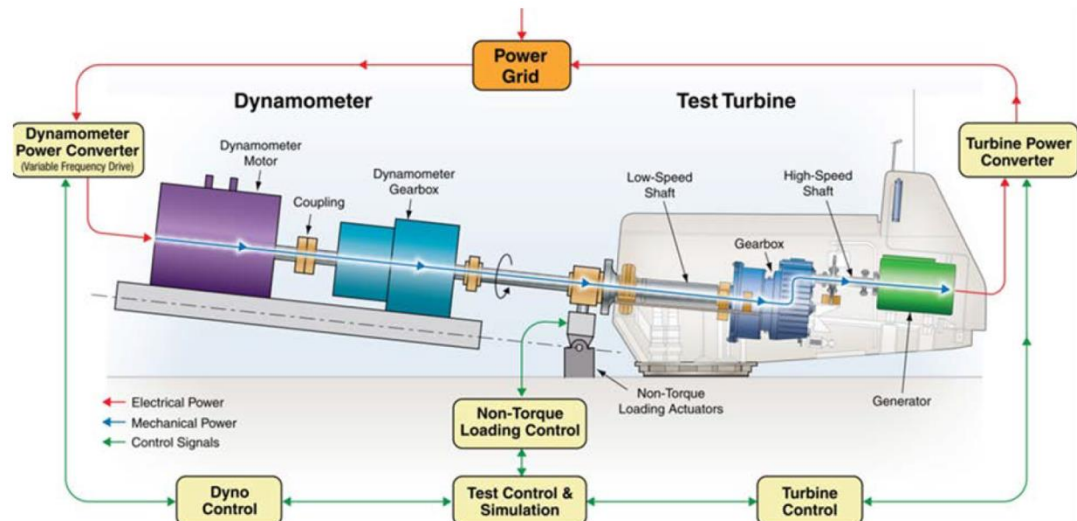
Figure 6.2: Schematic of the NREL 2.5 MW dynamometer test facility (Sheng, 2012).

Figure 6.3: NREL dynamometer test stand with the 750 kW gearbox installed, photograph by Lee Jay Fingersh/NREL 16913.

6.2.2.   Gearbox Description

The gearbox under test was a three-stage design featuring one LS planetary stage and two parallel stages, an intermediate-speed (IS) and HS,

169

respectively. The NREL nomenclature for the gearbox internal elements is described in the schematic in Figure 6.4, and the gear teeth number are listed in Table 6.1.
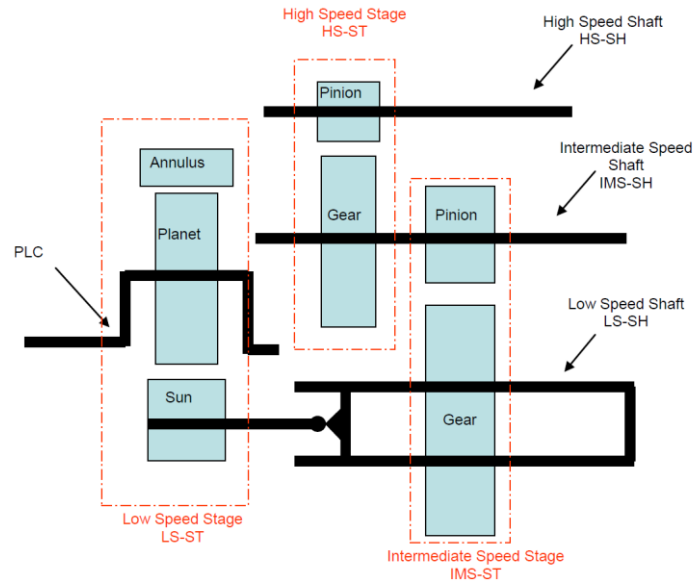
Figure 6.4: Schematic diagram of the NREL GRC gearbox transmission stages (Sheng, 2012).

Table 6.1: NREL 750 kW gearbox nomenclature and teeth number.

Gear Element	Location	Number of Teeth	Mate Teeth	Ratio
Ring Gear	LS planetary stage	99	39	–
Planet Gear	LS planetary stage	39	99	–
Sun Pinion	LS planetary stage	21	39	–
				5.71
Intermediate Gear	IS Parallel Stage	82	23	–
Intermediate Pinion	IS Parallel Stage	23	82	–
				3.57
HS Gear	HS Parallel Stage	88	22	–
HSS Pinion	HS Parallel Stage	22	88	–
				4.0
Overall ratio				81.491

The overall gear ratio between input and output shafts is 1:81.491. Based on the information provided in Table 6.1 the operating gear mesh characteristic frequencies can be easily calculated.

6.2.3. Vibration Data Acquisition System

During the dynamometer retest of the damaged gearbox, data was collected by a vibration DAS customized by NREL. It is composed of twelve accelerometers mounted on the gearbox frame, generator and main bearing, with locations chosen to reflect typical sensor placement practices seen in commercial WT drivetrain vibration-based CMSs, as described in detail in (Sheng, 2012). Data was collected at 40 kHz sampling rate per channel using a National Instruments PXI-4472B high-speed DAS. LSS torque and generator speed were recorded, in addition to the accelerometer data. The HSS speed measurement was obtained by an optical encoder.

6.2.4. Test Conditions and Actual Gearbox Damage

The vibration data was collected under the test conditions shown in Table 6.2. The highest test load applied was 50% of rated power to reduce the chances of a catastrophic gearbox failure. Under each test condition, ten minutes of data was collected.

Table 6.2: NREL WT Gearbox CM Round Robin project test conditions, adapted from (Sheng, 2012).

Test Case	LSS Speed (rev/min)	Nominal HSS Speed (rev/min)	Electric Power (% of rated)	Duration (min)
CM_2a	14.72	1200	25%	10
CM_2b	22.09	1800	25%	10
CM_2c	22.09	1800	50%	10

Once the dynamometer retest was completed, the gearbox was disassembled and a detailed failure analysis was conducted (Errichello and Muller, 2012). Severe scuffing of the HS shaft gear set was one of the 12 instances of damage found during the failure analysis. Figure 6.5 shows the damaged HSS pinion with clear scuffing marks. The root cause of the faults was assembly damage and oil starvation resulting from the two oil loss events in the field test.
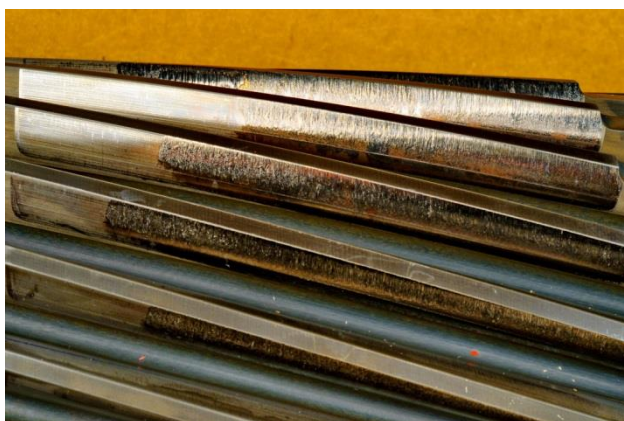
Figure 6.5: HSS pinion damage on the NREL 750 kW gearbox, photograph from GEARTECH/NREL 19743.

It should be noted that, according to the GRC CM Round Robin project final report (Sheng, 2012), HSS misalignment was one source of gearbox actual damage which could potentially be detected by vibration analysis as well, but most project partners considered it to be an operational condition and not damage. The complete list of the actual damage on the test gearbox is given in Sheng (2012) and a full discussion of this issue is beyond the scope of this Thesis.

6.2.5.   Baseline Data

Baseline data was collected on the dynamometer test stand from an identical healthy test gearbox, which had no operational experience. The healthy dataset refers to the 1800 rev/min and 50% rated power test condition,

corresponding to the CM_2c test case in the faulty dataset in Table 6.2. Vibration signals from several accelerometers mounted on the test gearbox, when it was considered healthy, were recorded and processed by a commercial CMS. The Hanning window has been applied to the vibration signals during the CMS FFT analysis. The produced spectra have 3200 resolution lines for a 2 kHz bandwidth with a resulting frequency resolution of 0.625 Hz/line. For each accelerometer, one healthy gearbox FFT spectrum, referring to a measurement time window of 1.6 seconds, was shared with the project partners.

6.3.   Gearbox Vibration Signature Analysis

The task of the research presented in this Thesis was to validate the $SBPF_{gear}$ analysis of the vibration data to detect and diagnose the NREL gearbox HSS pinion damage by using data collected by two independent accelerometers, namely AN6 and AN7 according to the NREL accelerometer nomenclature, mounted radially on the gearbox ISS and HSS, respectively. Both these sensors were PCB IMI 622B01 integrated-circuit piezoelectric-type accelerometers with a sensitivity of 100 mV/g, a frequency range of 0.2 to 15 kHz and ±50 g measuring range. The transducers were mounted as close as possible to the gearbox HS stage to get the best quality signals when evaluating the HSS pinion health condition.

The dataset from the two identical 750 kW WT gearboxes tested on the NREL test stand, available to the Author for analysis, refers to the HSS speed of 1800 rev/ min and to 50% of the rated power. For each accelerometer, it contains:

- For the healthy gearbox: 1 single FFT spectrum with 2 kHz bandwidth collected by a commercial CMS for a duration of 1.6 s;
- For the faulty gearbox: 40 kHz raw vibration data collected continuously for 10 min.

A methodological approach similar to that used for the 30 kW WTCMTR data, described in previous Section 4.7 and Section 5.2, has been adopted to analyse and process the 750 kW NREL gearbox vibration signals. In this case, the dataset presented some challenges for deriving a SB amplitude comparison system baseline. This was overcome by windowing data from the faulty gearbox through a 1.6 s time window and then processing the data by using the built-in FFT algorithm in MATLAB. The Hanning window was applied to the raw vibration signals. For each accelerometer, the resulting 375 FFT spectra have then been consistently compared against the available healthy spectrum, presenting the same frequency resolution of 0.625 Hz/Line.

Normalised order spectra (X) were used to facilitate the comparison of the FFT spectra and to identify the effect of the faulty tooth on the 750 kW NREL gearbox vibration signature. The NREL test gearbox has 22 teeth on the HSS pinion, Table 6.1, thus, according to what discussed in Section 3.4.6, the normalised HS stage meshing frequency is

$$f_{mesh,HS} = 22\,X \tag{6.1}$$

Although the full frequency range spectra are available, for clarity and conciseness, only their zoomed version around the HS stage meshing frequency second harmonic, $2xf_{mesh,HS}$, relevant to the work presented in this Thesis, are presented here. Figure 6.6 and Figure 6.7 show an example of the zoom-in view of the healthy and the faulty HSS order vibration spectra around the $2xf_{mesh,HS}$ second harmonic, given by

$$2xf_{mesh,HS} = 44\,X \tag{6.2}$$

for the AN6 and the AN7 accelerometer data, respectively.

In both cases, when comparing the degraded gearbox with the nominal baseline healthy gearbox, the increase in the energy content of the $2xf_{mesh,HS}$, harmonic and its SBs can be clearly seen.
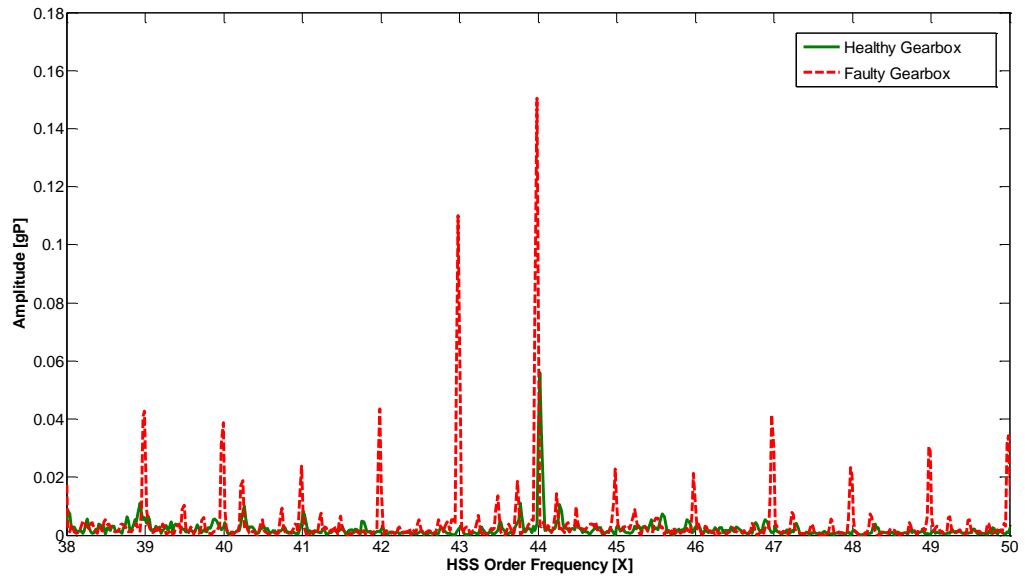
Figure 6.6: Accelerometer AN6 ISS Radial vibration FFT spectra in the $[38 - 50]$ X HSS order frequency bandwidth for the healthy and faulty identical 750 kW gearboxes.
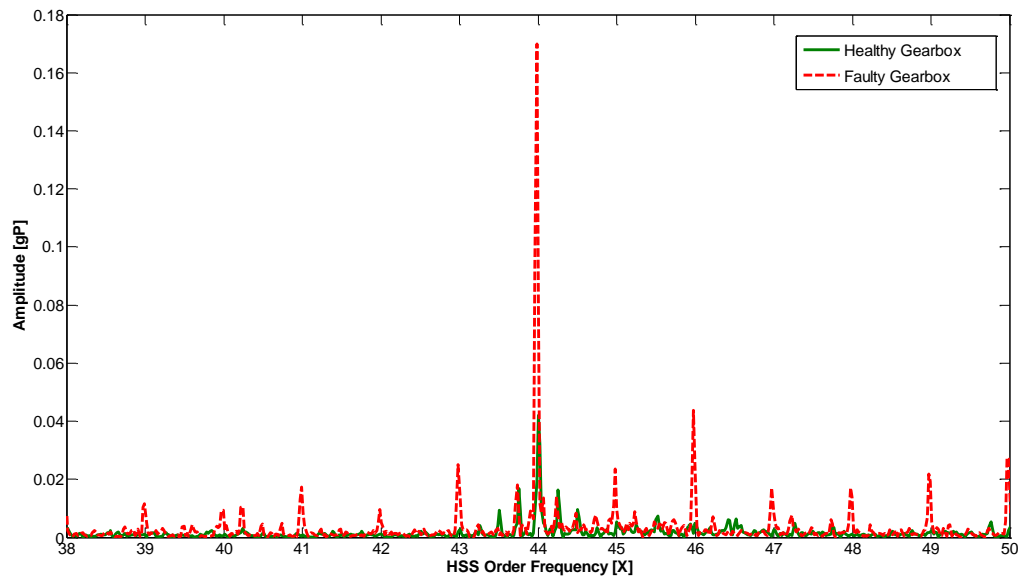
Figure 6.7: Accelerometer AN7 HSS Radial vibration FFT spectra in the $[38 - 50]$ X HSS order frequency bandwidth for the healthy and faulty identical 750 kW gearboxes.

In the faulty spectrum, the HS meshing frequency second harmonic is heavily modulated by the HSS rotational speed, $f_{HSS} = 1\ X$, clearly indicating

fault detection on the HS stage gear mesh. Furthermore, the SB spacing indicates severe damage on the HSS pinion.

These results confirm the validity of the small-scale WTCMTR experimental approach and strengthen the previous findings about the effectiveness of the $2xf_{mesh,HS}$ SBs tracking in the detection and diagnosis of HSS pinion defects.

6.4.   SBPF$_{gear}$ Algorithm Implementation

To quantify these observations from the vibration data, $SBPF_{gear}$ values were extracted from the baseline spectrum and the 375 degraded gearbox spectra for both accelerometers. The $SBPF_{gear}$ analysis procedure of the NREL dataset was implemented with the MATLAB code developed and built by the Author.

The results are shown in Figure 6.8 and Figure 6.9 for AN6 and AN7, respectively. In both cases, despite its low amplitude oscillations around the mean value, resulting from the random and the oscillatory vibration noise, the $SBPF_{gear}$ magnitude is much larger for the degraded gearbox compared with the baseline gearbox, representing an average value of 0.021 (gP)² and 0.013 (gP)², respectively. From the $SBPF_{gear}$ methodology, there is a strong indication that there is damage on the HSS pinion.

These results, on a full-size 750 kW gearbox, provide further credibility to the $SBPF_{gear}$ algorithm, already proven on the 30 kW WTCMTR, for a timely detection and diagnosis of gear damage. It should be noted that the HSS pinion detection and diagnostic task in the Round Robin project was more challenging because the drivetrain damage was more complex than in a typical operational WT. Therefore, the $SBPF_{gear}$ technique presented in this Thesis could potentially perform better when deployed in the field.
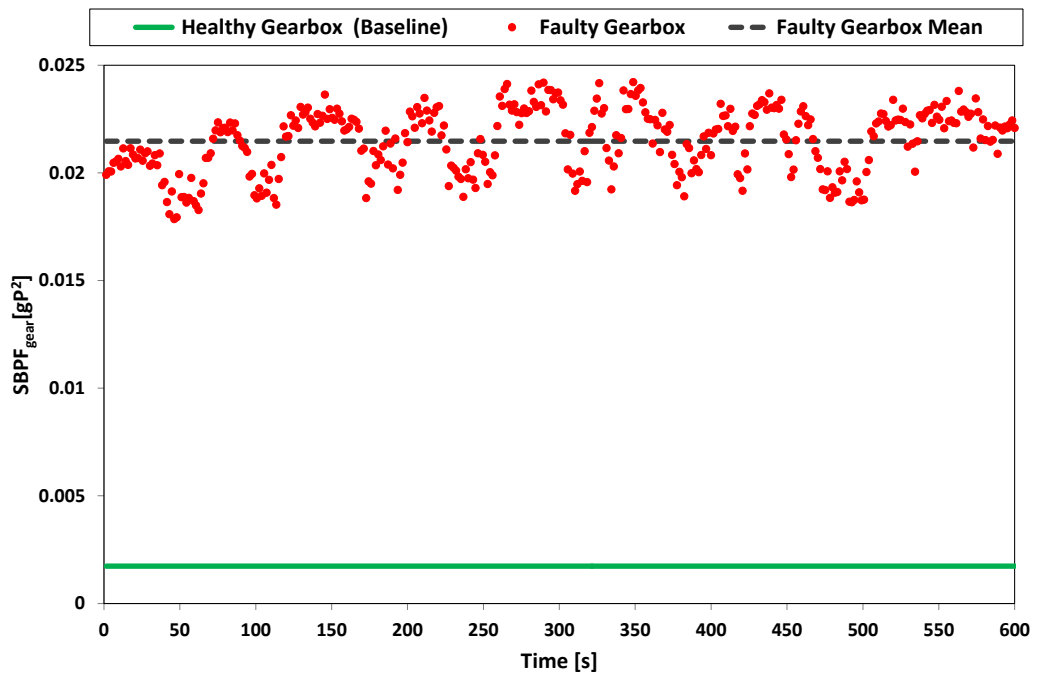
Figure 6.8: Accelerometer AN6 ISS Radial $SBPF_{gear}$ comparison between healthy and faulty identical 750 kW gearboxes.
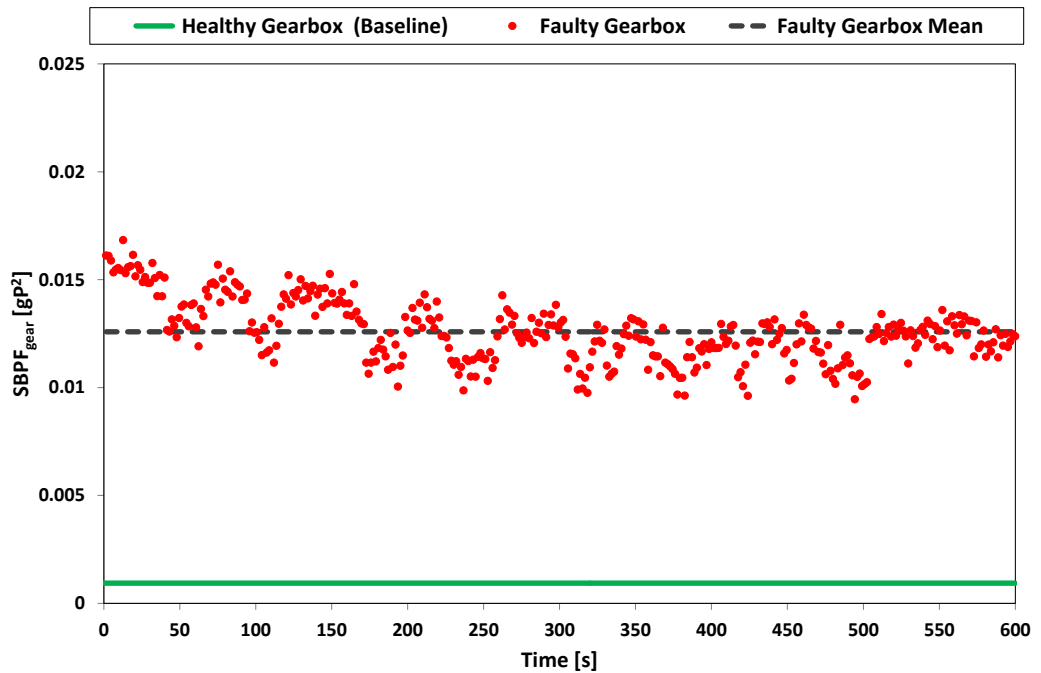
Figure 6.9: Accelerometer AN7 HSS Radial $SBPF_{gear}$ comparison between healthy and faulty identical 750 kW gearboxes.

In the NREL validation case study, the use of the vibration signals collected from two independent accelerometers located at strategic positions on the gearbox casing improves the confidence in the $SBPF_{gear}$ fault detection and diagnosis capability, eventually reducing false alarms. This is particularly interesting when considering that one issue around the CMS data interpretation is to rely on a single signal, which could lead to false alarms from the monitoring process (Feng et al., 2013).

Although no baseline data was available for comparison for the CM_2a and CM_2b test cases of the NREL faulty test gearbox dataset in Table 6.2, the corresponding $SBPF_{gear}$ values were calculated and compared against those obtained from the CM_2c test case. This allowed the investigation of the effect of changes in the machine speed and load on the magnitude of the proposed gear condition indicator. The results are shown in Figure 6.10 and Figure 6.11 for AN6 and AN7, respectively. In both cases, the $SBPF_{gear}$ magnitude increases with the HSS test speed consistently throughout the full testing period of 10 min, showing the highest values for the CM_2b and CM_2c test conditions, referring to the HSS speed of 1800 rev/min and 25% and 50% of the rated power, respectively. Moreover, at the same test speed of 1800 rev/min the $SBPF_{gear}$ magnitude shows the highest values for the CM_2c test conditions, corresponding to the highest electric power tested. The increase of the $SBPF_{gear}$ magnitude with the machine load confirms the behaviour observed on the Durham WTCMTR for a larger range of load investigated, Figure 5.11. However, further work is needed to validate these results with more datasets.
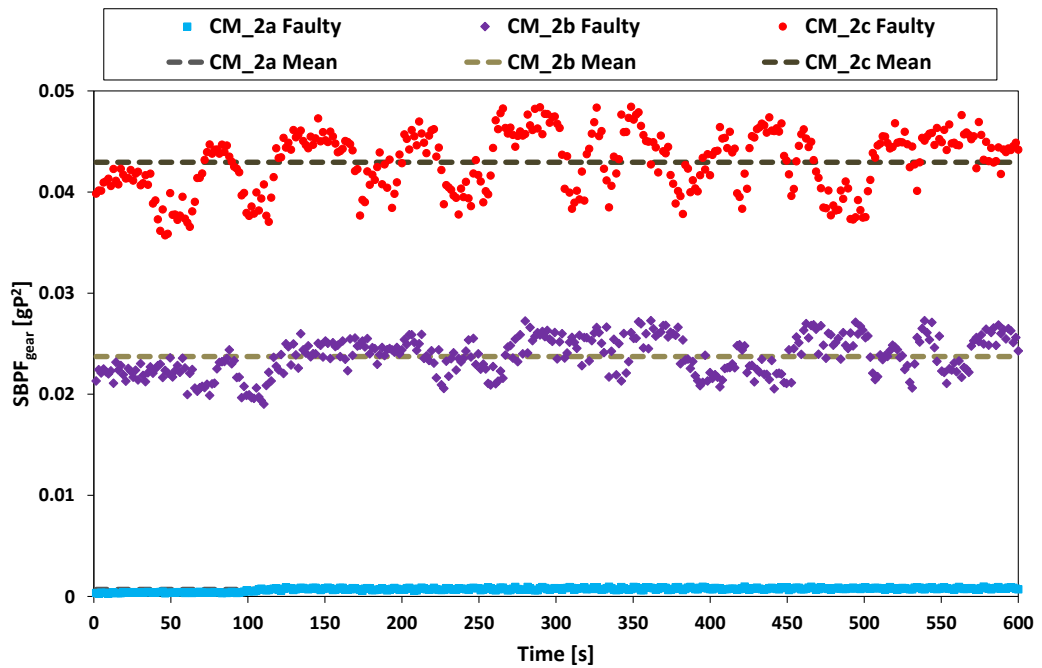
Figure 6.10: Accelerometer AN6 ISS Radial $SBPF_{gear}$ comparison between CM_2a, CM_2b and CM_2c faulty gearbox test cases.
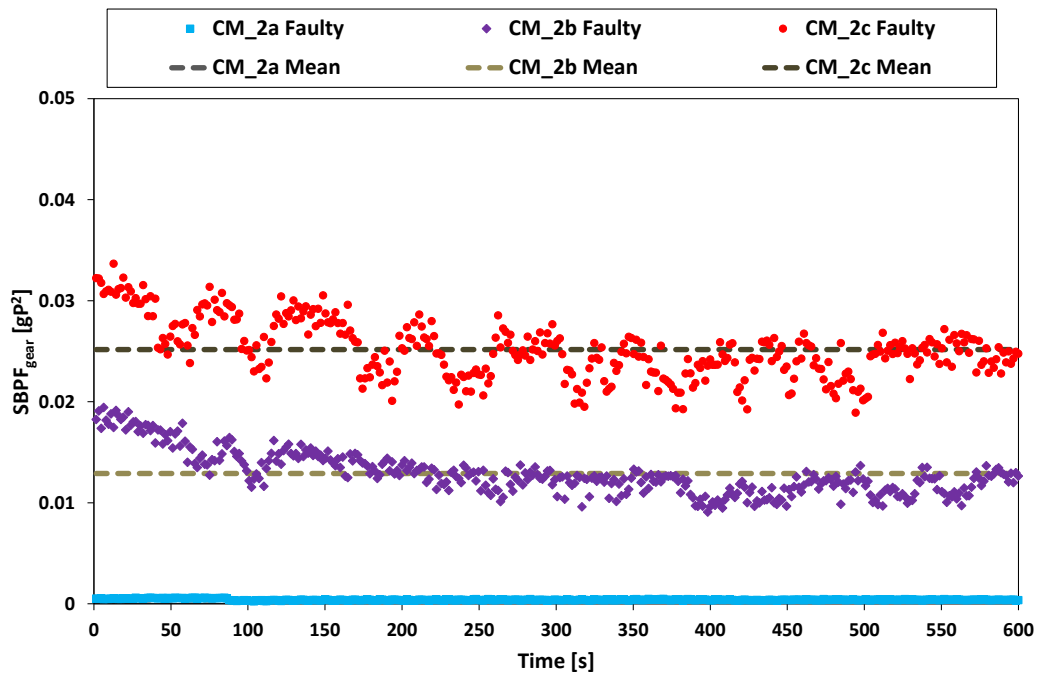
Figure 6.11: Accelerometer AN7 HSS Radial $SBPF_{gear}$ comparison between CM_2a, CM_2b and CM_2c faulty gearbox test cases.

179

6.5. Fault Detection Sensitivity

The $SBPF_{gear}$ detection sensitivity to the tooth damage, $\%SBPF_{gear}$, has been calculated according to equation (5.11) by determining, for the available healthy and faulty NREL datasets, the percentage change of the $SBPF_{gear}$ value. Table 6.3 summarises the average $SBPF_{gear}$ detection sensitivities to the HSS pinion damage for the 750 kW NREL gearbox datasets and, for comparison, the 30 kW Durham gearbox results presented in Section 5.7.1.

Table 6.3: Durham (30 kW) and NREL (750 kW) gearbox average $\%SBPF_{gear}$.

Gearbox	HSS Pinion Fault Severity	Accelerometer location	Average $\%SBPF_{gear}$
NREL – 750 kW gear box datasets	severe scuffing	AN6 ISS radial	1140%
	severe scuffing	AN7 HSS radial	1251%
Durham – 30 kW seeded fault tests	early stages of tooth wear	HSS vertical	100%
	missing tooth	HSS vertical	320%

As the gearbox scales up to the full-size WT design, the NREL $\%SBPF_{gear}$ shows increased values compared to the small-scale WTCMTR gearbox despite the lower level of fault severity experienced by the HSS pinion. In the case of the NREL dataset, although the gearbox damage was more complex than in a typical operational WT (Sheng, 2012) and the dataset provided refers to only one speed and load operational condition, the $SBPF_{gear}$ detection and diagnostics technique proves successful in the detection of the HSS pinion damage, with an average detection sensitivity of 1140 and 1251% for the AN6 ISS radial and the AN7 HSS radial accelerometers, respectively. Since the analysed dataset contains multiple gearbox progressed faults, it is

believed that the $SBPF_{gear}$ diagnostic performance could be improved when deployed in the field, bearing in mind the smaller number of the faults usually present during the early stages of the gearbox fault evolution.

These results show how the proposed $SBPF_{gear}$ methodology, based on the experimental analysis of the dynamics of the gears, can easily be scaled to the higher WT power levels. However, this would probably imply an increase in the spectral background noise because of the higher complexity of the WT drive trains compared with the small-scale WTCMTR.

6.6.   Summary

This chapter presents the successful validation of the proposed $SBPF_{gear}$ as automatic WT gear tooth fault detection and diagnosis technique through signals from a full-size WT gearbox studied in the NREL CM Round Robin project. After experiencing severe HSS gear set scuffing in the field, the full-size test gearbox was retested under controlled conditions in the NREL dynamometer test stand. A methodological approach similar to that used for the small-scale WTCMTR gearbox data, described in Chapter 5 has been adopted to analyse and process the large-scale NREL gearbox vibration signals. The results of the automated $SBPF_{gear}$ algorithm were corroborated with visual spectral analysis.

The available dataset presented some challenges and peculiarities. In particular, the absence of raw, time-domain data from a healthy system made it difficult to baseline the system for comparison purposes. This was overcome by processing the time-domain faulty gearbox data through an accurately chosen time window in order to get directly comparable spectra.

Although referring to only one steady-state operating condition, confidence in the NREL gearbox results is enhanced by a strong $SBPF_{gear}$

detection and diagnosis evidence from two independent accelerometers. Further work is needed to validate these results with more datasets.

The successful validation of the proposed $SBPF_{gear}$ technique on vibration data from two widely different gearbox designs and size strengthens its adaptability for application to a variety of geared WT technologies.

7

Conclusions & Further Work

7.1. Conclusions

Wind energy has an important role in providing sustainable energy. By the end of 2013, global wind power installed capacity had reached more than 318 GW (Fried et al., 2014), compared to a total installed electrical generation capacity of around 5.4 TW (Central Intelligence Agency, 2013). Offshore wind has significant generation potential in Europe, especially in the UK, but the market is not growing as fast as expected. The main challenges still facing the offshore wind industry are to reduce the capital cost, ensure that the technology is reliable enough and avoid premature component failures that lead to increased O&M costs, both increasing the cost of wind energy especially with the current growth in turbine size and capacity and the installation in increasingly remote and difficult-to-access offshore locations. The development of reliable and effective CM techniques can play a crucial role in minimising O&M costs of WT components, making wind power more competitive compared to conventional sources. WT CM is a fundamental input to advanced diagnostic techniques for a mature condition-based maintenance strategy.

In this Thesis, the state of the art, limitations and challenges of current commercially available WT CMSs have been investigated and discussed. This has highlighted that, although all new turbines are now fitted with some form of CMS, for certification and insurance reasons, very few operators make use of the available monitoring information for maintenance purposes because of the volume and the complexity of the data related to the WT variable speed operation and stochastic aerodynamic load. To use CM information successfully in the challenging offshore environment and to

183

deliver actionable recommendations for optimal O&M strategies, systems that can automatically analyse and interpret large volumes of data are needed.

High level reliability surveys have highlighted that the most critical drive train sub-assemblies for modern variable speed WT are in the drive train and particularly in the gearbox and generator. These technologies are mature, but the application to the wind industry is new and combines a number of acute challenges for their CM and the WT reliability which have been discussed.

It has been the purpose of this Thesis to experimentally devise advanced signal processing algorithms for WT automatic gearbox and generator fault detection and diagnosis.

Experimental work on small-scale CM test rigs has allowed the implementation of seeded-fault testing under controlled conditions. There are a number of benefits of using a test rig over full-scale WT field tests for evaluating CM techniques and these have been described.

Three classes of seeded-fault tests were performed:

- Gearbox high-speed pinion tooth damage;
- Generator rotor electrical asymmetry;
- Generator bearing faults.

In each case, characteristic fault frequencies have been identified and investigated by using conventional FFT spectra of mechanical and electrical signals provided by commercial WT CMSs. This was done to demonstrate that the research proposals in this Thesis could be implemented on a practicable, industrial CMS. The experimental results indicated a clear relationship between the magnitude of the identified spectral components and the presence of seeded-faults.

Based on the experimental evidence, three novel automatic fault detection and diagnosis algorithms have been designed to track reliably the observed fault component as the WT speed and load vary.

Considerable effort has been made throughout this Thesis to provide algorithms that are clear, easy to implement and use. The rationale behind their definition was to collate the power associated to the identified characteristic fault frequencies in the investigated CM signals in order to enhance the fault detection capabilities and reliability. To test their robustness the algorithms have been applied to data recorded from the CM test rigs and their sensitivity to fault detection have been assessed. The results presented in this Thesis demonstrate that the proposed techniques can provide WT component performance assessment and early fault identification, thereby giving the operators sufficient time to make more informed decisions regarding the maintenance of their machines.

The Gear Sideband Power Factor algorithm, $SBPF_{gear}$, was specifically developed to aid in the detection of WT gear tooth damage in non-stationary vibration monitoring signals. The proposed $SBPF_{gear}$ algorithm proved to be a reliable gear health indicator, effective in detecting the presence of both early and final stages of HSS pinion tooth damage introduced into the small-scale test rig gearbox, that is, damage location, and in identifying the precise damaged gear, that is, damage diagnosis, with a detection sensitivity of 100% and 320%, respectively. The $SBPF_{gear}$ successfully allowed the assessment of the pinion fault severity by tracking the progressive tooth damage introduced on the test rig gearbox during variable speed and load conditions.

The experimentally defined $SBPF_{gear}$ was successfully tested against the vibration data from an NREL full-scale WT gearbox, which had experienced severe HSS pinion scuffing in the field. Confidence in the NREL gearbox results was enhanced by a strong $SBPF_{gear}$ detection and diagnosis evidence

from two independent accelerometer signals, with detection sensitivities of 1140 and 1251%, respectively.

The Rotor Sideband Power Factor algorithm, $SBPF_{rotor}$, was specifically developed to aid in the automatic detection of WRIG rotor asymmetry through electrical signature analysis when analysing the non-stationary signals produced by modern WT variable speed operation. The proposed $SBPF_{rotor}$ techniques has proved capable of enabling clear fault detection, for both early and advanced stages of rotor asymmetry, with average detection sensitivity of 743% and 1897%, respectively. The experimental results have clearly shown the benefits of tracking the $SBPF_{rotor}$ under non stationary, variable speed, wind-driving conditions.

A knowledge of WT load is fundamental to the effective application of the $SBPF_{gear}$ and $SBPF_{rotor}$ techniques. Current commercially available CMSs usually provide turbine load information. This will allow the SBPF techniques to work in context with the machine load. Otherwise, in case the turbine load is not available, the operator has to take the SBPF measurements only when the machine is at its full load.

The Harmonic Power Factor algorithm, HPF, was specifically developed for automatic generator bearing fault detection by using conventional FFT analysis of vibration data produced by commercial WT CMSs. The HPF algorithm has proved to be a reliable indicator of the outer race bearing faults investigated during the seeded-fault tests performed under steady-state conditions. The experimental results have shown the HPF algorithm ability to clearly discriminate the fault severity regardless of the generator speed. The work presented in this Thesis clearly demonstrates the potential of developing WT real-time tracking applications based on the HPF algorithm.

The $SBPF_{gear}$, $SBPF_{rotor}$ and HPF methodology can easily be scaled to the higher WT power and speed levels. However, this would probably imply an

increase in the spectral background noise because of the higher complexity of the WT drive trains compared with the small-scale test rig.

The use of characteristic fault frequencies extracted from the generator vibration signature as an indicator of rotor electrical asymmetry has also been examined and discussed. Rotor asymmetry detection was enabled by tracking the changes in magnitude of the $|2s|f_s$ upper SB of the supply frequency second harmonic in the Durham test rig generator vibration signature. Further experimental investigation on the Manchester test rig, under similar seeded-fault conditions, could provide useful insights complementing the promising findings from the Durham test rig.

Previously proposed WT fault detection techniques were generally based on narrow band spectral analysis of single signals and relied on modest changes between faulty and healthy conditions resulting in low fault detection sensitivities (Crabtree, 2011; Hameed et al., 2009; Hyers et al., 2006; Tavner, 2012). This approach works well in the case of multi-parameter monitoring, where the fault detection results from the combination of indications arising from two or more independent sensors. However, when only one signal is analysed and monitored high detection sensitivity are needed in order to provide convincing and satisfactory results to support WT operator maintenance decision strategy. The main aim of this research was to devise automatic techniques to improve CM reliability using field-fitted equipment and to reduce the work-load on WF operators. The results presented in this Thesis demonstrate that the proposed algorithms will be valid for application to full-size offshore WTs.

In summary, the main advantages of the novel algorithms presented in this Thesis are:

- The reduction of the uncertainty involved in analysing CM signals by concentrating on raising fault detection sensitivity so that higher

reliability is achieved compared to previously proposed WT fault detection techniques. Enhanced detection sensitivity is obtained by considering a wideband spectral analysis of the CM signals and by identifying and collating the power of characteristic fault frequencies which could be tracked as the WT speed varies.

- The ability of auto-detecting and distinguishing WT component defect signatures within an overall CM signal, reducing each FFT spectrum to only one relevant parameter for each data acquisition. This significantly simplifies the complex and time consuming manual FFT analysis currently required.

- On-line automatic analysis and interpretation of the large volumes of data usually produced by a CMS in a WF with a significant reduction of the quantity of CM information that WT operators must handle, providing improved detection and timely decision-making capabilities.

- Clear ability to accurately discriminate the severity of mechanical and electrical faults providing an early detection and diagnosis warning of developing WT component damage crucial for effective maintenance optimization to prevent major component failures. Faults can be detected while the defective component is still operational and thus necessary repair actions can be planned in time.

- Easy implementation into existing commercial WT CMSs, as has been done in this research, avoiding costly extra new transducers, hardware components and data processing, for efficient analysis of data captured to get the most out of the CMS without requiring expert knowledge.

- The proposed algorithms are ideally suited for the WT industry and can be monitored over time, trended and compared with one or more predetermined magnitude threshold levels to provide warnings and alarms to the WT operators indicating when optimal maintenance action needs to be performed.

- Compared with the conventional FFT approach used in the current commercial CMSs, requiring a time consuming visual spectra analysis, the proposed approaches enable an automatic detection and diagnosis of the faults with a low risk of false alarms. This will lead to an increased accuracy of the WT drive-train CM.

- The proposed algorithms are a promising possibility for automating WT gearbox and generator CM and they can be also used in combination with other existing techniques in order to further strengthen the confidence in their results.

7.2. Further Work

The following areas for further work have arisen from the investigations presented in this Thesis.

- **Extend $SBPF_{gear}$ algorithm applicability.** The $SBPF_{gear}$ technique can be easily adapted to detect gear damage on all the WT gearbox parallel stages, while its applicability to the planetary stages still requires more investigation. For the gearbox parallel stages, the $SBPF_{gear}$ is easily applicable to the harmonics of each fundamental gear mesh frequency using both the gear and the pinion SBs, once the multistage gearbox configuration and the number of the teeth of each gear element are known. For each stage, this information allows for the calculation of the gear damage features, such as the meshing frequencies, their harmonics and the spacing of the SBs caused by the gear wear modulation phenomena, and the extraction of the corresponding $SBPF_{gear}$ values. For the planetary stages, the analysis of the SB patterns could be more complicated because of the low mechanical transmissibility from the gear components and the multiple contact points between each planet gear meshing and the sun and ring gears. Conventional gear diagnostic features are limited for planetary gear

component fault detection because of the changing transmission path, multiple mesh points and moving location of the fault. As such, special consideration should be given to fault detection of these components. Damage detection related to the WT gearbox low-speed side is an area that needs more research and engineering attention in the future.

- **Development of a WT electric model for CMS.** A similar method such as that used to generate CMS FFT spectral cursors for vibration interpretation can be developed to aid electrical interpretation and allow the easy implementation of the $SBPF_{rotor}$ rotor algorithm.

- **WTCMTR bearing seeded-fault testing.** To further validate the potential of developing WT real-time tracking applications based on the HPF algorithm, designed under rig steady-state operating conditions, it is suggested to perform further tests on the Durham WTCMTR at wind-like variable speed conditions.

- **Algorithm validation in the field.** It is recommended to further test the algorithms discussed in this Thesis with field measurements from real WTs. Their incorporation into the CMS of an operational WT would then allow complete on-line testing in the field.

- **WTCMTR DFIG operation.** The work in this Thesis operated the generator as a WRIG. However, thanks to its recent development the rig can now also operate as a fully variable speed WT-driven DFIG bringing it yet closer to the most widely installed WT configuration. The investigation of electrical and mechanical faults in this controlled environment using SKF WindCon CMS will be even more valuable.

- **Rotor electrical asymmetry detection through vibration analysis.** It is recommended to perform more tests on the Manchester test rig, under rotor asymmetry conditions similar to those of the Durham experiments, in order to further investigate the applicability of the $|2s|f_s$ upper SB of the supply frequency second harmonic as an

indicator of rotor electrical asymmetry in the generator vibration signature.

- **Data integration.** Fusing the proposed algorithm results with those from other sensors, including valuable information from SCADA systems, such as operational parameters, would help complete the diagnostic coverage and improve the reliability of the monitoring equipment detection. A number of monitoring signals from disparate sources presenting confirmatory fault data would increase confidence in their indications and would be a confidence-building to O&M managers and technicians. In particular, oil debris, oil temperature, and casing temperature would provide additional evidence of impending failures of gears and bearings.

- **Integration with maintenance tools.** Further work could be done to link the output of a more automatic CMS to maintenance tools in order to schedule maintenance at appropriate times of low energy production and favourable weather windows, after CMS detection, to defer and avoid failure.

- **Algorithm application to marine turbine CMSs.** The techniques proposed in this Thesis might find interesting application for CM of emerging marine renewable technologies, such as tidal and wave devices, whose O&M will face challenges comparable to those encountered by offshore WTs due to the very remote and difficult-to-access location. Reliable and effective CMSs would then be valuable because even a small improvement in reliability, or maintainability, could yield significant cost of energy savings.

References

Alewine, K. and Chen, W. (2010). Wind Turbine Generator Failure Modes Analysis and Occurrence. *Proceedings of WindPower 2010*. Dallas, Texas.

Amirat, Y., Benbouzid, M. E. H., Al-Ahmar, E., Bensaker, B. and Turri, S. (2009). A Brief Status on Condition Monitoring and Fault Diagnosis in Wind Energy Conversion Systems. *Renewable and Sustainable Energy Reviews*. **13**(9): 2629-2636.

Amirat, Y., Benbouzid, M. E. H., Bensaker, B. and Wamkeue, R. (2007). Condition Monitoring and Fault Diagnosis in Wind Energy Conversion Systems: A Review. *Proceedings of IEEE International Electric Machines & Drives Conference, 2007. IEMDC '07*

Andrawus, J., Watson, J. and Kishk, M. (2007). Wind Turbine Maintenance Optimisation: Principles of Quantitative Maintenance Optimisation. *Wind Engineering*. **31**(2): 101-110.

Arapogianni, A., Genachte, A. B., Ochagavia, R. M., Vergara, J. P., Castell, D., Tsouroukdissian, A. R. et al. (2013). 'Deep Water'. European Wind Energy Association available at http://www.ewea.org/publications/, last accessed 24th April 2014.

Arwas, P., Charlesworth, D., Clark, D., Clay, R., Craft, G., Donaldson, I. et al. (2012). 'Offshore Wind Cost Reduction Pathways Study'. The Crown Estate, available at http://www.thecrownestate.co.uk/media/305094/offshore-wind-cost-reduction-pathways-study.pdf, last accessed 14th May 2014.

Bengtsson, M. (2004). *Condition Based Maintenance Systems: An Investigation of Technical Constituents and Organizational Aspects.* Mälardalen University, Sweden. PhD Thesis.

Besnard, F. (2009). On Optimal Maintenance Management for Wind Power Systems; KTH Royal Institute of Technology School of Electrical Engineering Division of Electromagnetic Engineering, Stockholm, Sweden. Licentiate Thesis.

Besnard, F. (2013). *On Maintenance Optimization for Offshore Wind Farms.* KTH Royal Institute of Technology School of Electrical Engineering Division of Electromagnetic Engineering, Stockholm, Sweden. PhD Thesis.

Besnard, F., Nilsson, J. and Bertling, L. (2010). On the Economic Benefits of Using Condition Monitoring Systems for Maintenance Management of Wind Power Systems. *Proceedings of 2010 IEEE 11th International Conference on Probabilistic Methods Applied to Power Systems (PMAPS)*. Singapore.

Blödt, M., Granjon, P., Raison, B. and Rostaing, G. (2008). Models for Bearing Damage Detection in Induction Motors Using Stator Current

Monitoring. *IEEE Transactions on Industrial Electronics*. **55**(4): 1813-1822.

Bracewell, R. N. (1978). *The Fourier Transform and Its Applications* (2nd ed.). London: McGraw-Hill.

Brüel&Kjaer. (2013). 'PULSE Analyzer Platform'. available at http://www.bksv.com/products/pulse-analyzer, last accessed 5th February 2014.

Burton, T., Sharpe, D., Jenkins, N. and Bossanyi, E. (2011). *Wind Energy Handbook* (2nd ed.): John Wiley & Sons.

Byon, E. and Ding, Y. (2010). Season-Dependent Condition-Based Maintenance for a Wind Turbine Using a Partially Observed Markov Decision Process. *IEEE Transactions on Power Systems*. **25**(4): 1823-1834.

Central Intelligence Agency. (2013). 'The World Factbook 2013-14'. available at https://www.cia.gov/library/publications/the-world-factbook/index.html, last accessed 10th September 2014.

Chapman, S. J. (1999). *Electric Machinery Fundamentals* (3rd ed.). Boston: McGraw-Hill.

Chen, B., Matthews, P. C. and Tavner, P. J. (2013). Wind Turbine Pitch Faults Prognosis Using A-Priori Knowledge-Based ANFIS. *Expert Systems with Applications*. **40**(17): 6863-6876.

Chen, B., Zappalá, D., Crabtree, C. J. and Tavner, P. J. (2014). 'Survey of Commercially Available SCADA Data Analysis Tools for Wind Turbine Health Monitoring'. Durham University and the SUPERGEN Wind Energy Technologies Consortium, available at http://dro.dur.ac.uk/12563/ and http://www.supergen-wind.org.uk/dissemination.html, last accessed 10th June 2014.

Ciang, C. C., Lee, J.-R. and Bang, H.-J. (2008). Structural Health Monitoring for a Wind Turbine System: a Review of Damage Detection Methods. *Measurement Science and Technology*. **19**(12): 1-20.

Cooley, J. W. and Tukey, J. W. (1965). An Algorithm for the Machine Calculation of Complex Fourier Series. *Mathematics of Computation*. **19**(90): 297-301.

Crabtree, C. J. (2011). *Condition Monitoring Techniques for Wind Turbines*. Durham University, UK. PhD Thesis.

Crabtree, C. J. (2012). Operational and Reliability Analysis of Offshore Wind Farms. *Proceedings of the Scientific Track of the European Wind Energy Association Conference*. Copenhagen, Denmark.

Crabtree, C. J., Djurović, S., Tavner, P. J. and Smith, A. C. (2010a). Condition Monitoring of a Wind Turbine DFIG by Current or Power Analysis.

Proceedings of 5th IET International Conference on Power Electronics, Machines and Drives, PEMD 2010 Brighton, UK.

Crabtree, C. J., Djurović, S., Tavner, P. J. and Smith, A. C. (2010b). Fault Frequency Tracking During Transient Operation of Wind Turbine Generators. *Proceedings of XIX International Conference on Electrical Machines, ICEM 2010*. Rome, Italy.

Crabtree, C. J., Zappalá, D. and Tavner, P. J. (2014). 'Survey of Commercially Available Condition Monitoring Systems for Wind Turbines'. Durham University and the SUPERGEN Wind Energy Technologies Consortium, available at http://dro.dur.ac.uk/12497/ and http://www.supergen-wind.org.uk/dissemination.html, last accessed 10th June 2014.

Dalpiaz, G., Rivola, A. and Rubini, R. (2000). Effectiveness and Sensitivity of Vibration Processing Techniques for Local Fault Detection in Gears. *Mechanical Systems and Signal Processing*. **14**(3): 387-412.

Davies, A. (1998). *Handbook of Condition Monitoring: Techniques and Methodology*. London, UK: Springer.

de Silva, C. W. (1999). *Vibration: Fundamentals and Practice* (2nd ed.): CRC Press.

DECC. (2011). 'UK Renewable Energy Roadmap'. available at http://www.decc.gov.uk/en/content/cms/meeting_energy/renewable_ener/re_roadmap/re_roadmap.aspx, last accessed 14th May 2014.

Delorm, T. M., Zappalá, D. and Tavner, P. J. (2012). Tidal Stream Device Reliability Comparison Models. *Proceedings of the Institution of Mechanical Engineers, Part O: Journal of Risk and Reliability*. **226**(1): 6-17.

Djurović, S., Crabtree, C. J., Tavner, P. J. and Smith, A. C. (2012a). Condition Monitoring of Wind Turbine Induction Generators with Rotor Electrical Asymmetry. *IET Renewable Power Generation*. **6**(4): 207-216.

Djurović, S., Vilchis-Rodriguez, D. S. and Smith, A. C. (2012b). Vibration Monitoring for Wound Rotor Induction Machine Winding Fault Detection. *Proceedings of XXth International Conference on Electrical Machines, ICEM 2012* Marseille, France.

Djurović, S. and Williamson, S. (2008). A Coupled-Circuit Model for a DFIG Operating Under Unbalanced Conditions. *Proceedings of the 18th International Conference on Electrical Machines, ICEM 2008* Vilamoura, Portugal.

Djurović, S., Williamson, S. and Renfrew, A. (2009). Dynamic Model for Doubly-Fed Induction Generators with Unbalanced Excitation, Both

With and Without Winding Faults. *IET Electric Power Applications.* **3**(3): 171-177.

Doner, S. (2009). 'Winergy Condition Diagnostics System Enterprise-Wide Fleet Management Roadmap to Advanced Condition Monitoring'. NREL Wind Turbine Condition Monitoring Workshop, available at http://wind.nrel.gov/public/Wind_Turbine_Condition_Monitoring_Work shop_2009/, last accessed 12th June 2014.

EC. (2002a). 'COMMUNICATION FROM THE COMMISSION TO THE COUNCIL AND THE EUROPEAN PARLIAMENT - Final Report on the Green Paper "Towards a European Strategy for the Security of Energy Supply"'. Commission of the European Communities COM(2002) 321 final, available at http://eur-lex.europa.eu/legal-content/EN/TXT/?uri=CELEX:52002DC0321, last accessed 18th August 2011.

EC. (2002b). Council Decision 2002/358/EC of 25 April 2002 concerning the approval, on behalf of the European Community, of the Kyoto Protocol to the United Nations Framework Convention on Climate Change and the joint fulfilment of commitments thereunder; Official Journal of the European Communities L 130 of 15/05/2002, p.1-3.

EC. (2009). Directive 2009/28/EC of the European Parliament and of the Council of 23 April 2009 on the promotion of the use of energy from renewable sources and amending and subsequently repealing Directives 2001/77/EC and 2003/30/EC; Official Journal of the European Communities L140 of 05/06/2009, p.16-62.

EC. (2014). 'COMMUNICATION FROM THE COMMISSION TO THE EUROPEAN PARLIAMENT, THE COUNCIL, THE EUROPEAN ECONOMIC AND SOCIAL COMMITTEE AND THE COMMITTEE OF THE REGIONS - A Policy Framework for Climate and Energy in the Period from 2020 to 2030'. Commission of the European Communities COM(2014) 015 final, available at http://eur-lex.europa.eu/legal-content/EN/TXT/?uri=CELEX:52014DC0015, last accessed 9th May 2014.

Eggersglüß, W. (1995-2004). Wind Energie IX-XIV, Praxis -Ergebnisse 1995-2004. Landwirtschaftskammer Schleswig-Holstein, Osterrönfeld, Germany.

Errichello, R. and Muller, J. (2012). 'Gearbox Reliability Collaborative Gearbox 1 Failure Analysis Report'.NREL/SR-5000-530262, available at http://www.nrel.gov/docs/fy12osti/53062.pdf, last accessed 15th September 2013.

Fan, X. and Zuo, M. J. (2006). Gearbox Fault Detection Using Hilbert and Wavelet Packet Transform. *Mechanical Systems and Signal Processing.* **20**(4): 966-982.

Faulstich, S., Durstewitz, M., Hahn, B., Knorr, K. and Rohrig, K. (2008). 'German Wind Energy Report 2008'. Institut für Solare Energieversorgungstechnik available at http://windmonitor.iwes.fraunhofer.de/wind/download/Windenergie_Report_2008_en.pdf, last accessed 4th June 2014.

Faulstich, S., Hahn, B. and Tavner, P. J. (2011). Wind Turbine Downtime and Its Importance for Offshore Deployment. *Wind Energy*. **14**(3): 327-337.

Feng, Y., Qiu, Y., Crabtree, C. J., Long, H. and Tavner, P. J. (2013). Monitoring Wind Turbine Gearboxes. *Wind Energy*. **16**(5): 728-740.

Feng, Y., Tavner, P. J. and Long, H. (2010). Early Experiences with UK Round 1 Offshore Wind Farms. *Proceedings of the Institution of Civil Engineers : energy.* **163**(4): 167-181.

Fischer, K. (2012). 'Maintenance Management of Wind Power Systems by means of Reliability-Centred Maintenance and Condition Monitoring Systems'. Chalmers University, available at http://www.chalmers.se/en/projects/Pages/Maintenance-Management-of-Wind-Power-Systems.aspx, last accessed 9th June 2014.

Fried, L., Sawyer, S., Shukla, S. and Qiao, L. (2014). 'Global Wind Report Annual Market Update 2013'. GWEC, available at http://www.gwec.net/wp-content/uploads/2014/04/GWEC-Global-Wind-Report_9-April-2014.pdf, last accessed 16th May 2014.

Garcia Marquez, F. P., Tobias, A. M., Pinar Perez, J. M. and Papaelias, M. (2012). Condition Monitoring of Wind Turbines: Techniques and Methods. *Renewable Energy*. **46**: 169-178.

Germanischer Lloyd. (2007). Guideline for the Certification of Condition Monitoring Systems for Wind Turbines; Hamburg, Germany.

Giordano, F. and Stein, R. (2011). The Operator's Assessment of Condition Monitoring: Practical Experience and Results. *Proceedings of the European Wind Energy Association Conference*. Brussels, Belgium.

GL Garrad Hassan. (2013). 'Offshore Wind Operations And Maintenance Opportunities In Scotland'. Scottish Enterprise, available at http://www.scottish-enterprise.com/~/media/SE/Resources/Documents/MNO/Offshore%20wind%20operations%20and%20maintenance%20opps.pdf, last accessed 21st May 2014.

Goldman, S. (1999). *Vibration Spectrum Analysis: a Practical Approach* (2nd ed.). New York, NY: Industrial Press Inc.

Gram & Juhl A/S. (2010). 'TCM® Turbine Condition Monitoring'. available at http://www.rotomech.com/pdf/brochure-eng.pdf, last accessed 12th June 2014.

Gray, C. S. and Watson, S. J. (2010). Physics of Failure Approach to Wind Turbine Condition Based Maintenance. *Wind Energy*. **13**(5): 395-405.

Gritli, Y., Stefani, A., Chatti, A., Rossi, C. and Filippetti, F. (2009). The Combined Use of the Instantaneous Fault Frequency Evolution and Frequency Sliding for Advanced Rotor Fault Diagnosis in DFIM under Time-Varying Condition. *Proceedings of 35th Annual Conference of IEEE Industrial Electronics. IECON '09.* .

Hahn, B., Durstewitz, M. and Rohrig, K. (2007). Reliability of Wind Turbines, Experience of 15 years with 1,500 WTs. *Wind Energy - Proceedings of the Euromech Colloquium.* Springer, Berlin, Germany.

Hameed, Z., Hong, Y. S., Cho, Y. M., Ahn, S. H. and Song, C. K. (2009). Condition Monitoring and Fault Detection of Wind Turbines and Related Algorithms: A Review. *Renewable and Sustainable Energy Reviews*. **13**(1): 1-39.

Harris, F. J. (1978). On the Use of Windows for Harmonic Analysis with the Discrete Fourier Transform. *Proceedings of the IEEE*. **66**(1): 51-83.

Hatch, C. T., Hess, D. D., Weiss, A. A., Woodson, S. M. and Kalb, M. B. (2012). *Sideband Energy Ratio Method For Gear Mesh Fault Detection*; US Patent 2012/0073364.

Hau, E. (2006). *Wind Turbines: Fundamentals, Technologies, Application, Economics* (2nd ed.). Berlin: Springer.

Howard, I. (1994). 'A Review of Rolling Element Bearing Vibration: "Detection, Diagnosis and Prognosis"'. Aeronautical and Maritime Research Laboratory Airframes and Engines Division, available at http://www.dsto.defence.gov.au/publications/2624/DSTO-RR-0013.pdf, last accessed 27th June 2014.

Hsu, W. (2008). Measurements on a Wind Turbine Condition Monitoring Test Rig; Master's thesis, Durham University.

Hyers, R. W., McGowan, J. G., Sullivan, K. L., Manwell, J. F. and Syrett, B. C. (2006). Condition Monitoring and Prognosis of Utility Scale Wind Turbines. *Energy Materials: Materials Science and Engineering for Energy Systems*. **1**(3): 187-203.

IEC 61400-4. (2012). Wind Turbines - Part 4: Design Requirements for Wind Turbine Gearboxes.

ISO 14224:2006. 'Petroleum, Petrochemical and Natural Gas Industries - Collection and Exchange of Reliability and Maintenance Data for Equipment'.

Kaldellis, J. K. and Kapsali, M. (2013). Shifting Towards Offshore Wind Energy - Recent Activity and Future Development. *Energy Policy*. **53**: 136-148.

Karyotakis, A. (2011). *On the Optimisation of Operation and Maintenance Strategies for Offshore Wind Farms.* University College London, UK. PhD Thesis.

Kay, S. M. (1988). *Modern Spectral Estimation: Theory and Application.* Englewood Cliffs, NJ: Prentice Hall.

Krohn, S., Morthorst, P. E. and Awerbuch, S. (2009). 'The Economics of Wind Energy'. European Wind Energy Association, available at http://www.ewea.org/policy-issues/economics/, last accessed 5th March 2014.

Li, H. and Chen, Z. (2008). Overview of Different Wind Generator Systems and their Comparisons. *IET Renewable Power Generation.* **2**(2): 123-138.

Lu, B., Li, Y., Wu, X. and Yang, Z. (2009). A Review of Recent Advances in Wind Turbine Condition Monitoring and Fault Diagnosis. *Proceedings of 2009 IEEE Symposium on Power Electronics and Machines in Wind Applications. PEMWA 2009.* Lincoln, Nebraska.

Mark, W. D., Lee, H., Patrick, R. and Coker, J. D. (2010). A Simple Frequency-domain Algorithm for Early Detection of Damaged Gear Teeth. *Mechanical Systems and Signal Processing.* **24**(8): 2807-2823.

McFadden, P. D. (1986). Detecting Fatigue Cracks in Gears by Amplitude and Phase Demodulation of the Meshing Vibration. *Transactions of the ASME Journal of Vibration Acoustics Stress and Reliability in Design.* **108**(2): 165-170.

McGowin, C., Walford, C. and Roberts, D. (2006). 'Condition Monitoring of Wind Turbines - Technology Overview, Seeded-Fault Testing and Cost-Benefit Analysis'. EPRI, available at http://www.epri.com/abstracts/Pages/ProductAbstract.aspx?ProductId=000000000001010419, last accessed 13th June 2014.

McMillan, D. and Ault, G. W. (2007). Quantification of Condition Monitoring Benefit for Offshore Wind Turbines. *Wind Engineering.* **31**(4): 267-285.

McMillan, D. and Ault, G. W. (2008). Condition Monitoring Benefit for Onshore Wind Turbines: Sensitivity to Operational Parameters. *IET Renewable Power Generation.* **2**(1): 60-72.

Mobley, R. K. (1999). *Vibration Fundamentals.* Boston, MA: Butterworth-Heinemann.

Mobley, R. K., Higgins, L. R. and Wikoff, D. J. (2008). *Maintenance Engineering Handbook* (7th ed.): McGraw-Hill.

Moccia, J., Arapogianni, A., Wilkes, J., Kjaer, C., Gruet, R., Azau, S. et al. (2011). 'Pure Power - Wind Energy Targets for 2020 and 2030'. European Wind Energy Association, available at

http://www.ewea.org/fileadmin/ewea_documents/documents/publications/reports/Pure_Power_III.pdf, last accessed 24th April 2014.

Musial, W., Butterfield, S. and McNiff, B. (2007). Improving Wind Turbine Gearbox Reliability. *Proceedings of the European Wind Energy Conference*. Milan, Italy.

Musial, W., Butterfield, S. and Ram, B. (2006). Energy from Offshore Wind. *Proceedings of the 2006 Offshore Technology Conference*. Houston, TX.

Musial, W. and McNiff, B. (2000). Wind Turbine Testing in the NREL Dynamometer Test Bed. *Proceedings of the American Wind Energy Association's WindPower 2000 Conference* Palm Springs, CA.

Musial, W. and Ram, B. (2010). 'Large-Scale Offshore Wind Power in the United States: Assessment of Opportunities and Barriers '. NREL No. TP-500-40745, available at http://www.nrel.gov/wind/pdfs/40745.pdf, last accessed 28th May 2014.

Nilsson, J. and Bertling, L. (2007). Maintenance Management of Wind Power Systems Using Condition Monitoring Systems - Life Cycle Cost Analysis for Two Case Studies. *IEEE Transactions on Energy Conversion*. **22**(1): 223-229.

NoordzeeWind, S. (2007-2009). 'Egmond aan Zee Operations Reports 2007, 2008, 2009'. available at www.noordzeewind.nl, last accessed 10th October 2013.

NREL. (2010). 'Dynamometer Testing (Fact Sheet)'. NREL No. FS-5000-45649, available at http://www.nrel.gov/docs/fy11osti/45649.pdf, last accessed 13th August 2014.

Oppenheim, A. V., Schafer, R. W. and Buck, J. R. (1999). *Discrete-time Signal Processing*. Upper Saddle River, NJ: Prentice Hall.

Pinar Pérez, J. M., García Márquez, F. P., Tobias, A. and Papaelias, M. (2013). Wind Turbine Reliability Analysis. *Renewable and Sustainable Energy Reviews* **23**: 463-472.

Pineda, I., Azau, S., Moccia, J. and Wilkes, J. (2014). 'Wind in Power 2013 European Statistics'. European Wind Energy Association, available at http://www.ewea.org/statistics/european/, last accessed 23rd May 2014.

Qiu, Y., Feng, Y., Tavner, P., Richardson, P., Erdos, G. and Chen, B. (2012). Wind Turbine SCADA Alarm Analysis for Improving Reliability. *Wind Energy*. **15**(8): 951-966.

Randall, R. B. (1982). A New Method of Modelling Gear Faults. *Transactions of the ASME Journal of Mechanical Design*. **104**(2): 259-267.

Randall, R. B. (1987). *Frequency Analysis* (3rd ed.). Copenhagen: Brüel & Kjaer.

Randall, R. B. (2011). *Vibration-Based Condition Monitoring: Industrial, Aerospace and Automotive Applications*: John Wiley & Sons, Ltd.

RenewableUK. (2014). 'Offshore Wind', http://www.renewableuk.com/en/renewable-energy/wind-energy/offshore-wind/index.cfm, last accessed 21st May 2014.

Ribrant, J. and Bertling, L. M. (2007). Survey of Failures in Wind Power Systems with Focus on Swedish Wind Power Plants During 1997-2005. *IEEE Transactions on Energy Conversion.* **22**(1): 167-173.

Shah, D., Nandi, S. and Neti, P. (2009). Stator-Interturn-Fault Detection of Doubly Fed Induction Generators Using Rotor-Current and Search-Coil-Voltage Signature Analysis. *IEEE Transactions on Industry Applications.* **45**(5): 1831-1842.

Sheng, S. (2011). Investigation of Various Condition Monitoring Techniques Based on a Damaged Wind Turbine Gearbox. *Proceedings of the 8th International workshop on Structural Health Monitoring, Condition-based Maintenance and Intelligent Structures.* Stanford, California.

Sheng, S. (2012). 'Wind Turbine Gearbox Condition Monitoring Round Robin Study - Vibration Analysis'. NREL No. TP-5000-54530, available at http://www.nrel.gov/docs/fy12osti/54530.pdf, last accessed 25th July 2013.

Sheng, S. and Veers, P. (2011). Wind Turbine Drivetrain Condition Monitoring - An Overview. *Proceedings of Machinery Failure Prevention Technology (MFPT) Society 2011 Conference.* Virginia Beach, Virginia.

Shin, K. and Hammond, J. (2008). *Fundamentals of Signal Processing for Sound and Vibration Engineers.* Chichester, UK: Wiley.

SKF Reliability Systems. (2010). @ptitude Observer; User Manual, Part No. 32170900, Revision G.

Smith, J. D. (1989). *Vibration Measurement and Analysis*: Butterworths.

Smolders, K., Long, H., Y., F. and Tavner, P. J. (2010). Reliability Analysis and Prediction of Wind Turbine Gearboxes. *Proceedings of the Scientific Track of the European Wind Energy Conference.* Warsaw, Poland.

Sørensen, J. D. (2009). Framework for Risk-Based Planning of Operation and Maintenance for Offshore Wind Turbines. *Wind Energy.* **12**(5): 493-506.

Spinato, F., Tavner, P. J., van Bussel, G. J. W. and Koutoulakos, E. (2009). Reliability of Wind Turbine Subassemblies. *IET Renewable Power Generation.* **3**(4): 387-401.

Stefani, A., Yazidi, A., Rossi, C., Filippetti, F., Casadei, D. and Capolino, G. A. (2008). Doubly Fed Induction Machines Diagnosis Based on Signature Analysis of Rotor Modulating Signals. *IEEE Transactions on Industry Applications.* **44**(6): 1711-1721.

SUPERGEN Wind. (2014). 'Supergen Wind Energy Technologies Consortium ', http://www.supergen-wind.org.uk/, last accessed 6th May 2014.

Tavner, P., Faulstich, S., Hahn, B. and van Bussel, G. J. W. (2010). Reliability & Availability of Wind Turbine Electrical & Electronic Components. *EPE Journal.* **20**(4): 45-50.

Tavner, P. J. (2008). Review of Condition Monitoring of Rotating Electrical Machines. *IET Electric Power Applications.* **2**(4): 215-247.

Tavner, P. J. (2012). *Offshore Wind Turbines: Reliability, Availability and Maintenance* (1st ed.). London: The Institution of Engineering and Technology.

Tavner, P. J., Ran, L., Penman, J. and Sedding, H. (2008a). *Condition Monitoring of Rotating Electrical Machines.* London: Institution of Engineering and Technology

Tavner, P. J., Spinato, F., Van Bussel, G. J. W. and Koutoulakos, E. (2008b). Reliability of Different Wind Turbine Concepts with Relevance to Offshore Application. *Proceedings of the Scientific Track of the European Wind Energy Association Conference.* Brussels, Belgium.

Tavner, P. J., Van Bussel, G. J. W. and Spinato, F. (2006). Machine and Converter Reliabilities in Wind Turbines. *Proceedings of the 3rd IET International Conference on Power Electronics, Machines and Drives.* Dublin, Ireland.

Tavner, P. J., Xiang, J. and Spinato, F. (2007). Reliability Analysis for Wind Turbines. *Wind Energy.* **10**(1): 1-18.

Thomson, W. T. and Fenger, M. (2001). Current Signature Analysis to Detect Induction Motor Faults. *IEEE Industry Applications Magazine.* **7**(4): 26-34.

Val, D. V. (2009). Aspects of Reliability Assessment of Tidal Stream Turbines. *Proceedings of the 10th International Conference on Structural Safety and Reliability - ICOSSAR 2009.* Osaka, Japan.

Van Bussel, G. J. W. and Schöntag, C. (1997). Operation and Maintenance Aspects of Large Offshore Wind Farms. *Proceedings of the Scientific Track of the European Wind Energy Association Conference.* Dublin, Ireland.

Van Hulle, F. and Fichaux, N. (2010). 'Powering Europe: Wind Energy and the Electricity Grid'. European Wind Energy Association, available at http://www.ewea.org/publications/, last accessed 20th June 2014.

Vilchis-Rodriguez, D. S., Djurović, S., Djukanovic, S. and Smith, A. C. (2013a). Analysis of Wound Rotor Induction Generator Transient Vibration Signal Under Stator Fault Conditions. *Proceedings of the Scientific Track of the European Wind Energy Association Conference*. Vienna, Austria.

Vilchis-Rodriguez, D. S., Djurović, S. and Smith, A. C. (2013b). Wound Rotor Induction Generator Bearing Fault Modelling and Detection Using Stator Current Analysis. *IET Renewable Power Generation*. **7**(4): 330-340.

Walford, C. and Roberts, D. (2006). 'Condition Monitoring of Wind Turbines: Technology Overview, Seeded-Fault Testing and Cost-Benefit Analysis '. EPRI No. 1010419, available at http://www.epri.com/abstracts/Pages/ProductAbstract.aspx?ProductId= 000000000001010419, last accessed 5th June 2014.

Walford, C. A. (2006). 'Wind Turbine Reliability: Understanding and Minimizing Wind Turbine Operation and Maintenance Costs'. Sandia National Laboratories SAND2006-1100, available at http://prod.sandia.gov/techlib/access-control.cgi/2006/061100.pdf, last accessed 20th April 2013.

Watson, S. J., Xiang, B. J., Yang, W. X., Tavner, P. J. and Crabtree, C. J. (2010). Condition Monitoring of the Power Output of Wind Turbine Generators Using Wavelets. *IEEE Transactions on Energy Conversion*. **25**(3): 715-721.

Whittle, M. W. G. (2013). *Wind Turbine Generator Reliability: An Exploration of the Root Causes of Generator Bearing Failures*. Durham University, UK. PhD Thesis.

Wieringa, H., De Kraker, A. and Stakenborg, M. J. L. (1986). Cepstrum Analysis as a Useful Supplement to Spectrum Analysis for Gear-Box Monitoring. *Proceedings of the VIIIth International Conference on Experimental Stress Analysis*. Amsterdam, The Netherlands.

Wiggelinkhuizen, E., Verbruggen, T., Braam, H., Rademakers, L., Xiang, J. P. and Watson, S. (2008). Assessment of Condition Monitoring Techniques for Offshore Wind Farms. *Transactions of the ASME Journal of Solar Energy Engineering*. **130**(3): 9.

Wilkinson, M. (2011). Measuring Wind Turbine Reliability - Results of the Reliawind Project. *Proceedings of the Scientific Track of the European Wind Energy Association Conference*. Brussels, Belgium.

Wilkinson, M., Hendriks, B., Spinato, F., Gomez, E., Bulacio, H., Roca, J. et al. (2010). Methodology and Results of the ReliaWind Reliability Field Study. *Proceedings of the Scientific Track of the European Wind Energy Association Conference*. Warsaw, Poland.

Wilkinson, M., Spinato, F., Knowles, M. and Tavner, P. J. (2006). Towards the Zero Maintenance Wind Turbine. *Proceedings of the 41st International Universities Power Engineering Conference*. Vol 1. pp.74-78, Newcastle, UK.

Wilkinson, M. R. (2008). *Condition Monitoring of Offshore Wind Turbines.* Newcastle University, UK. PhD Thesis.

Wilkinson, M. R., Spinato, F. and Tavner, P. J. (2007). Condition Monitoring of Generators & Other Subassemblies in Wind Turbine Drive Trains. *Proceedings of 2007 IEEE International Symposium on Diagnostics for Electric Machines, Power Electronics and Drives (SDEMPED 2007).* Cracow, Poland.

Williamson, S. and Djurović, S. (2009). Origins of Stator Current Spectra in DFIGs with Winding Faults and Excitation Asymmetries. *Proceedings of IEEE International Electric Machines and Drives Conference, IEMDC '09* Miami, USA.

Wolfram, J. (2006). On Assessing The Reliability and Availability of Marine Energy Converters: The Problems of a New Technology. *Proceedings of the Institution of Mechanical Engineers, Part O: Journal of Risk and Reliability.* **220**(1): 55-68.

Yang, W., Tavner, P. J. and Crabtree, C. J. (2009a). An Intelligent Approach to the Condition Monitoring of Large Scale Wind Turbines. *Proceedings of the Scientific Track of the European Wind Energy Association Conference.* Marseille, France.

Yang, W., Tavner, P. J., Crabtree, C. J., Feng, Y. and Qiu, Y. (2014). Wind Turbine Condition Monitoring: Technical and Commercial Challenges. *Wind Energy.* **17**(5): 673-693.

Yang, W., Tavner, P. J., Crabtree, C. J. and Wilkinson, M. (2010). Cost-Effective Condition Monitoring for Wind Turbines. *IEEE Transactions on Industrial Electronics.* **57**(1): 263-271.

Yang, W., Tavner, P. J. and Wilkinson, M. R. (2009b). Condition Monitoring and Fault Diagnosis of a Wind Turbine Synchronous Generator Drive Train. *IET Renewable Power Generation.* **3**(1): 1-11.

Yazidi, A., Henao, H., Capolino, G. A. and Betin, F. (2010). Rotor Inter-Turn Short Circuit Fault Detection in Wound Rotor Induction Machines. *Proceedings of XIX International Conference on Electrical Machines, ICEM 2010.* Rome, Italy.

Zaggout, M. N. (2013). *Wind Turbine Generator Condition Monitoring via the Generator Control Loop.* Durham University, UK. PhD Thesis.

Zaggout, M. N., Tavner, P. J., Crabtree, C. J. and Ran, L. (2014). Detection of Rotor Electrical Asymmetry in Wind Turbine Doubly-fed Induction

Generators. *IET Renewable Power Generation* (Article first published online:30 June 2014, DOI: 10.1049/iet-rpg.2013.0324).

Zaher, A., McArthur, S. D. J., Infield, D. G. and Patel, Y. (2009). Online Wind Turbine Fault Detection Through Automated SCADA Data Analysis. *Wind Energy*. **12**(6): 574-593.

Zappalá, D. (2010). Reliability Evaluation of Tidal Stream Turbines; Master's thesis, Durham University.

Zappalá, D., Crabtree, C. J., Vilchis-Rodriguez, D. S., Tavner, P. J., Djurović, S. and Smith, A. C. (2014a). Advanced Algorithms for Automatic Wind Turbine Generator Fault Detection and Diagnosis. *Proceedings of the Scientific Track of the European Wind Energy Association Conference*. Barcelona, Spain.

Zappalá, D., Tavner, P. J. and Crabtree, C. J. (2012). Gear Fault Detection Using WindCon Frequency Tracking. *Proceedings of the Scientific Track of the European Wind Energy Association Conference*. Copenhagen, Denmark.

Zappalá, D., Tavner, P. J., Crabtree, C. J. and Sheng, S. (2013). Sideband Algorithm for Automatic Wind Turbine Gearbox Fault Detection and Diagnosis. *Proceedings of the Scientific Track of the European Wind Energy Association Conference*. Vienna, Austria.

Zappalá, D., Tavner, P. J., Crabtree, C. J. and Sheng, S. (2014b). Side-Band Algorithm for Automatic Wind Turbine Gearbox Fault Detection and Diagnosis. *IET Renewable Power Generation*. **8**(4): 380-389.

Appendix: Survey of Commercially Available Condition Monitoring Systems for Wind Turbines

Survey of Commercially Available Condition Monitoring Systems for Wind Turbines

Christopher J Crabtree, Donatella Zappalá and Peter J Tavner
Revision: 05, May 2014

Confidentiality

This document is the copyright property of Durham University School of Engineering and Computing Sciences and the SUPERGEN Wind Energy Technologies Consortium. No part of this document may be copied or reproduced without the permission of the author. This document is subject to constant review.

Previous Versions

The first survey completed, named *Survey of Commercially Available Wind Turbine Condition Monitoring Systems*, was initially prepared by P. J. Tavner (Durham University School of Engineering and Computing Sciences) as part of the SUPERGEN Wind Energy Technologies Consortium with help and contributions from W. Yang (Durham University, now Newcastle University), C. Booth (University of Strathclyde) and S. Watson (Loughborough University). It was then subject to constant revision up to April 2009 by W. Yang.

The current document is based on this earlier survey and is written by C. J. Crabtree (Durham University School of Engineering and Computing Sciences) as part of the UK EPSRC SUPERGEN Wind Energy Technologies Consortium, EP/D034566/1. It contains information contributed by the C. J. Crabtree, P. J. Tavner, Y. Feng and M. W. G. Whittle, obtained at European Wind Energy Conferences 2009 and 2010.

The survey of commercially available condition monitoring systems for wind turbines has been further revised by D. Zappalá & P. J. Tavner, as part of the UK EPSRC SUPERGEN Wind Energy Technologies programme, EP/H018662/1, who added information gathered at:

- European Wind Energy Conference 2011 held in Brussels, Belgium, from 14th to 17th of March 2011;

- European Wind Energy Conference 2012 held in Copenhagen, Denmark, from 16th to 19th of April 2012;

- Husum Wind Fair, Husum, Germany, 18th to 22nd September 2012;

- European Wind Energy Conference 2013 held in Vienna, Austria, from 4th to 7th of February 2013;

- European Wind Energy Conference 2014 held in Barcelona, Spain, from 10th to 13th of March 2014.

This document contains 22 (twenty two) pages including the cover page.

Abstract

As wind energy assumes greater importance in remote and offshore locations, effective and reliable condition monitoring techniques are required. Failure rate and downtime studies have also highlighted a need for condition monitoring of particular wind turbine drive train components. This survey discusses the reliability of wind turbines and different monitoring configurations currently in use. The document contains a survey of commercially available condition monitoring systems for wind turbines including information on their monitoring technologies based on available literature and discussion with the companies responsible. Observations are made concerning the nature of systems that are currently available and the apparent direction of future monitoring systems.

Contents

1. Introduction

As wind energy assumes greater importance in remote and offshore locations, affective and reliable condition monitoring (CM) techniques are required. Conventional CM methods used in the power generation industry have been adapted by a number of industrial companies and have been applied to wind turbines (WT) commercially.

This survey discusses commercially available condition monitoring systems (CMS) which are currently being applied in the WT industry. Information has been gathered over several years from conferences and websites and includes information available from product brochures, technical documents and discussion with company representatives. The research was carried out as part of:

- Theme X of the SUPERGEN Wind Energy Technologies Consortium, Phase 1, [1] whose objective was to devise a comprehensive CMS for practical application on WTs;
- Theme 2 of the SUPERGEN Wind Energy Technologies Consortium, Phase 2, [2] whose objective, built on the work in SUPERGEN Wind 1, was to develop turbine monitoring targeted at improving the reliability and availability of offshore wind farms.
- Theme 4.3 of the SUPERGEN Wind Energy Technologies Consortium, Phase 2, [3] whose objective was to develop fault identification methodologies for electrical and mechanical drivetrain systems.

The report also identifies some of the advantages and disadvantages of existing commercial CMSs alongside discussion of access, cost, connectivity and commercial issues surrounding the application of WT CMSs.

2. Reliability of Wind Turbines

Quantitative studies of WT reliability have recently been carried out based on publically available data [4][5]. These studies have shown WT gearboxes to be a mature technology with constant of slightly deteriorating reliability with time. This would suggest that WT gearboxes are not an issue however surveys by WMEP and LWK [6] have shown that gearboxes exhibit the highest downtime per failure among onshore subassemblies. This is shown graphically in Figure 1 where we clearly see consistently low gearbox failure rate between two surveys with high downtime per failure. Similar results have also been shown for the Egmond aan Zee wind farm [7] where gearbox failure rate is not high but the downtime and resulting costs are. The poor early reliabilities for gearbox and drive train reliability components has led to an emphasis in WT CMSs on drive train components and therefore on vibration analysis.

The high downtime for gearboxes derives from complex repair procedures. Offshore WT maintenance can be a particular problem as this involves specialist equipment such as support

vessels and cranes but has the additional issue of potentially unfavourable weather and wave conditions. The EU funded project ReliaWind has developed a systematic and consistent process to deal with detailed commercial data collected from operational wind farms. This includes the analysis of 10 minute average SCADA data as discussed above, automated fault logs and operation and maintenance reports. The research aimed to identify and understand WT gearbox failure mechanisms in greater detail [8]. However, more recent information on WT reliability and downtime, especially when considering offshore operation suggests that the target for WT CMSs should be widened from the drive train towards WT electrical and control systems [9].

As a result of low early reliability, particularly in large WTs, interest in CMSs has increased. This is being driven forward by the insurer Germanischer Lloyd who published guidelines for the certification of CMSs [10] and certification of WTs both onshore [11] and offshore [12].

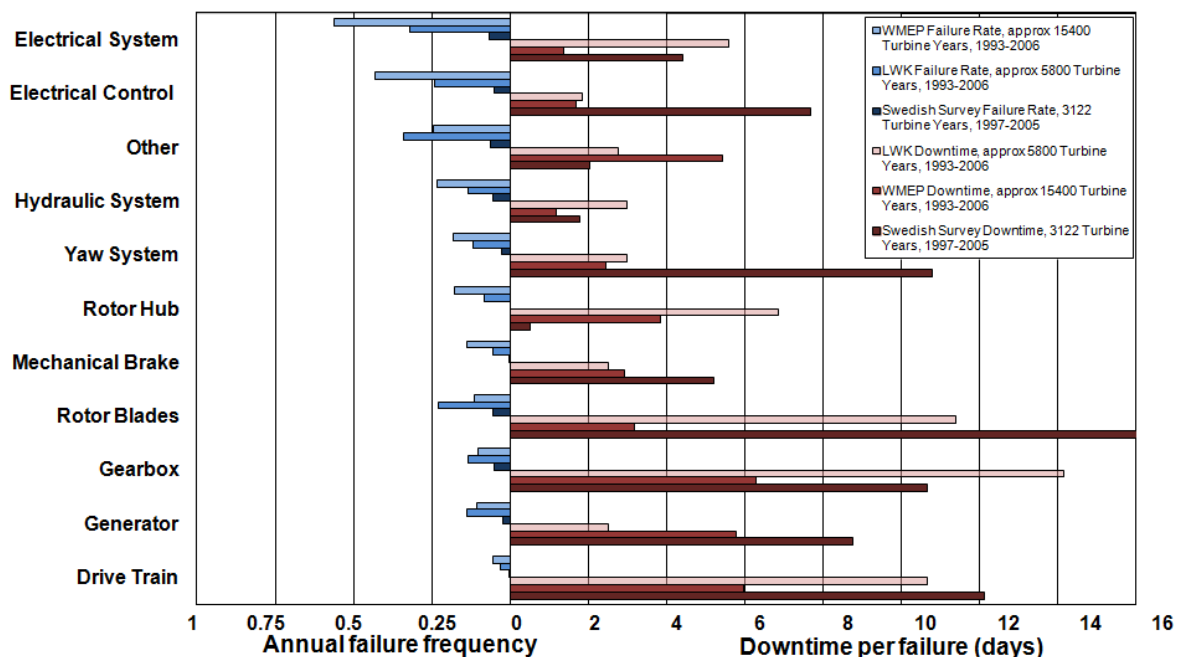**Figure 1: Wind turbine sub-assembly failure rate and downtime per failure from three surveys including over 24000 turbine years of data as published in [13]**

3. Monitoring of Wind Turbines

WTs are monitored for a variety of reasons. There are a number of different classes into which monitoring systems could be placed and these are shown in Figure2, showing the general layout and interaction of the various classes.
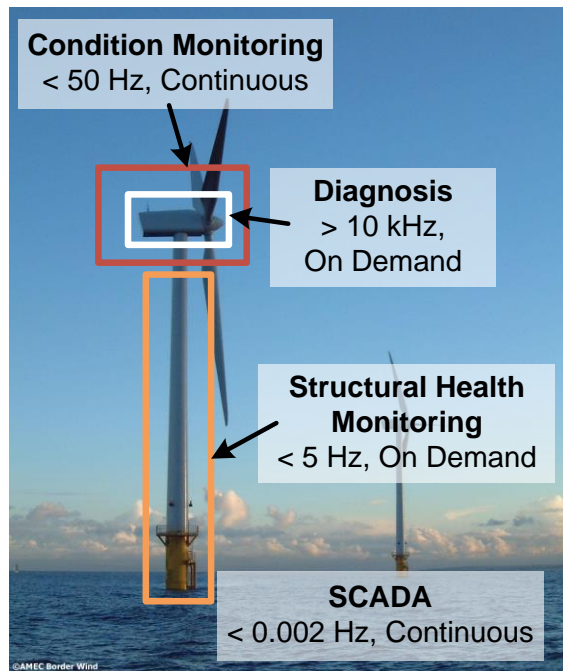
Figure 2: Structural health and condition monitoring of a wind turbine

Firstly, we have Supervisory Control and Data Acquisition (SCADA) systems. Initially these systems provided measurements for a WT's energy production and to confirm that the WT was operational through 5-10 minute averaged values transmitted to a central database. However, SCADA systems can also provide warning of impending malfunctions in the WT drive train. According to Zaher et al. [14][14] 10 minute averaged signals often monitored in modern SCADA systems include:

- Active power output (and standard deviation over 10 min interval);
- Anemometer-measured win d speed (and standard deviation over 10 min interval);
- Gearbox bearing temperature;
- Gearbox lubrication oil temperature;
- Generator winding temperature;
- Power factor;
- Reactive power;
- Phase currents, and;
- Nacelle temperature (1 hour average).

This SCADA configuration is designed to show the operating condition of a WT but not necessarily give an indication of the health and a WT. However, the much up to date SCADA systems include additional alarm settings based not only on temperature transducers mentioned above but also on vibration transducers. Often we find several transducers fitted to the WT gearbox, generator bearings and the turbine main bearing. The resultant alarms are

based on the level of vibration being observed over the 10 minute average period. Research has being carried out into the CM of WTs through SCADA analysis in the EU project ReliaWind [15]. The research consortium consisted of a number of University partners alongside industrial consultants and WT manufacturers.

Secondly, there is the area of structural health monitoring (SHM). These systems aim to determine the integrity of the WT tower and foundations. SHM is generally carried out using low sampling frequencies below 5Hz.

While SCADA and SHM monitoring are key areas for WT monitoring, this survey will concentrate on the remaining two classes of CM and diagnosis systems.

Monitoring of the drive train is often considered to be most effective through the interaction of these two areas. CM itself may be considered as a method for determining whether a WT is operating correctly or whether a fault is present or developing. A WT Operator's main interest is likely to be in obtaining reliable alarms based on CM information which can enable them to take confident action with regard to shutting down for maintenance. The operator need not know the exact nature of the fault but would be alerted to the severity of the issue by the alarm signal. Reliable CM alarms will be essential for any operator with a large number of WTs under its ownership. On this basis, CM signals should not need to be collected on a high frequency basis as this will reduce bandwidth for transmission and space required for storage of data.

Once a fault has been detected through a reliable alarm signal from the CMS, a diagnosis system could be activated either automatically or by a monitoring engineer to determine the exact nature and location of the fault. For diagnosis systems, data recorded at a high sampling frequency is required for analysis however this need only be collected on an intermittent basis. The operational time of the system should be configured to provide enough data for detailed analysis but not to flood the monitoring system or data transmission network with excess information.

Finally, Figure3 gives an indication of three sections of a WT which may require monitoring based on reliability data such as that in Figure1 [13]. While each of the three areas are shown as separate entities it is possible that CM of the areas may well blur the boundaries between them in order to provide clear alarms and, subsequently, diagnostic information.

Many of the CMSs included in this survey are a combination of CMSs and diagnostic systems due to the high level of interaction that can exist between the two types of system.
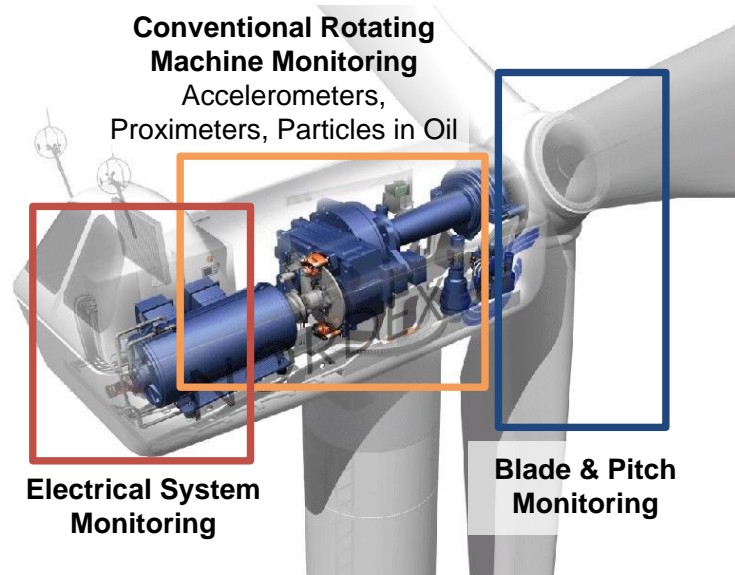
Figure 3: General layout of three areas for condition monitoring and diagnosis within the nacelle

4.   Commercially Available Condition Monitoring Systems

Table1, found on page 217 of this survey, provides a summary of a number of widely available and popular CMSs for WTs. The information in this table has been collected from interaction with CMS manufacturers, WT manufacturers and product brochures over a long period of time and is up to date as of the time of writing. However, since some information has been acquired through discussion with sales and product representatives and not from published brochures, it should be noted that the table may not be fully definitive and is as accurate as possible given the available information. The systems in Table1 are arranged alphabetically by product name.

The first observation to make from Table1 is that the CMSs nearly all focus on the same WT subassemblies. Moving through the WT these are:

- Blades
- Main bearing
- Gearbox internals
- Gearbox bearings
- Generator bearings

A quick summery of Table1 shows that there are:

- 27 systems primarily based on drive train vibration analysis (1 – 27)

- 1 system using Motor Current Signature Analysis, Operational Modal Analysis and Acoustic Emission techniques (28)
- 4 systems solely for oil debris monitoring (29 – 32)
- 1 system using vibration analysis for WT blade monitoring (33).
- 3 systems based on fibre optic strain measurement in WT blades, mast and foundation (34, 35, 36)

It is quite clear when reading through the table that the majority of systems are based around monitoring methods originating from other, traditional rotating machinery industries. Indeed 27 of the 36 systems in the table are based on vibration monitoring using accelerometers typically using a configuration similar to that in Figure4 for the Mita-Teknik WP4086 CMS (27).
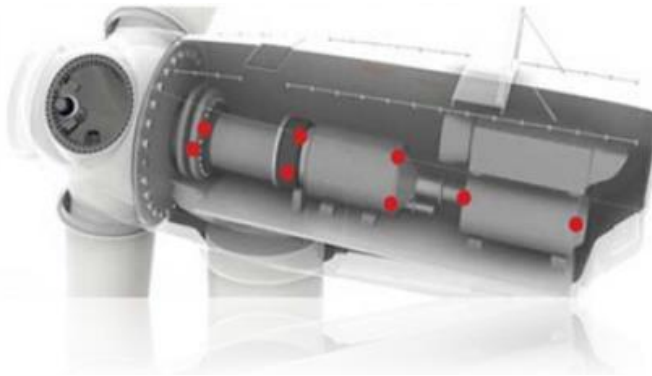

Figure 4: Typical accelerometer positions [16]

Of these 27 CMSs, all have the capability to carry out some form of diagnostic procedure once a fault has been detected. In most cases this is done through fast Fourier transform (FFT) analysis of high frequency data in order to detect fault-specific frequencies. In the case of the SKF WindCon 3.0 (23), the ACOEM OneProd Wind CMS (15) and several others, high data acquisition is triggered by operational parameters. For example, the SKF WindCon 3.0 CMS can be configured to collect a vibration spectrum on either a time basis or when a specific load and speed condition is achieved. The aim of this is to acquire data that is directly comparable between each point and, importantly, to allow spectra to be recorded in apparently stationary conditions. This is an important point to note when using traditional signal processing methods such as the FFT which require stationary signals in order to obtain a clear result. The Mita-Teknik WP4086 system (27), however, states that it includes advanced signal processing techniques such as comb filtering, whitening and Kurtogram analysis which in combination with re-sampling and order alignment approaches, allow the system to overcome the effects of WT speed variations.

An innovative vibration-based CMS is OrtoSense APPA (2) which is based on Auditory Perceptual Pulse Analysis. This patented technology outperforms the human ear by capturing a detailed interference pattern and detecting even the smallest indication of damaged or worn elements

within the machine/turbine. OrtoSense states that its product is 4 to 10 time more sensitive compared to prevailing systems.

CMSWind (7) is still in the development phase but it represents an advanced system for WT CM utilising three new and novel techniques, specifically designed for wind turbines and their components. Motor Current Signature Analysis, Operational Modal Analysis and Acoustic Emission techniques will be used to monitor the condition of the generator, the gearbox and rotary components, respectively. All systems will be tied together through SCADA to provide supervisory control, data logging & analysis.

Six of the vibration-based CMSs also state that they are able to monitor the level of debris particles in the WT gearbox lubrication oil system. Further to this, included in the table are four systems which are not in themselves CMSs. These four (29 – 32) are oil quality monitoring systems or transducers rather than full CMSs but are included as discussion with industry has suggested that debris in oil plays a significant role in the damage and failure of gearbox components. Systems using these debris in oil transducers are using either cumulative particle counts or particle count rates.

Several of the 27 vibration-based CMSs also allow for other parameters to be recorded alongside vibration such as load, wind speed, generator speed and temperatures although the capabilities of some systems are unclear given the information available. There is some interest being shown as regards the importance of operational parameters in WT CM. This arises from the fact that many analysis techniques, for example the FFT, have been developed in constant speed, constant load environments. This can lead to difficulties when moving to the variable speed, variable load WT however experienced CM engineers are able to use these techniques and successfully detect faults.

Recent CM solutions, as (1), (7), (11), (13), (19), (24), (27), (28), (30), can be adapted and fully integrated with existing SCADA systems using standard protocols. Thanks to this integration, the analysis of the systems installed on the wind energy plant can also directly consider any other signals or variables of the entire controller network, as for example current performance and operating condition, without requiring a doubling of the sensor system. The database, integrated into a single unified plant operations' view, allows a trend analysis of the condition of the machine.

In some cases the CMS company offers also custom service solutions from 24/7 remote monitoring to on-demand technical support, examples are GE Energy ADAPT.wind (1), Moventas CMaS (10), ABS Wind Turbine In-Service (24) and several others.

Recently patented condition-based turbine health monitoring systems, as (4), (5), (13), (19), feature diagnostic and prognostic software unifying fleet wide CMS and SCADA enabling the

identification of both source and cause of the fault and the application of prognostics to establish the remaining operational life of the component.

Three CMSs in the table (34, 35, 36) are based on strain measurement using fibre optic transducers. FS2500 (34) and RMS (35) are aimed at detection of damage to WT blades and, in the case of the Moog Insensys system (35), blade icing, mass unbalance or lightning strikes. SCAIME system (36) allows turbine structural monitoring with sensors mounted on the blades, the mast and the foundations. These three systems may be fitted to WT retrospectively. Compared to vibration monitoring techniques, these systems can be operated at low sampling rates as they are looking to observe changes in time domain. They are usually integrated in the WT control system but there are also some cases of integration, as an external input, into commercial available conventional vibration-based CMSs. In addition to (34) (35) and (36) there is the IGUS system (33) using accelerometers to monitor blade damage, icing and lightning strikes. This system compares the blade accelerometer FFT with stored spectra for similar operating conditions and has the power to automatically shut down or restart a WT based on the results. The system appears to be popular within industry.

5. Comments on Numbers of CMS Installed & Centrally Monitored

5.1. Bruel & Kjaer Vibro

It has been reported that B & K had sold 4000 Vibro systems world-wide, all for wind turbines with 2500 connected to their central monitoring service. It has been reported that Bachmann, a wind turbine controller manufacturer, is now a serious competitor. B & K take signals from CMS transducers and SCADA, as allowed by the WT OEM, which is straightforward with Vestas, where the B & K system is fitted to new turbines.

5.2. Gram & Juhl

It was reported that G & J had 6000 CMS systems installed worldwide but not all in wind turbines and that 2-3000 wind turbine systems are connected to the G & J monitoring centre. G & J take signals from CMS transducers and SCADA, as permitted by the WT OEM, which is straightforward with Siemens, where the G & J system is fitted to new turbines.

The process of automating CMS detection has proved very hard because it depends upon specific drive-train designs and required some learning of machine operation, that generally came from experienced CMS technicians.

5.3. Pruftechnik

Pruftechnik has more than 2000 systems installed in the wind industry with 800 wind turbine systems connected to their monitoring centre. They are not selling directly to wind turbine OEMs, except in rare cases, but did supply their system to gearbox OEMs, for example Winergy. They are also supplying an oil debris counter and handheld and alignment devices.

5.4. SKF Windcon

SKF have thousands of Windcon units fitted to wind turbines world-wide with about 1000 Windcons connected to their Hamburg Wind Centre.

It was reported that CMS is a difficult sell for wind turbines, as some Operators refuse to recognise the value of CMS because it cannot prevent failure without interpretation. Their philosophy is run to failure. However, on large wind farms in the US there is a growing interest as Operators begin to recognise the disadvantage of simple Availability benchmarks for operational performance measurement, where these can only be achieved at high O&M cost. Some Operators, particularly of large wind farms, are recognising the benefit of maintenance planning using integrated SCADA & CMS data.

5.5. Mita-Teknik

Mita-Technik continue to offer their CMS option within their SCADA offering. The value of integration between SCADA and CMS was stressed and only Mita Technik appeared to offer that advantage to Operators.

6. The Future of Wind Turbine Condition Monitoring

As can be seen from this survey of current CMSs there is a clear trend towards vibration monitoring of WTs. This is presumably a result of the wealth of knowledge gained from many years work in other fields. It is likely that this trend will continue however it would be reasonable to assume that other CM and diagnostic techniques will be incorporated into existing systems.

Currently these additions are those such as oil debris monitoring and fibre optic strain measurement. However, it is likely that major innovation will occur in terms of developing signal processing techniques. In particular, the industry is already noting the importance of operational parameters such as load and speed and so techniques may begin to adapt further to the WT environment leading to more reliable CMSs, diagnostics and alarm signals.

Automation of CM and diagnostic systems may also be an important development as WT operators acquire a larger number of turbines and manual inspection of data becomes impractical. Further to this, it is therefore essential that methods for reliable, automatic diagnosis are developed with consideration of multiple signals in order to improve detection and increase operator confidence in alarm signals. It is clear that CMS automation is difficult, because of individual plant peculiarities, but that with larger wind farms it is becoming more attractive for Operators.

However, it should be noted that a major hindrance to the development of CMSs and diagnostic techniques could be data confidentially meaning that few operators are able to divulge or obtain information concerning their own WTs. This is an issue which should be addressed if the art of CM is to progress quickly. Confidentiality has also led to a lack of publicly available cost justification of WT CM, which seems likely to provide overwhelming support for WT CM, particularly in the offshore environment where availability is at a premium.

Table 1: Table of commercially available condition monitoring systems

	Product and Company Information			Product Details (based on available literature and contact with industry including EWEC 2008, 2009, 2010, 2011, 2012, 2013, 2014)				
Ref.	Product	Supplier or Manufacturer (Known Users)	Country of Origin	Description	Main Components Monitored	Monitoring Technology	Analysis Method(s)	Data Rate or Sampling Frequency
1	ADAPT.wind	GE Energy	USA	Up to 150 static variables monitored and trended per WT. Planetary Cumulative Impulse Detection algorithm to detect debris particles through the gearbox planetary stage. Dynamic Energy Index algorithm to spread the variation over five bands of operation for spectral energy calculations and earlier fault detection. Sideband Energy Ratio algorithm to aid in the detection of gear tooth damage. Alarm, diagnostic, analytic and reporting capabilities facilitate maintenance with actionable recommendations. Possible integration with SCADA system.	Main bearing, gearbox, generator	Vibration (Accelerometer) Oil debris particle counter	FFT frequency domain analysis Time domain analysis	-
2	APPA System	OrtoSense	Denmark	Oscillation technology based on interference analysis that replicates the human ear's ability to perceive sound.	Main bearing, gearbox, generator	Vibration	Auditory Perceptual Pulse Analysis (APPA)	-
3	Ascent	Commtest	New Zealand	System available in 3 complexity levels. Level 3 includes frequency band alarms, machine template creation, statistical alarming.	Main shaft, gearbox, generator	Vibration (Accelerometer)	FFT frequency domain analysis Envelope analysis Time domain analysis	-
4	Brüel & Kjaer Vibro	Brüel & Kjaer (Vestas)	Denmark	Local data acquisition units, alarm management and review by the Condition Monitoring Centre analysts, reports on actionable information to customers. Vibration and process data automatically monitored at fixed intervals and remotely sent to the diagnostic server. Monitoring to specific power loadings and filtering out irrelevant alarms. Time waveform automatically stored before and after user-defined event for advanced vibration post-analysis. Severity classes, each related to an estimated lead-time. Severity is first estimated automatically by the Alarm Manager, followed by the diagnostic expert final assessment.	Main bearing, coupling, gearbox, generator, nacelle, support structure. Nacelle temperature. Noise in the nacelle	Vibration Temperature sensor Acoustic	Time domain FFT frequency analysis	Variable up to 40kHz. 25.6kHz.
5	Brüel & Kjaer VibroSuite	Brüel & Kjaer (Vestas)	Denmark	Stand-alone software packages, completely client-owned, enable end-users and operators to host, process and analyse the data in-house. AlarmManager processes and simplifies data, provides developing faults automated evaluation, severity level and lead-time to failure; AlamTracker for quick access to live alarms with alarm history and high-end functionality; WTG.Analyser diagnostic tool interprets signals and identifies root causes; EventMaster facilitates time and event based diagnostic data acquisition.	Main bearing, coupling, gearbox, generator, nacelle, support structure. Nacelle temperature. Noise in the nacelle	Vibration Temperature sensor Acoustic	Time domain FFT frequency analysis	Variable up to 40kHz. 25.6kHz.

6	CMS	Nordex	Germany	Start-up period acquires vibration 'fingerprint' components. Actual values automatically compared by frequency, envelope and order analysis, with the reference values stored in the system. Some Nordex turbines also use the Moog Insensys fibre optic measurement system.	Main bearing, gearbox, generator	Vibration (Accelerometer)	Time domain based on initial 'fingerprint'	-
7	Condition Based Maintenance System (CBM)	GE (Bently Nevada)	USA	This is built upon the Bently Nevada ADAPT.wind technology and System 1. Basis on System 1 gives monitoring and diagnostics of drive train parameters such as vibration and temperature. Correlate machine information with operational information such as machine speed, electrical load, and wind speed. Alarms are sent via the SCADA network.	Main bearing, gearbox, generator, nacelle Optional bearing and oil temperature	Vibration (Accelerometer)	FFT frequency domain analysis Acceleration enveloping	-
8	Condition Based Monitoring System	Bachmann electronic GmbH	Austria	Up to 9 piezoelectric acceleration sensors per module. Basic vibration analysis with 7 sensors. PRÜFTECHNIK solid borne sound sensors for low frequency diagnostics of slowly rotating bearings on the WT LSS. Three channels for the ±10V standard signal per module. Audibile sensor signals to assess the spectra acoustically. Fully integration in automation control system to link the measured values to operating parameters and increase diagnostic reliability. Traffic light system indicates if predefined thresholds are exceeded. Data analyzed by experienced diagnostics specialists using extensive tools, such as envelope and amplitude spectra, or frequency-based characteristic values. Integrated database enables data trend analysis.	Main drive train components Generator	Vibration (Accelerometer) Acoustic	Time domain FFT frequency analysis	24-bit res 190 kHz sample rate per channel 0.33 Hz (solid borne sound sensors)
9	Condition Diagnostics System	Winergy	Denmark	Up to 6 inputs per module. Advanced signal processing of vibration levels, load and oil to give automated machinery health diagnostics, forecasts and recommendations for corrective action. Automatic fault identification is provided. Relevant information provided in an automated format to the Operations and Maintenance centre, without any experts being involved. Information delivered to the appropriate parties in real time. Pitch, controller, yaw and inverter monitoring can also be included.	Main shaft, gearbox, generator	Vibration (Accelerometer) Oil debris particle counter	Time domain FFT frequency domain analysis	96kHz per channel
10	Condition Management System (CMaS)	Moventas	Finland	Compact remote system measuring temperature, vibration, load, pressure, speed, oil aging and oil particle count. 16 analogue channels can be extended with adapter. Performance monitoring, anticipate possible upcoming failures by providing timely updates and alerting maintenance crews. Data stored, analysed and reported to remote server via standard TCP/IP protocol. Mobile interface available. Moventas Remote Centre provides proactive gear expertise with specialists available for all customers on-call 24 hours a day, seven days a week.	Gearbox, main bearing, generator, rotor, turbine controller	Temperature Vibration Load Pressure RPM Oil condition/particles	Time domain (Possible FFT)	-

#	Name	Manufacturer	Country	Description	Monitored components	Monitored parameters	Analysis methods	Sampling
11	Distributed Condition Monitoring System	National Instruments	USA	Up to 32 channels; default configuration: 16 accelerometer/microphone, four proximity probe and eight tachometer input channels. Also provided mixed-measurement capability for strain, temperature, acoustics, voltage, current and electrical power. Oil particulate counts and fiber-optic sensing can also be added to the system. Possible integration into SCADA systems.	Main bearing, gearbox, generator	Vibration Acoustic	Spectral analysis Level measurements Order analysis Waterfall plots Order tracking Shaft centre-line measurements Bode plots	24-bit res 23.04 kHz of bandwidth with antialiasing filters per accelerometer/ microphone channel
12	HAICMON	Hainzl	Austria	The Monitoring Unit (CMU), mounted in the nacelle, performs the data acquisition, analysis and local intermediate storage. Up to 32 vibration inputs, 8 digital and optional 16 analog inputs. Web interface for configuration and visualization purpose. Automatic data analysis directly on the CMU with automatic alarming features. CMU can operate in standalone mode or in connection with the superior HAICMON ANALYSIS CENTER which features more computing power or database access functionality for advanced trend analysis. It also allows comparing different plants among each other and provides a reporting module.	Rotor bearing, gearbox, generator	Vibration Load Rotation speed Oil temperature	Time domain FFT frequency analysis Envelope analysis Cepstrum analysis	Variable up to 40kHz.
13	InSight intelligent Diagnostic System (iDS)	Romax Technology Ltd	UK	Diagnostic and prognostic software unifying fleet wide CMS and SCADA data. Suite of predictive maintenance technologies and services comprising: Inspection and Analysis; iDS that integrates vibration, SCADA and maintenance record data. This hardware independent software platform harmonises data from multiple manufacturers CMSs. Intuitive user interface and advanced diagnostic rules. iDS Manger provides managers with a clear dashboard displaying wind turbines' condition and notifying of alarm events via email. InSight Expert is a diagnostic platform aimed at vibration analysis experts which enables the identification of both fault source and cause and the application of prognostics.	Main drive train components	Vibration Temperature Oil debris particle counter	Time domain FFT frequency analysis	-
14	OMNITREND	Prüftechnik	Germany	WebReport creates customizable reports for analysing machine conditions, color-coded alarm classes in the status report identify machine problems at a glance; Online View, visualizes measurement data from online systems and machine conditions in real time; network capable multiuser PC software OMNITREND saves measurement data in a database, arranges routes for data collection and visualizes the results in easy-to-read diagrams. Practical tools support data evaluation and documentation. Data exchange between OMNITREND and a Computerized Maintenance Management System allows exchanging measurement data, sending status messages and using master data from ERP systems.	Main drive train components	Vibration	FFT frequency domain analysis	-

15	OneProd Wind System	ACOEM (01dB-Metravib)	France	8 to 32 channels; operating conditions trigger data acquisitions. Repetitive and abnormal shock warnings enable detection of failure modes; built-in diagnostic tool. Optional additional sensors for shaft displacement and permanent oil quality monitoring; structure low frequency sensors; current&voltage sensors. Graphics module for vibration analysis including many representation modes as trend, simple or concatenated spectrum, waterfall spectrum, time signal, circular view, and orbit; advanced cursors and post-processing are available. SUPERVISION web application provides information on alarm status together with expert diagnoses and recommendations.	Main bearing on LSS, Bearing on gearbox LSS, Bearing on intermediate gearbox shaft, on gearbox high-speed shaft, on generator Oil debris, structure, shaft displacement, electrical signals	Vibration Acoustic Electrical signals Thermography Oil debris particle counter	Time domain FFT frequency analysis Electrical signature analysis	-
16	SIPLUS CMS4000	Siemens	Germany	Acquisition and evaluation of analog and binary signals in individual wind turbines or complex wind farms. Data acquisitions and pre-processing performed with interface nodes that enable the recording of highly dynamic processes. Software X tools for analysis, diagnostics, visualisation and archiving for wind power plants. Data displayed via traffic lights, integrated message systems and spectrum-view in CMS X-Tools. Library of standard function blocks for FFT, envelope curve analysis, input filters, mathematical and communication functions and graphical creation of diagnostic models. Analysis blocks can be interconnected graphically to resolve specific measuring and diagnostic tasks. Modular, scalable system can be integrated into existing wind turbines and new ones.	Bearings , gearbox, tower	Vibration	FFT frequency domain analysis Envelope curve analysis Fingerprint comparison Trend Analysis Input filters	Exceeding 40kHz
17	SMP-8C	Gamesa Eolica	Spain	Continuous on-line vibration measurement of main shaft, gearbox and generator. Comparison of spectra trends. Warnings and alarm transmission connected to Wind Farm Management System.	Main shaft, gearbox, generator	Vibration	FFT frequency domain	-
18	System 1	Bently Nevada (GE)	USA	Monitoring and diagnostics of drive train parameters such as vibration and temperature. Correlate machine information with operational information such as machine speed, electrical load, and wind speed.	Main bearing, gearbox, generator, nacelle Optional bearing and oil temperature	Vibration (Accelerometer)	FFT frequency domain Acceleration enveloping	-

19	TCM (Turbine Condition Monitoring) Enterprise V6 Solution with SCADA integration	Gram & Juhl A/S	Denmark	Advanced signal analysis and process signals combined with automation rules and algorithms for generating references and alarms. M-System hardware features up to 24 synchronous channels, interface for Structural Vibration Monitoring and RPM sensors, extern process parameters and analog outputs. TCM Site Server stores data and does post data processing (data mining) and alarm handling. TCM Ocular Modeller models drive train and sensor configuration to relate measurement data to the kinematics of the turbine. Control room with web based operator interface. TCM Enterprise allows centralised remote monitoring on a global scale. Optional Structural Vibration Monitoring sensor to measure low frequency signals associated with tower sway, rotor imbalance and machine over speed. Integration with SCADA through OPC UA.	Tower, blades, shaft, nacelle Main bearing, gearbox, generator	Vibration (Accelerometer) Sound analysis Strain analysis Process signals analysis	FFT and Wavelet frequency domain analysis Envelope, time and frequency domain [analytic/Hilbert] analysis Cepstrum, Kurtosis, Spectral kurtosis, Skewness RMS analysis Order tracking analysis	40.960/81.920 kHz
20	TurbinePhD (Predictive Health Monitoring)	NRG Systems	USA	Automatically integrates multiple condition indicators into a single readily understandable health indicator for each turbine's drive train component delivering future health predictions. Actionable indicators and data supporting the diagnosis accessible via Internet. Optimise turbine maintenance schedules by predicting when components in the turbine's drive train are likely to fail and scheduling repairs at the most cost-effective time. Advanced diagnostic algorithms from the aerospace industry accounting for varying speed and torque conditions. Residual, energy operator, narrow band and modulation analysis tools for gear analysis; spectrum and envelope for bearing analysis; synchronous average for shaft analysis.	Main shaft, gearbox, main bearing	Vibration (Accelerometer)	FFT frequency domain analysis	0.78 to 100 Hz @24 bits (High Speed Vibration Sensor) 8 to 500 Hz (Low Speed Vibration Sensor)
21	VIBstudio WIND	EC Systems KAStrion project	Poland	Integrated embedded system for data acquisition; real-time verification through algorithms for automatic signal validation, to avoid generating false alarms, and advanced signal processing. Up to 24 vibration channels, 4 analog channels, 2 digital inputs and 3 digital outputs. Automated generation of analyses and thresholds; individually tuned, automated configuration of machine operational state; intelligent data selection and storage; tolerance for loss of connectivity. VIBmonitor Astrion module for automatic vibration analysis. VIBmonitor SMESA module for generator fault detection by electrical signature analysis.	Bearings, shaft, gearbox, generator	Vibration (Accelerometer)	Wideband analyses: PP, RMS, VRMS, Crest, Kurtosis Narrowband analyses: energy in the band, order spectrum and envelope spectrum	Vibration channels: Variable up to 100 kHz Process variable channels: up to 1 kHz
22	Wind AnalytiX	ICONICS	USA	This software solution uses Fault Detection and Diagnostics technology which identifies equipment and energy inefficiencies and provides possible causes that help in predicting plant operations, resulting in reduced downtime and costs related to diagnostic and repair.	Main WT components	Vibration (Accelerometer)	Unknown	-

No	Name	Company	Country	Description	Components Monitored	Measurement Type	Analysis	Frequency Range
23	WindCon 3.0	SKF	Sweden	Monitoring solution including sensors, data export, analysis and lubrication. Turbine health monitoring through vibration sensors and access to the turbine control system by means of the SKF WindCon software. WindCon 3.0 collects, analyses and compiles operating data that can be configured to suit management, operators or maintenance engineers. The system can be stand alone or linked together using SKF's WebCon, the web solution for data hosting and remote monitoring. WindCon can also be linked to the turbine lubrication system and fully integrated with the WindLub system for automated condition based lubrication and monitoirng of the lubrication pump.	Blade, main bearings, shaft, gearbox, generator, tower, generator electrical	Vibration (Accelerometer, proximity probe) Oil debris particle counter	FFT frequency domain analysis Envelope analysis Time domain analysis	Analogue: DC to 40kHz (Variable, chan dependent) Digital: 0.1 Hz - 20kHz
24	Wind Turbine In-Service	ABS Consulting	USA	Data gathered from inspections, vibration sensors and SCADA system. Ekho for WIND software features regular diagnostics, dynamic performance reports, key performance indicators, fleet-wide analysis, forecasts/schedules, and asset benchmarking. It generates alarms and notifications or triggers work orders for inspections or repairs.	Main bearing, gearbox, generator Gearbox and gear oil, rotor blades and coatings	Vibration Inspections	FFT frequency domain analysis Time domain analysis	-
25	WinTControl	Flender Service GmbH	Germany	Vibration measurements are taken when load and speed triggers are realised. Time and frequency domain analysis are possible.	Main bearing, gearbox, generator.	Vibration (Accelerometer)	FFT frequency domain Time domain analysis	32.5kHz
26	WiPro	FAG Industrial Services GmbH	Germany	Measurement of vibration and other parameters given appropriate sensors. Time and frequency domain analysis carried out during alarm situations. Allows speed-dependent frequency band tracking and speed-variable alarm level.	Main bearing, shaft, gearbox, generator, temperature. (Adaptable inputs)	Vibration (Accelerometer)	FFT frequency domain Time domain analysis	Variable up to 50kHz
27	WP4086	Mita-Teknik	Denmark	Up to 8 accelerometers for real-time frequency and time domain analysis. Warnings/Alarms set for both time and frequency domains based on predefined statistical/thresholds-based vibration limits. Operational parameters recorded alongside with vibration signals/spectra and full integration into Gateway SCADA system. Algorithm Toolbox for diagnostic analysis. Approx 5000 – 8000 variables covering different production classes.	Main bearing, gearbox, generator	Vibration (Accelerometer)	FFT amplitude spectra FFT envelope spectra Time domain magnitude Comb filtering, whitening, Kurtogram analysis	12-bit chan res Variable up to 10kHz
28	CMSWind (still in development phase)	CMSWind project	European Research & Development Project	Advanced condition monitoring system which utilises Motor Current Signature Analysis, Operational Modal Analysis and Acoustic Emission techniques to monitor the condition of the generator, the gearbox and rotary components, respectively. All systems are tied together through SCADA to provide supervisory control, data logging & analysis. Wireless sensors for rotating components monitoring using high performance powering and energy harvesting technologies.	Gearbox (including Main bearing, Yaw System, Hub), generator	Electrical signals operational paramters, acoustic	Motor Current Signature Analysis Operational Modal Analysis Acoustic Emission techniques	-

29	HYDACLab	HYDAC Filtertechnik GmbH	Germany	Permanent monitoring system to monitor particles (including air bubbles) in hydraulic and lube oil systems.	Lubrication oil & cooling fluid quality	Oil debris particle counter	N/A	-
30	Oil Contamination Monitor (OCM 30X)	C.C. Jensen	Denmark	Early warning for gearbox breakdown by measuring wear generation. Especially designed for high viscous oils, such as gear oils, and equipped with an air removal device to enable correct measurements. Very stable flow over a large viscosity range allows sensor accurate readings. Different options for communication with the SCADA system and wen based trends.	Lubrication oil quality and cleankiness	Oil debris particle counter Oil cleanliness sensor	N/A	-
31	PCM200	Pall Industrial Manufacturing (Pall Europe Ltd)	USA (UK)	Fluid cleanliness monitor reports test data in real-time so ongoing assessments can be made. Can be permanently installed or portable.	Lubrication oil cleanliness	Oil cleanliness sensor	N/A	-
32	TechAlert 10 TechAlert 20	MACOM	UK	TechAlert 10 is an inductive sensor to count and size ferrous and non-ferrous debris in circulating oil systems. TechAlert 20 is a magnetic sensor to count ferrous particles.	Lubrication oil quality	Inductive or magnetic oil debris particle counter	N/A	-
33	BLADEcontrol	IGUS ITS GmbH	Germany	Accelerometers are bonded directly to the blades and a hub measurement unit transfers data wirelessly to the nacelle. Blades are assesed by comparing spectra with those stored for common conditions. Measurement and analysis data are stored centrally and blade condition displayed using a web browser.	Blades	Accelerometer	FFT frequency domain	≈ 1kHz
34	FS2500	FiberSensing	Portugal	BraggSCOPE measurement unit designed for industrial environments to interrogate up to 4 Fiber Bragg Grating sensors. Acceleration, tilt, displacement, strain, temperature and pressure measurable.	Blades	Fibre optic	Unknown	Up to 2kHz
35	RMS (Rotor Monitoring System)	Moog Insensys Ltd.	UK	Modular blade sensing system consisting of 18 sensors, 6 per blade, installed in the cylindrical root section of each blade to provide edgewise and flapwise bending moment data. Can be designed-in during turbine manufacture or retrofitted. Monitors turbine rotor performance, mass and aerodynamic imbalance, blade bending moments, icing, damage and lightning strikes. Possible integration, as an external input, in commercial available CMSs.	Blades	Fibre optic strain	Time domain strain analysis	25 Hz/sensor
36	SCAIME Condition Monitoring Solutions	SCAIME	France	Fibre optic systems for structural monitoring. Sensors, made of glass fibre reinforced plastic or aluminium alloys, measure the stresses on the blades, the mast and the foundations. MDX400 data acquisition unit with an integrated web server for remote system and sensor setup. Emergency alarms generated when loads become too high and blade loads data used for pitch controller input. Data processing provides remaining life estimation, defect and ice detection. In the mast, sensors measure bending moments at different heights to monitor tower deformations and oscillations. Sensors monitor foundation aging due to load accumulation, soil pressure, grouting.	Blades Mast Foundation	Strain and temperature sensors Long base extensometers Displacement sensors Tilt-meters Accelerometers	Time domain analysis	100 Hz

7. Conclusions

From this survey we can conclude that:

- Current WT reliability is reasonable however in the offshore environment the failure rate will be unacceptable;
- Cost effective and reliable CM is required to enable planned maintenance, reduce unplanned WT downtime and improve capacity factors;
- Successful CMSs must be able to adapt to the non-stationary, variable speed nature of WTs;
- There is a wide variety of commercially available CMSs currently in use on operational WTs;
- Monitoring technology is currently based on techniques from other, conventional rotating machine industries;
- Vibration monitoring is currently favoured in commercially available systems using standard time and frequency domain techniques for analysis;
- These traditional techniques can be applied to detect WT faults but require experienced CM engineers for successful data analysis and diagnosis;
- Some commercially available CMSs are beginning to adapt to the WT environment and to be fully integrated into existing SCADA systems, and;
- Recently patented condition-based turbine health monitoring systems feature diagnostic and prognostic software enabling the identification of both source and cause of the fault and the application of prognostics to establish the remaining operational life of the component.
- A diverse range of new or developing technologies are moving into the WT CM market.

Finally, it should be noted that there is not currently a consensus in the WT industry as to the correct route forward for CM of WTs. Work in this document and its references suggest that CM of WTs will be beneficial for large onshore WTs but essential for all offshore development and should be considered carefully by the industry as a whole.

8. References

[1] SUPERGEN Wind, *Theme X: Drive train loads and monitoring*, www.supergen-wind.org.uk/research_x0.html, last accessed 8th February 2010.

[2] SUPERGEN Wind, *Theme 2: The Turbine*, http://www.supergen-wind.org.uk/research_2.html, last accessed 10th May 2014.

[3] SUPERGEN Wind, *Theme 4: The wind farm as a power station*, http://www.supergen-wind.org.uk/research_4.html, last accessed 10th May 2014.

[4] Tavner, P.J., Xiang, J.P., Spinato, F., *Reliability analysis for wind turbines*, Wind Energy, Vol. 10, Issue 1, 2006.

[5] Spinato, F., Tavner, P.J., van Bussel, G.J.W., Koutoulakos, E., *Reliability of wind turbine subassemblies*, IET Renewable Power Generation, Vol. 3, Issue 4, pp. 1-15, 2009.

[6] Faulstich, S., et al., *Windenergie Report Deutschland 2008*, Institut für Solare Energieversorgungstechnik (Hrsg.), Kassel, 2008.

[7] Various Authors, *Operations Report 2007, Document No. OWEZ_R_000_20081023*, Noordzee Wind, 2008.

[8] Wilkinson, M.R., et al., *Methodology and results of the ReliaWind reliability field study*, Scientific Track Proceedings, European Wind Energy Conference 2010, Warsaw, 2010.

[9] Wilkinson, M.R, et al., *Measuring Wind Turbine Reliability: Results of the ReliaWind Project*, Scientific Track Proceedings, European Wind Energy Conference 2011, Brussels, 2011.

[10] Germanischer Lloyd, *Rules and Guidelines, IV Industrial Services, 4 Guideline for the Certification of Condition Monitoring Systems for Wind Turbines*, Edition 2007.

[11] Germanischer Lloyd, *Guideline for the Certification of Wind Turbines, Edition 2003 with Supplement 2004*, Reprint 2007.

[12] Germanischer Lloyd, *Guideline for the Certification of Offshore Wind Turbines, Edition 2005*, Reprint 2007.

[13] Crabtree, C.J., Feng, Y., Tavner, P.J., *Detecting Incipient Wind Turbine Gearbox Failure: A Signal Analysis Method for Online Condition Monitoring, Scientific Track Proceedings*, European Wind Energy Conference 2010, Warsaw, 2010.

[14] Zaher, A., McArthur, S.D.J., Infield, D.G., *Online Wind Turbine Fault Detection through Automated SCADA Data Analysis*, Wind Energy, Vol. 12, Issue 6, pp. 574-593, 2009.

[15] ReliaWind, www.reliawind.eu, last accessed 8th February 2010.

[16] Isko, V., Mykhaylyshyn, V., Moroz, I., Ivanchenko, O., Rasmussen, P., *Remote Wind Turbine Generator Condition Monitoring with WP4086 System*, Materials Proceedings, European Wind Energy Conference 2010, Warsaw, 2010.